Newark Basin – View from the 21st Century

Field Guide and Proceedings

Edited by
Alexander E. Gates
Rutgers University-Newark

Geological Association of New Jersey

XXII Annual Meeting

October 7-8, 2005
The College of New Jersey
Trenton, New Jersey

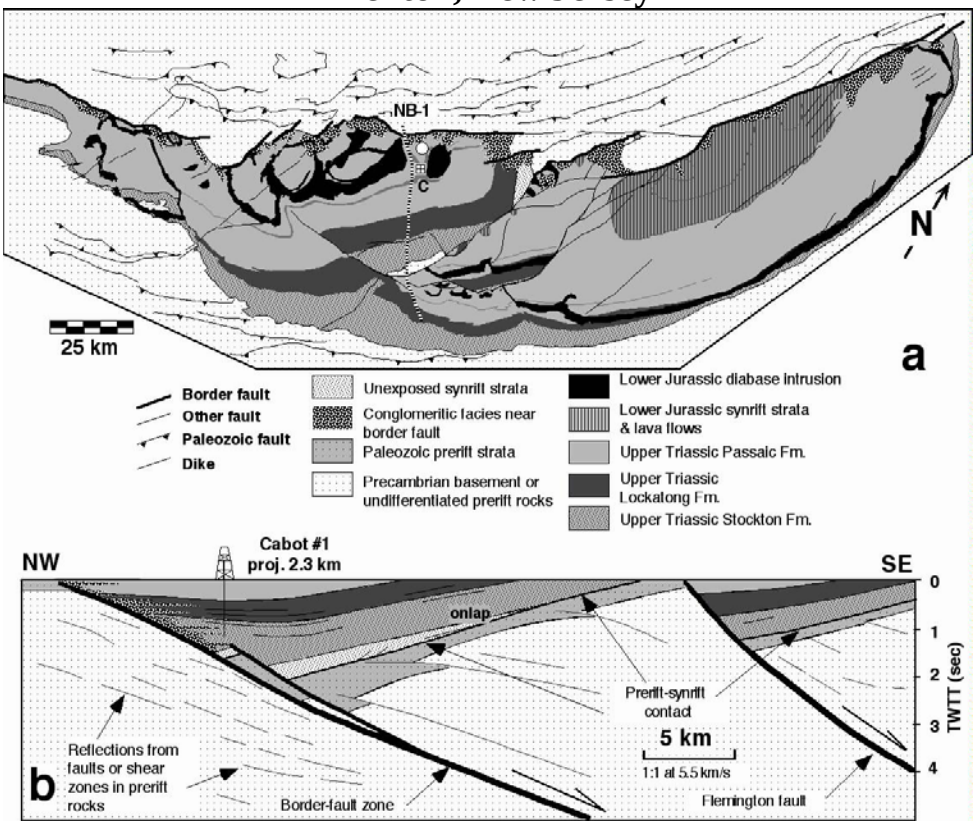

Newark Basin –

View from the 21st Century

Field Guide and Proceedings

Edited by
Alexander E. Gates
Rutgers University-Newark

Twenty-Second Annual Meeting
Geological Association of New Jersey

October 7-8, 2005
The College of New Jersey
Trenton, New Jersey

CORPORATE SPONSORS OF THE MEETING

CORPORATE SPONSORS OF THE MEETING

GEOLOGICAL ASSOCIATION OF NEW JERSEY

2005 Executive Board

President	Dr. William Montgomery, *New Jersey City University*
Past President	Dr. Michael J. Hozik, *Richard Stockton College of New Jersey*
President Elect	Dr. Alexander E. Gates, *Rutgers University-Newark*
Recording Secretary	Mr. Steve Urbanik, *New Jersey Dept. of Environmental Protection*
Membership Secretary	Ms. Suzanne Macaoay, *Sadat Associates Inc.*
Treasurer	Dr. Alan Benimoff, *College of Staten Island/CU*NY
Councilor at Large	Dr. John Puffer, *Rutgers University-Newark*
Councilor at Large	Dr. George Randall, *Rowan University*
Councilor at Large	Mr. Michael Fedosh, *Ecol Sciences, Inc*.
Director of Publications	Dr. Richard Kroll, *Kean University*
Webmaster	Dr. Gregory Herman, *New Jersey Geological Survey*

GEOLOGICAL ASSOCIATION OF NEW JERSEY

Field Guide and Proceedings of Annual Meetings

Guidebooks may be purchased from:

Dr. Richard Kroll
Department of Geology and Meteorology
Kean University
Union, NJ 07083
E-mail: rkroll@kean.edu

Guidebooks are $20.00 each; postpaid
Checks or money orders must be made payable to GANJ.

2004 GANJ XXI	**NEOPROTEROZOIC, PALEOZOIC, AND MESOZOIC INTRUSIVE ROCKS OF NORTHERN NEW JERSEY AND SOUTHEASTERN NEW YORK.** Puffer**,** J. and Volkert, R.A.
2003 GANJ XX	**PERIGLACIAL FEATURES OF SOUTHERN NEW JERSEYAND ADJACENT AREAS,** Hozik, M.J. and Mihalasky, M.J., eds.
2002 GANJ XIX	**GEOLOGY OF THE DELAWARE WATER GAP AREA**, Dana D'Amato, ed.
2001 GANJ XVIII	**GEOLOGY IN THE SERVICE OF PUBLIC HEALTH**, LaCombe, P. and Herman, G., eds.
2000 GANJ XVII	**GLACIAL GEOLOGY OF NEW JERSEY**, Harper, D.P. and Goldstein, F.R., eds.
1999 GANJ XVI	**NEW JERSEY BEACHES AND COASTAL PROCESSES FROM A GEOLOGICAL AND ENVIRONMENTAL PERSPECTIVE**, Puffer, J.H., ed.
1998 GANJ XV	**ECONOMIC GEOLOGY OF CENTRAL NEW JERSEY**, Puffer, J.H., ed.
1997 GANJ XIV	**ECONOMIC GEOLOGY OF NORTHERN NEW JERSEY**, Benimoff, A.I. and Puffer, J.H., eds.
1996 GANJ XIII	**KARST GEOLOGY OF NEW JERSEY AND VICINITY**, Dalton, R.F. and Brown, J.O., eds.
1995 GANJ XII	**CONTRIBUTIONS TO THE PALEONTOLOGY OF NEW JERSEY**, Baker, J., ed.
1994 GANJ XI	**GEOLOGY OF STATEN ISLAND**, Benimoff, A.I., ed.
1993 GANJ X	**GEOLOGIC TRAVERSE ACROSS THE PRECAMBRIAN ROCKS OF THE NEW JERSEY HIGHLANDS**, Puffer, J.H., ed.
1992 GANJ IX	**ENVIRONMENTAL GEOLOGY OF THE RARITAN RIVER BASIN**, Ashley, G.M. and Halsey, S.D., eds.

1991 GANJ VIII	**EVOLUTION AND ASSEMBLY OF THE PENNSYLVANIA-DELAWARE PIEDMONT**, Crawford, M.L. and Crawford, W.A., eds.
1990 GANJ VII	**ASPECTS OF GROUNDWATER IN NEW JERSEY**, Brown, J.O. and Kroll, R.L., eds.
1989 GANJ VI	**PALEOZOIC GEOLOGY OF THE KITTATINNY VALLEY AND SOUTHWEST HIGHLANDS AREA, NEW JERSEY**, Grossman, I.G., ed.
1988 GANJ V	**GEOLOGY OF THE CENTRAL NEWARK BASIN**, Husch, J.M. and Hozik, M.J., eds.
1987 GANJ IV	**PALEONTOLOGY AND STRATIGRAPHY OF THE LOWER PALEOZOIC DEPOSITS OF THE DELAWARE WATER GAP AREA**, Gallagher, W.B., ed.
1986 GANJ III	**GEOLOGY OF THE NEW JERSEY HIGHLANDS AND RADON IN NEW JERSEY**, Husch, J.M. and Goldstein, F.R., eds.
1985 GANJ II	**GEOLOGICAL INVESTIGATION OF THE COASTAL PLAIN OF SOUTHERN NEW JERSEY**, Talkington, R.W. and Epstein, C.M., eds.
1984 GANJ I	**IGNEOUS ROCKS OF THE NEWARK BASIN: PETROLOGY, MINERALOGY, AND ORE DEPOSITS**, Puffer, J.H., ed.

ABSTRACTS

Control Of Fractured Bedrock Structure On The Movement Of Chlorinated Volatile Organics In Bedrock And Overburden Aquifers, Newark Basin Of New Jersey

Robert M. Bond, PG and Katherine E. Linnell, PG
Langan Engineering and Environmental Services, Inc., Doylestown, Pennsylvania, USA.

We have developed a conceptual model of groundwater flow and contaminant migration in the Passaic Formation and overlying Rahway Till in the Newark Basin of New Jersey as part of a remedial site investigation at a former industrial facility in Middlesex County. Historic releases of chlorinated volatile organic compounds (CVOCs) have caused groundwater contamination in overburden and bedrock that extend up to 4,200 feet downgradient and have affected surface water quality. Our conceptualization of bedrock structure and groundwater flow generally follows the dipping multi-layered leaky aquifer system model. We have mapped out major bedding partings and characterized fracture zones that control the migration of dissolved contaminants in the bedrock aquifer using rock coring, analytical sampling, groundwater elevation data, packer testing, acoustic televiewer logging, and other downhole geophysical techniques. The bedrock in the area of investigation includes the Metlars, Livingston and Kilmer members of the Passaic Formation. The lithology is generally described as red mudstones with intervals of purple mudstone, the latter of which we used as marker beds to correlate boring logs.

The study area spans a slope-aquifer system from contaminant source areas located near a topographic high with strong downward hydraulic gradients to a receiving stream at the base of the slope. The discharge area is characterized by flowing artesian conditions in overburden and bedrock wells. We have found that major bedding-parallel water-bearing zones identified in multiple boreholes subcrop below the overburden as buried valleys, having been preferentially eroded because of structural weakness before and during the deposition of the Rahway Till. The geometry of the buried valleys controls the overburden groundwater flow direction, act as pathways for plumes and generally contain the highest concentrations of CVOCs. In recharge areas, the most elevated CVOCs in the overburden groundwater therefore drain, in part, directly into the major bedding-parallel water-bearing zones of the bedrock aquifer. The contaminant distribution in bedrock indicates that the primary direction of groundwater transport from the source areas is along strike, however, significant down-dip transport has been observed. Impacts in bedrock have traveled at least 2,300 feet along strike within the water-bearing zones to the location of a potential near-vertical fracture zone or fault, which is a groundwater discharge zone. This fracture zone feature is expressed as a regional linear valley in the top of bedrock oriented roughly north-south, an orientation consistent with mapped faults in the area. In the current conceptual model, a steeply dipping north-south fracture zone would intercept groundwater flow and be generally protective of aquifer use areas to the west. We continue to investigate this site to complete delineation of the impacts in the bedrock aquifer and assess remedial options.

A Beginners Guide to the Geology and Landscapes of the New Jersey Piedmont

Dr. Richard L. Kroll
Department of Geology and Meteorology, Kean University, Union, New Jersey

The New Jersey portion of the Piedmont Province is characterized by a broad lowland to the east that is interrupted by ridges to the west. The lowland is underlain by relatively soft and easily erodable sedimentary rocks of the Newark Supergroup and the ridges are formed of basalts and diabases. Three basalt formations (Orange Mountain, Preakness , Hook Mountain) are interlayered with sedimentary formations (Passaic, Feltville, Towaco, Boonton). The more resistant basalts form the ridges that stretch from near the New York-New Jersey state line, south for approximately 40 miles to the Somerville area. The ridges are known as the First and Second Watchung Mountains, and Hook Mountain. Given their structural tilt to the west and the resulting alternating exposures, the basalts form ridges separated by intervening valleys. The westerly tilt, in combination with columnar structures in the basalts, form ridges with steep easterly edges and gently tilting westerly slopes. A gentle fold causes the ridges to curve to the west and northwest in the Somerville area.

Numerous steep sided, NW-SE trending valleys (gorges?) cut through the First Watchung Mountain (Orange Mountain Basalt), and are probably the result of minor fault phenonomena. These cuts provided transportation access routes for the earliest colonists and are still the major east-west access routes.

The most prominent diabase body, the Palisades Sill, forms the west shore of the Hudson River. The Palisades are formed by the west tilting columnar structures that provide the dramatic east-facing cliffs.. Smaller diabase bodies, probably southerly extensions of the Palisades Sill, form ridges and hills south of the Somerville area such as Sourland Mountain and Rocky Hill.

Interrupting the general north south grain of the topography is the east-west trending Wisconsin Terminal Moraine. In places it is barely noticeable, but in other places it forms a significant topographic feature and is partly responsible for forming the Great Swamp. Other glacial deposits provide a variety of topographic landforms.

An exercise in topographic profiling and sketching a geologic cross-section is included.

Trace fossils from the Newark basin of New Jersey and southeastern Pennsylvania

Robert Metz
Department of Geology and Meteorology, Kean University, Union, New Jersey 07083, rmetz@kean.edu

Strata representing largely lake-shoreline deposits of the Upper Triassic Passaic Formation and Lower Jurassic Towaco formation of New Jersey and southeastern

Pennsylvania have yielded an assemblage of trace fossils. Dominated by burrowing forms and represented by the *Scoyenia* ichnofacies, specimens include: *Cochlichnus anguineus, Didymaulichnus lyelli, Helminthoidichnites tenuis, Helminthopsis hieroglyphica, Mermia carickensis, Palaeophycus alternatus, Palaeophycus tubularis, Planolites annularis, Planolites beverleyensis, Scoyenia gracilis, Spongeliomorpha milfordensis, Treptichnus bifurcus, Treptichnus pollardi,* paired trails, insect trackway, as well as scratch circles.

Reddish brown, sporadically green siltstones and mudstones, and gray claystones have produced all of the trace fossils. Where trace fossils are found to be diverse and abundant, field evidence indicates that a variety of paleoenvironments including lake-margin, very shallow water, and floodplains with their ephemeral puddles and ponds offered optimum conditions for feeding and tracemaking by insects and arthropods. These deposits were later subject to periodic desiccation alternating with fine-grained sediment influx during rainstorms, favoring trace preservation.

Genetic Classification of Mesozoic Copper Deposits of New Jersey using Contemporary USGS and CGS Criteria

JOHN H. PUFFER and GEOFFREY E. GRAHAM
Department of Earth and Environmental Science, Rutgers University, Newark, NJ 07930
jpuffer@andromeda.rutgers.edu

Reexamination of several Mesozoic copper mines including some key exposures of mineralized diabase breccia plus some new geochemical data has lead to a clearer understanding of the genesis of these deposits.

The Palisades diabase sill intruded into unconsolidated Mesozoic sand and silt that was saturated with brackish water. The diabase magma was contaminated with this water until it was expelled during cooling. Copper leached from cooling diabase magma was carried to the surface via an epithermal hot spring system where it precipitated on solfataras and in mud under shallow ponds. These copper concentrations were quickly buried under Orange Mountain basalt that was extruding while the co-magmatic sill was intruding. Most of the copper deposits of New Jersey, such as the Bound Brook and Somerville deposits, are found in the resulting hornfels at the base of the basalt flow. Some additional copper deposits, such as the Schuyler and Flemington deposits, are found in hornfels around the margins of shallow diabase offshoots of the Palisades sill and in explosion breccias where these offshoots intruded into wet sediment. Hot brine-water leached additional copper from cooling basalt flows where it precipitated in flow-top amygdule deposits, such as the Hoffman mine, and may have contributed to the basal hornfels deposits. A few minor New Jersey deposits are found in gray beds where some copper has precipitated around carbonized plant remains.

Most New Jersey copper deposits are typical of those designated by the United States Geological Survey as “Basaltic Cu” such as the Denali, Alaska and Keweenaw, Michigan deposits; and of those designated by the Canadian Geological Survey as “Volcanic Redbed Cu” such as the Sustut, British Columbia and Buena Esperanze, Chile deposits. The few minor New Jersey occurrences associated with carbonized plant remains qualify as USGS “Redbed Cu” or CGS “Redbed-type”.

Structure Of The Hopewell Fault, North Segment, Belle Mead, Nj

Stephen E. Laney, CPG 7519

The central part of the Hopewell fault in New Jersey forms an arcuate scarp extending from near Hillsborough on the north end to near Harbourton at the southwest end. The Hopewell Fault has been typically characterized as being a normal fault structure, juxtaposing the Passaic formation hanging wall against the older Lockatong and Stockton formations footwall. Mapping conducted near Belle Mead, NJ indicates that the fault zone is a shear zone at least 500 feet wide. Four areas within the fault zone were studied. The innermost part of the exposed deformation in the footwall consists of large-scale drag folding and reverse faulting, the middle part by a dextral strike-slip zone and the outer part by a heavily brecciated zone. The hanging wall consists of relatively undeformed mudstone. Brittle deformation dominates the shear zone, but brittle-ductile features are common. This is the first field evidence of right-lateral movement on the fault.

Joints and Veins in the Newark Basin, New Jersey In Regional Tectonic Perspective

Gregory C. Herman
N.J. Geological Survey, P.O. Box 427, Trenton, N.J. 08625
greg.herman@dep.state.nj.us

Late Triassic and Early Jurassic bedrock in the Newark basin is pervasively fractured as a result of early Mesozoic rifting and subsequent wrench faulting of the eastern North American margin. Systematic sets of tectonic extension fractures, including ordinary and mineralized joints, are arranged in structural arrays having the geometry of normal dip-slip shear zones. Together with complimentary sets of cross fractures, they contributed to crustal stretching, sagging, and eventual faulting of the thick pile of basin rift deposits. Extension fractures developed during rifting stages of the basin display progressive linkage and spatial clustering that probably controlled incipient fault growth. They cluster into three prominent strike sets correlated to early- (S1, about 30^{o}E to N60^{o}E), intermediate- (S2, about N15^{o} to N30^{o}E), and late-stage (S3, about N-S) stretching events in the basin. Extension fractures display three-dimensional spatial variability but consistent geometric relations. S1 fractures are unevenly distributed throughout Late Triassic sedimentary strata and occur in conjunction with border faults and subparallel segments of intrabasin faults. They are locally folded normal to bedding owing to sedimentary compaction during lithification and show complex vein and vein-cement morphologies. They also show geometric interaction with subsequent S2 extension fractures. Such fractures parallel Early Jurassic igneous dikes around the SW part of the basin and cut Early Jurassic basalt and diabase farther to the NE in New Jersey. S2 and S3 fractures locally terminate against preexisting S1 fractures and commonly have fibrous-calcite vein cements in the Passaic Formation. S2 fractures are most pervasive in

intrabasin fault blocks in conjunction with subparallel fault segments of the Flemington, Hopewell, and New Brunswick fault systems. The S2 extension phase marks a period of accelerated stretching and large-scale faulting of Early Mesozoic strata with highest strains in the center of the basin. S2 fractures are transitional in orientation to S3 extension fractures that cluster near tip lines of intrabasin faults in the NE. S3 fractures locally terminate against both earlier sets. Other sets of prominent, E-W striking S3 extension fractures are aligned across strike at high angles to all earlier sets. These cross fractures (S3C sets) formed late in areas where block faults with S2 transform and oblique normal slip components were inverted with opposing slip during later crustal compression and uplift of the continental margin. Both S2 and S3 phase brittle faults extend into and involve surrounding bedrock of the older continental interior and younger oceanic margin. The geometry, spatial distribution, and morphology of the extension fractures indicate progressive counterclockwise rotation of the regional, principal extension axis from NW-SE during the Late Triassic to E-W after the Late Cretaceous. S3 fractures record late stages of crustal stretching followed by compression oriented subparallel to the contemporary principal stress axis.

An Interpretative Analysis Of The Sedimentary Fabric Represented In An Approximately 84-Meter Core Recovered From The Passaic Formation In Central-Eastern, New Jersey

John A. Anton
Hudson Environmental Services, Inc., 4 MARK ROAD, SUITE C, Kenilworth, New Jersey 07033

An interpretative analysis of sedimentary fabric recorded in an 84-meter core recovered from the Passaic Formation in Rahway, Union County, New Jersey was performed to reconstruct the represented paleoenvironments. This locality is situated proximal to the northeastern margin of the Triassic-Jurassic continental rift complex known as the Newark Basin and well described due to its exceptional documentation of geological history. The core is primarily composed of alternating shale and siltstone beds that indicate generally coarsening upward sequences characteristically associated with fluctuating water levels in lacustrine settings and prograding fluvial systems. Paleosol (e.g., brecciated mudcracks, root casts, reworked gypsum soil) and fluvial depositional features (e.g., laminae) served as marked indicators of pronounced ecological shifts in response to rift activity. Downhole geotechnical methodologies (e.g., gamma ray, electrical resistivity, etc.) were applied following core recovery to identify subtle lithologic variation and depositional cycles.

TABLE OF CONTENTS

TECHNICAL REPORTS

FIELD GUIDE

Genetic Classification of Mesozoic Copper Deposits of New Jersey using Contemporary USGS and CGS Criteria

JOHN H. PUFFER and GEOFFREY E. GRAHAM Department of Earth and Environmental Science**,** Rutgers University**,** Newark, NJ 07930
jpuffer@andromeda.rutgers.edu

ABSTRACT

Reexamination of several Mesozoic copper mines including some key exposures of mineralized diabase breccia plus some new geochemical data has lead to a clearer understanding of the genesis of these deposits.

The Palisades diabase sill intruded into unconsolidated Mesozoic sand and silt that was saturated with brackish water. The diabase magma was contaminated with this water until it was expelled during cooling. Copper leached from cooling diabase magma was carried to the surface via an epithermal hot spring system where it precipitated on solfataras and in mud under shallow ponds. These copper concentrations were quickly buried under Orange Mountain basalt that was extruding while the co-magmatic sill was intruding. Most of the copper deposits of New Jersey, such as the Bound Brook and Somerville deposits, are found in the resulting hornfels at the base of the basalt flow. Some additional copper deposits, such as the Schuyler and Flemington deposits, are found in hornfels around the margins of shallow diabase offshoots of the Palisades sill and in explosion breccias where these offshoots intruded into wet sediment. Hot brine-water leached additional copper from cooling basalt flows where it precipitated in flow-top amygdule deposits, such as the Hoffman mine, and may have contributed to the basal hornfels deposits. A few minor New Jersey deposits are found in gray beds where some copper has precipitated around carbonized plant remains.

Most New Jersey copper deposits are typical of those designated by the United States Geological Survey as "Basaltic Cu" such as the Denali, Alaska and Keweenaw, Michigan deposits; and of those designated by the Canadian Geological Survey as "Volcanic Redbed Cu" such as the Sustut, British Columbia and Buena Esperanze, Chile deposits. The few minor New Jersey occurrences associated with carbonized plant remains qualify as USGS "Redbed Cu" or CGS "Redbed-type".

PRODUCTION AND DEVELOPMENT HISTORY

Lewis (1907) summarized the production and development of the New Jersey copper mining industry during its declining years of activity. "Since early in the eighteenth century the copper deposits of New Jersey have attracted more or less attention, and have been the objects of repeated attempts to mine and smelt them. From time to time, however, one locality or another has been taken up, some of the old

workings reopened and perhaps a little additional work done, only to be abandoned again after a few months or a few years. Such, in brief, has been the history of the New Jersey copper industry for nearly two centuries." Lewis (1907) goes on to say "Whether or not any of these mines shall ever again prove commercially profitable, they constitute an exceedingly interesting example of a class of ore-deposits, and are of considerable importance in investigating the principals of their origin." Since 1907 none of these mines ever proved commercially profitable but we agree with his recognition of their importance.

GEOLOGIC SETTING

All of the larger Mesozoic Cu mines of New Jersey are found along the upper or lower contact of the Orange Mountain Basalt or near thin early Jurassic dikes and sills that intrude the Passaic Formation (Figure 1). Copper ore is most commonly found in: 1) Passaic hornfels within 1 m below the base of the Orange Mountain Basalt; 2) Passaic hornfels within 1 m above or below thin shallow dikes or sills of Orange Mountain composition and; 3) in Orange Mountain Basalt within 2 m above the base of the first flow or within 1 m below flow tops. A few minor copper occurrences are found in the unmetamorphosed red-beds of the Passaic Formation.

The Orange Mountain Basalt consists of three flows that together measure about 180 m thick. The Orange Mountain Basalt is a subaerial continental flood basalt but is locally pillowed where it extruded into shallow brackish ponds. The composition of the three flows is highly uniform although non-ore Cu concentrations range from 90 to 405 ppm averaging 127 ppm (Puffer, 1992). This compares to Cu concentrations in the unmineralized Preakness Basalt that overlies the Orange Mountain, of 39 to 112 ppm averaging 63 ppm (Puffer, 1992).

The upper Passaic Formation that is the host-rock of most copper ore was deposited as lacustrian and fluvial sediment characterized by the effects of alternating Melankovich forced climatic cycles (Olsen, l986) that resulted in expansion and contraction of lakes across alluvial plains. In general, the water level of the lakes and depositional rates decreased during Passaic sedimentation then rapidly increased at the onset of volcanic activity (Olsen and others, l996). Calcium sulfate precipitation in the Passaic sediments and in amygdules in pillowed Orange Mountain Basalt indicates that the water was brackish.

The thermal metamorphic effect of the extrusion of the first flow of Orange Mountain flood basalt onto the Passaic sediments is highly variable. Although the flow was 70 m thick only 5 to 10 cm of gray hornfels was typically generated under the base of the flow. However, wherever copper mineralization is concentrated, the thickness of the hornfels

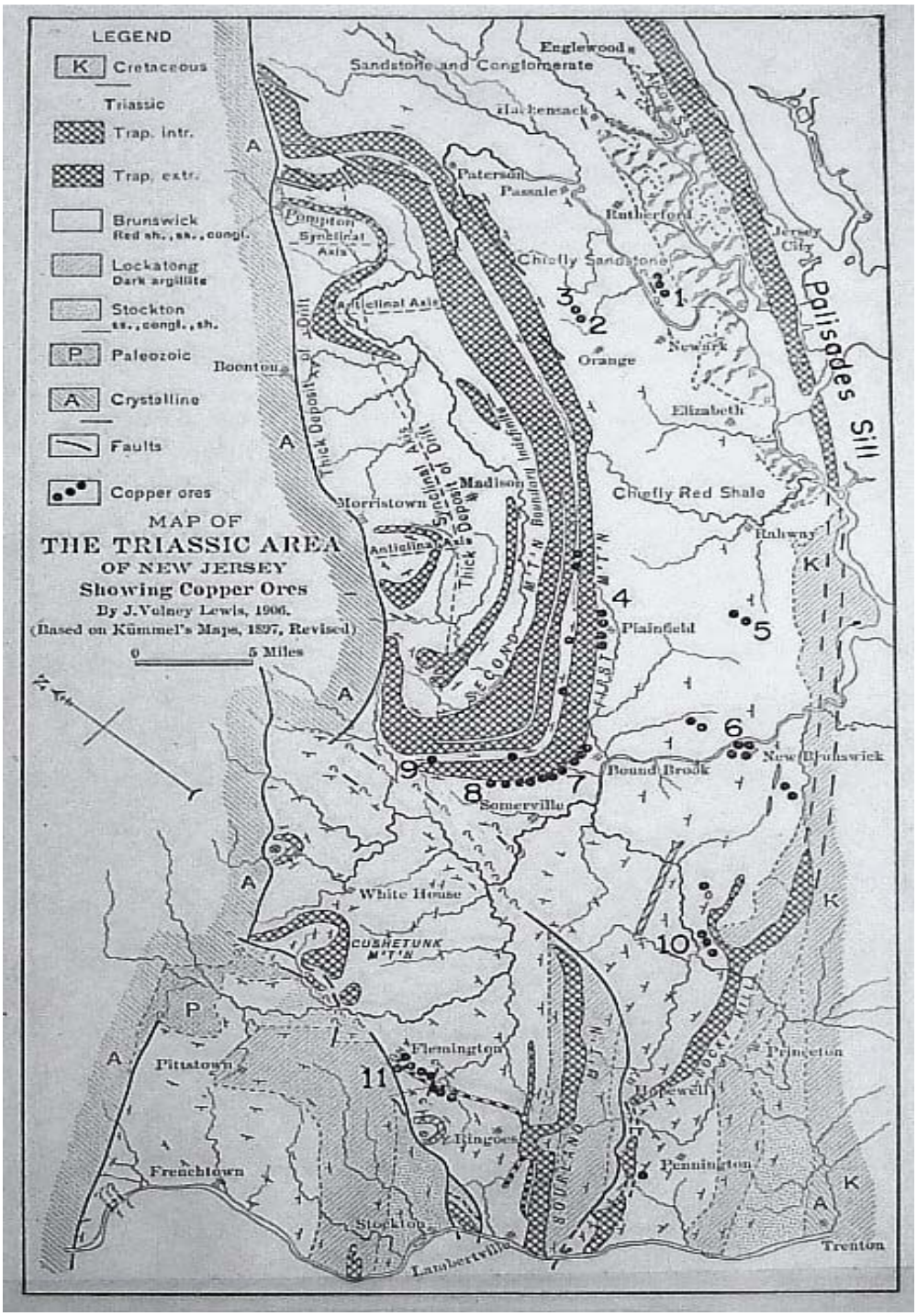

Figure 1. Copper deposits of the Newark Basin (after Lewis, 1907) with numbered locations: 1. Schuyler mine, 2. Dod mine, 3. Glen Ridge Mine, 4. Stony Brook mine, 5. Menlo Park mine, 6. New Brunswick mine, 7. Chimney Rock mine, 8. American (Bridgewater) mine, 9. Hoffman mine, 10. Griggstown (Franklin) mine, 11. Flemington mines.

increases to about one to two meters and local salt fluxing has resulted in a few occurrences of sediment fusion (Puffer and others, l993).

COPPER MINES

Lewis (1907) indicated 29 copper mine locations on a geologic map of New Jersey (Figure 1), and grouped them into four categories:

Category 1. Those associated with "altered sedimentary rock" (hornfels) near the foot-wall contact of a west dipping 17 m thick diabase dike.

The Grigstown (Rocky Hill, or Franklin) mine

Category 2. Those associated with sedimentary rocks intersected by small diabase intrusions.

The Arlington (Schuyler) mine

The Flemington mines (three)

Category 3. Those found along the upper and lower contact of basalt flows (Orange Mountain Basalt).

The Pluckamin (Hoffman) mine at the upper contact

The Somerville mines (five mines along the lower contact)

The Bound Brook mine at the lower contact

The Plainfield mines (three mines along the lower contact)

Four unnamed mines along the upper contact

Category 4. Those found in sedimentary rock (Passaic Formation) locations that are not close to known exposures of igneous rock.

The New Brunswick mines

The Glen Ridge mines (three)

The Newtown silver occurrence

Each of these mine locations have been visited by the principal author of this report (except for Glen Ridge, Newtown, and four of the mines along the upper Orange Mountain contact). In most cases there is very little that remains today (2005) of the former working except for occasional samples of discarded ore and host-rock. In the case of the Glen Ridge and Newtown mines there is no trace of former workings. However, the underground workings at the Schuyler mine were examined on several occasions during 1970-1975 by the principal author. Good exposures of ore and country rock are still accessible, although the underground workings have been sealed off. Good exposures of ore and country rock are also still accessible at the Somerville mines, particularly the American Mine.

Although descriptions of individual mines can be found in several sources the most comprehensive descriptions were written by Lewis (1907) when some of them were still in development. The following mine descriptions, therefore, draw heavily on the observations of Lewis (1907) together with additional first hand observations made by the authors of this report.

Lewis Category 1: The Griggstown (Rocky Hill) mine

"It is said that 160 Welsh miners were employed in the mine at one time before the Revolutionary War, and that considerable ore was concentrated and shipped to

England." (Lewis, 1907). The principal shaft was 190 feet deep and a drainage tunnel 1080 feet long was developed (Lewis, 1907). The host rock was described by Lewis (1907) as "shale" that was "dark purple to black with chlorite nodules up to an inch across". This dark purple "shale" is more accurately described as a hornfels and is typical of New Jersey copper ore. The hornfels lacks bedding or cleavage and is a meta-argillite. Lewis (1907) reported that the ore veins consist of chalcocite that "occurs in fissures and brecciated zones in the hard, flinty hornstone"

Lewis Category 2:

The Arlington (Schuyler) mine

The Schuyler mine is the oldest mine in New Jersey and was probably the first copper mine operated in America. It was discovered early in the eighteenth century, probably about 1719, and a shipment of 110 casks of ore from New York in 1721 was probably the first exported from this mine. About 200 laborers were employed in the mine and mills (Lewis, 1907).

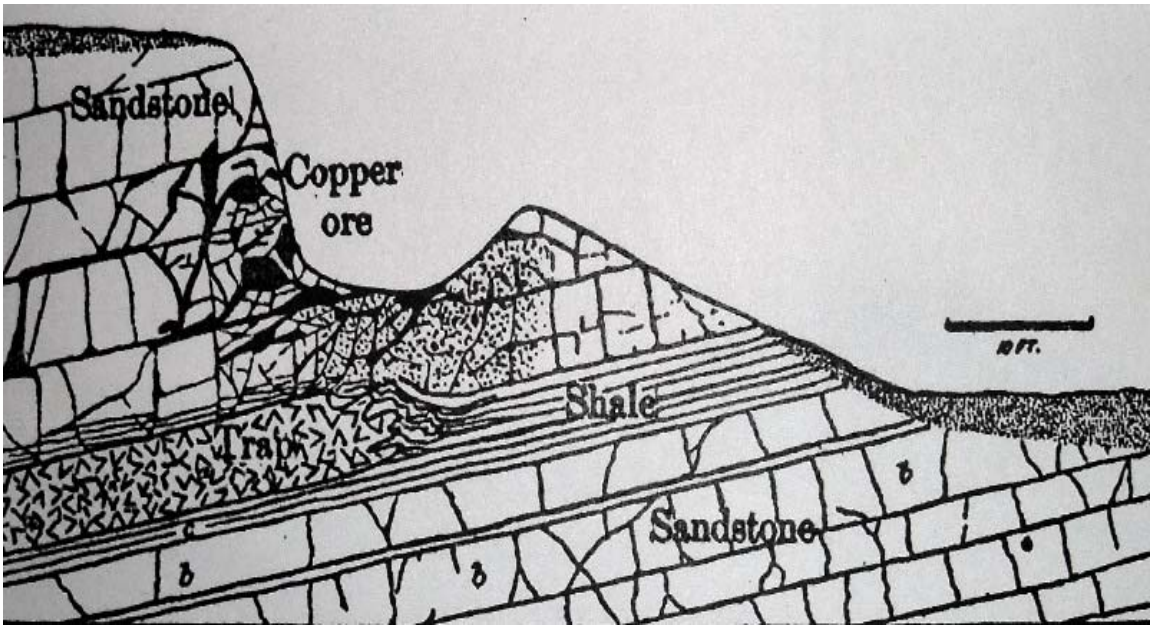

Figure 2. Cross section through the Schuyler copper mine (after Darton 1902) illustrating relationship of copper ore to thin veins of fine grained diabase (black) over diabase sill (labeled trap) intruded into Passaic shale. Stippled area at the termination of the trap sheet is explosion breccia.

The "Victoria shaft" is reported to be 347 feet deep (Lewis 1907) and an extensive network of underground working were developed, some of which consist of adits dug into the east slope of the hill upon which the town of Arlington is located. Some of these adits were accessible until the early 1970s and were explored on several occasions by the principal author before being sealed off. The ore consists of chalcocite together with minor native copper, cuprite, malachite, and chrysocolla. Lewis reports that "The chalcocite is found chiefly in branching veins and seams in the sandstone near the small dikes and in the frequent fault breccias of sandstone and trap." However upon

Figure 3. Explosion breccia exposed at the termination of the diabase sill intruded into the Passaic Formation at the Schuyler mine consisting of fine grained diabase clasts in a matrix of sand mineralized with chalcocite. US 25 cent coin for scale.

Figure 4. Explosion breccia sampled at the Schuyler mine consisting of diabase clasts in copper enriched sandstone.

Table 1.
Chemical composition of diabase from Schuyler mine compared with average Orange Mountain basalt and Palisades chill zone

Name	Schuyler	Orange Mt.	Palisades
	sill	flow	lower CZ
I.D.	S-1		80B-1
Samples	1	av. 11	1
Weight percent normalized to 100 percent anhydrous			
SiO_2	49.81	52.68	55.4
TiO_2	1.26	1.12	1.05
Al_2O_3	14.26	14.25	14.27
FeO_t	10.74	10.15	8.92
MnO		0.18	0.16
MgO	5.93	7.81	6.6
CaO	9.13	10.80	9.09
Na_2O	2.6	2.45	1.74
K_2O	0.43	0.43	0.64
P_2O_5		0.13	
LOI	2.87	0.00	
total	97.03	100.00	97.87
ppm			
Cu	1910.0	127.0	100.0
Zn	420.0	85.0	80.0
Pb	9.0	6.0	
Rb	9.0	15.0	26.0
Ba	94.0	119.0	134.0
Sr	145.0	192.0	160.0
Th	2.2	2.0	1.5
Zr	95.0	99.0	108.0
Hf	2.8	2.4	2.1
Nb	7.2	6.9	
Ni	50.0	99.0	48.0
Cr	240.0	309.0	229.0
La	10.2	10.2	9.0
Ce	22.7	22.1	20.5
Nd	12.5	11.8	10.3
Sm	3.4	3.4	2.8
Eu	1.2	1.1	1.0
Tb	0.6	0.6	0.5
Yb	2.2	2.1	1.8
Lu	0.3	0.3	0.3
Y	21.0	20.4	17.0

Note. Schuyler data is new analyses of a black unweathered fine-grained diabase sample by Jeffery Steiner and Karen Block of City College of New York, Orange Mountain data after Puffer (2001), Palisades data after Sherley (1987) except for Cu, Y, Zn, and Zr from same sample after Gottfried et al. (1991).

careful observation, the common breccia interpreted by Lewis as a "fault breccia" is actually an explosion breccia or breccia pipe confined to the margins of the thin diabase sill that terminates at the mine. There is no field indication of faulting at the mine that intersects the breccia ore. Lewis (1907) also observed that "…the (diabase) sheet also sends several offshoots up into the sandstone". Some of these thin offshoots are extremely thin, (2-5 cm) and penetrate the highest grade ore (Figure 2). They are very fine grained and were probably intruded into wet mud at shallow depths. The explosion breccia (Figures 3 and 4) that surrounds the termination of the sill is evidence of wet sediment.

Most ore recovered at the Schuyler mine consisted of hornfels along the upper contact of the diabase sill (Figure 5).

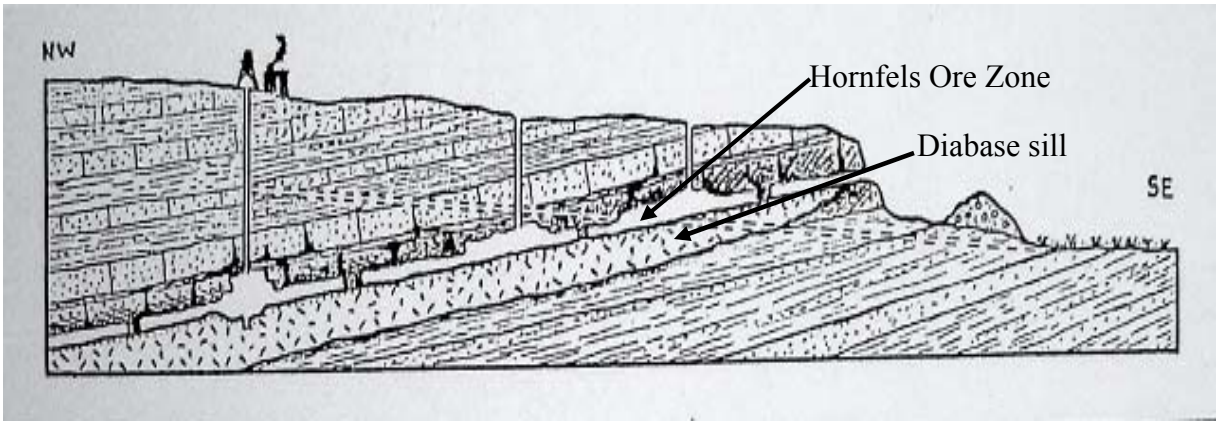

Figure 5. Cross section through the Schuyler mine (after Woodward, 1944). The mine workings followed the upper contact of the thin Arlington sill.

A black, unaltered, fine grained sample of diabase from the Schuyler mine was chemically analyzed by Steiner and Block at The City College of New York (Table 1). The immobile and insoluble Rare Earth Element content of the diabase is almost identical to average Orange Mountain basalt (Puffer, 2001) and closely compares with the Palisades diabase chill zone indicating a co-magmatic relationship. However, the Cu, Zn, and Pb contents of the Schuyler diabase are highly enriched and the sodium content elevated compared with Orange Mountain basalt and Palisades diabase (Table 1). The Schuyler diabase does not appear to have undergone any fractionation but is hydrated and has been slightly depleted in some of its most water soluble components (Ca, Mg, Table 1). If, as is probable on the basis of elevated sodium content (Table 1) and the brackish environment of deposition of the country rock (Olsen et al, 1996), this hydration included unanalyzed chlorine and sulfur, the copper content could have been stabilized by these ligands until water saturation levels were reached during cooling and dehydration. Similar processes are probably responsible for most of Earths copper ore deposits.

The Flemington mines

Lewis (1907) reports that "The ore was found in partly altered brownish-red and purplish shales in the vicinity of trap dikes." However, again, the purplish "shale" is a

hornfels. The ore was described by Professor H.D. Rogers of Philadelphia to Lewis (1907) as "… intimately blended or incorporated with the semi-indurated and altered sandstone, and the mass has therefore somewhat the aspect in certain portions of a conglomerate of recemented fragments, the metalliferous part being the cement." Roger's description of "recemented fragments" resemble breccia samples of Flemington ore observed by the principle author consisting of hornfels clasts cemented with chalcocite with minor cuprite chrysocolla, and malachite. We agree with both Lewis (1907) and Woodward (1944) who suggests that the Flemington mines closely resemble the Schuyler mine.

Lewis Category 3:

The Somerville (Bridgewater / American) mines

According to Lewis (1907) "Active work was again begun in 1821 and continued more or less intermittently at many points from this mine (Bridgewater) southeastward to Chimney Rock, a distance of 4 miles, during the next two decades" He continues "...drifts were run into the mountain side (First Watchung) along the contact of the trap and the underlying shales." At the Somerville mines the ore consists of disseminated nuggets of native copper partially altered to cuprite together with chalcocite (Figure 6). The basalt-Passaic contact is well exposed and samples of ore are still easily obtained at several locations along this 4 mile (7 km) series of discontinuous outcrop through Somerville.

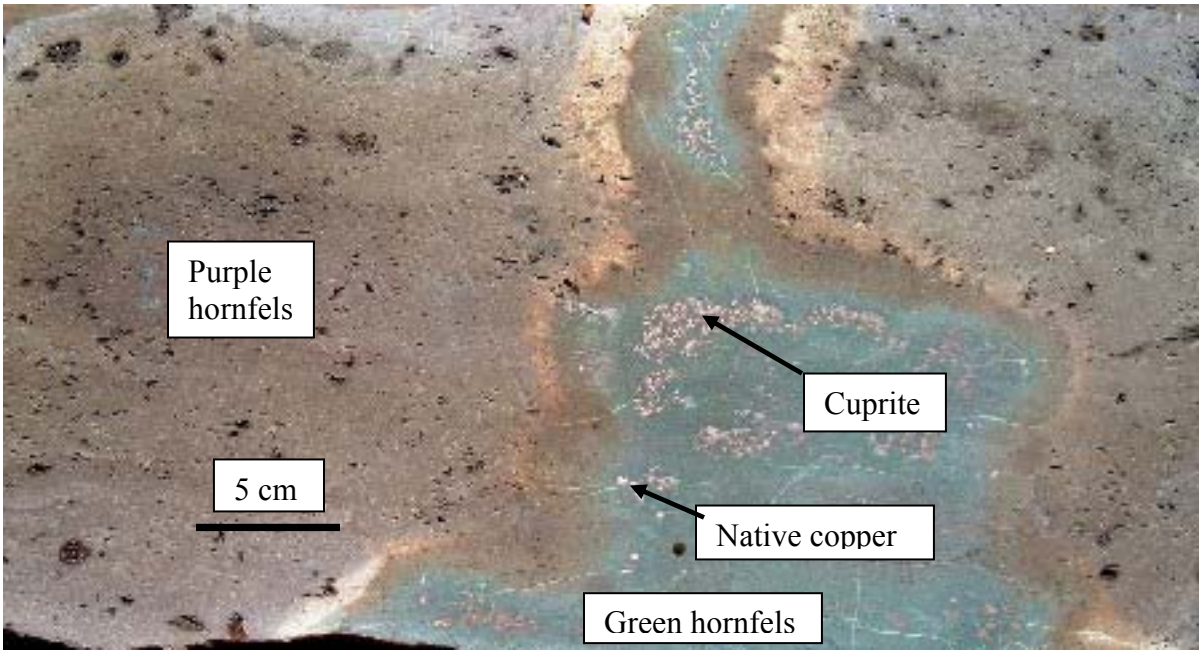

Figure 6. Ore sample collected at the American mine consisting of purple, porous, but impermeable hornfels (meta-mudstone) completely devoid of any bedding containing bleached amoeboid shaped structures consisting of green chlorite rich hornfels mineralized with native copper and cuprite with minor chalcocite. Chemical analyses of purple and green hornfels from this sample appear in Table 2.

The ore zone is fine grained, with no bedding, and is best described as an argillite hornfels (Figure 6). A mine map of the American mine formerly known as the Bridgewater mine (Figure 7, after Lewis, 1907) indicates the confinement of the ore to the vesicular base of the first Orange Mountain flow and the hornfels within 1.0 m below the flow. The American Mine ore-body at Somerville is also described in some detail by Reiff and Bond (1902) and Cattafi et el (1998).

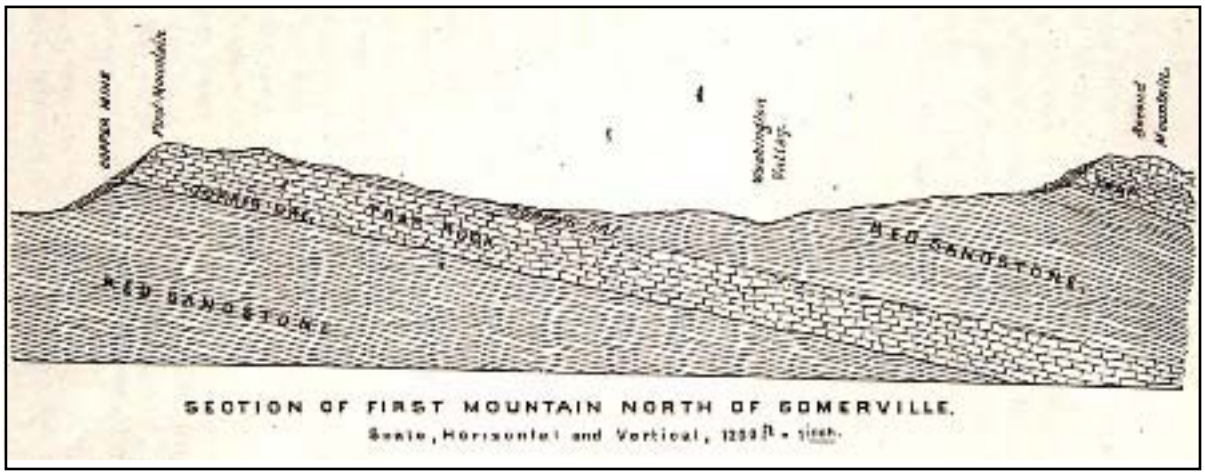

Figure 7. Idealized section through copper mines north of Somerville after Lewis (1907) illustrating confinement of ore to the contacts of the "First Mountain" Orange Mountain basalt.

Table 2.

Chemical composition of rocks from the American Copper Mine, New Jersey
Data after Cattafi et al., (1998)

	Redbed 15 m below ore	Purple hornfels at ore zone	White hornfels at ore zone	Green hornfels at ore zone	Orange Mt basalt m above ore zon
SiO2	61.23	52.56	42.2	37.42	51.87
TiO2	0.97	1.02	0.74	0.73	1.09
Al2O3	18.1	15.49	20.05	8.31	14.12
FeOt	6.11	11.36	6.41	3.45	10.1
MgO	3.59	8.14	7.32	4.86	7.71
CaO	0.29	0.38	5.96	0.56	10.68
Na2O	1.57	7.1	4.32	3.68	2.41
K2O	2.66	0.22	0.29	0.13	0.39
P2O5	0.05	0.16	0.17	0.17	0.14
LOI	5.12	2.67	6.98	32.3	1.29
Cu	0.01	0.08	2.83	6.85	0.01
total	99.7	99.18	98.27	98.46	99.81
ppm					
Cu	62	839	28341	68529	125
Zn	141	150	119	121	84
Sr	209	127		65	190
Zr	259	129		64	101
Ni	73	94			97

Mines at Plainfield and Chimney Rock

The mines near Plainfield and at Chimney Rock are similar to those at Summerville. Chimney Rock is currently a major trap quarry where large sheets of native copper are easily collected in the Passaic hornfels in contact with the Orange Mountain basalt and in unaltered joints in the basalt within 2 m above the contact (Figure 8). Small sheets of native silver have also been found here.

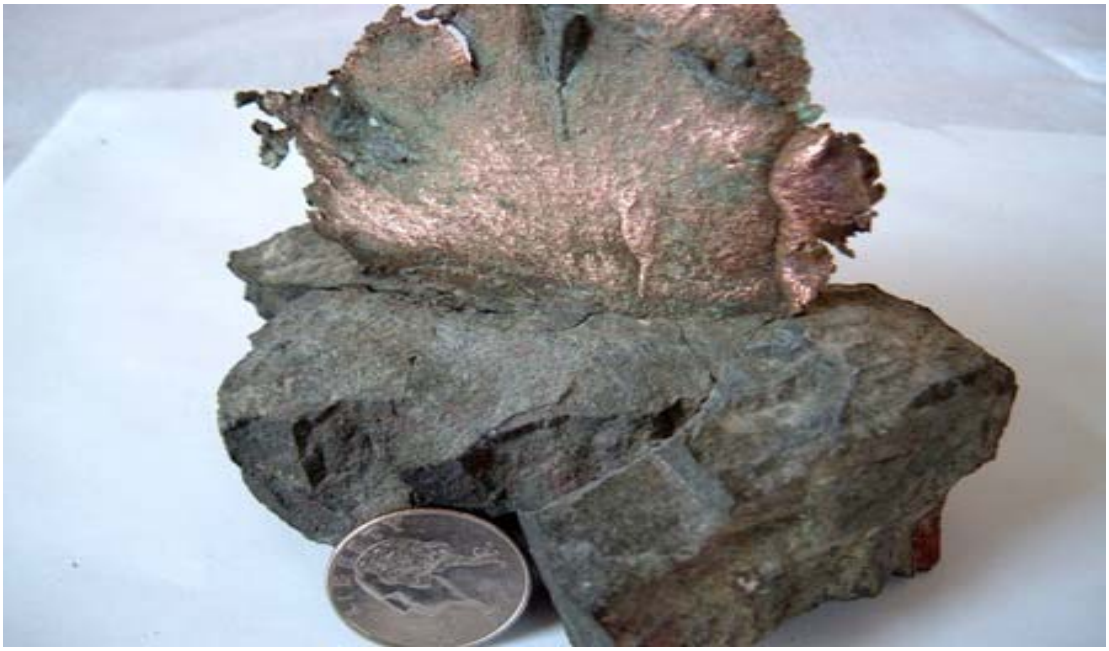

Figure 8. Sheet of native copper in basalt joint sampled at Chimney Rock.

Back of First Mountain (Hoffman mine)

According to Lewis (1907) the ore at the Hoffman mine is 4 feet thick consisting of chalcocite with some native copper and malachite in both Feltville Formation sandstone and in brecciated and vesicular Orange Mountain flow top basalt. Presumably the ore in the Feltville sandstone was eroded from underlying basalt.

Lewis Category 4:

New Brunswick mines (French and Raritan)

French mine - According to Lewis (1907) "About 1748 to 1750 many lumps of native copper weighing from 5 to 30 pounds each, upwards of 200 pounds in all, were plowed up in the field of Philip French, now Neilson Campus of Rutgers College, at New Brunswick. A company was formed to mine for copper in 1750 and work was begun by sinking a shaft the following year. A stamp-mill was erected and many tons are said to have been shipped to England." Lewis (1907) go on to say "…copper is found in a zone

of bleached grayish shale and in spots of gray mottled with the normal red color along an east-west fissure. The conditions are an exact duplicate of those found at Menlo Park… The usual red shales of the region were penetrated, with occasional purplish and sandy layers. The purple shales, which are also occasionally seen at the surface in this vicinity, may indicate the presence of intrusive trap at no great depth."

There is no trace of the original mine and native copper has not been recently plowed up at the campus of Rutgers, New Brunswick. However "purple shale" is the same description that Lewis (1907) applies to the hornfels at the American Mine and elsewhere. Proximity of copper ore to igneous intrusions is confirmed by Woodward (1944) who reports that small diabase dikes intrude the sedimentary rock near the mine and also reports the occurrence of "trap rock" in the mine dumps. Samples of ore from the Brunswick mine observed by the principal author are similar to Figure 6. The clear igneous association of the ore indicates that the French mine (and the Raritan mine) should be reclassified as Lewis category 2 mines

The Raritan mine - The Lewis (1907) description of the Raritan mine is about the same as New Brunswick mine. Lewis (1907) states the "The rock of these shafts lying at the mouth of the mine is mostly red and bluish shales. Very little trap was seen in these rubbish heaps." The ore was mostly malachite.

Menlo Park mine

Lewis (1907) interpreted the mineralization of the Menlo Park mine as controlled by a fault through the Passaic Formation. The ore was apparently very poor and no trace of copper mineralization is currently exposed there. Lewis (1907) states that "The fault-breccia, varying from 6 inches to 2 feet in thickness, and about 3 feet of each wall of the fissure are composed of the dark-gray, nearly black, soft shale referred to as carrying the ore". He goes on to state "Mr. Thomas A. Edison, who did some work here about twenty-five years ago (1881), writes in answer to an inquiry: 'The ores were too lean to pay. Of the streak we worked, which was about four feet wide, the average was about one-half percent'."

Glenn Ridge mines (Glen Ridge, Dod, Wigwam Brook)

Woodward (1944) states that three small copper mines once operated near what is now the city of East Orange. "These mines seem not to have been active since the 18th century, and are now scarcely more than historical relics. Their total production of ore was only a few hundred tons." (Woodward, 1944).

Glenn Ridge mine - Lewis (1907) states that "Traces of old workings are still to be seen at Glen Ridge, 4 miles northwest of Newark, in the area just east of the public school building. Chalcocite and chrysocolla are found penetrating and largely replacing bituminous plant remains in black glossy masses looking much like anthracite coal." He goes on to state that "No trap is known to occur here…"

Dod mine – The Dod mine located just south of the Glenn Ridge mine in East Orange (Figure 1) is not described by Lewis (1907) but was a minor deposit briefly described by Woodward (1944) that is also not associated with basalt or diabase.

Wigwam Brook mine – Woodward (1944) on the basis of an exhaustive compilation of all historical New Jersey copper mining records concludes with respect to the Wigwam Brook mine that "There is no evidence in the vicinity, nore in any available records, that any of these workings ever returned a reward"

Newtown silver occurrence

Lewis (1907) states that "Native silver in small scales and specks occurs in gray sandstone stained with chrysocolla on George Drake's farm at Newtown, 4 miles north of New Brunswick. Only surface specimens have been collected, and there has been no prospecting for ores."

LITHOLOGY

Samples from each of the named mines (except the Glen Ridge and Newtown ocurrences) have been examined on sight, typically at outcrops and mine dumps, by the principal author of this report and/or during examination of a large collection of New Jersey copper ore samples donated to Rutgers University, New Brunswick by Princeton University and subsequently donated to Rutgers University, Newark.

Of each of the ore samples (rocks containing at least 1 percent copper mineralization) examined by the principal author approximately 75 percent are hornfels, 10 percent are breccia from the Schuyler Mine and Flemington Mine, 5 percent are basalt from near the lower Orange Mountain contact, 5 percent are amygdaloidal basalt from the upper contact, and the remaining 5 percent are siltstones that do not appear to have been metamorphosed. Most ore (including the ore observed by Lewis, 1907) is found within the meter of Passaic meta-siltstone and meta-mudstone located directly below the Orange Mountain Basalt and within basalt within 15 cm above the contact. Lewis (1907) however, reported finding copper mineralization in siltstone located up to 5 m below the lower contact and in basalt up to 15 m above the lower contact.

MINERALOGY

Chalcocite, native copper, and chrysocolla are found in most ore samples together with minor malachite, and cuprite. Pyrite is a common gangue mineral in samples of hornfels and trace amounts of chalcopyrite is found in most samples of massive basalt. Chrysocolla is easily observed at most mine exposures, and flakes and sheets of native copper are readily observed in high grade samples. However, observation of disseminated chalcocite and native copper typically requires microscopic observation of polished sections. Cuprite is commonly found as a thin coating along joints through hornfels samples but is easily mistaken for hematite and requires testing for conformation. At the Somerville mine the ore is disseminated nuggets of native copper partially altered to cuprite in a purple hornfels (Figure. 6). At Chimney Rock sheets of native Cu are found in joints in basalt (Figure. 8) and in redbed shale both within 1 m of the contact. At the Schuyler mine chalcocite is finely disseminated in sand between fragments of diabase in a breccia (Figures 3 and 4).

GENETIC CLASSIFICATION

The United States Geological Survey and the Canadian Geological Survey have each published descriptions of mineral deposit models that include genetic classifications applying to most global ore deposits. The USGS models were compiled by Cox and Singer (1986) although modifications (including Cox et al. 2003) to some of the models have been made since 1986. The most recent comprehensive CGS list was published by Eckstrand et al (1995) although, again, some updates have been recently published. Models that might pertain to the Mesozoic copper deposits of New Jersey were screened from the USGS and CGS listings (Table 3) to include all models that 1) are related to mafic extrusive rocks and their intrusive counterparts and/or 2) are related to clastic sedimentary rocks.

Deposits related to subaerial mafic extrusive rocks (USGS Model 23 and CGS Model 9) were considered because most of the Watchung flows were subaerial flood basalts such as the host for most examples of the class.

Deposits related to marine mafic extrusive rocks (USGS Models 24a and 24b and CGS Model 6.3) were considered because some of the Orange Mountain basalt is pillowed where it flowed into brackish water bodies of unknown but probably shallow depth. In addition, the spreading center out of which the Orange Mountain and other CAMP flood basalts extruded, later developed into a marine basin.

Deposits related to subaerial felsic to mafic extrusive rocks (USGS Models 25a and 25b) were considered because the Orange Mountain basalt geochemically resembles andesite more closely than it resembles most global continental flood basalt (Puffer, 2001). The shallow explosion breccia at the Schuyler and Flemington mines also resembles the explosion breccia that is a characteristic of Model 25a and the Orange Mountain basalt has extruded over sedimentary rocks containing saline fluids near a normal fault system which is the principal characteristic of Model 25b.

Deposits in clastic sedimentary rocks (USGS Model 30b and CGS Model 8.3a and 8.3b) were considered because the Passaic redbeds are the host to most of the Mesozoic rocks of New Jersey.

Table 3.
USGS Mineral Deposit Models (Cox and Singer, 1986; Cox et al. 2003)

Deposits related to subaerial mafic extrusive rocks

Model 23 Basaltic Cu
Amygdaloidal basalt flow tops, native Cu, chalcocite, Keweenaw MI, Denali AK

Deposits related to marine mafic extrusive rocks

Model 24a Cyprus massive sulfide
Ophiolite assemblage, hot springs related to submarine volcanoes, Cyprus deposits

Model 24b Besshi massive sulfide
Clastic terrigenous sedimentary rocks and basalts, submarine hot springs, Besshi, Japan

Deposits related to subaerial felsic to mafic extrusive rocks

Model 25a hot-spring Au-Ag
Ore in shallow seams, veins, explosion breccia, and breccia dikes

Model 25b Creede epithermal veins
Andesites over sedimentary rocks containing saline fluids near normal fault system, Creede CO

Deposits in clastic sedimentary rocks

Model 30b.1 Sediment-hosted copper
General category of sediment-hosted deposits formed independently of igneous processes

Model 30b.2 Reduced-facies subtype
Reduced-facies (shales) interbedded with redbeds or subaerial basalt, Kuperschiefer-type

Model 30b.3 Redbed Cu
Permeable SS near plant debris, chalcocite, native Cu, Corocoro BLVA, Nacimiento and Stauber NM

Model 30b.4 Revett Cu
Bleached zones in deltaic SS near marine basin with oil & gas, chalcocite, Spar Lake MN

CGS Mineral Deposit Models (Eckstrand el al., 1995)

Exhalative base metal sulphides

Model 6.3 Volcanic-associated massive sulphide base metals
Marine volcanism with fine-grained sediments associated with faults, Noranda/Kuroko Canada

Sediment-hosted stratiform Cu

Model 8.3a Kupferschiefer-type
Reduced-facies (shales) interbedded with redbeds or subaerial basalt

Model 8.3b Redbed-type
Permeable SS near plant debris, chalcocite, native Cu, Corocoro BLVA, Nacimiento NM

Deposits related to subaerial mafic extrusive rocks

Model 9 Volcanic redbed copper
Amygdaloidal basalt flow tops, native Cu, chalcocite, Sustut Canada, Buena Esperanza Chile

Basis for choice of best fit model (USGS Basaltic Cu ~ CGS Volcanic Redbed Cu)

USGS Model 23 is approximately equivalent to CGS Model 9 and most of the same characteristics and examples are shared by each. Although as indicated in the previous section an argument could be made supporting any of several genetic models the Mesozoic copper deposits of New Jersey (Lewis Categories 1-3) share more characteristics with the Basaltic Cu / Volcanic Redbed Cu model than any other choice.

The essential characteristics of the Basaltic Cu / Volcanic Redbed Cu model are listed in Table 4 and compared with the Mesozoic Cu deposits of New Jersey. The comparison is not perfect and would require some modification for a perfect fit but the overlap is clear

Table 4.
Best Fit Model

	USGS Model 23 Basaltic Cu **CGS Model 9 Volcanic Redbed Cu**	**Mesozoic Cu Deposits of New Jersey**
Rock Types	Subaerial to shallow marine basalt, red-bed sandstone	Subaerial to shallow marine basalt, red-bed sandstone
Textures	Amygdules, flow-top breccias, sediments with high original porosity	Flow bottom joints, breccia pipes, sediments with high original porosity
Depositional Environment	Copper-rich (100-200 ppm) basalt interlayered with red clastic beds	Copper-rich (90-405 ppm) basalt interlayered with red clastic beds
Tectonic Setting	Intracontinental rift	Intracontinental rift
Ore Minerals	Native Cu, chalcocite	Native Cu, chalcocite
Gangue Minerals	hematite, quartz, chlorite, zeolites	hematite, quartz, chlorite, zeolites
Examples	Sustut BC (Wilson and Sinclair, 1988) Keweenaw MI (White, 1968) Denali AK (Seraphim, 1975) Buena Esperanza, Chile (Sillitoe, 1977)	
Genetic Controls	Metamorphic release of Cu-rich fluids from underlying volcanic rock. (White, 1968) Epithermal migration of Cu-rich fluids to solfataric vents (Sillitoe, 1977; Seraphim, 1975)	Leaching of Cu from diabase into epithermal hot-spring system with precipitation in explosion breccia and near solfataric vents, then buried under comagmatic basalt flows

Characteristics of "Basaltic Cu" deposits (Table 4) that apply to most or all of the Mesozoic Cu deposits of New Jersey include:
1.) Host rock is subaerial to shallow marine (brackish water) basalt and interbedded red-beds.

2.) Ore textures include precipitation in basalt amydgules and in adjacent sediments with high original porosity.
3.) Association of ore with copper-rich basalt (100-200 ppm) and interbedded red-beds.
4.) An intercontinental rift tectonic setting.
5.) A native copper – chalcocite ore
6.) A gangue of hematite, quartz, chlorite, and zeolites.

Characteristics of "Basaltic Cu" deposits that do not apply to most of the Mesozoic Cu deposits of New Jersey include:
1.) The flow-top breccia characteristic (Table 1) pertains to a few New Jersey deposits but not to the mines that are located at the base of the Orange Mountain basalt or to those associated with intrusive diabase.
2.) The New Jersey deposits differ in metamorphic history to some of the type-examples of the Basaltic Cu model
3.) The basaltic rock association clearly pertains to most New Jersey deposits but does not pertain to the Glen Ridge mines.

Modification of Basaltic Cu / Volcanic Redbed Cu model to accommodate some of the New Jersey deposits

The three New Jersey characteristics listed above that do not comply with the "Basaltic Cu" model require some modification of the model to accommodate some of the New Jersey deposits. These modifications are accomplished by incorporating aspects of USGS Model 24b (Besshi massive sulfide) and USGS Model 25a (Hot-spring Au-Ag). USGS Model 30b.3 (Redbed Cu) and CGS Model 8.3 (Redbed-type) may pertain to the Glen Ridge mines.

Application of Cyprus (USGS Model 24a) and Besshi (USGS Model 24b

The Cyprus massive sulfide model applies best to marine spreading centers over active ridges where ophiollites are forming such as the Cyprus ophiollite. The Besshi massive sulfide model applies best to basalts or andesites in a subduction zone setting such as Besshi Japan. In both cases mineralization is precipitated around marine hot-springs or black smokers.

Although none of the copper deposits of New Jersey are typical black smokers the deposits at the base of the Orange Mountain basalt were precipitated during a major volcanic event over a shallow sill that clearly must have generated major hot-springs and solfataras. Cox (1986) describes the characteristic depositional environment of Besshi deposits as "Possibly deposition by submarine hot springs related to basaltic volcanism. Ores may be localized within permeable sediments and fractured volcanic rocks in anoxic marine basins." Although the mud ponds where the ore bearing argillites of the New Jersey copper ores were deposited are not marine they were at least brackish. On the basis of related carbonaceous plant fossil remains at the same strata as the ore, they were probably also anoxic. The "fractured volcanic rock" characteristic of Besshi host rock describes the native copper precipitated in joints within the Orange Mountain basalt at several New Jersey deposits (Figure 8). A supply of sulfate and chloride rich water was probably available within the Passaic Formation groundwater and in surface ponds that could have acted as a ligand source for the leaching of copper from the underlying

network of diabase sills and perhaps from the overlying basalt flows. Transport of copper to basalt cooling fractures and to the surface muds under the flows would have involved minimal distances.

Application of Hot-Spring Au-Ag (USGS Model 25a) and Creed epithermal vein (USGS Model 25b) models

The Hot-spring and Creed models apply best to Au, Ag, He, and As mineralization in calc-alkaline volcanic rock systems with associated sedimentary rocks. However, characteristic mineralogy also includes copper sulfosalts and chalcopyrite. The breccia dikes and low angle veins of ore found at the Schuyler and Flemington mines together with surface precipitation of ore found at the deposits under the Orange Mountain basalt are characteristics of both Hot-spring and Creed models (Cox and Singer, 1986). In the case of the Creed model the depositional environment is described by Mosier et al (1986) as "Deposits related to sources of saline fluids in prevolcanic basement such as evaporates or rocks with entrapped seawater" Mosier et al (1986) do not indicate whether the source of copper was prevolcanic basement (such as the Passaic Formation?) or the volcanic rock that is the characteristic ore host. However volcanic rock is an essential ingredient of the model, without which it would be classified with "Deposits in clastic sedimentary rocks". We suggest that in the case of the New Jersey deposits at least some copper was leached from the igneous rocks (intrusive and perhaps extrusive) by ligand enriched waters that were contained within the Passaic Formation.

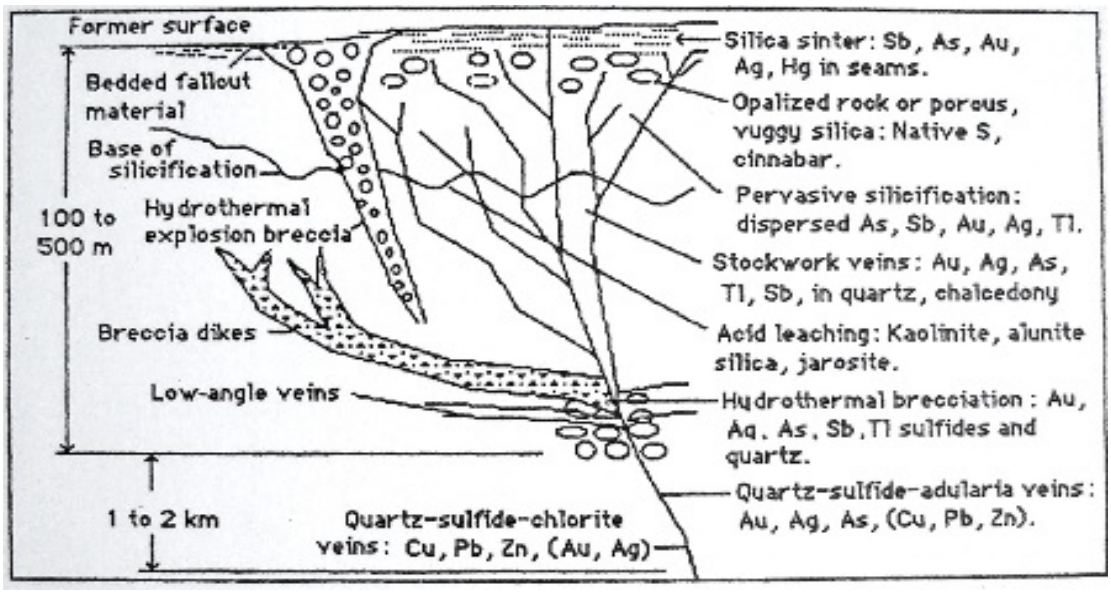

Figure 9. Cross section through USGS Hot-spring Model 25a (Cox and Singer, 1986)

Restricted application of Redbed Cu (USGS Model 30b.3) and Redbed-type (CGS Model 8.3b) models.

An essential characteristic of each of the USGS "Deposits in clastic sedimentary rocks" models (Table 3) is that ore deposition must be independent of igneous processes (Cox and Singer, 1986). Application of this criterion to most New Jersey deposits would totally ignore the very intimate spatial association of most of the New Jersey deposits with Orange Mountain Basalt or co-magmatic shallow intrusives. The only useful application of the Redbed models to New Jersey is, therefore, restricted to the relatively minor Glen Ridge mines.

Nevertheless, Robinson and Sears (1988) have classified most of the New Jersey Cu deposits as "… sediment-hosted, stratabound, and vein-type mineralized occurrences associated with the migration of brines within the basins, apparently unrelated to igneous intrusion." This classification is approximately the same as the USGS Redbed model. However, despite considering "skarn deposits", "hornfels deposits", and "late-stage igneous segregations and veins within and bordering diabase sheets" Robinson and Sears (1988) conclude that all of the New Jersey deposits are unrelated to igneous intrusion. Some of the deposits they specifically describe as unrelated to igneous intrusion include the Grigstown, Schuyler, and Flemington mines despite the fact that all of the ore at these mines was recovered from mineralized diabase breccia (Figures 3 and 4) or hornfels located within about 2 m from diabase intrusions (Figures 2 and 5). The reasoning behind the Robinson and Sears (1988) application of a "sediment-hosted stratabound" model to the New Jersey deposits is not indicated in their report and there is no indication that they actually examined the New Jersey deposits.

Smoot and Robinson (1988) examined several sandstone deposits in the Culpeper, Newark, and Hartford basins and also classify each New Jersey occurrence as "sediment-hosted stratabound base metal occurrences" again in keeping with an approximately "Redbed" model. They accurately describe the "host-rock lithology" of the Hoffman, Stony Brook, Bridgewater, and Chimney Rock deposits as "basalt" but for some unexplained reason list these deposits under their "sediment-hosted" category. Smoot and Robinson (1988) recognize the possibility that the circulation of mineralizing fluids may have been initiated by Jurassic igneous activity but conclude that copper enrichment of the New Jersey deposits was controlled by organic material in permeable medium- to coarse-grained sandstones. However, most of the New Jersey deposits are fine-grained argillite hornfels such as (Figure 6) that are totally devoid of any organic material. In agreement with Smoot and Robinson (1988) we have also observed some carbonized plant remains in a few gray beds interbedded with the dominant redbeds at the Schuyler mine, but the only beds that are mineralized with copper are those in close proximity to a diabase sheet (Figures 2 and 5).

There are at least two facts that argue against the application of a "Redbed" model to the Schuyler mine and similar deposits or to deposits at the base of the Orange Mountain basalt.

1.) At the Schuyler mine beds of gray shale containing carbonized plant remains are intersected by a shallow diabase intrusion. However, copper mineralization <u>is confined to the margins of the intrusion</u> (Figures 2 and 5) where the richest ore is contained in an explosion breccia (Figures 3 and 4). Ore values within each lithology adjacent to the diabase (well sorted sandstone, argillite, reddish siltstone, and gray shale) decrease in direct proportion to distance from the termination of the intrusion. Each of the several thin gray shale beds, some containing traces of carbonized plant remains are

exposed along a steep cliff outcrop parallel to an industrial park; none of which contain any visible evidence of copper mineralization at distances exceeding 10 m from the diabase sill exposed near the top of the approximately 300 m of continuous outcrop. Clearly, if ore mineralization was controlled by copper precipitation out of connate water wherever reduction was forced by carbonized gray strata, proximity to the diabase intrusion should not be a factor. It could be argued that the copper deposits at the base of the first Orange Mountain flow were precipitated at the surface in an anoxic environment before the basalt extruded and that local remobilization of copper heated by the flow account for its precipitation in basalt joints. However, if the source of copper at the Schuyler mine was Orange Mountain magma, it is logical that similar mineralization at the base of the Orange Mountain flow was also Orange Mountain magma.

2.) The copper content of the Schuyler diabase is 1910 ppm and the copper content of Orange Mountain basalt is within and locally exceeds the 100-200 "copper rich" range characteristic of the "Basaltic Cu" model. However, the copper content of most flows that overly the Orange Mountain such as the Preakness Basalt fall below the 100-200 ppm range and are not mineralized. The copper content of the Hook Mountain flows fall within the 100-200 ppm range but the base of these flows is not mineralized because there was no known shallow diabase sill that intruded beneath them when they were extruded that could have generated a solfatara.

PROPOSED ORIGIN

The diversity of the Mesozoic copper deposits of New Jersey make it impossible to categorize all of them into any one USGS or CGS genetic model. However with few minor exceptions (Lewis Category 4) the best fit for Lewis Categories 1-3 is the USGS "Basaltic Cu" model which is approximately equivalent to the CGS "Volcanic redbed copper" model.

Our proposed origin is consistent with the fact that most of Earth's known copper deposits (including black smokers and porphyry copper deposits) were derived from igneous magmas that were contaminated with saline water that in turn leached or extracted hydrothermal copper out of the magma during cooling.

Lewis Categories 1-3

A few New Jersey copper deposits (Lewis Category 3) comply in all respects to the Basaltic Cu model, particularly the deposits located within the amygdaloidal flow-top of the Orange Mountain basalt including the Pluckamin (Hoffman) mine. In agreement with the Basaltic Cu model a close association of copper mineralization with subaerial basalt or comagmatic diabase is a characteristic of all the Lewis Category 1-3 deposits of New Jersey. However, copper in the mines at the base of the Orange Mountain basalt was probably precipitated in surface muds, probably boiling "mud-pots", in the solfatara that with little doubt characterized the Newark Basin immediately preceding the extrusion of the Orange Mountain basalt (Figure 10). The underlying Palisades Sill and shallow off-shoots fed these copper rich flows as it intruded beneath wet Preakness redbeds.

It is not clear how much copper was leached directly out of the first Orange Mountain flow as it extruded across wet solfatara and brackish ponds. However, leaching of copper from the first flow would have been limited to any surface water that

was able to penetrate the lower portion of the first flow. Circulation of water through the basalt flows and the mud and sand under the first flow would have rapidly decreased as soon as impermeable hornfels were formed. In contrast, water circulation through the intrusive system of copper enriched diabase could have leached considerable copper at higher water pressures and slower cooling rates.

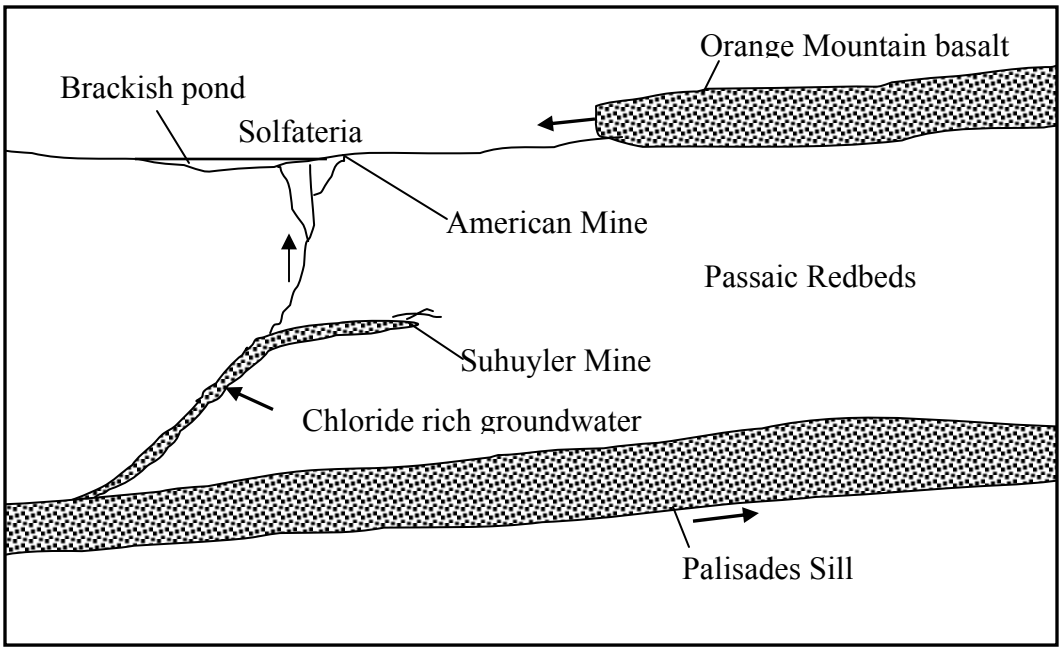

Figure 10. Idealized cross section through Passaic redbeds illustrating the leaching of copper from diabase into epithermal brines followed by movement to solfataric vents at the surface. Copper precipitation in explosion breccia occurred wherever thin diabase offshoots encountered wet sedimentary horizons.

Copper leached from the intrusive system would have been driven toward the surface as complex ions in hydrothermal solutions. Some copper was probably concentrated in the muds of solfatara or may have formed small Besshi-type hot-spring precipitates at the bottom of any water bodies. Where shallow diabase sills encountered wet muds, Hot-Spring-type explosion breccias would have formed, such as those of the Schuyler mine together with a network of thin veins.

Evidence that the Palisades diabase magma was contaminated with saline water includes the elevated levels of sodium (3.0 to 4.3 percent) within upper interior levels that can not be accounted for by fractionation processes (Puffer and Steiner, in prep.).

Ore deposits genetically similar to Lewis Category 1-3

Several examples of Basaltic Cu deposits are listed by the USGS (Cox and Singer, 1986) and of Volcanic Redbed Copper by the CGS (Eckstrand el al, 1995) including the Keweenaw and Denali deposits, (and Kennicott) in the US, the Redstone, Sustut, and White River deposits in Canada and the Buena Esperanza deposit of Chile.

The Buena Esperanza deposits of Chile

Gilbert and Park (1985) speculate that the Buena Esperanza copper deposit of Chile and other similar deposits may be I-type extrusive equivalents of porphyry coppers. These deposits are typically mantos types (flat, bedded, and sheet like) and are stratabound in Jurassic andesitic flow tops, breccias, and interbedded sediments and are mineralized with native copper and chalcocite. Sillitoe (1977) proposed a Valley of Ten Thousand Smokes analogy that closely agrees with our proposed origin of most New Jersey deposits. Sillitoe's fluid inclusion data indicate epithermal temperatures in a 112 to 195 ^{o}C range. He also suggested some involvement of shallow lagoonal or lacustrine water, again similar to what we envision for some of the New Jersey deposits.

The Keweenaw Michigan deposits

The copper deposits in subaerial continental flood basalt are mineralized with native copper and contain very little sulfur, unlike the New Jersey deposits. The ore is confined to flow tops and breccias, again unlike the New Jersey deposits although in both cases they have been metamorphosed to prehnite-pumpellyite facies. Stoiber and Davidson (1959) propose that metamorphism of the basalt released copper and low temperature fluids that carried copper to flow-tops near the surface where it precipitated. However, metamorphism probably played a less important role in New Jersey where most copper is concentrated in impermeable argillite hornfels. In addition, metamorphism would not account for the confinement of copper ore at the Schuyler mine and its close proximity to thin diabase sheets. Metamorphism of the New Jersey deposits, however, probably re-equilibrated the copper mineral assemblage to metamorphic temperatures and pressures and may have remobilized some copper that precipitated as native copper in basalt joints within the flow bottoms.

The Denali deposits, Alaska

The Denali deposits are found along a zone of Triassic sediment-volcanic intercalation. The mineralized beds lie under or in front of the flows are "… squeezed and crumpled, presumably by the loading of the flows" (Seraphim, 1975). Unlike the Keweenaw and Kennecott deposits the Denali deposits are not metamorphosed. According to Seraphim (1975) "The copper-rich solutions were probably derived from the leaching of the abundant copper mineralization in the volcanic flow tops or from solfataric vents." In the case of the New Jersey deposits, solfataric vents are a more likely factor because most of the deposits are located at the base of the first flow.

The Sustut deposit, British Columbia

The Sustut copper deposit occurs in Upper Triassic volcanic conglomerate with local tuffaceous layers that have been metamorphosed to prehnite-pumpellyite facies. The ore is mineralized with chalcocite, bornite, chalcopyrite, and native copper. The ore fluids are interpreted by Wilton and Sinclair (1988) as derived from below during metamorphism.

Lewis Category 4

A few minor copper deposits (the Glen Ridge mines and possibly the Menlo Park mine) are not apparently associated with igneous rocks. The Glen Ridge mines are, however, associated with carbonized plant remains (Lewis, 1907) and, therefore, qualify as USGS Model 30b.3 "Redbed Cu" or CGS Model 8.3b "Redbed-type Sediment-Hosted Stratiform Cu".

Shockey et al. (1974) have proposed that redbed Cu deposits are similar to uranium roll-front deposits and result from oxygenated formation water flushing through permeable reduced sediments and depositing ore minerals at oxidation-reduction interfaces. The pore fluids in redbed Cu host sediments are generally thought to be saline with elevated chloride content. Rose et al (1986) and Rose (1989) propose leaching of copper from redbeds into chloride bearing pore fluids followed by movement through permeable beds until organic reductants (such as carbonized plant remains) are encountered. The transmission of copper as a chloride complex is, therefore, similar to the "Basaltic Cu" model, however temperatures are much lower resulting in diminished solubility and ore grade. The copper content of detrital redbed sediment sources is also generally less than the copper content of typical igneous sources (Table 2) again resulting in lower ore grades. However some redbed deposits may represent deposition of copper enriched sediment derived from a copper rich provenance.

Ore deposits genetically similar to Lewis Category 4

The Corocoro deposit, Bolivia

The Corocoro native copper and chalcocite deposit is found in thick Cenozoic redbed sediment that was deposited in a subaerial environment. This redbed deposit superficially resembles the Lewis category 4 deposits of New Jersey. However, Entwistle and Gouin (1955) observed that most Corocoro ore consists of interstitial chalcocite grains that are concentrated at the base of red sandstone beds indicating that the copper was localized at, or soon after, the time of sedimentation perhaps from a copper enriched source. Some chalcocite has altered to native copper. No igneous rocks are known near the ore deposits.

The Sierra Nacimiento, New Mexico deposit

The Nacimiento deposits consist of chalcocite, malachite, chrysocolla, and azurite that fill interstices and fractures in Chinle sandstones of Triassic age. Woodward et al (1974) propose that the ore was deposited by ground-water solutions moving through paleochannels shortly after deposition of the host rock. They propose that the ultimate source of the copper was older Precambrian rocks and that mineralization occurred where there was a reducing environment, principally carbonaceous material.

CONCLUSIONS

The Palisades sill and some shallow offshoots intruded into unconsolidated redbed sediments. These diabase magmas were contaminated with basin brine. Copper

extracted from the diabase upon saturation was carried into the surrounding sediments and explosion breccias as a chloride complex where it precipitated as sulfides or native copper during cooling. Some copper was carried by epithermal hot-spring systems to the surface where it precipitated in solfatara or in mud at the base of shallow brackish ponds. These surface deposits were quickly buried under thick co-magmatic basalt flows and baked into hornfels. Additional copper may have been leached from the basalt upon encountering shallow brackish water bodies and then precipitated in amygdules. The primary copper mineral assemblage may have been remobilized during subsequent zeolite facies burial metamorphism and re-equilibrated. However the low permeability of the argillite hornfels host-rock of the copper ore argues against significant redistribution.

The resulting copper deposits described in this report, therefore, qualify as "Basaltic Cu" (Model 23) on the basis of current USGS criteria (Cox and Singer, 1986) and as "Volcanic Redbed copper" (Model 9) on the basis of current CGS criteria (Eckstrand et al. 1995).

A few minor occurrences near Glen Ridge are not associated with igneous rock but are associated with carbonized plant remains. These Glen Ridge deposits qualify as "Redbed-type" deposits (Model 30b.3) on the basis of current USGS criteria (Cox et al. 2003) and as "Redbed-type" deposits (Model 8.3b) on the basis of current CGS criteria (Eckstrand et al. 1995).

ACKNOWLEDGMENTS

We wish to thank Ted Proctor for field assistance at the Schuyler mine during the years1990-1994 and for analyses of samples collected there. We thank Karen Block and Jeffery Steiner at the City College of New York for chemical analytical help.

REFERENCES

Cattafi, P.P; Mahon, J.C; Shaw, M.F; Stefanik, A; Syred, T.A; Villacis, J.P; and Puffer, J.H; 1998, The American Mine Copper Deposit of New Jersey. *in* Puffer, J. H., (editor), The Economic Geology of Central New Jersey. Field Guide and Proceedings; Fifteenth Annual Meeting of the Geological Association of New Jersey, V. 15, p. 50-66.

Cox, D. P., 1986, Descriptive model of Besshi massive sulfide in Cox, D. P., and Singer, D. A., eds., Ore deposit Models: United States Geological Survey Bulletin 1693, p. 132.

Cox, D. P., and Singer, D. A., 1986, Ore deposit Models: United States Geological Survey Bulletin 1693, 379p.

Cox, D. P., Lindsey, D. A., Singer, D. A, and Diggles, M. F., 2003; "Sediment-Hosted Copper Deposits of the World: Deposit Models and Database." United States Geological Survey Open File Report 03-107.

Darton, 1902, Annual Report of State Geologist for 1901, p. 129.

Berger, B. R., and Silberman, M. L., l985, Relationship of trace-element patterns to geology in hot-spring-type precious-metal deposits: *in* Berger, B. R., and Bethke, P. M., (editors),Geology and Geochemistry of epithermal systems, Reviews in Economic Geology V. 2, Society of Economic Geologists, p. 233-255.

Eckstrand O. R., Sinclair, W. D., and Thorpe, R. I., 1995, Geology of Canadian Mineral Deposit Types, Geological Survey of Canada: Geology of Canada No. 8

Entwistle, L. P., and Gouin L. O., 1955, The chalcocite-ore deposits at Corocoro, Bolivia, Economic. Geology., V. 50, p. 555-564.

Gilbert J. M., and Park, C. F., 1985, The geology of Ore deposits, W. H. Freeman and Company / New York, 985 pp.

Gottfried, D. Froelich, A. J., and Grossman, J. N., 1991, Geochemical data for Jurassic diabase associated with early Mesozoic basins in the Eastern United States: Eastern Newark Basin, New York and New Jersey, U. S. Geological Survey Open-File Report 91-322-C, 6 pp.

Lewis, J. V., 1907, The Newark (Triassic) Copper Ores of New Jersey. Annual Report of the State Geologist for the Year 1906, p. 131-164.

Mosier, D. L., Singer, D. A., and Cox, D. P., 1986, Grade and tonnage model of sediment-hosted Cu; in Mineral Deposit Models, Cox, D. P. and Singer, D. A., Editors, United States Geological Survey Bulletin 1693. p. 206-208.

Olsen, P.E., l986, A 40-million year lake record of early Mesozoic orbital climate forcing: Science, v. 234, p. 842-848.

Olsen, P. E., Kent, D.V., Cornet, B., Witte, W.K., and Schlische, R.W., l996, High resolution stratigraphy of the Newark Rift Basin (early Mesozoic, Eastern North America): Geological Society of America Bulletin. V. 108, p. 40-77.

Puffer, J. H., 1984, Copper Mineralization of the Newark Basin, New Jersey : *In* Puffer J. H. (editor) Igneous Rocks of the Newark Basin: Petrology, Mineralogy, Ore Deposits, and Guide to Field Trip: Geological Association of New Jersey, 1st Annual Field Conference, p. 127-136.

Puffer, J. H., 1987, Copper Mineralization of the Mesozoic Passaic Formation, Northern New Jersey. *in* Vassiliou, A, H. (editor), Process Mineralogy VII, The Metallurigical Society of AIME-SEM p. 303-313.

Puffer, J. H., 2001, Contrasting high field strength element content of continental flood basalts form plume versus reactivated-arc sources: Geology, v. 29, p. 675-678.

Puffer, J. H., 1992, Eastern North American Flood Basalts in the Context of the Incipient Breakup of Pangea. In Puffer, J. H., and Ragland, P. C., (Editors) Eastern North American Mesozoic Magmatism: Geological Society of America, Special Paper 268, p. 95-119.

Puffer, J. H., and Proctor, T., 1992, Copper Mineralization at the Base of the Orange Mountain Basalt, Newark Basin, New Jersey. Geological Society of America, Annual Meeting, Cincinnati, Ohio, Abstracts With Program, V. 24, p. 23.

Puffer, J. H., and Proctor, T., 1994, Distribution of Copper in the Orange Mountain Basalt, Related Diabase Dikes, and Underlying Passaic Formation, New Jersey: Geological Society of America, Annual Meeting, Seattle, Washington, Abstracts with Program, V. 26, p. A-402.

Reiff, J. C., and Bond, J. 1902, The American Copper Mine, Somerville, Annual Report of the State Geologist for the year 1901, Geological Survey of New Jersey, p. 151-152.

Robinson, G. R., Jr., and Sears, C, 1987, Inventory of Metal Occurrences Associated with the Early Mesozoic Basins of the Eastern United States. *in* Froelich, A. J., and

Robinson, G. R., Jr. (editors) Studies of the Early Mesozoic Basins of the Eastern United States, U. S. Geological Survey Bulletin 1776, p. 265-302.

Rose, A.W., l989, Mobility of copper and other heavy metals in sidimentary environments: *in* Boyle, R.W., Brown, A.C., Jefferson, C.W., Jowett, E.C., and Kirkham, R. V., (editors)., Sediment-hosted stratiform copper deposits: Geological Association of Canada, Special Paper 36, p. 97-110.

Rose, A.W., Smith, A.T., Lustwerk, R.L., Ohmoto, H., and Hoy, L.D., l986, Geochemical aspects of stratiform and Red-Bed copper deposits in the Catskill Formation (Pennsylvania, USA) and Redstone Area (Canada). Sequence of Mineralization in sediment-hosted copper deposits (Part 3) *in* G.H. Friedrich et al. (editors), Geology and Metallogeny of Copper Deposits: Springer-Verlag, Berlin Heidelberg, p. 412-421.

Schmitt, H. A., l950, The fumarolic-hot spring and "epithermal" mineral deposit environment: Quarterly Colorado School Mines, V. 45,1B, p. 209-229.

Seraphim, R. H., 1975, Denali- A nonmetamorphosed stratiform sulfide deposit: Economic. Geology. V. 70, p. 949-959.

Shirley, D. N., 1987, Differentiation and compaction in the Palisades Sill, New Jersey: Journal of Petrology, V. 28, p. 835-865.

Shockey, P. N., Renfro, A. R., and Peterson, R. J., 1974, Copper-silver solution fronts at Paoli, Oklahoma: Economic Geology V. 69, p. 266-268.

Silltoe, R.H., l977, Metallic mineralization affiliated to subaerial volcanism: a review: *in* Volcanic Processes in Ore Genesis. London: Inst. Min. Metall., Special. Paper. 7, 188 pp.

Smoot, J. P., and Robinson, G. R., 1988, Sedimentology of stratabound base-metal occurrences in the Newark Supergroup *in* Froelich, A. J., and Robinson, G. R., Jr. (editors) Studies of the Early Mesozoic Basins of the Eastern United States, United States Geological Survey Bulletin 1776, p. 356-376..

Stoiber R. S., and Davidson E. S., 1959, Amygdule Mineral Zoning in the Portage Lake Lava Series, Michigan Copper District. Economic Geology, V. 54, p. 1250-1277.

White, W. S., 1968, The native-copper deposits of Northern Michigan; in Ore Deposits of the United States, 1933-1967; The Graton-Sales Volume, Ridge, J. D., Editor, American Institute of Mining, Metallurgy and Petroleum Engineers, Inc., New York, p. 303-325.

Wilton, D. H. C., and Sinclair, A. J., 1988, The geology and genesis of a strata-bound disseminated copper deposit at Sustut, British Columbia, Economic Geology, V. 83, p. 30-45.

Woodward, H. P., 1944, Copper mines and mining in New Jersey: Dept of Cons. and Dev. State of New Jersey, Bulletin, V. 57, 156 pp.

Woodward, L. A., Kaufman, W. H., Schumacher, O. L., and Talbott, L. W., 1974, Strata-bound copper deposits in Triassic Sandstone of Sierra Nacimiento, New Mexico, Economic Geology, V. 69, p. 108-120.

Trace fossils from the Newark basin of New Jersey and southeastern Pennsylvania

Robert Metz
Department of Geology and Meteorology, Kean University, Union, New Jersey 07083, rmetz@kean.edu

ABSTRACT

Strata representing largely lake-shoreline deposits of the Upper Triassic Passaic Formation and Lower Jurassic Towaco formation of New Jersey and southeastern Pennsylvania have yielded an assemblage of trace fossils. Dominated by burrowing forms and represented by the *Scoyenia* ichnofacies, specimens include: *Cochlichnus anguineus, Didymaulichnus lyelli, Helminthoidichnites tenuis, Helminthopsis hieroglyphica, Mermia carickensis, Palaeophycus alternatus, Palaeophycus tubularis, Planolites annularis, Planolites beverleyensis, Scoyenia gracilis, Spongeliomorpha milfordensis, Treptichnus bifurcus, Treptichnus pollardi,* paired trails, insect trackway, as well as scratch circles.

Reddish brown, sporadically green siltstones and mudstones, and gray claystones have produced all of the trace fossils. Where trace fossils are found to be diverse and abundant, field evidence indicates that a variety of paleoenvironments including lake-margin, very shallow water, and floodplains with their ephemeral puddles and ponds offered optimum conditions for feeding and tracemaking by insects and arthropods. These deposits were later subject to periodic desiccation alternating with fine-grained sediment influx during rainstorms, favoring trace preservation.

INTRODUCTION

Ichnology has been defined by Frey (1973, p. 9) as the "….overall study of traces made by organisms, including their description, classification, and interpretation." These traces include burrows, trails, tracks, borings, and similar features occurring in both fossil and modern form. Though the term has been employed for over 150 years, it has often been neglected compared to body fossils. However, within the last four decades, there has been a significant increase of interest in ichnology. There are a number of reasons for this resurgence including: 1) what is preserved is both fossil as well as sedimentary structure 2) the change from soft sediment into a rock may alter or destroy body fossils, yet has little if any effect on the traces present, and 3) in many cases trace fossils are found preserved where body fossils are lacking (Ekdale et al., 1984). Thus, when combined with other features of the substrate (e.g., physical and chemical), trace fossils have proven to be very useful in providing insight into past environments.

Research on modern nonmarine environments indicates that a great diversity of invertebrate traces, mostly by arthropods, are formed (e.g., Chamberlain, 1975; Ratcliffe and Fagerstrom, 1980; Tevesz and McCall, 1982; Metz, 1987a, 1987b). Nevertheless, some workers noted that considerably fewer of these traces are represented in fossil form (Frey et al., 1984). Interestingly, Frey et al. (1984) questioned whether the low diversity was due to poor preservational potential or more a lack of comprehensive study. As noted by Pickerill (1992), it most certainly appears to be more of the latter. Thus, recent studies

(Tevesz and McCall, 1982; Sarkur and Chaudhuri, 1992; Pickerill, 1992; Buatois and Mángano, 1995, 1998; Hasiotis, 2002; Uchman et al., 2004) suggest that a wide range of trace fossil assemblages existed under nonmarine conditions.

GEOLOGIC SETTING

The Newark Basin is the largest of the exposed rift basins formed along eastern North America during the breakup of Pangea in Late Triassic to Early Jurassic time (Manspeizer, 1988; Olsen, et al., 1989). This half-graben basin received thick accumulations of continental deposits spanning a period of approximately 30 million years. Although these deposits were originally thought to largely lack fossils, they have since been shown to contain one of the richest Mesozoic faunas, especially vertebrates (Olsen, 1988; Olsen and Flynn, 1989; Olsen et al., 1989).

The Stockton, Lockatong, Passaic, Feltville, Towaco, and Boonton Formations (Late Triassic-Early Jurassic) form the major nonmarine sedimentary units comprising the strata of the Newark Basin of New Jersey and southeastern Pennsylvania. They consist of reddish brown, gray, gray-green, and black largely lacustrine and fluvial deposits of siltstone, mudstone, and fine-grained sandstone (Olsen, 1980a). Olsen (1980a) indicated that all the sedimentary deposits above the Stockton Formation exhibit repetitive transgressive-regressive lake-level successions, designated Van Houten Cycles (Olsen, 1985), reflecting climate modifications which affected rates of inflow versus evaporation (see also Van Houten, 1964, 1969; Smoot and Olsen, 1988).

Though the geology of the formations has been extensively detailed (Van Houten, 1964, 1969; Olsen, 1980a; Smoot and Olsen, 1988; Olsen and Flynn, 1989; Olsen et al., 1989; Smoot, 1991), evidence of trace fossils has remained largely unreported (Boyer, 1979; Olsen, 1980b; Olsen et al., 1989). This paper describes the trace fossils found within the Passaic and Towaco Formations, comments on the paleoenvironment, and represents an update (Metz, 1991, 1996a, 1996b, 1998, 2000) of previous investigations by the author (Metz, 1989, 1992, 1993a, 1993b, 1995).

SYSTEMATIC ICHNOLOGY

Ichnogenus *Cochlichnus* Hitchcock 1858
Cochlichnus anguineus Hitchcock 1858
Figure 1A

Description: Sinusoidal, unbranched, unlined epichnial trails preserved as positive hyporeliefs. Diameter ranges from 0.5-2.0 mm; visible lengths up to 6 cm; wave amplitude ranges from 1.0-3.5 mm, wavelength varies from 3 to 18 mm.
Remarks: *Cochlichnus* is a distinctive trace fossil characterized by a sinusoidal form. Gluszek (1995) observed that the original diagnosis of *Cochlichnus* (Hitchcock, 1858) stipulating "Trackway a continuous serpentine furrow, resembling a compressed corkscrew," had not been sufficiently defined by Häntzschel (1975), thus, almost any sinusoidal trail could be assigned to this ichnogenus. Metz (1998), however, noted that Hitchcock (1858) in adding a "Spire not unfrequently gradually diminishing towards one extremity", implied that not all examples of *Cochlichnus* encountered by him fit this

description. Interestingly, as noted by Metz (1998), detailed investigation of all available type specimens of *Cochlichnus* of Hitchcock (1858) indicates that most, in fact, do not exhibit a corkscrew appearance. Therefore, this limitation in shape posed by Gluszek (1995) seems unwarranted.

Fillion and Pickerill (1990), Keighley and Pickerill (1997) and Buatois et al. (1997) discussed the status of several ichnospecies of *Cochlichnus*, specifically those whose descriptions relied on whether the trace referred to a burrow or trail. The general consensus is to include both trails and burrows within this ichnogenus, since in many cases deciphering between them is difficult to impossible (see Rindsberg, 1994). Thus, the researchers concluded that several ichnospecies of *Cochlichnus* should be relegated to junior synonyms of *C. anguineus* (e.g., see Keighley and Pickerill (1997), for details).

Worms or worm-like animals are the most commonly proposed tracemakers for *Cochlichnus* (e.g., Hitchcock, 1858; Moussa, 1970; Eagar et al., 1985), although insect larvae (Michaelis, 1972; Metz, 1987c) have also been suggested.

Ichnogenus *Didymaulichnus* Young 1972
***Didymaulichnus lyelli* (Rouault 1850)**
Figure 1B

Description: Smooth, straight or gently curving burrow, 1.5-2.0 mm in diameter, preserved length 9 cm. Consists of smooth bilobate form bisected by a distinctive central furrow, parallel to bedding plane, preserved in convex hyporelief.
Remarks: A well preserved specimen of *Didymaulichnus* which most closely resembles *D. lyelli* Rouault 1850, except for its smaller size. It lacks the marginal bevels of *D. miettensis* Young 1972 and *D. tirasensis* Palij 1974; the pit-like depressions of *D. nankervisi* Bradshaw 1981; and the change from shallow to deeper impressed sections of *D. alternatus* Pickerill et al. 1984.

Didymaulichnus is virtually identical to *Aulichnites*. They are commonly distinguished on the basis of *Didymaulichnus* being found preserved in convex hyporelief on the sole of bedding surfaces, while *Aulichnites* is found in convex epirelief on the top of bedding surfaces (Pickerill, 1994). The specimen is also similar to the ichnotaxon *Palaeobullia*. However, it lacks evidence of some form of surface sculpture (e.g., ribbing, knobs, striations) exhibited by *Palaeobullia* and, again, is smaller in diameter (Häntzschel, 1975; Miller and Knox, 1985). The presence of a smooth bilobate form distinguishes this specimen from the ichnotaxon *Cruziana* which processes transverse scratch marks (MacNaughton and Pickerill, 1995).

Didymaulichnus occurs in nonmarine (e.g., Miller, 1986; Aceñolaza and Buatois, 1993) and marine (e.g., Young, 1972; Crimes and Anderson, 1985) strata. It has been recorded from Precambrian to Cretaceous. The tracemaker of *Didymaulichnus* has been attributed to molluscs (Glaesser, 1969), trilobites (Crimes, 1970), and gastropods (Hakes, 1977), although its origin remains obscure (Pickerill et al. 1984). Other potential tracemakers in nonmarine environments include arthropods and bivalves (Buatois, personal communication, 1995). The specimen of *Didymaulichnus* is associated on the same bedding plane with *Spongeliomorpha* and *Scoyenia*, and desiccation cracks, and is believed to have been formed by an insect.

Ichnogenus *Helminthoidichnites* Fitch 1850
***Helminthoidichnites tenuis* Fitch 1850**
Figure 1C

Description: Simple, small, unbranched, straight to gently winding traces preserved as positive hyporeliefs. Trace fill is similar in composition to the surrounding sediments. Diameter ranges from 0.7 to 1.5 mm, and is constant within individual specimens; preserved length up to 24.5 cm. Crossover between different specimens is common.
Remarks: Although Häntzschel (1975) placed *Helminthoidichnites* in with *Gordia*, Hoffman and Patel (1989) did not concur, citing the secondary amount of looping of their specimens compared to the distinctive self-overcrossing of *Gordia*. Hoffman and Patel (1989) also noted that *Helminthoidichnites* is less sinuous and does not exhibit the type of meander habit of *Helminthopsis*. A number of researchers agree with their assessment, including this author, and consider *Helminthoidichnites* a valid ichnogenus (e.g., Narbonne and Aitken, 1990; Hoffman et al., 1994; Jensen, 1997; Buatois et al., 1997). This trace is very similar to *Unisulcus minutus* (Hitchcock, 1858).

Buatois et al. (1997) interpreted this ichnotaxon as a grazing trace produced by nematomorphs or insect larvae. Based on the present specimens and comparison to modern nonmarine traces (Metz, 1987a, 1987b), this author agrees with Buatois et al. (1997), and would add small insects to the list of probable tracemakers. *Helminthoidichnites* has been reported from nonmarine and marine deposits. Nonmarine settings include the Carboniferous and Permian of Argentina (Buatois and Mángano, 1993a, Buatois et al., 1997) the Jurassic of China (Buatois et al., 1996), the Cretaceous of Spain (Fregenal Martinez et al., 1995), and the Oligocene of Switzerland (Uchman et al., 2004). Thus, the present specimens represent the first nonmarine record of *Helminthoidichnites* from North America (see Metz, 2000). The record of this ichnogenus ranges in age from the Late Precambrian to the Cretaceous (Narbonne and Aitken, 1990; Fregenal Martinez et al., 1995).

Ichnogenus *Helminthopsis* Heer 1877
***Heminthopsis hieroglyphica* Wetzel and Bromley 1996**
Figure 1D

Description: Horizontal, unbranched, irregularly meandering burrows or trails. Burrow fill is similar to the enclosing rock. Specimen width is constant and ranges from 0.5-2.0 mm, with maximum preserved length of 24 cm. Typically, specimens exhibit low-amplitude, irregular meanders separated by straight segments, less commonly meanders are bell-shaped, but not horseshoe-shaped. Preserved in positive hyporelief, a few in negative epirelief.
Remarks: The greater sinuosity and irregular meandering differentiates *Helminthopsis* from *Helminthoidichnites* (Hoffman and Patel, 1989). *Helminthopsis* is distinguished from *Gordia* by its tendency to meander and lack of self-overcrossing (Pickerill, 1981). Recent in-depth reviews by Han and Pickerill (1995) and Wetzel and Bromley (1996) suggested retaining only three of the previously established ichnospecies (up to 22) of this ichnogenus. However, they differed as to which three ichnospecies should be valid, with Han and Pickerill (1995) designating *H. granulate, H. abeli,* and *H. hieroglyphica,* and Wetzel and Bromley (1996) choosing *H. abeli, H. tenuis,* and *H. hieroglyphica* (see

also Wetzel et al. (1998) and Pickerill et al. (1998) for further details). There does appear, however, to be general agreement for *H. hieroglyphica,* specifically, the distinctive display of straight segments between irregular meanders.

Helminthopsis is considered to represent a grazing trail produced by a deposit-feeding organism (Buatois et al., 1997). Proposed tracemakers for *Helminthopsis* include worm or worm-like forms (Chamberlain, 1971; Dam, 1990) and polychaetes and priapulans (Książkiewicz, 1977). Nonmarine producers may include arthropods and nematodes (Metz, 1996b; Mángano et al., 1996). Nonmarine records of *Helminthopsis* include those by Pickerill (1992), Metz (1992, 1996b), Buatois and Mángano (1993a), Buatois et al. (1996), Keighley and Pickerill (1997), and Buatois et al. (1997).

Ichnogenus *Mermia* Smith 1909
***Mermia carickensis* Smith 1909**
Figure 1E

Description: Smooth, very narrow (0.5 mm), unornamented sinuous to intensely looped trails. Numerous individuals, commonly crossing one another, although any single trail is generally difficult to follow due to sheer density. Preserved in convex hyporelief.
Remarks: *Gordia* is similar in appearance but lacks the intense looping of *Mermia* and is more worm-like (Walker, 1985; Buatois and Mángano, 1993b). In addition, occasional individual trails of *Mermia* that can be "followed" do not display the level crossings typical of *Gordia*. *Mermia* is a rare ichnotaxon, thus far limited to lacustrine deposits of the Devonian (Smith, 1909; Pollard and Walker, 1984; Walker, 1985), Carboniferous (Buatois and Mángano, 1993b), and Triassic (Metz, 1996a). *Mermia* occurs on the same bedding surface as *Scoyenia, Helminthopsis,* and *Spongeliomorpha*. It has been interpreted to represent surface feeding by small arthropods (Walker, 1985), and grazing trails (Buatois and Mángano, 1993b). Buatois and Mángano (1993b) noted the similarity between *Mermia* and the trails of modern horsehair worms (Chamberlain, 1975).

Ichnogenus *Palaeophycus* Hall 1847
***Palaeophycus alternatus* Pemberton and Frey 1982**
Figure 1F

Description: Straight to slightly curved thinly lined horizontal burrows (2.0-2.5 mm in diameter, preserved length up to 4 cm), well-developed annulations (approximately 10 per cm) and fine wavy longitudinal striae. No evidence of burrow collapse or branching. Burrow fill is similar to surrounding sediment. Preserved in convex hyporelief.
Remarks: These specimens represent some of the most morphologically distinctive ones found thus far for this ichnospecies. The specimens of *P. alternatus* most closely resemble the illustrative portion of *Palaeophycus,* type-B of Osgood (1970, Plate 77, figure 6). Pemberton and Frey (1982) indicated that *Palaeophycus* could be differentiated from *Planolites* by the presence of a wall and having fill identical to that of the surrounding rock. Keighley and Pickerill (1995) provided a definitive and historic discussion concerning the difficulties associated with assigning a given specimen to *Palaeophycus* or *Planolites*. They concurred with Pemberton and Frey (1982) in that they recommended that the primary ichnotaxabase for *Palaeophycus* be the presence of a lined simple burrow, while *Planolites* is an unlined burrow (also see Fillion, 1989; Fillion and

Pickerill, 1990). *Palaeophycus* has been interpreted to represent the infaunal pathway of a food searching organism (Osgood, 1970), a dwelling structure formed by a predaceous or suspension-feeding animal (Pemberton and Frey, (1982), feeding and locomotion burrows of a worm-like animal, or burrows formed by predators/scavengers or grazers (Miller, 1993). Modern analogues proposed include annelids (James, 1885), and various types of polychaetes (Osgood, 1970; Schäfer, 1972; Howard and Frey, 1975). *Palaeophycus* is a facies-crossing trace and has been recognized in a variety of nonmarine settings (see Buatois and Mángano, 1993b, for details). This author concurs with Buatois and Mángano (1993b) who noted that insects as well as other arthropods are likely producers under nonmarine conditions.

Ichnogenus *Palaeophycus* Hall 1847
***Palaeophycus tubularis* Hall 1847**
Figure 1G

Description: Smooth, straight to curved, unbranched, horizontal, thinly lined burrows exhibiting partial collapse. Variable burrow diameter in each specimen (overall range 2.0-4.5 mm), maximum preserved length is 10 cm. Burrow fill is structureless and similar to the host rock. Preserved in convex hyporelief.
Remarks: a combination of simple, smooth, lined burrows filled with structureless sediment identical to the surrounding rock allow these specimens to be assigned to *P. tubularis* (Pemberton and Frey, 1982). *P. tubularis* has been recorded from nonmarine (e.g., Pickerill, 1992; Buatois and Mángano, 1993b) and marine (e.g., Howard and Frey, 1984; Hoffman and Patel, 1989; Pickerill and Peel, 1990) deposits.

Ichnogenus *Planolites* Nicholson 1873
***Planolites annularis* Walcott 1890**
Figure 1H

Description: Straight to curved, horizontal, cylindrical to ellipsoidal, unbranched burrows exhibiting regularly spaced annulations. Burrow diameter nearly uniform (1.0-1.5 mm), preserved length is 4.5 cm. A burrow lining is not present and the structureless fill differs from that of the host sediment. Preserved in convex hyporelief.
Remarks: *Planolites* is distinguished from *Palaeophycus* by the lack of a wall lining and having burrow fill that differs from the host rock (Pemberton and Frey, 1982). It has been reported from nonmarine (e.g., Gierlowski-Kordesch, 1991; Metz, 1992; Pickerill, 1992; Buatois and Mángano, 1993b) as well as marine (e.g., Heinberg and Birkelund, 1984; Uchman, 1991; Buatois and Lopez Angriman, 1992; MacNaughton and Pickerill, 1995) strata. Specimens of *P. annularis* are most comparable to a similar ichnotaxon in Osgood (1970, Plate, 77, figure 3), as well as badly weathered specimens from the same location (cf. Osgood, 1970) collected by the author (1996a). *Planolites* represents active backfilling of a temporary burrow formed by a mobile deposit-feeding organism (Pemberton and Frey, 1982).

Ichnogenus *Planolites* Nicholson 1873
***Planolites beverleyensis* (Billings 1862)**
Figure 2A

Description: Simple, circular to ellipsoidal, smooth-walled unlined burrows. Single burrows, parallel to bedding, 2-3 mm in diameter, maximum preserved length is 3 cm. Burrow fill differs from and is lighter than the surrounding sediment. Preserved in convex hyporelief.
Remarks: *P. beverleyensis* differs from *P. montanus* in being more gently curved and of larger size (Pemberton and Frey, 1982). Previous reports of *P. montanus* in Newark basin strata (Metz, 1992, 1995) indicated an average diameter of 1 mm.

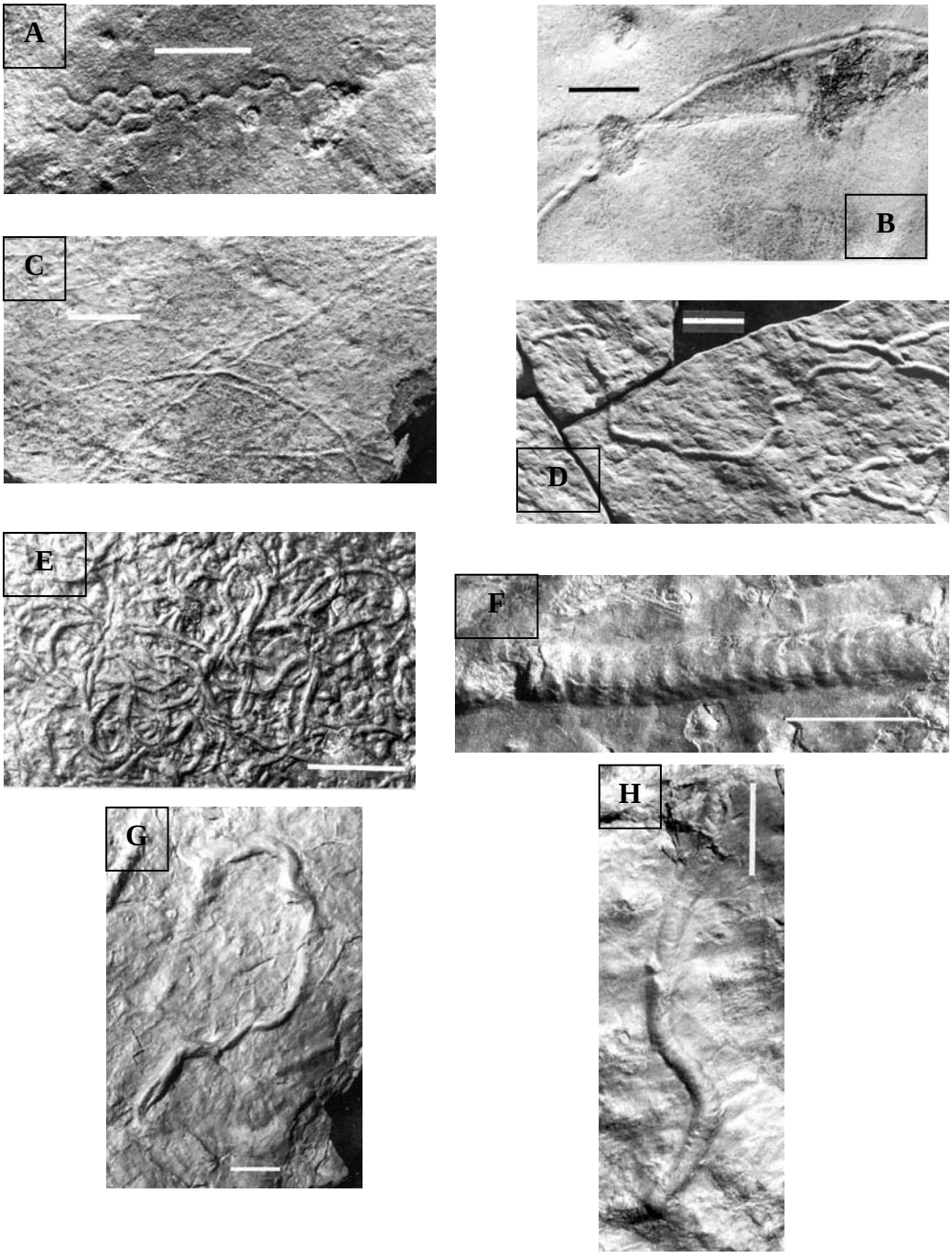

Figure 1. Ichnotaxa of the *Scoyenia* ichnocoenosis. A. *Cochlichnus anguineus* produced by a nematode. Scale = 5 mm. B. *Didymaulichnus lyelli* . Scale = 1 cm. C. *Helminthiodichnites tenuis* illustrating straight to gently winding traces. Scale = 1 cm. D. *Helminthopsis hieroglyphica*. Scale = 1 cm. E. Many examples of *Mermia carickensis*. Scale = 1 cm. F. *Palaeophycus alternatus*. Scale = 5 mm. G. *Palaeophycus tubularis*. Scale = 1 cm. H. *Planolites annularis*. Scale = 1 cm. A preserved in concave epirelief, B-H preserved in convex hyporelief. After Metz, 1996a, 1998, 2000.

Ichnogenus *Scoyenia* White 1929
***Scoyenia gracilis* white 1929**
Figure 2B

Description: Straight to gently curved burrows possessing overlapping bract-like longitudinal striations and are parallel or oblique to the bedding surface with cross-overs being common. Burrow diameter 1-10 mm (each one possessing a nearly constant size), maximum preserved length 4.7 cm. A few poorly preserved weathered specimens exhibit curved, internal menisci and wall linings. Preserved in positive and negative hyporelief and epirelief.
Remarks: Suggested tracemakers for *Scoyenia* include decapod crustaceans (Olsen, 1977), arthropods (Frey et al., 1984), and specialized insects or polychaetes (Bromley and Asgaard, 1979; D'Alessandro et al., 1987). The most common trace fossil in nonmarine strata of the Newark basin (Smoot and Olsen, 1988), *Scoyenia* has been recorded from Permian floodplain deposits (White, 1929), lacustrine sediments of Triassic and Jurassic age (Bromley and Asgaard, 1979; Metz, 1992, 1996a), Jurassic alluvial plain deposits (Gierlowski-Kordesch, 1991) and Eocene braided and meandering stream deposits (D'Alessandro et al., 1987). Though reported from Carboniferous shallow marine strata (Turner and Benton, 1983), Metz (1996a) noted the lack of descriptive or photographic evidence of meniscate structures, suggesting instead that their material may be considered *Palaeophycus striatus* (see also Frey et al., 1984).

Ichnogenus *Spongeliomorpha* Saporta
***Spongeliomorpha milfordensis* Metz 1993a**
Figure 2C

Description: Mostly straight to slightly curved, unlined, cylindrical to ellipsoidal horizontal burrows, with structureless burrow fill similar to the enclosing rock. Burrows are 3-5 mm in diameter, maximum length up to 5 cm, and display incised wall striations, majority crossing each other, with individual striae forming acute angle with the axis of the burrow. Preserved in positive and negative hyporelief and positive epirelief.
Remarks: *Spongeliomorpha* occurs in nonmarine and marine sediments, and has been commonly reported from lake-margin deposits of the Newark basin (Metz, 1993a, 1993b, 1995, 1996). Suggested tracemakers for *Spongeliomorpha* include sponges (Saporta, 1887), callianassid excavations (Fürsich, 1973), algae (Darder, 1945), other crustaceans (Calzada, 1981; D'Alessandro and Bromley, 1995), and other arthropods, including, probably insects (Bromley and Asgaard, 1979; Metz, 1993a). Four ichnospecies have been assigned to *Spongeliomorpha*: *S. iberica* Saporta 1887, *S. carlbergi* Bromley and Asgaard, 1979 (see Ekdale et al., 1984; Bromley and Asgaard, 1991), *S. milfordensis* Metz 1993a, and *S. sicula* D'Alessandro and Bromley 1995. The first three ichnospecies differ from each other by the orientation of the striations, while *S. sicula* in contrast, display ovoid chambers above branching points (D'Alessandro and Bromley, 1995).

Ichnogenus *Treptichnus* Miller 1889
***Treptichnus bifurcus* Miller 1889**
Figure 2D

Description: Straight to curved horizontal burrows, 1 mm in diameter, with short projections, 1-2 mm in length, having thickened knob-like terminations extending from junctures between longer segments, creating a zigzag pattern. Preserved in concave and convex hyporelief.
Remarks: Maples and Archer (1987) emended the original description of *Treptichnus* while Buatois and Mángano (1993a) provided a thorough reevaluation of the ichnotaxon. Where the burrow segments of *T. bifurcus* are straight, projections occur on alternate sides, where curved, projections occur on outside of curved portion. Projections represent bedding plane indications of oblique shafts (Maples and Archer, 1987; Buatois and Mángano, 1993a).

Ichnogenus *Treptichnus* Miller 1889
***Treptichnus pollardi* Buatois and Mángano 1993a**
Figure 2E

Description: Trace fossil consisting of zigzag, curved, or straight burrow segments with small pits, indicating openings of vertical shafts situated either at junction between, or at some position within individual segments. Diameter of segments 0.5-1.0 mm; length of segments 4-32 mm. The maximum number of burrow segments is 8, most systems have 5 or less. Some burrow segments have short projections at junctures, similar to *T. bifurcus*. Specimens preserved in convex hyporelief.
Remarks: The presence of number of burrow segments, pits, burrow diameter, and range of segment length compare well to *T. pollardi* from Carboniferous lacustrine deposits of Argentina (Buatois and Mángano, 1993a). Occurring in nonmarine and marine strata, *Treptichnus* likely represents a feeding structure produced by insect larvae or vermiform animals (Tessier et al., 1995; Buatois and Mángano, 1998). This is the third reported occurrence of *T. pollardi* in North America, all within strata of the Newark basin (see Metz, 1995, 1996a, 1996b).

Paired Trails
Figure 2F

Description: Straight to gently winding parallel ridges preserved in positive hyporelief. Ridges lack ornamentation and can be traced up to 5 cm. Internal width of the ridges ranges from 2.5-5.0 mm; external width ranges from 3.5-6.5 mm.
Remarks: These traces resemble *Diplopodichnus biformis* which has been interpreted as a locomotion trace (Brady, 1947). However, due to the lack of ornamentation (e.g., punctuate markings, striae), a median furrow (Keighley and Pickerill, 1997) or small appendage imprints, the author prefers to retain these specimens in open nomenclature. The trace is likely attributable to a worm-like or arthropod form or gastropod trail.

Unidentified Trackway
Figure 2G

Description: Single, simple, straight to slightly curved trackway, 8 mm in width, approximately 9 cm long, comprising two rows of linear traces elongated parallel to direction of movement. Preserved in concave epirelief.
Remarks: Interpreted as trackway of an insect.

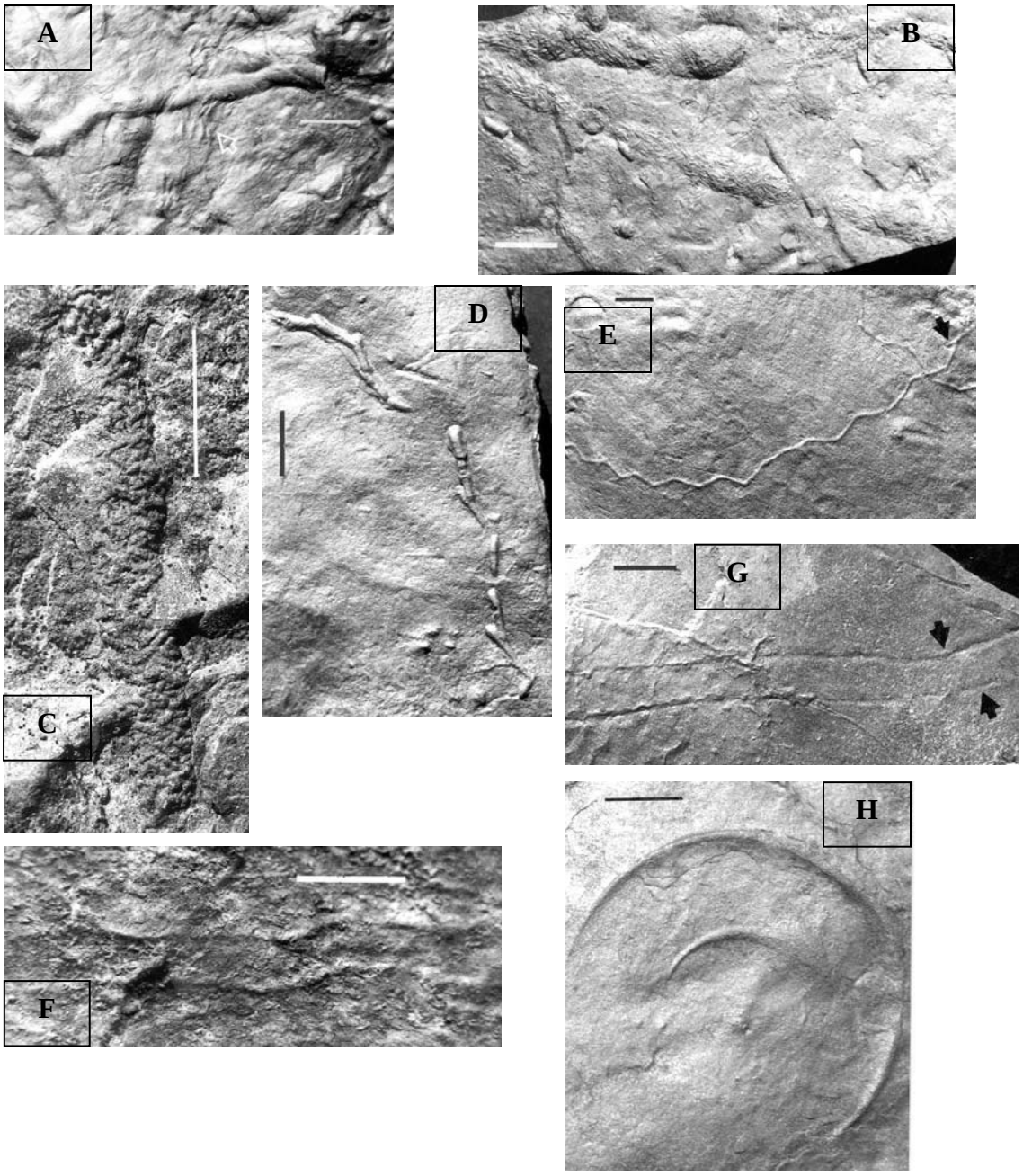

Figure 2. Ichnotaxa of the *Scoyenia* ichnocoenosis. A. *Planolites beverleyensis* crossed by a later formed *Scoyenia* (arrow). Scale = 5 mm. B. *Scoyenia gracilis*. Scale = 1 cm. C. *Spongeliomorpha milfordensis*. Scale = 1 cm. D. *Treptichnus bifurcus*. Scale = 1 cm. E. *Treptichnus pollardi* illustrating zigzag burrow segments with pits, occasional transition to *T. bifurcus* (arrow), as well as crossovers. Scale = 1 cm. F. Paired trails. Scale = 1 cm. G. Unidentified trackway likely formed by an insect. Scale = 1 cm. H. Scratch circles, likely formed by a plant. Scale = 5 mm. A-F, H preserved in convex hyporelief, G preserved in concave epirelief. After Metz, 1991, 1996a, 1996b, 2000.

Scratch Circles
Figure 2H

Description: Two partial scratch circles preserved in convex hyporelief. Maximum diameter of the outer scratch circle is 22 mm. At the center of the circles is a narrow, filled tube interpreted to have been occupied previously by a plant stem. Plant fragments were found at the same level as the scratch circles. In addition, evidence of desiccation cracks and drag marks is present on the same surface as the scratch circles.
Remarks: Based on bedding types, lithology, and associated sedimentary structures, and previous work by Olsen (1980b) and Gallagher (1983), the scratch circles are interpreted as having formed on an ancient floodplain, perhaps close to a natural levee. Shallow migrating streams in this region were subject to periodic heavy rains. Subsequently, sediments eroded from upland sources were carried by these swollen streams onto the floodplain. Water currents may have partially jarred the plant stem, while the plant leaves etched out impressions of partial scratch circles as they were swirled around on the sediment surface of the floodplain. At the same time, inorganic grains and/or plant fragments moved by the currents across this surface grooved it, forming drag marks. Eventually, a thin veneer of mud was deposited, filling the scratch circles and drag marks. Subsequent drying formed desiccation cracks.

DISCUSSION

Seilacher (1967) designated the *Scoyenia* ichnofacies to represent characteristic ichnotaxons found in nonmarine sandstones and shales. Seilacher (1987) noted, however, that a problem existed in identifying nonmarine conditions. As such, redbeds commonly exhibited a low diversity of trace fossils, not one of which was by itself suggestive of nonmarine conditions. Frey et al. (1984) implied that the *Scoyenia* ichnofacies was but one of a wide range of feasible trace fossil assemblages that existed under nonmarine conditions. Furthermore, they noted that the *Scoyenia* ichnofacies be limited to one characterized by a relatively low diversity of traces formed in wet or moist lake or stream sediment intermittently exposed to air. In contrast, Buatois and Mángano (1995) proposed the *Mermia* ichnofacies to characterize a moderate to high diversity of trace fossils associated with well-oxygenated, low-energy lake bottoms. This ichnofacies typified stable conditions, although periodic disruptions by underflow or turbidity currents might occur. As such, a pre-event trace fossil assemblage may be replaced by a post-event, low diversity opportunistic suite. Investigation of Newark basin strata has commonly produced trace fossil assemblages indicative of the *Scoyenia* ichnofacies. Interestingly, in one study (Metz, 2000), the ichnotaxa and their associated traces, as well as a distinctive lack of meniscate burrows strongly suggested comparison to the *Mermia* ichnofacies. In contrast, however, the Passaic deposits exhibited evidence of subaerial exposure (e.g., raindrop impressions, desiccation cracks). This is not intended to imply that the *Mermia* ichnofacies should be extended to include post-depositional conditions.

The trace fossils detailed in this report are associated largely with reddish brown, sporadically green to gray, mudstones, siltstones, and fine-grained sandstones. Associated sedimentary structures commonly include raindrop impressions, desiccation cracks, ripple marks, tool marks, and cross-bedding. Field evidence indicates that flood-plains with their associated puddles and ponds, newly exposed lake-margins, and shallow water

deposits yield the greatest diversity and abundance of trace fossils. These paleoenvironments offered optimum conditions for inhabitation and tracemaking by a variety of opportunistic organisms, particularly arthropods (e.g., insects, insect larvae). Interestingly, however, the greatest diversity of these traces is found associated with a limited number of bedding surfaces. Thus, while under modern conditions, one can view a plethora of traces being formed in the above environments, preservation is far from automatic. Experience has shown, particularly for surficial traces (e.g., trails), that subsequent desiccation is needed to provide hardening of the sediment. In turn, to avoid reworking and destruction of the trace, sediment influx during rainstorms provides a cover for potential trace fossil preservation.

ACKNOWLEDGMENTS

I particularly thank Paul E. Olsen for the sheer amount of time and effort he has provided to me in discussions over the years, without which, this research could not have been completed. I also thank the Geological Association of New Jersey for offering me the opportunity to contribute this paper.

REFERENCES CITED

Aceñolaza, F.G., and Buatois, L.A., 1993, Non marine perigondwanic trace fossils from the Late Paleozoic of Argentina: Ichnos, v. 2, p.183-201.

Boyer, P.S., 1979, Trace fossils *Biformites* and *Fustiglyphus* from the Jurassic of New Jersey: New Jersey Academy of Science, v. 24, p. 73-77.

Brady, L.F., 1947, Invertebrate tracks from the Coconino Sandstone of northern Arizona: Journal of Paleontology, v. 21, p. 466-472.

Bromley, R.G., and Asgaard, U., 1979, Triassic freshwater ichnocoenoses from Carlsberg Fjord, East Greenland: Palaeogeography, Palaeoclimatology, Palaeoecology: v. 28, p. 39-80.

Buatois, L.A., and Lopez Angriman, A.O., 1992, The ichnology of a submarine braided channel complex: the Whisky Bay Formation, Cretaceous of James Ross Island, Antarctica: Palaeogeography, Palaeoclimatology, Palaeoecology, v. 94, p. 119-140.

Buatois, L.A., and Mángano, M.G., 1993a, The ichnotaxonomic status of *Plangtichnus* and *Teptichnus*: Ichnos, v. 2, p. 217-224.

Buatois, L.A., and Mángano, M.G., 1993b, Trace fossils from a Carboniferous turbiditic lake: Implications for the recognition of additional nonmarine ichnofacies: Ichnos, v. 2, p. 237-258.

Buatois, L.A., and Mángano, M.G., 1995, The paleoenvironmental and paleoecological significance of the lacustrine *Mermia* ichnofacies: an archetypical subaqueous nonmarine trace fossil assemblage: Ichnos, v. 4, p. 151-161.

Buatois, L.A., and Mángano, M.G., 1998, Trace fossil analysis of lacustrine facies and basins: Palaeogeography, Palaeoclimatology, Palaeoecology, v. 140, p. 367-382.

Buatois, L.A., Mángano, M.G., Wu, X., and Zhang, G., 1996, Trace fossils from Jurassic turbidites of the Anyao Formation (central China) and their environmental and evolutionary significance: Ichnos, v. 4, p. 287-303.

Buatois, L.A., Jalfin, G., and Aceñolaza, F.G., 1997, Permian nonmarine invertebrate trace fossils from southern Patagonia, Argentina: Journal of Paleontology, v. 71, p. 324-336.

Calzada, S., 1981, Revisión del icno *Spongeliomorpha iberica* Saporta, 1887 (Mioceno de Alcoy, España): Boletin de la Real Sociedad Española de Historia Natural (Geologica), v.79, p. 189-195.

Chamberlain, C.K., 1971, Morphology and ethology of trace fossils from the Quachita Mountains, southeastern Oklahoma: Journal of Paleontology, v. 45, p. 212-246.

Chamberlain, C.K., 1975, Recent lebensspuren in nonmarine aquatic environments, *in* Frey, R.W., ed., The study of trace fossils: Springer-Verlag, New York, p. 431-458.

Crimes, T.P., 1970, Trilobite tracks and other trace fossils from the Upper Cambrian of North Wales: Geological Journal, v. 7, p. 47-67.

Crimes, T.P., and Anderson, N.M., 1985, Trace fossils from Late Precambrian-Early Cambrian strata of southeastern Newfoundland (Canada): temporal and environmental implications: Journal of Paleontology, v. 59, p. 310-343.

D'Alessandro, A., and Bromley, R.G., 1995, A new ichnospecies of *Spongeliomorpha* from the Pleistocene of Italy: Journal of Paleontology, v. 69, p. 393-398.

D'Alessandro, A., Ekdale, A.A., and Picard, M.D., 1987, Trace fossils in fluvial deposits of the Duchesne River Formation (Eocene), Uinta Basin, Utah: Palaeogeography, Palaeoclimatology, Palaeoecology, v. 61, p. 285-301.

Dam, G., 1990, Taxonomy of trace fossils from the shallow marine Lower Jurassic Neill Klinter Formation, East Greenland: Bulletin of the Geological Society of Denmark, v. 38, p. 119-144.

Darder, B., 1945, Estudio geológico del sur de la provincial de Valencia y norte de la Alicante: Boletin del Instituto Geológico y Minero de España, v. 57, p. 59-362.

Eagar, R.M.C., Baines, J.G., Collinson, J.D., Hardy, P.G., Okolo, S.A., and Pollard, J.E., 1985, Trace fossil assemblages and their occurrence in Silesian (Mid-Carboniferous) deltaic sediments of the Central Pennine Basin, England, *in* Curran, H.A., ed., Biogenic structures: their use in interpreting depositional environments: Society of Economic Paleontologists and Mineralogists Special Publication 35, p. 99-149.

Ekdale, A.A., Bromley, R.G., and Pemberton, S.G., 1984, Ichnology. The use of trace fossils in sedimentology and stratigraphy: Society of Economic Paleontologists and Mineralogists, Short Course 15, 317 p.

Fillion, D., 1989., Les critères discriminants à l'intérieur du triptyque *Palaeophycus-Planolites-Macaronichnus.* Essai de synthèse d'un usage critique: Comptes rendus de l'Académie des Sciences de Paris, Série 2, v. 309, p. 169-172.

Fillion, D., and Pickerill, R.K., 1990, Ichnology of the Upper Cambrian? to Lower Ordovician Bell Island and Wabana groups of eastern Newfoundland, Canada: Palaeontographica Canadiana, v. 7, p. 1-119.

Fregenal Martinez, M.A., Buatois, L.A., and Mángano, M.G., 1995, Invertebrate trace fossils from Las Hoyas fossil site (Serrania de Cuenca, Spain), Paleoenvironmental interpretations: Extended Abstracts Second International Symposium on Lithographic Limestones, Lleida-Cuenca, p. 67-70.

Frey, R.W., 1973, Concepts in the study of biogenic sedimentary structures: Journal of Sedimentary Petrology, v. 43, p. 6-19.

Frey, R.W., Pemberton, S.G., and Fagerstrom, J.A., 1984, Morphological, ethological, and environmental significance of the ichnogenera *Scoyenia* and *Ancorichnus*: Journal of Paleontology, v. 58, p. 511-528.

Fürsich, F.T., 1973, A revision of the trace fossils *Spongeliomorpha, Ophiomorpha,* and *Thalassinoides*: Neues Jahrbach für Geologie und Paläeontologie, Monatshefte, 1973, p. 719-735.

Gallagher, W.B., 1983, Paleoecology of the Delaware Valley region Part 1: Cambrian to Jurassic: The Mosasaur, v. 1, p. 23-42.

Gierlowski-Kordesch, E., 1991, Ichnology of an ephemeral lacustrine/alluvial plain system: Jurassic East Berlin Formation, Hartford Basin, USA: Ichnos, v. 1, p. 221-232.

Glaesser, M.F., 1969, Trace fossils from the Precambrian and basal Cambrian: Lethaia, v. 2, p. 369-393.

Gluszek, A., 1995, Invertebrate trace fossils in the continental deposits of an Upper Carboniferous coal-bearing succession, Upper Silesia, Poland: Studia Geologica Polonica, v. 108, p. 171-202.

Hakes, W.G., 1977, Trace fossils in Late Pennsylvanian cyclothems, Kansas, *in* Crimes, T.P., and Harper, J.C., eds., Trace fossils 2: Geological Journal, Special Issue 9, p. 209-226.

Han, Y., and Pickerill, R.K., 1995, Taxonomic review of the ichnogenus *Helminthopsis* Heer1877 with a statistical analysis of selected ichnospecies: Ichnos, v. 4, p. 83-118.

Häntzschel, W., 1975, Trace fossils and problematica, *in* Teichert, C., ed., Treatise on invertebrate paleontology, part w, miscellanea, supplement 1: Geological Society of America and University of Kansas Press, Boulder, Colorado and Lawrence, Kansas, W269 p.

Hasiotis, S.T., 2002, Continental trace fossils: Society of Economic Paleontologists and Mineralogists Short Course Notes No. 51, 132 p.

Hitchcock, E., 1858, Ichnology of New England. A report on the sandstone of the Connecticut Valley, especially its footprints: W. White, Boston, 220 p.

Hofmann, H.J., and Patel, I.M., 1989, Trace fossils from the type Etcheminian Series (Lower Cambrian Ratcliffe Brook Formation), Saint John area, New Brunswick, Canada: Geological Magazine, v. 126, p. 139-157.

Hoffman, H.J., Cecile, M.P., and Lane, L.S., 1994, New occurrences of *Oldhamia* and other trace fossils in the Cambrian of the Yukon and Ellesmere Island, artic Canada: Canadian Journal of Earth Sciences, v. 31, p. 767-782.

Howard, J.D., and Frey, R.W., 1975, Estuaries of the Georgia coast, U.S.A.: sedimentology and biology. II Regional animal-sediment characteristics of Georgia estuaries: Senckenbergiana Maritima, v. 7, p. 33-103.

Howard, J.D., and Frey, R.W., 1984, Characteristic trace fossils in nearshore to offshore, Upper Cretaceous of east-central Utah: Canadian Journal of Earth Science, v. 21, p. 200-219.

James, J.F., 1885, Fucoids of the Cincinnati Group: Cincinnati Society of Natural History Journal, v. 7, p. 151-166.

Jensen, S., 1997, Trace fossils from the Lower Cambrian Mickwitzia sandstone, south-central Sweden: Fossils and Strata, v. 42, p. 1-110.

Keighley, D.G., and Pickerill, R.K., 1995, The ichnotaxa *Palaeophycus* and *Planolites*:

historical perspectives and recommendations: Ichnos, v. 3, p. 301-309.
Keighley, D.G., and Pickerill, R.K., 1997, Systematic ichnology of the Mabou and Cumberland groups (Carboniferous) of western Cape Breton Island, eastern Canada, 1: burrows, pits, trails, and coprolites: Atlantic Geology, v. 33, p. 181-215.
Książkiewicz, M., 1977, trace fossils in the flysch of the Polish Carpathians: Paleontologica Polonica, v. 36, p. 1-200.
MacNaughton, R.B., and Pickerill, R.K., 1995, Invertebrate ichnology of the nonmarine Lepreau Formation (Triassic), southern New Brunswick, eastern Canada: Journal of Paleontology, v. 69, p. 160-171.
Mángano, M.G., Buatois, L.A., and Claps, G.L., 1995, Grazing trails formed by soldier fly larvae (Diptera: Stratiomyidae) and their paleoenvironmental and paleoecological implications for the fossil record: Ichnos, v. 4, p. 163-167.
Manspeizer, W., ed., 1988, Triassic-Jurassic Rifting, Continental Breakup and the Origin of the Atlantic Ocean and Passive Margins: Elsevier, New York, Parts A and B, 998 p.
Maples, C.G., and Archer, A.W., 1987, Redescription of Early Pennsylvanian trace-fossil holotypes from the nonmarine Hindostan Whetstone beds of Indiana: Journal of Paleontology, v. 61, p. 890-897.
Metz, R., 1987a, Insect traces from nonmarine ephemeral puddles: Boreas, v. 16, p. 189-195.
Metz, R., 1987b, Insect traces by invertebrates in aquatic nonmarine environments: Bulletin New Jersey Academy of Science, v. 32, p. 19-24.
Metz, R., 1987c, Sinusoidal trail formed by a recent biting midge (Family Ceratopogonidae): trace fossil implications: Journal of Paleontology, v. 61, p. 312-314.
Metz, R., 1989, *Scoyenia* ichnofacies from the Passaic Formation (Upper Triassic) near Milford, New Jersey: Northeastern Geology, v. 14, p. 29-34.
Metz, R., 1991, Scratch circles from the Towaco Formation (Lower Jurassic), Riker Hill, Roseland, New Jersey: Ichnos, v. 1, p. 233-235.
Metz, R., 1992, Trace fossils from the Lower Jurassic Towaco Formation, New Jersey: Northeastern Geology, v. 14, p. 29-34.
Metz, R., 1993a, A new ichnospecies of *Spongeliomorpha* from the Late Triassic of New Jersey: Ichnos, v. 2, p. 259-262.
Metz, R., 1993b, Ichnology of the Boonton Formation (Early Jurassic), Rockaway River, Boonton, New Jersey: Northeastern Geology, v. 15, p. 170-175.
Metz, R., 1995, Ichnologic study of the Lockatong Formation (Late Triassic), Newark Basin, southeastern Pennsylvania: Ichnos, v. 4, p. 43-51.
Metz, R., 1996a, Newark Basin ichnology: the Late Triassic Perkasie Member of the Passaic Formation, Sanatoga, Pennsylvania: Northeastern Geology and Environmental Sciences, v. 18, p. 118-129.
Metz, R., 1996b, Nonmarine trace fossils from the Late Triassic and Early Jurassic of New Jersey: Bulletin New Jersey Academy of Science, v. 41, p. 1-5.
Metz, R., 1998, Nematode trails from the Late Triassic of Pennsylvania: Ichnos, v. 5, p. 303-308.
Metz, R., 2000, Triassic trace fossils from lacustrine shoreline deposits of the Passaic Formation, Douglassville, Pennsylvania: Ichnos, v. 7, p. 253-266.

Michaelis, H., 1972, Die Lebensspur einer Dipterenlarve im Dünensand: Natur und Museum, v. 102, p. 421-424.

Miller, G.D., 1986, The sediments and trace fossils of the Rough Neck Group on Cracken Edge, Derbyshire: Mercian Geologist, v. 10, p. 189-202.

Miller, W. III, 1993, Trace fossil zonation in Cretaceous turbidite facies, northern California: Ichnos, v. 3, p. 11-28.

Miller, M.F., and Knox, L.W., 1985, Biogenic structures and depositional environments of a Lower Pennsylvanian coal-bearing sequence, northern Cumberland Plateau, Tennessee, U.S.A: *in* Curran, H.A., ed., Biogenic structures: their use in interpreting depositional Environments: Society of Economic Paleontologists and Mineralogists Special Publication 35, p. 67-97.

Moussa, M.T., 1970, Nematode fossil trails from the Green River Formation (Eocene) in the Uinta Basin, Utah: Journal of Paleontology, v. 44, p. 304-307.

Narbonne, G.M., and Aitken, J.D., 1990, Ediacaran fossils from the Sekwi brook area, Mckenzie Mountains, northwestern Canada: Palaeontology, v. 33, p. 945-980.

Olsen, P.E., 1977, Stop 11-Triangle Brick Quarry, *in* Bain, G.L., and Harvey, B.W., eds., Field guide to the geology of the Durham Basin: Carolina Geological Society Fortieth Anniversary Meeting, p. 59-60.

Olsen, P.E., 1980a, The latest Triassic and early Jurassic formations of the Newark basin (eastern North America, Newark Supergroup): stratigraphy, structure, and correlation: Bulletin New Jersey Academy of Science, v. 25, p. 25-51.

Olsen, P.E., 1980b, Triassic and Jurassic formations of the Newark basin, *in* Manspeizer, W., ed., Field studies of New Jersey geology and guide to field trips: 52nd annual meeting of the New York State geological association: Rutgers University, Newark, p. 2-39.

Olsen, P.E., 1985, Distribution of organic-matter-rich lacustrine rocks in the early Mesozoic Newark Supergroup, *in* Robinson, G.R., and Froelich, A.J., eds., Proceedings of the second U.S. Geological Survey workshop on the Early Mesozoic basins of the eastern United States: United States Geological Survey Circular 946, p. 61-64.

Olsen, P.E., 1988, Paleontology and paleoecology of the Newark Supergroup (early Mesozoic, Eastern North America), *in* Manspeizer, W., ed., Triassic-Jurassic rifting, continental breakup and the origin of the Atlantic Ocean and passive margins: Elsevier, New York, Parts A and B, p. 185-230.

Olsen, P.E., and Flynn, J.J., 1989, Field guide to the vertebrate paleontology of Late Triassic age rocks in the southeastern Newark basin (Newark Supergroup, New Jersey and Pennsylvania): The Mosasaur, v. 4, p. 1-43.

Olsen, P.E., Schlische, R., and Gore, P.J., eds., 1989, Tectonic, Depositional, and Paleoecological History of Early Mesozoic Rift Basins, Eastern North America: International Geological Congress Field Trip Guidebook, T-351, 174 p.

Osgood, R.G., 1970, Trace fossils of the Cincinnati area. Palaeontographica Americana: v. 6, p. 277-444.

Pemberton, S.G., and Frey, R.W., 1982, Trace fossil nomenclature and the *Planolites-Palaeophycus* dilemma: Journal of Paleontology, v. 56, p. 843-881.

Pickerill, R.K., 1981, Trace fossils in a Lower Paleozoic submarine canyon sequence-the Siegas Formation of northwestern New Brunswick, Canada: Maritime Sediments and Atlantic Geology, v. 17, p. 157-163.

Pickerill, R.K., 1992, Carboniferous nonmarine invertebrate ichnocoenoses from southern New Brunswick, eastern Canada: Ichnos, v. 2, p. 21-35.

Pickerill, R.K., 1994, Nomenclature and taxonomy of invertebrate trace fossils, *in* Donovan, S. K., ed., The palaeobiology of trace fossils: John Wiley and Sons, Chichester, p. 3-42.

Pickerill, R.K., and Peel, J.S., 1990, Trace fossils from the Lower Cambrian Bastion Formation of East Greenland: Rapport Gronlands Geologiske Undersogelse, v. 147, p. 5-43.

Pickerill, R.K., Romano, M., and Melendez, B., 1984, Arenig trace fossils from the Salamanca area, western Spain: Geological Journal, v. 19, p. 249-269.

Pickerill, R.K., Han, Y., and Jiang, D., 1998, Taxonomic review of the ichnogenus *Helminthopsis* Heer 1877 with a statistical analysis of selected ichnospecies-a reply: Ichnos:5:313-316.

Pollard, J.E., and Walker, E., 1984, Reassessment of sediments and trace fossils from Old Red Sandstone (Lower Devonian) of Dunure, Scotland, described by John Smith (1909): Geobios, v. 17, p. 567-576.

Ratcliffe, B.C., and Fagerstrom, J.A., 1980, Invertebrate lebensspuren of Holocene floodplains: Their morphology; origin and paleoecological significance: Journal of Paleontology, v. 54, p. 614-630.

Rindsberg, A.K., 1994, Ichnology of the Upper Mississippian Hartselle Sandstone of Alabama, with notes on other Carboniferous formations: Geological Survey of Alabama, Bulletin, v. 158, p. 1107.

Saporta, G., de 1887, Nouveaux documents relatifs aux organisms pronlématiques des anciennes mers: Société Géologique de France Bulletin, Séries 3, v. 15, p. 286-302.

Sarkur, S., and Chaudhuri, A.K., 1992, Trace fossils in Middle to Late Triassic fluvial redbeds, Pranhita-Godavari Valley, south India: Ichnos, v. 2, p. 7-19.

Schäfer, W., 1972, Ecology and Palaeoecology of Marine Environments: University of Chicago Press, Chicago, 568 p.

Seilacher, A., 1967, Bathymetry of trace fossils: Marine Geology, v. 5, p. 413-428.

Smith, J., 1909, Upland fauna of the Old Red Sandstone Formation of Carrick, Ayrshire: Kilwinning Cross, 60 p.

Smoot, J.P., 1991, Sedimentary facies and depositional environments of early Mesozoic Newark Supergroup basins, eastern North America: Palaeogeography, Palaeoclimatology, Palaeoecology, v. 84, p. 369-423.

Smoot, J.P., and Olsen, P.E., 1988, Massive mudstones in basin analysis and paleoclimatic interpretation of the Newark Supergroup, *in* Manspeizer, W., ed., Triassic-Jurassic rifting, continental breakup and the origin of the Atlantic Ocean and passive margins: Elsevier, New York, Parts A and B, p. 250-274.

Tessier, B., Archer, A.W., Lanier, W.P., and Feldman, H.R., 1995, Comparison of ancient tidal rhythmites (Carboniferous of Kansas and Indiana, USA) with modern analogues (the Bay Mont-Saint Michel, France), *in* Fleming, B.W., and Bartholomä, A., eds., Tidal signatures in modern and ancient sediments: International Association of Sedimentologists Special Publication 24, p. 259-271.

Tevesz, M.J.S., and McCall, P.L., 1982, Geological significance of aquatic nonmarine trace fossils, *in* McCall, P.L., and Tevesz, M.J.S., eds., Animal-sediment relations: Plenum Press, New York, p. 257-285.

Turner, B.R., and Benton, M.J., 1983, Paleozoic trace fossils from the Kufra Basin, Libya: Journal of Paleontology, v. 57, p. 447-460.

Uchman, A., Pika-Biolzi, M., and Hochuli, P.A., 2004, Oligocene trace fossils from temporary fluvial ponds: An example from the freshwater molasses of Switzerland: Eclogae Geologicae Halvetae, v. 97, p. 133-148.

Van Houton, F.B., 1964, Cyclic lacustrine sedimentation, Upper Triassic Lockatong Formation, central New Jersey and adjacent Pennsylvania: Kansas Geological Survey Bulletin, v. 169, p. 497-531.

Van Houton, F.B., 1969, Late Triassic Newark Group, north central New Jersey and adjacent Pennsylvania and New York, *in* Subitzky, S., ed., Geology of selected areas in New Jersey and eastern Pennsylvania: Rutgers University Press, New Brunswick, New Jersey, p. 314-347.

Walker, E., 1985, Arthropod ichnofauna of the Old Red Sandstone at Dunure and Montrose, Scotland: Transactions of the Royal Society of Edinburgh: Earth Sciences, v. 76, p. 287-297.

Wetzel, A., and Bromley, R.G., 1996, Re-evaluation of the ichnogenus *Helminthopsis*-a new look at the type material: Palaeontology, v. 39, p. 1-19.

Wetzel, A., Kamelger, A., and Bromley, R.G., 1998, Taxonomic review of the ichnogenus *Helminthopsis* Heer 1877 with a statistical analysis of selected ichnospecies-a discussion: Ichnos, v. 5, p. 309-312.

White, C.D., 1929, Flora of the Hermit Shale, Grand Canyon, Arizona: Carnegie Institute of Washington Publication 405, p. 1-221.

Young, F.G., 1972, Early Cambrian and older trace fossils from the southern Cordillera of Canada: Canadian Journal of Earth Sciences, v. 9, p. 1-17

AN INTERPRETATIVE ANALYSIS OF THE SEDIMENTARY FABRIC REPRESENTED IN AN APPROXIMATELY 84-METER CORE RECOVERED FROM THE PASSAIC FORMATION IN CENTRAL-EASTERN, NEW JERSEY

John A. Anton
Hudson Environmental Services, Inc.
4 Mark Road, Suite C
Kenilworth, New Jersey 07033

ABSTRACT

An interpretative analysis of sedimentary fabric recorded in an 84-meter core recovered from the Passaic Formation in Rahway, Union County, New Jersey was performed to reconstruct the represented paleoenvironments. This locality is situated proximal to the northeastern margin of the Triassic-Jurassic continental rift complex known as the Newark Basin and well described due to its exceptional documentation of geological history. The core is primarily composed of alternating shale and siltstone beds that indicate generally coarsening upward sequences characteristically associated with fluctuating water levels in lacustrine settings and prograding fluvial systems. Paleosol (e.g., brecciated mudcracks, root casts, reworked gypsum soil) and fluvial depositional features (e.g., laminae) served as marked indicators of pronounced ecological shifts in response to rift activity. Downhole geotechnical methodologies (e.g., gamma ray, electrical resistivity, etc.) were applied following core recovery to identify subtle lithologic variation and depositional cycles.

INTRODUCTION

The geologic history of New Jersey is dynamic and essential to understanding the active processes that continue to shape this planet. One of the most studied geologic features in New Jersey is the extensive Newark Basin that shares a comparably detailed history to other Triassic-Jurassic rift structures that occupy portions of the eastern North American continental margin. This structure extends westward into Pennsylvania and northward into New York and has an approximate areal extent of 7,000 square kilometers (Olsen et al., 1996). The Newark Basin approaches a total maximum thickness of five kilometers (Olsen et al., 1996) and predominantly consists of sedimentary units punctuated by mafic igneous sills and dikes. Metamorphic rock is only modestly represented throughout the Newark Basin. Unconsolidated deposits associated with the Illinoian and Wisconsinan glacial advances cover portions of the Piedmont Physiographic Province in which the Newark Basin is situated (Stanford, 2000).

The geologic formations defining the Newark Basin are well described. They provide a detailed record of the rifting event that resulted as the African and North American plates separated. The Newark Basin is interpreted as a half-graben (Olsen, et al., 1996; Schlische, 1991, 1995b) that preferentially received sediment from the African plate owing to the basin's westward dip.

The goal of this study was to reconstruct the paleoenvironments recorded in an 84-meter core performed in the Passaic Formation of the Newark Basin. This formation is one of several late Triassic-early Jurassic sedimentary units that preceded the deposition of mid-Cretaceous deposits comprising New Jersey's Coastal Plain.

DATA COLLECTION

A two-tiered approach was applied to data collection. The initial phase entailed continuous rock coring at a site located in the southern portion of Rahway, Union County, New Jersey (Figure 1). The boring was advanced to 92.6 meters below grade using a Mobile B-90 drill rig equipped with a NQ-2 wireline system to recover a five-centimeter diameter core. Coring was conducted in 1.52- meter intervals and commenced 8.8 meters below grade following the installation of temporary casing to compensate for 7.6 meters of overlying glacial till and 1.2 meters of regolith.

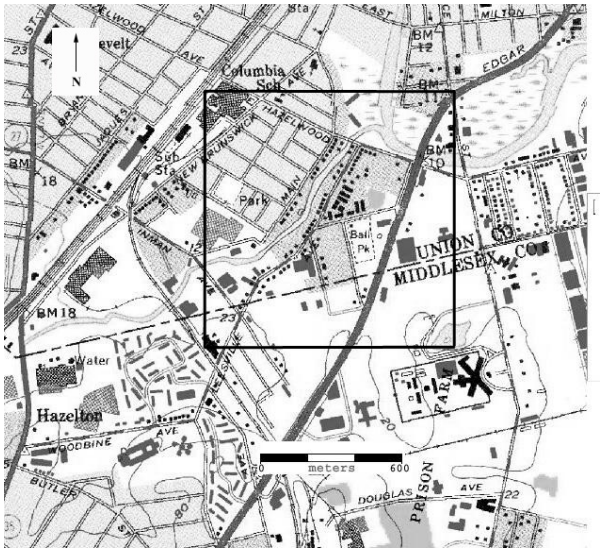

Figure 1. The study area was located in Rahway, Union County, New Jersey at approximately 40°35'51" N latitude and 74°16'31" W longitude. USGS 7.5'x7.5' Rahway, N.J. Map, 1981.

The core was photographed, logged (Figure 2) and boxed for reference. Logging included documentation of standard characteristics including color, fractures, bedding planes, lithology, and stratigraphic features.

The second phase of the investigation involved employing various geotechnical methodologies to the borehole proper to complement the data amassed by visual core inspection. Geotechnical parameters included caliper, resistivity, and natural gamma radiation measurements among others that are part of a larger scale study and not pertinent to the discussion at hand.

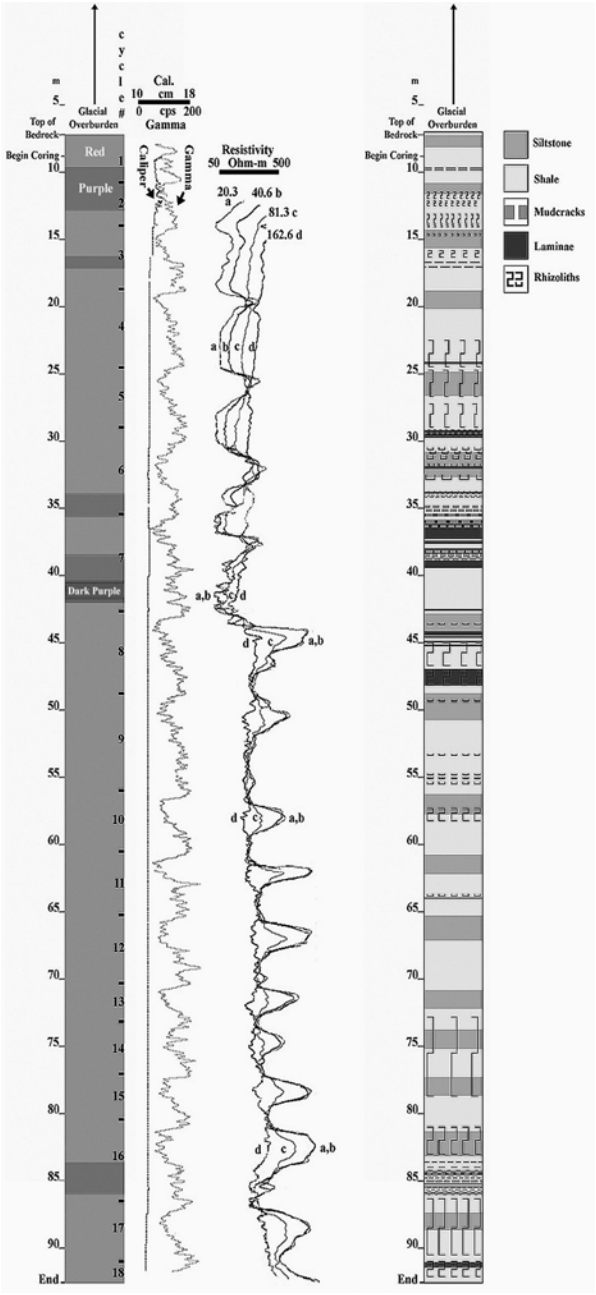

Figure 2. Generalized Geologic Log. Note the change in average grain size recorded in cycle #8 and maintained through cycle #1. Units are as stated.

Caliper Measurements

Three-arm caliper measurements were conducted using a MGX digital logging system manufactured by the Mount Sopris Instrument Company, to identify changes in borehole width attributable to degree of rock competency and possible lithologic variation. The same equipment was used throughout the geotechnical investigation except where noted. Likewise, data collection was performed at a frequency of one measurement

per five centimeters except in the case of the optical televiewer where it was obtained at approximately 0.122-centimeter intervals.

Resistivity Measurements

Resistivity values are typically reported in ohms per meter and reflect the rudimentary properties of geologic units. Resistivity, which is essentially controlled by matrix and fluid availability, is generally considered reliable for discerning rock type and depositional cyclicity. The separation between electrodes was adjusted to collect resistivity data horizontally at distances approximately 20.3, 40.6, 81.3, and 162.6 centimeters with respect to the borehole wall. Data collected at greater distances from the borehole wall are more reflective of formation characteristics as opposed to those induced by drilling fluids that enter geological units via fractures or along bedding planes.

Gamma Ray Measurements

Relative clay content in the rock units was evaluated by measuring natural gamma radiation resulting from the decay of radioelements (e.g., potassium, thorium, and uranium) that commonly occur in fine grain sedimentary units. Data was recorded as counts per second and subsequently plotted. The plots were evaluated to determine whether depositional patterns emerged, and if so, what ecologic settings would be appropriate models for interpreting the type of paleoenvironments represented throughout the core.

Digital Optical Televiewer

Fracture and bed orientation was determined using a Robertson Geologging Micrologger System II and digital optical televiewer probe that recorded and stacked undistorted 360^{o} 24-bit color images orientated to true north. Radial resolution was limited to one degree. Only bedding information is briefly discussed herein.

FINDINGS

Description of the Core

The core is primarily composed of multiple shades of red and purple siltstone, shale and mudstone. Color diversity is chiefly attributed to various oxidation states of iron-bearing minerals. This is also manifested along select fracture zones where anaerobic conditions presumably occurred in response to historic groundwater storage. The result is the appearance of gleyed contacts (Figure 3) and precipitation of unoxidized manganese and iron minerals within fractures. In other cases lighter minerals, such as calcite, analcime, and presumably chlorite dominate as prevailing fracture precipitates. An exhaustive assessment of fracture orientation and secondary minerals was not feasible for inclusion in this paper but will be undertaken and reported separately due to time constraints and their lack of significant contribution to sedimentary fabrics.

There did not appear to be a definitive correlation between color and grain size. The range in grain size is not pronounced and one may argue with reasonable certainty that in

given circumstances transitional intervals may be classified as either siltstone or shale in the absence of grain size analysis or other appropriate quantitative validation. Consequently, geotechnical data, and more specifically, natural gamma radiation measurements proved invaluable for discerning large-scale depositional cycles and trends.

Sedimentary features were used in conjunction with data obtained from geotechnical methods for reconstructing the paleoenvironments represented in the core. Such features included brecciated mudcracks

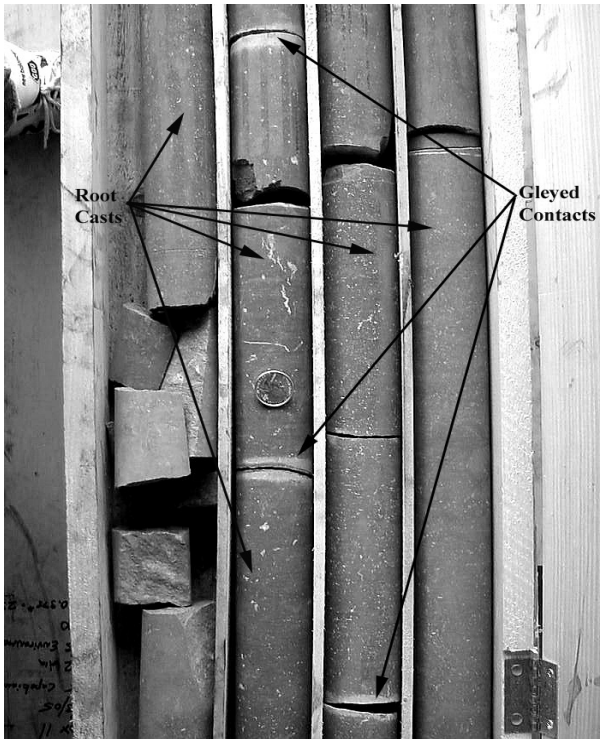

Figure 3. Gleyed staining indicates that anaerobic conditions formerly prevailed along specific fracture zones. The quarter's position corresponds to 59.4 meters below grade.

and laminae (Figure 4), rhizoliths (Figure 5), reworked gypsum soil (Figure 6), and banding (Figure 7). The presence of mudcracks superimposed on banded strata was of particular interest because the latter is *typically* associated with relatively quiet (e.g., low energy) depositional regimes reflective of deep lacustrine settings. It is also noteworthy that the majority of the core exhibited mineralized rhizoliths (e.g., "root casts"), the significance of which will be discussed later. Secondary minerals generally account for less than 15 percent of the rock composition at any given interval (Figure 3), but are fairly persistent throughout much of the core. In some cases, open (e.g., non-mineralized) channels prevail at former root sites. These features have the potential to complicate groundwater flow modeling even when fracture orientation, depth, and frequency are well established. In rare cases, the organic matter has maturated into coal (Figure 8).

Figure 4. The brecciated mudcracks (right) and complex fracture (left) occur at 38.7 meters and 41.7 meters below grade, respectively. Scale indicated by quarter.

Cyclosedimentologic signatures were not readily discernable based solely on visual inspection of the core due to the noted limited range of grain size observed throughout the column and the extended intervals over which grading occurs (e.g., several meters). Instead, an alternate approach was employed to reveal depositional cycles in the absence of obvious sedimentological markers. The method entailed placing preferential emphasis on the occurrence of stratigraphic and biotic features.

The brecciated mudcracks, laminae, and rhizoliths occurred persistently throughout the core. Solution features, small concretions (<5 mm diameter), and reworked gypsum paleosols were also identified but collectively constituted only a minor (<5%) core fraction. Significant color variation was also observed (e.g., shades of red and purple) and evaluated for cyclic expression.

The occurrence of the three dominant features (e.g., mudcracks, laminae, and rhizoliths) was plotted against each other to identify paleoenvironmental relationships with the anticipation that a distinct depositional frequency would emerge. Color transition (e.g., red versus purple matrices) was also graphed in this manner to ascertain whether it was tied to depositional nodes or secondary in nature. The graph is presented as Figure 9 and depicts the relationship between these features.

The results indicate that paleoecological criteria are reliable cycle indicators in the absence of strong sedimentological markers and therefore suitable for reconstructing feasible environmental relationships. The case for using this approach in cycle identification is supported in several ways.

First, the reoccurrence of these three individual features throughout the rock core were markedly similar. (They each occurred approximately 30 times over the 84-meter section.) Secondly brecciated mudcracks, when they occurred, were typically associated

with laminated intervals (Figure 9). Finally, rhizoliths and mudcracks occurred at distinct intervals with regard to each other indicating strong climatic controls over the paleoenvironment.

The data also indicated flora was well established, exhibited a propensity for flourishing, and that it dominated the landscape in this region of the Newark Basin. There was no obvious relationship between rhizoliths and laminae despite the benefits derived from the influx of transported inorganic nutrient ions. However, as noted, flora was sensitive to extreme changes in water availability (Figure 9) but not exclusively in regard to drought as periods of flooding also significantly impacted its ability to take root.

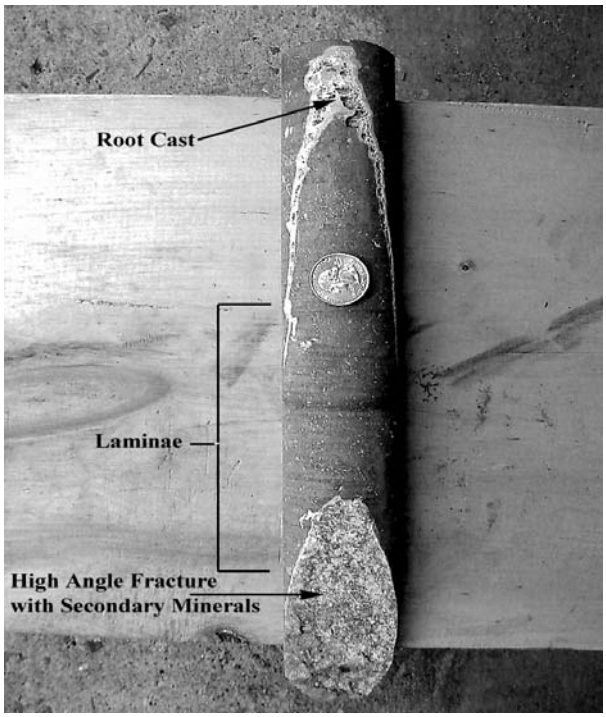

Figure 5. Root casts and banded laminae. The top of this core section represents 63.8 meters below grade. The core width is five centimeters and the quarter is for reference.

As for color, the data indicates that there is no coherent correlation between depositional regime and oxidation state (Figure 9). Initially it was unclear whether changes in oxidation states were also manifested as cycles, reflective of fluctuations in redox conditions through time (e.g., secondarily imposed), or of another origin. The purple coloration did not consistently correspond with deeper water settings. This observation is pertinent with respect to the subject core as data collected at other localities may yield considerable correlations relating to depth.

However, purple hues loosely correlate with the finer fraction (e.g., shale) of the sedimentological cycles as supported by the natural gamma radiation data (Figure 1). The implication is that redox markers may simply be secondary and contrived. Grain size may exert respectable constraints on mineralogic staining and induce coloration not necessarily complimentary of depositional regimes. Consider that fine-grained material, such as the clay minerals composing the shale, have the potential to starve the matrix of

oxygen due to their structure. The clay grains may have re-orientated themselves in response to burial pressure by uniformly flattening with time thereby promoting reducing conditions and creating the resultant purple hue.

Figure 6. Reworked gypsum soil. Arrowed region was recovered from 82.9 meters below grade. Each core is five centimeters in diameter.

The proposition that purple shades are in specific cases secondarily imposed within the rock matrix at this location is further substantiated by the presence of brecciated mudcracks (Figure 4) and carbonized roots (Figure 8) occupying these zones. An alternate explanation for the color shift is more appropriately presented under the discussion portion of this paper.

There are other remarkable examples where redox markers do not correlate with the type of depositional environments suggested by stratigraphic features. For instance, the low energy conditions required for the banding depicted in Figure 7 to develop conflicts with the notion that the clasts were subaerially exposed as inferred by the red matrix in which

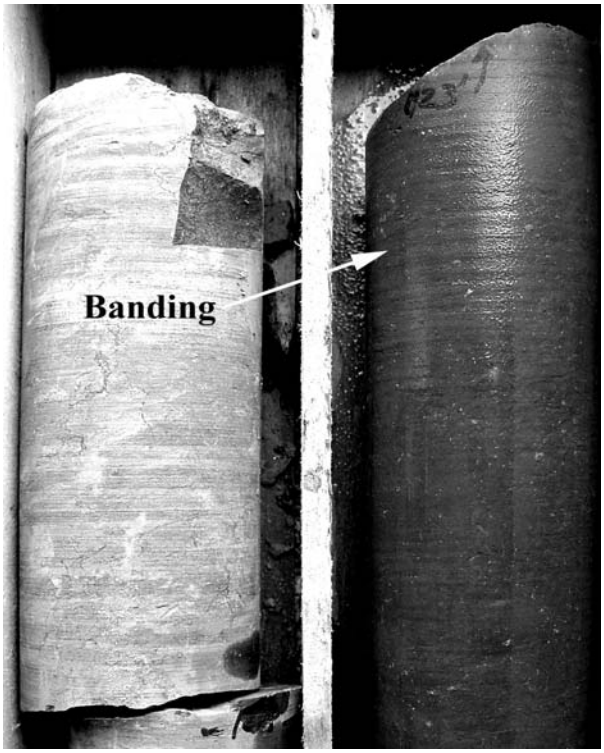

Figure 7. Banding. The cores are each five centimeters in diameter. In this section (37.5 m below grade), approximately 4.4 pairs occur within one centimeter of vertical span.

they are recorded. The banding is naturally reminiscent of non-glacial varves and routinely interpreted to reflect rapid short-term depositional fluctuation triggered by seasonal rhythms. In this case, the slightly lighter red bands are thicker (≤1.5 millimeters) and coarser (silt) than their corresponding darker clay counterparts.

Conventional thought implies that coarser laminae develop during warmer seasons when average precipitation reaches its pinnacle thereby allowing the transport of "heavier" clasts into deep lakes where they settle. The biased deposition of the finer fraction is executed during the remainder of the year when precipitation is reduced but adequate to selectively erode these particles into surface water bodies where they accumulate on the coarser grains. Deep inundated basins are ideal for preserving the advancing record of cyclic deposition in that they create a haven from disturbances spurred by more energetic environments that otherwise disrupt the their orderly appearance.

It is this aspect of the model that limits its appropriateness in explaining the seemingly opposing conditions under which sedimentation occurred based on redox and stratigraphic signatures. The formalities offered by generalized stratigraphic models dissolve in conspicuous disparities that invoke the realization of new historical perspectives without disregard or falsification of the former. The challenge that ensues when introducing alternate thought is to maintain congruency with the core premises of resolute models while adequately mitigating disparities in a manner that is both parsimonious and ubiquitous in application. An explanation for the observed paradoxes is

proposed following a discussion concerning the results of the geotechnical phase of this investigation.

Geotechnical Data

Caliper

Caliper measurements indicated that the borehole maintained a fairly consistent diameter of approximately 0.05 meters. The greatest variation occurred between 11 and 16 meters below grade where the borehole approached a maximum width of 0.1 meters. The irregularity within the given interval is attributable to weathering induced rugosity, after which the borehole diameter varied less than 10^{-3} meters.

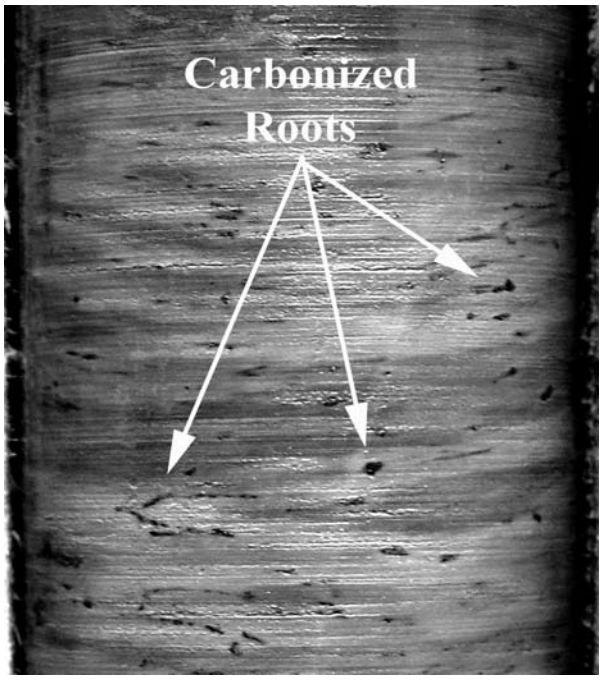

Figure 8. Carbonized roots occur in laminated purple substrate approximately 40.5 meters below grade. The core measures five centimeters in diameter.

Resistivity and Gamma Radiation

Resistivity and gamma radiation data complimented each other inversely and were paramount in identifying depositional cycles from a sedimentological perspective. Sixteen coarsening up sequences were documented (excludes two partial cycles) and each essentially represents two cycles identified using the discussed stratigraphic criteria. Certain cycles could be further subdivided depending on the criteria used for defining periodicity particularly if natural gamma radiation data receives greater attention than that afforded by other geotechnical methods. (Subdivisions may account for the additional stratigraphic cycles observed in the core.) For this paper, we will only acknowledge that finer cyclic divisions are possible and that they occur at the onset of larger cycles possibly indicating periods when depositional processes were suppressed.

Gamma radiation signatures appeared as "funnel" patterns, the boundaries of which were defined in part by electrical resistivity cycles that roughly correspond to sine functions (Figure 2). In this way, the interference posed by minor cycles was mitigated when defining boundary limits because they were solely manifested in the gamma radiation data. Cycle boundaries were rounded to the nearest foot but are summarized in Table 1 using metric notation.

#	Start	End	Δ	#	Start	End	Δ
1	?	10.7	?	10	56.1	60.6	4.5
2	10.7	14.0	3.3	11	60.6	65.3	4.7
3	14.0	18.7	4.7	12	65.3	70.3	5.0
4	18.7	24.4	5.7	13	70.3	73.2	2.9
5	24.4	29.0	4.6	14	73.2	77.2	4.0
6	29.0	35.4	6.4	15	77.2	80.3	3.1
7	35.4	42.7	7.3	16	80.3	86.5	6.2
8	42.7	48.7	6.0	17	86.5	91.0	4.5
9	48.7	56.1	7.4	18	91.0	?	?

Table 1. Summary of cycle boundaries (in meters) based on gamma radiation patterns. Cycle numbers correspond to those denoted on Figure 2.

Cycle thickness ranged between 2.9 and 7.4 meters. Additional work is required to determine whether these depositional sequences represent Van Houten cycles (Van Houten, 1980). No obvious pattern emerged with regard to cycle *thickness*, which should not be mistakenly correlated with depositional periodicity. However, the conspicuous increase in electrical resistivity and corresponding decrease in gamma radiation observed at the terminus of cycle #8 (Figure 2) indicates a 'sustained', but presumably not permanent trend from finer to coarser sedimentation. A distinct and persistent change in deposition pattern alludes to the signature of a large-scale cycle, only a portion of which is recorded in this particular core.

Such changes typically occur basin wide since they are driven by astronomically induced climate variation and expressed in diverse ways, the habit of which are dictated by local conditions. It is also noteworthy that in specific cases, the lack of recognition of large-scale cycles may be an artifact of core length or the type of cycle represented.

The gamma radiation signatures observed in the core are similar to those resulting from prograding fluvial systems or fluctuating water levels in lacustrine settings and will be discussed later.

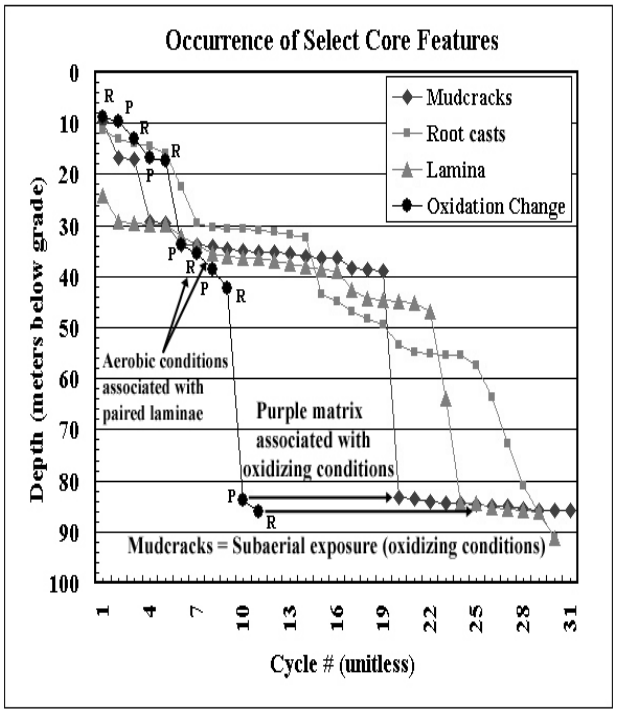

Figure 9. The recurrence of dominant features is highly cyclic. A close relationship exists between the appearance of mudcracks and laminae. Flora proliferated between dry episodes. Redox changes are not tied to paleoenvironment conditions. (R = red matrix; P = purple matrix). The cycle numbers denote the number of times a given feature occurs in the core. Correlations between features are identified along the abscissa as exemplified by the arrows.

Optical Televiewer

The Optical Televiewer recorded a continuous set of digital images throughout the borehole that provided raw data used for determining strike and dip of fracture sets and bedding surfaces. This paper does not discuss the fracture data, which is copious and to be reported independently. The Optical Televiewer did not readily identify bedding planes most likely because they exhibited relatively low dip angles (typically between 6^{o} and 19^{o}). It is particularly interesting though, that beds strike northeast-southwest and dip southeast. This trend is incongruent with reported bedding measurements in the Passaic Formation along the eastern portion of Newark Basin (Goldberg et al., 1994; Withjack and Schlische, 2002) when they are not attributable to structural influences (e.g., folding, faults, etc.). Instead, these disparities reflect locally distinct depositional processes that were operating concomitantly throughout the Newark Basin. For instance, beds associated with alluvial fans will exhibit greater dips than those resulting from flood plain deposits.

DISCUSSION

The core records alternating wet and dry cycles within this stratigraphic section of the Passaic Formation. This is a general trend documented at other localities throughout the Newark Basin and particularly within this unit. These cycles are routinely linked with the expansion and contraction of lacustrine settings during the development of the basin and controlled primarily by climate and sedimentation rates (Smoot et al., 1985).

However, local conditions were unique and mandate the development of special proposals to explain peculiarities such as the inconsistencies suggested by redox conditions and stratigraphic features. It was previously noted that reduction zones are commonly observed within stratigraphic intervals dominated by paleosols. The notion that grain size may force secondary redox conditions to overwrite primary markers was proposed earlier in this paper.

Another viable possibility is that the mineralogic staining observed in the core denotes regional redox conditions that are primary, atmospherically induced, and hence essentially detached from depositional processes. If changes in atmospheric character were pronounced, they would have been recorded across facies boundaries. It is noteworthy that significant atmospheric changes may be locally extensive (as opposed to global) and have the potential for altering climate.

In this case, the color changes imply fluctuating redox conditions that are not naturally assigned to isostatic adjustments, certain aspects of tectonism, or a host of other processes that affect climatic patterns. Instead, episodic outgassing may trigger them. This may be tested by tracing select purple zones throughout the basin and noting whether they transcend a wide variety of facies (e.g., deep water settings vs. paleosols) or analyzing for rare earth elements across color boundaries.

One interesting implication is that these anaerobic markers should not substantially share similar stratigraphic intervals as rhizoliths due to the assumed stress applied to flora and ensuing die-off. An exception would be at the initial onset or terminus of such conditions. This may also explain why the carbonized roots shown in Figure 8 are situated in purple matrix and the only circumstance where the two features occur together. Furthermore, low oxygen fugacity is a critical component in ensuring organic preservation. It is unlikely that natural die-off of ancient flora resulted in the development of anaerobic conditions for at least two reasons. First, the vast majority of rhizoliths occur in oxidized deposits. Secondly, low oxygen masking can be observed throughout mudcrack-bearing intervals where rhizoliths are absent.

Rhizoliths persist throughout much of the core and imply that a progressive low energy ecological setting transcended time. The late Triassic and early Jurassic landscape at this locale was quite lush and dominated by drainage systems and ephemeral ponds. The fluvial systems were shallow, exhibited low velocities, and received no influx of moderate to coarse-grained terrigenous material. Movement of turbid water through dense non-woody vegetation may have aided the development of non-paired laminae. It is perceivable that flora removed enough energy from the fluvial system during high stands to arrest saltation and force deposition of suspended loads. This explains the persistence of root casts through laminated sequences.

Soil was well aerated and possibly not transported vast distances prior to deposition due to restrictions imposed by the low energy environment. Weathering of channel banks

is evidenced by gray concretions, at least one of which contains a central carbonized root. In addition, some instances of convoluted flow were preserved in the core suggesting channel wall collapse. (The dips range from approximately 15^{o} to 35^{o} implying that the core was located fairly proximal to the source wall from which the collapsed material was derived and that the embankment was not vertically extensive.) In the most pronounced case, the matrix appears purple and may be perceived by some as indicative of an intermediate depth lacustrine setting.

Although this interpretation cannot be fully dismissed, it is more appropriate for explaining what is observed at given intervals at other core locations throughout the Newark Basin. Furthermore there are no stratigraphic or geophysical indicators supporting that a lake had developed immediately prior to the convoluted interval. Regardless, either interpretation suggests that water depth increased. Interestingly, the laminae in the purple matrix consist of variegated shades of red, purple, and gray once again suggestive of secondary redox controls that responded to slight variations of porosity and permeability and therefore oxygen availability.

Gray coloration suggests amplified anaerobic conditions prevailed but were extremely limited. In other studies, there is a correlation with deep lacustrine settings (Olsen et al., 1996). At this locality, the gray color results from oxygen depletion spurred by decaying organic detritus except when it occurs along structural joints. This position is supported by several observations including the presence of the mentioned concretions and solution features. Solution features are fairly limited in extent, occur as gray features set in red silty or clayey matrix, and commonly depict a vertical component indicative of movement in that aspect. They are believed to have formed in response to the decay of shallow pockets of organic material that prompted severely limited anaerobic conditions. (These areas may have experienced temporal flooding and represented throughout the region as vernal ponds or shallow lakes that expanded and contracted regularly.)

The gases that were produced as by-products of decay were the possible agents for the tendency of these structures to move upward. The highly oxidizing nature and tropical setting under which the Passaic Formation was laid down encouraged rapid organic decay such that reducing conditions would not sufficiently endure. The deficiency of gray hues throughout the core (e.g., <1% of core coloration) is testament to this. In the last case, the gray coloration pertains to reducing conditions associated with certain fracture sets and is not pertinent to this study.

Paired laminae are distinct from those induced or influenced by flora and intriguing due to their regularity and association with aerobic depositional conditions. These laminae are also unique in that no other observed stratigraphic feature is aligned with them or contributed to their formation. This uniqueness though does not require an elaborate explanation.

Both parts of each cycle are composed of fine detritus indicating that they were deposited under relatively quiet conditions. The interpretation of a fluvial depositional environment is favored over a lacustrine- based one for reasons posed earlier. Sedimentation rates are by and large higher in large rivers than lakes and the former promotes greater oxygen mixing without necessarily causing disturbances to accumulating sediments. The added dimension though in this case is the occurrence of paired laminae. A rapid sustained change in depositional energy is a criterion for their

formation. A deep lake can satisfy this criterion if sedimentation is strongly tied to seasonal variation.

But other low energy processes are equally capable of producing paired laminae. One such candidate is tides (Lobo et al., 2003). The implication of transient estuarine driven environments is tantalizing because it may signal the processes leading to the establishment of the Atlantic Ocean in the mid-Jurassic. Emerson (1898a) and Russell (1892) presented a similar proposal although it was too broad in its application. Even so, it is noteworthy that the identification of a given historic event or process may substantially post-date the initiation of same. From a geologic perspective, not much time separates the potential appearance of estuaries in the early Jurassic from indisputable evidence documenting the Atlantic Ocean's presence in the mid-Jurassic. Furthermore, the thickness of laminae defining each cycle is rather diminutive and would represent extraordinary low annual deposition rates if so interpreted. Rather, each half cycle may represent a tidal high and low and therefore record a lunar influence. No inferences are made to suggest that all cycles are preserved in the intervals yielding them.

Another noteworthy point is that paired laminae only occur sporadically throughout the core. This may indicate that the creation of the Atlantic Ocean within the rift basin met early opposition from sedimentation and the noted dry episodes. This would explain the appearance and subsequent loss of estuaries until the time that rifting advanced to a level where the ocean became established (e.g., middle Jurassic). Alternating wet and dry periods are atypical for equatorial regions unless they are located in continental interiors as in the case of the Newark Basin during the late Triassic and early Jurassic.

Currently, tropical wet and dry climates develop approximately 10^{o} poleward of the equator and may serve as a climatic analog for the *pattern* of alternating wet and dry periods observed in the core. In the latter case, the extended alternating wet and dry episodes may reflect climatic adjustments following major faulting events following incremental extension. The adjustments would presumably induce orographic effects and thereby alter long-term precipitation patterns.

CONCLUSIONS

The paleoenvironments represented in this cored interval of the Passaic Formation are more readily expressed cyclostratigraphically than sedimentologically due principally to constraints on clast range. Geotechnical methods proved invaluable in identifying depositional cycles (including portions of large scale ones indicative of basin wide ecological shifts) and complimented those recoded as dominant reoccurring stratigraphic features. This region of the Newark Basin experienced cyclic wet and dry periods that affected the expansion and contraction of shallow lacustrine and prograding fluvial systems. The landscape was exceeding lush during wet episodes and interrupted by climatic change possibly spurred by orographic effects and outgassing. Select fluvial systems appear tidally influenced potentially signaling the initiation of processes preceding the birth of the Atlantic Ocean in the mid-Jurassic.

REFERENCES

Emerson, B. K., 1898a, Geology of Old Hampshire County Massachusetts, comprising Franklin, Hampshire, and Hampden Counties: United States Geological Survey Monograph 29, 790 p.

Goldberg, D.; Reynolds, D.; Williams, C.; Witte, W. K.; Olsen, P. E.; and Kent, D. V., 1994, Well logging results from the Newark Rift Basin Coring Project: Scientific Drilling, v. 4, nos. 4-6, p. 267-279.

Lobo, F.J., Dias, J.M.A., Gonzalez, R., Hernandez-Molina, F.J., Morales, J.A., and Diaz Del Rio, V., 2003, High-Resolution Seismic Stratigraphy of a Narrow, Bedrock-Controlled Estuary: The Guadiana Estuarine System, SW Iberia, Journal of Sedimentary Research, v. 73, No. 6, p. 973-986.

Olsen, P. E.; Kent, D. V.; Cornet, B.; Witte, W. K.; and Schlische, R. W., 1996, High-resolution stratigraphy of the Newark rift basin (early Mesozoic, eastern North America): Geological Society of America Bulletin, v. 108, no. 1, p. 40-77.

Russell, I. C., 1892, Correlation papers. The Newark System: United States Geological Survey Bulletin 85, 344 p. (Conn. area on p. 80-82, 98-107; Index and bibliography, p. 131-339).

Schlische, R. W., 1991, Half-graben filling models: Implications for the evolution of continental extensional basins: Basin Research, v. 3, p. 123-141.

Schlische, R. W., 1995b, Geometry and origin of fault-related folds in extensional settings: American Association of Petroleum Geologists Bulletin, v. 79, no. 11, p. 1661-1678.

Smoot, J.P., and Olsen, P.E., 1985, Massive Mudstones in Basin Analysis and Paleoclimate Interpretation of the Newark Supergroup, in Robinson, G.R. and Froelich, A.J., eds., Proceedings of the Second United States Geological Survey Workshop on the Early Mesozoic Basins of the Eastern United States: U.S., Geological Survey Circular 946, p. 29-33.

Stanford, S. 2000, Overview of the Glacial Geology of New Jersey in "Glacial Geology of New Jersey, Field Guide and Proceedings of the Seventeenth Annual Meeting of the Geological Association of New Jersey."

Van Houten, F. B., 1980, Late Triassic Part of the Newark Supergroup, Delaware River Section, West Central New Jersey, in Manspeizer, W., ed. Field Studies of New Jersey Geology and Guide to Field Trips: New York Geological Association, 52nd Annual Meeting, Newark, New Jersey, Rutgers University, p. 264-269.

Withjack, M. and Schlische, R. W., 2002, Rift-Basin Structure and its Influence on Sedimentary Systems. Sedimentation in Continental Rifts. Society for Sedimentary Geology Special Publication No. 73.

JOINTS AND VEINS IN THE NEWARK BASIN, NEW JERSEY IN REGIONAL TECTONIC PERSPECTIVE

Gregory C. Herman
N.J. Geological Survey
P.O. Box 427
Trenton, N.J. 08625
greg.herman@dep.state.nj.us

ABSTRACT

Late Triassic and Early Jurassic bedrock in the Newark basin is pervasively fractured as a result of early Mesozoic rifting and subsequent wrench faulting of the eastern North American margin. Systematic sets of tectonic extension fractures, including ordinary and mineralized joints, are arranged in structural arrays having the geometry of normal dip-slip shear zones. Together with complimentary sets of cross fractures, they contributed to crustal stretching, sagging, and eventual faulting of the thick pile of basin rift deposits. Extension fractures developed during rifting stages of the basin display progressive linkage and spatial clustering that probably controlled incipient fault growth. They cluster into three prominent strike sets correlated to early- (S1, about 30^{o}E to N60^{o}E), intermediate- (S2, about N15^{o} to N30^{o}E), and late-stage (S3, about N-S) stretching events in the basin. Extension fractures display three-dimensional spatial variability but consistent geometric relations. S1 fractures are unevenly distributed throughout Late Triassic sedimentary strata and occur in conjunction with border faults and subparallel segments of intrabasin faults. They are locally folded normal to bedding owing to sedimentary compaction during lithification and show complex vein and vein-cement morphologies. They also show geometric interaction with subsequent S2 extension fractures. Such fractures parallel Early Jurassic igneous dikes around the SW part of the basin and cut Early Jurassic basalt and diabase farther to the NE in New Jersey. S2 and S3 fractures locally terminate against preexisting S1 fractures and commonly have fibrous-calcite vein cements in the Passaic Formation. S2 fractures are most pervasive in intrabasin fault blocks in conjunction with subparallel fault segments of the Flemington, Hopewell, and New Brunswick fault systems. The S2 extension phase marks a period of accelerated stretching and large-scale faulting of Early Mesozoic strata with highest strains in the center of the basin. S2 fractures are transitional in orientation to S3 extension fractures that cluster near tip lines of intrabasin faults in the NE. S3 fractures locally terminate against both earlier sets. Other sets of prominent, E-W striking S3 extension fractures are aligned across strike at high angles to all earlier sets. These cross fractures (S3C sets) formed late in areas where block faults with S2 transform and oblique normal slip components were inverted with opposing slip during later crustal compression and uplift of the continental margin. Both S2 and S3 phase brittle faults extend into and involve surrounding bedrock of the older continental interior and younger oceanic margin. The geometry, spatial distribution, and morphology of the extension fractures indicate progressive counterclockwise rotation of the regional, principal extension axis from NW-SE during the Late Triassic to E-W after the Late Cretaceous.

S3 fractures record late stages of crustal stretching followed by compression oriented subparallel to the contemporary principal stress axis.

INTRODUCTION

Steeply dipping joints are ubiquitous in Early Mesozoic strata in the Newark basin. This article examines the morphology, mineralogy, and spatial distribution of these fractures in outcrop and the shallow subsurface in the New Jersey part of the basin. It advances the hypothesis that steeply dipping joints are primary structures developed throughout the basin's history, resulting in stretching, sagging, and eventual faulting of accumulating crustal deposits in the rift basin and deformation in adjacent parts of the continental foreland and oceanic margin. It refines some earlier work in the GANJ XVIII proceedings describing fractures as an essential part of the hydrogeological framework of bedrock aquifers in the basin (Herman, 2001). Recent subsurface mapping using a digital optical televiewer in bedrock water wells has provided unprecedented access to the three-dimensional geometry and spatial distribution of fracture systems in the shallow subsurface, and corroborates structural observations and measurements made in outcrop.

Extension fractures provide effective, secondary porosity for storing and transmitting ground water within the basin's aquifers. However, this paper's scope is limited the structural aspects of these fractures and to their tectonic implications. Their physical properties are characterized using outcrop and hand-sample relationships, microscopic petrography, and regional maps that emphasize fracture geometry and the spatial distribution of fracture sets. Other fracture systems dipping at gentle- to moderate angles stemming from post-rifting tectonic compression and inversion, exhumation, erosion, glacial rebound, and weathering are treated only briefly.

GEOLOGICAL SETTING

The Newark basin is one of a series of tectonic rift basins of Mesozoic age formed on the eastern North American plate margin during the breakup of the supercontinent Pangea preceding formation of the Atlantic Ocean basin. It covers about 7500 km^2 and extends from southern New York across New Jersey and into southeastern Pennsylvania (Figure 1). The basin is filled with Upper Triassic to Lower Jurassic sedimentary and igneous bedrock that is fractured, faulted, tilted, and locally folded (see summaries in Schlische, 1992; 2003; and Olsen et. al., 1996a).

Various tectonic models invoking multiple phases of 'rifting' and 'shifting' have been proposed to account for the physical relationships observed in Mesozoic rift basins throughout the eastern continental margin of North America (Sanders, 1963, Lindholm, 1978; Manspeizer and Cousiminer, 1988, Swanson, 1986; de Boer and Clifford, 1988; Hutchinson and Klitgord, 1988; Lucas and others, 1988; Schlische and Olsen, 1988; Schlische, 1993, Schlische, 2003). Rifting in the Newark basin region probably began during the Middle Triassic and intensified in the latest Triassic and into the earliest Jurassic as evidenced by widespread igneous activity and a marked increase in sediment-accumulation rates (de Boer and Clifford, 1988; Schlische, 1992). Tectonic deformation and synchronous sedimentation in the region continued into the Middle Jurassic when

extensional faulting and associated folding ceased. At this stage, the basin experienced a period of post-rift contraction uplift (basin inversion) and erosion similar to that of other

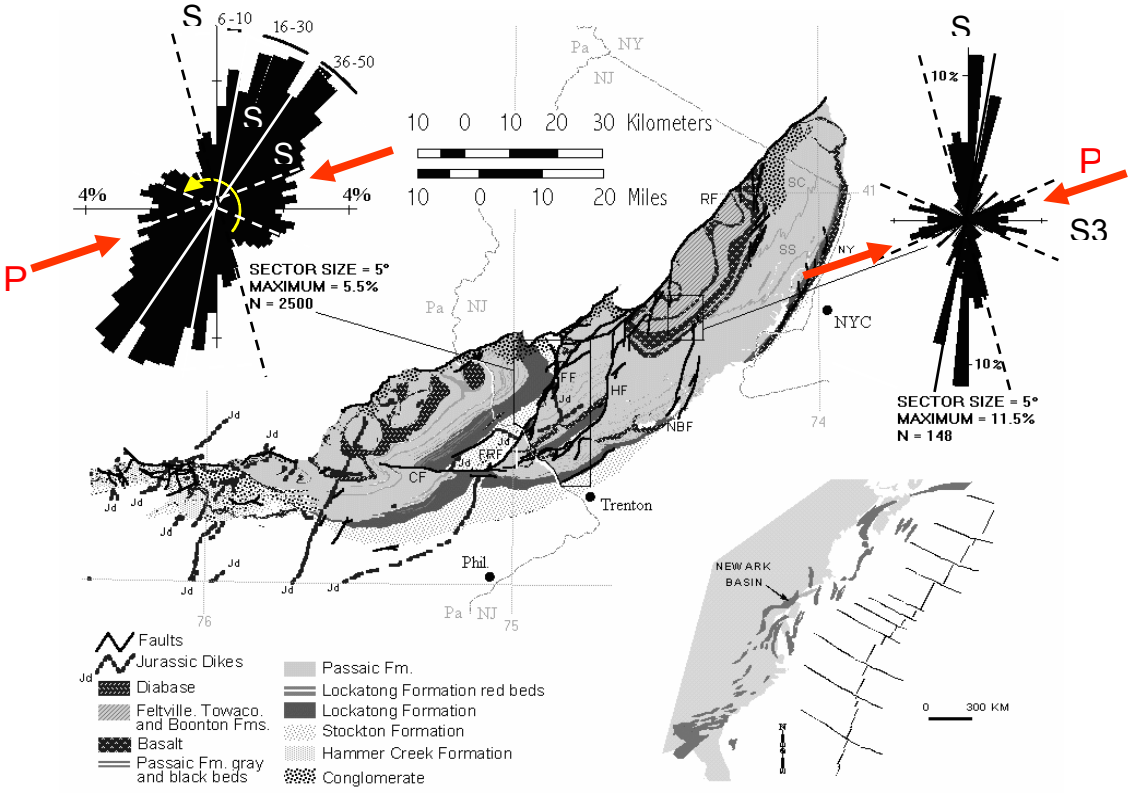

Figure 1. Bedrock geology map of the Newark basin showing faults, Jurassic dikes, and sedimentary facies compiled from geographic information system bedrock geology of New Jersey (Drake and others, 1996; Owens and others, 1998; N.J. Geological Survey, 2000), New York (Fischer and others, 1970; http://www.nysm.nysed.gov/gis/), and Pennsylvania (Berg and others, 1980; http://www.dcnr.state.pa.us/topogeo/map1/bedma.htm). The circular histogram on the left summarizes planar strike for 2500 sets of non-bedding, systematic tectonic fractures measured in about 1300 outcrops in a six-quadrangle area from the central part of the basin. These fractures in Triassic rocks predominantly strike N15°E to N50°E whereas those in younger Jurassic rocks (upper right histogram) strike more northerly (Monteverde and Volkert, 2005). Index map of Mesozoic basins on the East Coast (d) adapted from Schlische (1993). Steeply dipping joints cluster into three groups based on fracture strike and geometry including crosscutting and abutting relationships. These groups are interpreted to result from early (S1), intermediate (S2), and late (S3) phases of tectonic

Mesozoic rift basins (de Boer and Clifford, 1988; Withjack and others, 1998; Olsen and others, 1992).

DEFINITION, CLASSIFICATION, AND DESCRIPTION OF JOINTS AND VEINS

Extension fractures are crack-like discontinuities in rock that form perpendicular to the direction of maximum incremental stretching as a result of brittle or semi-brittle failure (Ramsey, 1980; Ramsey and Huber, 1983; and Figure 2). Extension fractures classify as joints when their two sides show no visible differential displacement (Mode I tensile fractures of Pollard and Aydin, 1988), as healed joints when the fracture walls are completely or partially joined together by secondary crystalline minerals, or as tectonic veins when a considerable thickness (> 1mm) of secondary minerals fills the space between fracture walls (Ramsay and Huber, 1987).

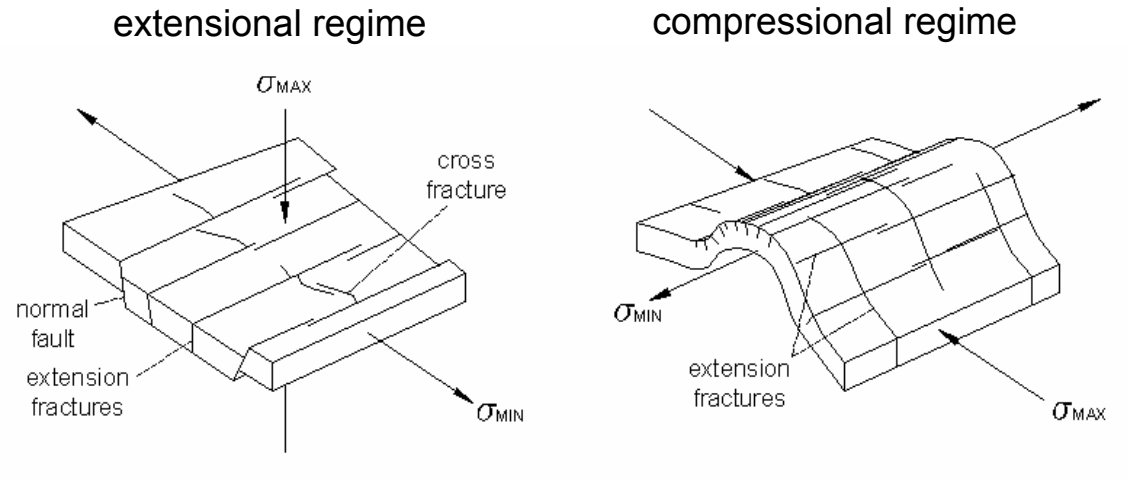

Figure 2. Block diagrams illustrating extension and cross fractures and normal faults in an extensional tectonic regime, and extension fractures in folded strata in a compressive tectonic regime; with respect to the maximum (S_{MAX}) and minimum (S_{MIN}) principal stress directions. Intermediate principal stress direction is not shown but is oriented orthogonal to the other principal stresses. S_{MAX} in the extensional regime is oriented subvertical and stems from sedimentary loading. Extension fractures in the extensional regime strike parallel to normal faults. Extension fractures in the compressional regime strike both perpendicular to and parallel to fold axes, allowing strata to be stretched both along the fold axes and in the outer arc of the fold. Note that cross fractures in the extensional regime strike subparallel to extension fractures in the compressional regime if the orientation of the principal axes remains unchanged and S_{MIN} is inverted to S_{MAX}.

In outcrop, extension fractures have elliptical surfaces (Figure 3) that are commonly straight, planar, and continuous over a distance of many meters (Figures 3 and 4). They display characteristic surface markings including plumose patterns (Figure 5), rib marks and hackles that reflect their tensile origin (Pollard and Adyin, 1988). Extension fractures are considered systematic when they occur in sets within which the fractures belonging to each set are parallel or subparallel (Hodgson, 1961). In contrast, nonsystematic extension fractures (Groshong, 1988) display more random orientations, often have curviplanar and irregular surfaces extending between and approximately normal to a systematic fracture set (Figure 6). This class of extension fracture includes cross-joints that commonly terminate against bedding and against other fractures (Hodgson, 1961). Cross fractures have comparatively little separation of fracture walls (interstices) than joints and veins and have little or no secondary mineralization.

Steeply-dipping extension fractures in igneous and sedimentary rocks throughout the Newark Basin are mapped as ordinary joints because secondary minerals that formerly cemented space between fracture walls have been removed near land surface by mineral dissolution and erosion (Herman, 2001). In excavated and cored sedimentary bedrock sampled below the weathered zone (Figure 7) fracture apertures are mostly cemented with secondary crystalline minerals (Lucas and others, 1988; Parnell and Monson, 1995; Herman, 2001). The secondary minerals include a variety of compositions and morphologies reflecting a locally variable and complex tectonic history. Vein-fill minerals include analcime, sodic feldspar (albite), potassium feldspar, calcite, gypsum, quartz, chlorite, epidote, pyrite, and relict hydrocarbons (bitumen) that generally reflect an evolved geochemical environment where early carbonate and silica cements were succeeded and locally replaced by later carbonate and sulfate cements including calcite and gypsum (Van Houten, 1964; 1965; Smoot and Olsen, 1994; Simonson and Smoot, 1994; Smoot and Simonson, 1994; Van der Kamp and Leak, 1996; El Tabakh and others, 1997; 1998). Albite (Na-feldspar) is among the early group of diagenetic cements commonly found in the Stockton Fm. and veins in the Lockatong Fm. (Figures 9a). Calcite most commonly cements fracture interstices in the Passaic Fm (Figures 8, 9b, and 10b). Calcite mineral fibers are commonly aligned perpendicular to the fracture plane and meet along a central suture line (Figure 8c, 9b, and 10b). These veins result from crystal growth from the vein wall inward toward the vein center as a result of repeated midpoint fracturing accompanying progressive dilation and crack-seal episodes (Durney and Ramsay, 1973; Groshong, 1988). Many of these veins have early albite growths on the fracture walls that are overgrown by calcite (Figure 8a). Some fibrous calcite-filled veins display twinned calcite (Figure 8a) from mechanical strain associated with localized tectonic compression. Other cements have curved and sheared fibers (Figure 8c, and Lucas and other, 1988) indicating local rotations of the incremental strain field and angular shearing postdating extension. Complex vein-fill cements have composite vein morphologies with relict grains of albite and K-spar embedded in a matrix of mosaic calcite with intergrown pyrite and bitumen (Figure 8b). Also common are veins of one strike set branching or splaying into a new strike orientation representative of later extensional phases (Figure 8a). Early veins are commonly crosscut and overprinted by younger vein sets having a different strike orientation (Figure 9b).

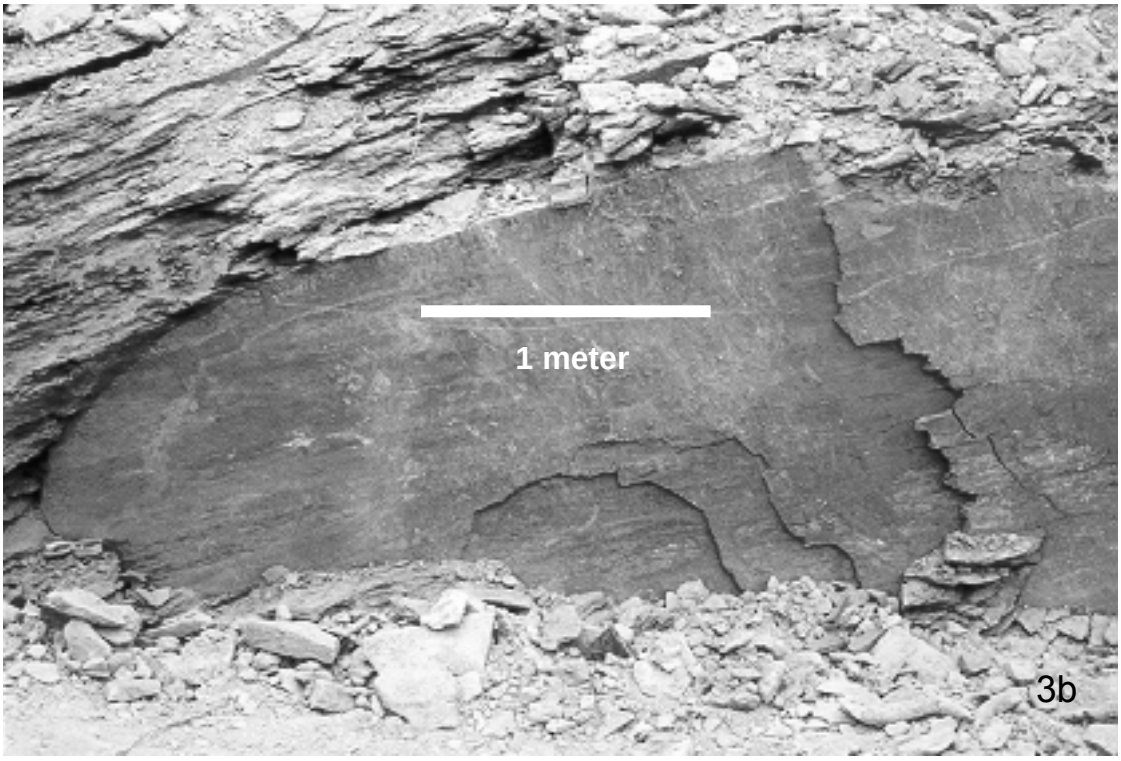

Figure 3. Extension fractures are typically mapped in outcrop as joints. They dip at high angles to bedding, occur in sets with individual fractures and have elliptical faces arranged in subparallel alignment. Photos (courtesy of Matt Muhall) show joints in red mudstone in the lower Passaic Formation from East Amwell Township, Hunterdon County.

Figure 4. Map view (above) and profile view (below) of systematic extension fractures arranged in sets with individual fractures in subparallel alignment. Extension fractures commonly terminate against beds or abrupty change orientation and inter-fracture spacing in adjacent sedimentary strata having differing mechanical properties. Top photo shows systematic joints in the Lockatong Formation in Raritan Township. Bottom photo shows joints in profile view of red mudstone and siltstone of the middle Passaic Formation, Branchburg Township (courtesy of Don Monteverde). Plastic netting on upper bench is about 1.5 m high.

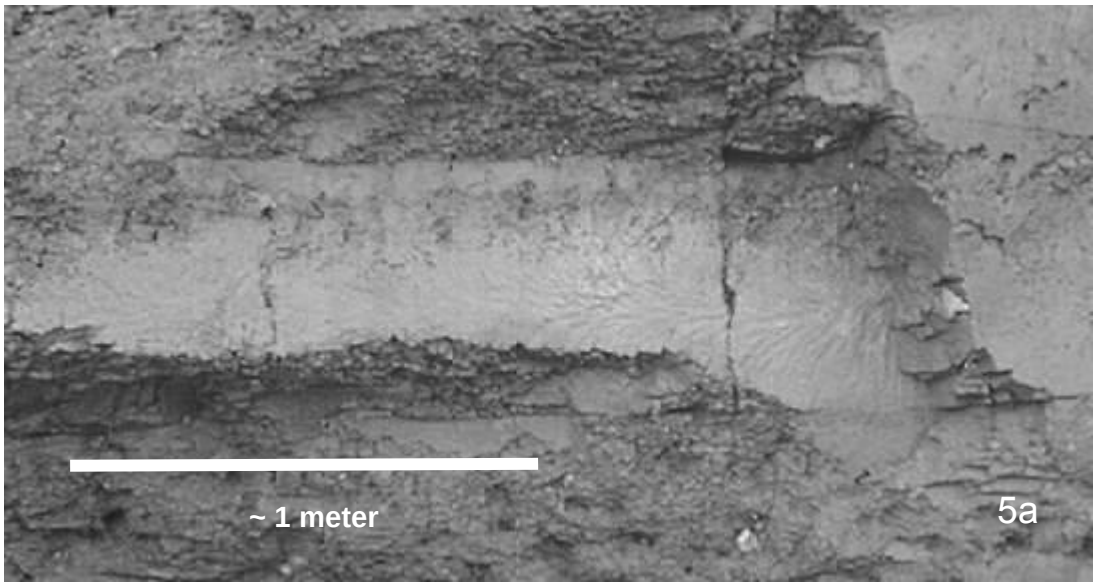

Figure 5. Extension fractures show characteristic surface markings, including plumose patterns, that indicate their tensile origin. The plume axis is commonly subparallel to the upper and lower boundaries of the rock unit it's in and fractures propagate such that plumes radiate outward from the axis (Hodgson, 1961). Top photo shows joints in red mudstone of the upper Passaic Formation from Bedminster Township, Hunterdon County. Bottom photo shows joints in early Jurassic diabase from the Pennington quarry in Hopewell Township, Mercer County.

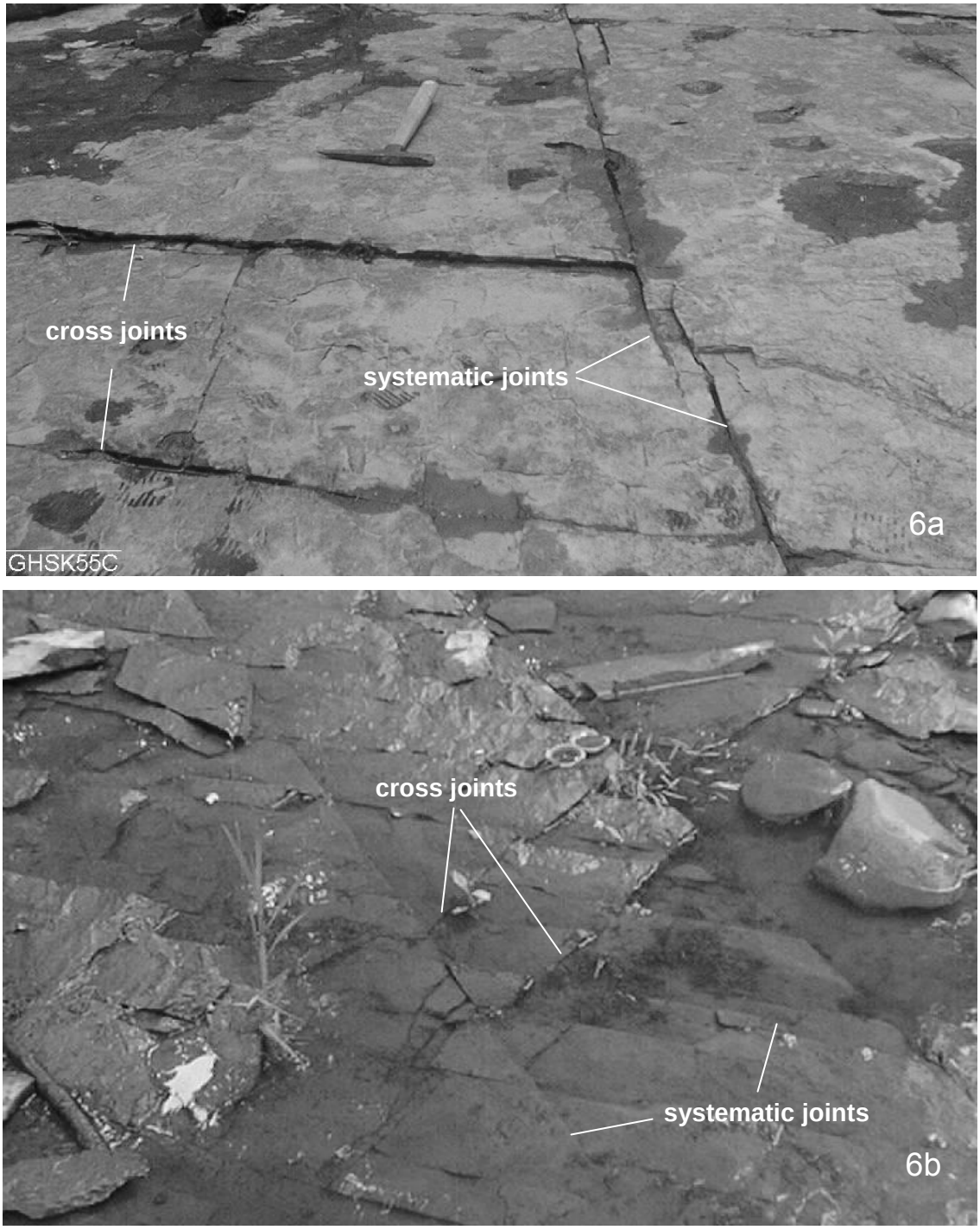

Figure 6. Nonsystematic 'cross joints' strike about perpendicular to, occur between, and terminate against, systematic extension fractures. They also are commonly curviplanar. Top photo shows systematic and cross joints in gray argillite of the Lockatong Formation in Raritan Township. Bottom photo shows two sets of crosscutting systematic fractures and cross joints in gray argillite of the Lockatong Formation in Delaware Township. Brunton compass in upper center view of bottom photo shows scale.

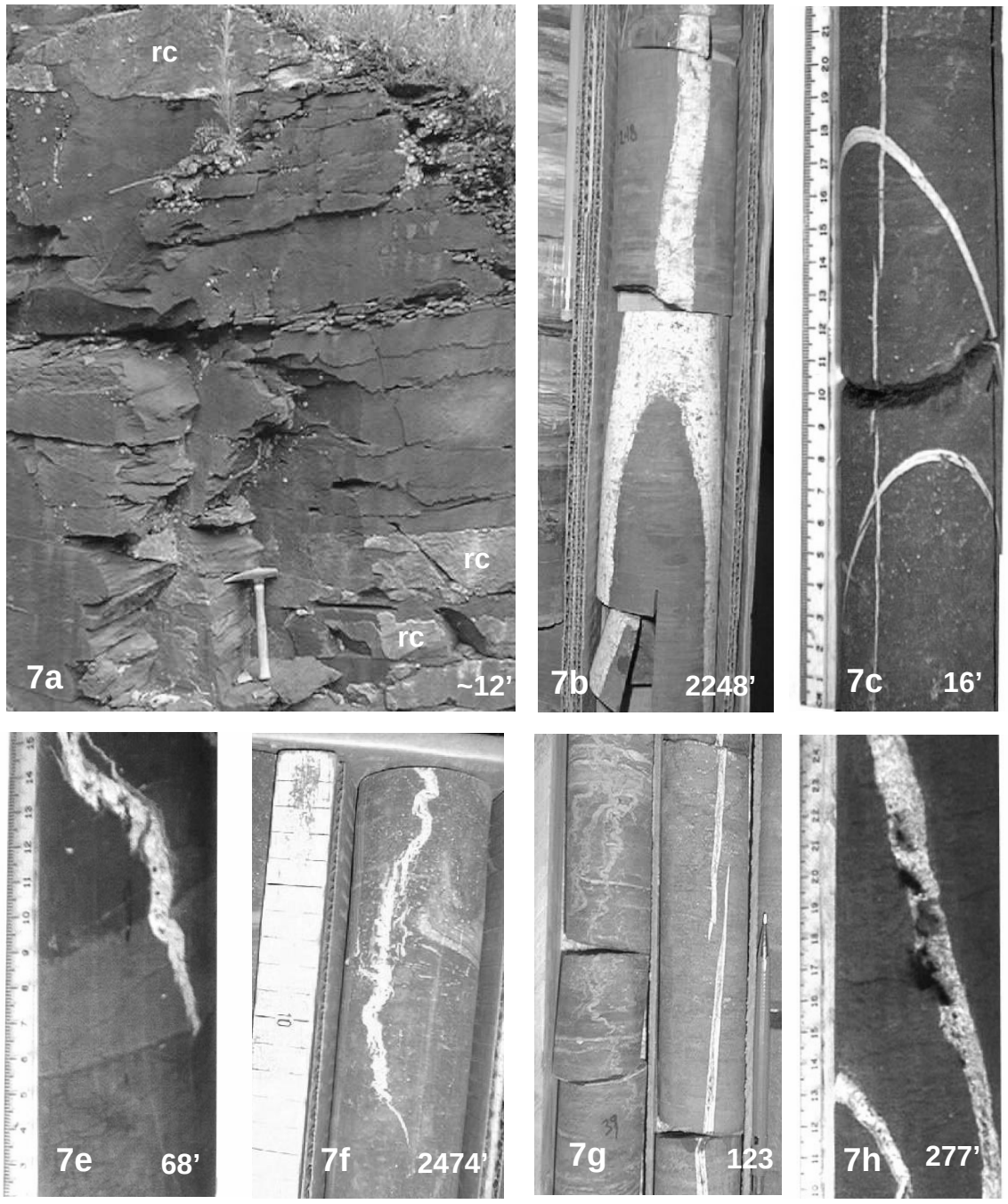

Figure 7. Extension-fracture interstices in the subsurface are cemented by secondary crystalline minerals such as calcite and classify as tectonic veins. Systematic joints mapped at the surface were also probably veins, but now appear as joints because secondary minerals were dissolved and removed, as seen in 7a and 7h, by weakly acidic ground water. Figure 7a – remnant calcite (rc) is almost entirely removed from fracture walls exposed in a railroad cut in Pennington, Mercer County. Figures 7b and 7f show veins in Passaic Formation from the Rutgers deep core (Olsen and others, 1996). Figures 7c, 7e, and 7h show veins from a 2-inch diameter core in the Passaic Formation taken by the NJGS at Hopewell. Figure 7g show veins and folded, clay-filled mudcracks in the Passaic Formation in a 2-inch diameter core from West Trenton, Mercer County. Numbers

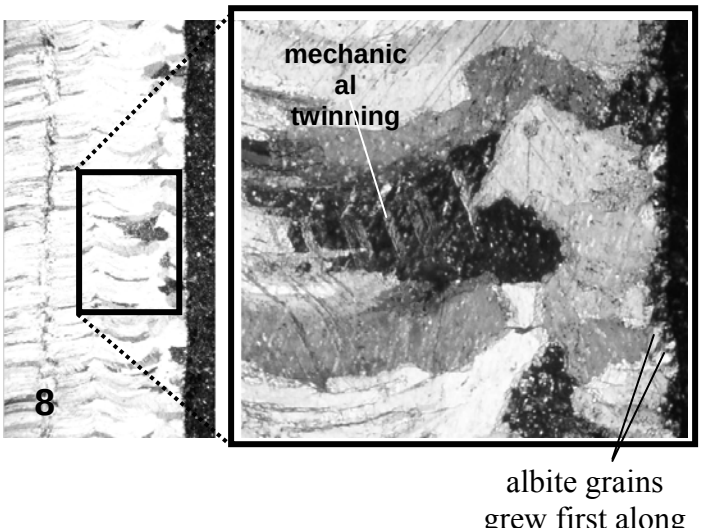

Figure 8. Examples of vein-fill morphologies. Calcite fibers (8a) postdate early albite crystal growth along the fracture walls and are locally curved and twinned. Curved fibers indicate incremental rotations of the principal extension direction and mechanical twinning indicates subsequent tectonic compression. Calcite vein in gray mudstone from the lower part of the Passaic Formation, Hopewell Township, Mercer County.

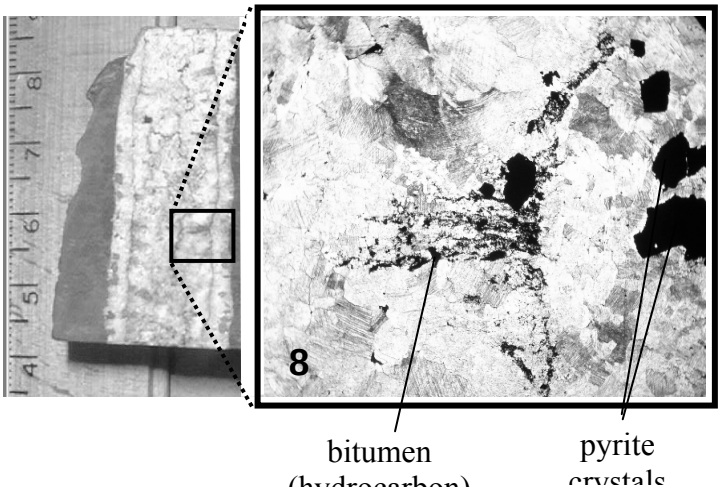

Figure 8b. Some veins are filled with mosaic calcite crystals containing interspersed sulphides (pyrite) and hydrocarbons Calcite vein in gray mudstone, Rutgers NBDCP core at 2248-foot depth. Vein fillings having multiple suture lines are evidence of 'crack-seal' growth (Ramsay, 1980) that give veins a 'banded' morphology (Wiltschko and Morse, 2001)

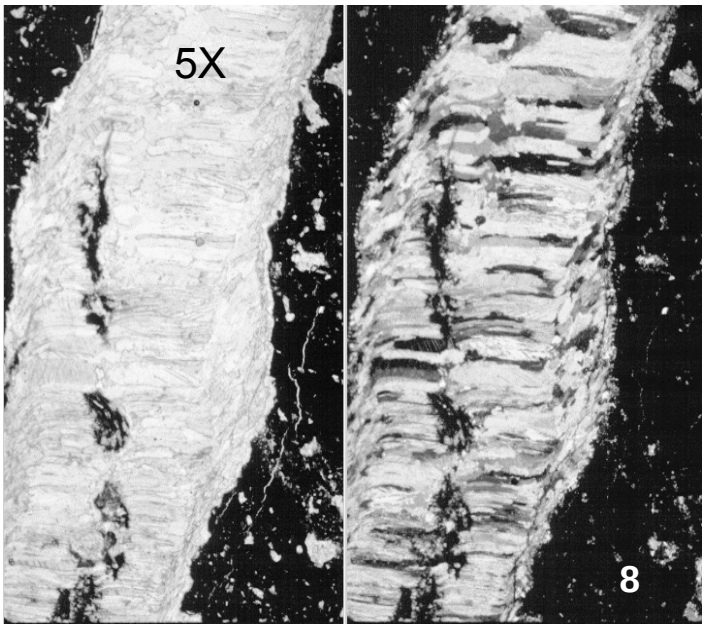

Figure 8c. Other veins have calcite fibers showing localized shearing along fracture walls and vein sutures indicating compressive shearing of earlier fabric. Sample on left shown in plane (left) and polarized (right) light

Gypsum-filled veins (Figure 9c) represent a unique class of fracture for they cut across all earlier structures and are mostly oriented sub-horizontal and orthogonal to the aforementioned tectonic extension veins. These gypsum veins show central sutures and morphologies linked to episodic growth and linkage, but are late-stage veins that may have resulted from unloading and exhumation (El Tabakh and others, 1998) or perhaps from late tectonic compression.

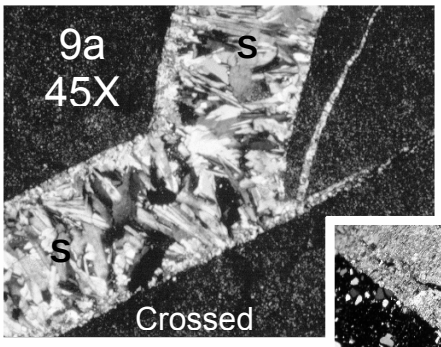

Figure 9a. S1 and S2 albite-filled veins in gray argillite of the Lockatong

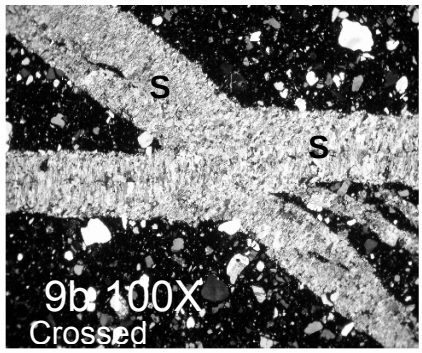

Figure 9b. S1 and S2 fibrous calcite veins in red mudstone of the Passaic Formation, Hopewell Borough, Mercer County

Figure 9. Common vein-cementing minerals include albite and calcite. Vein composition reflects host rock geochemisty. Veins in the Na- and Si-rich Locaktong Formation commonly have albite cements (Figure 9a) and veins in the Passaic Formation commonly have calcite- and gypsum-cements (Figures 9b and 9c).

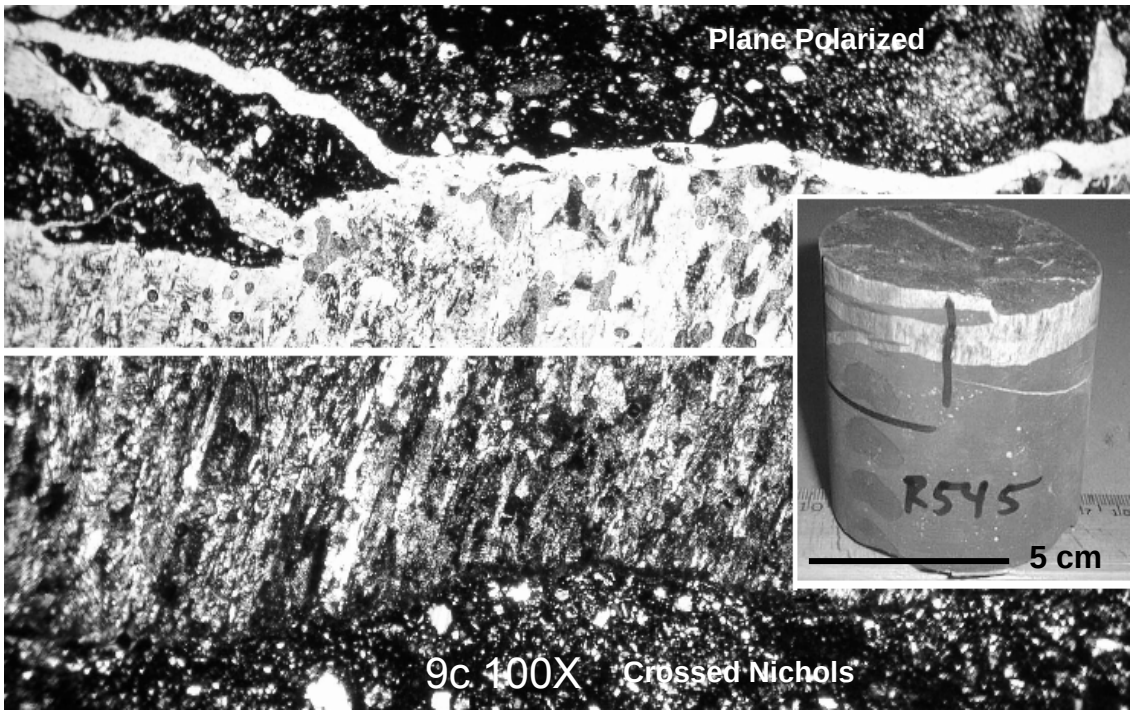

Figure 9c. Gypsum veins are late fillings, mostly oriented sub-horizontal to land surface with sub-vertical crystal fibers. Gypsum veins many centimeters thick are reported from depths exceeding 200 ft in cores from the northeast and central parts of the basin.

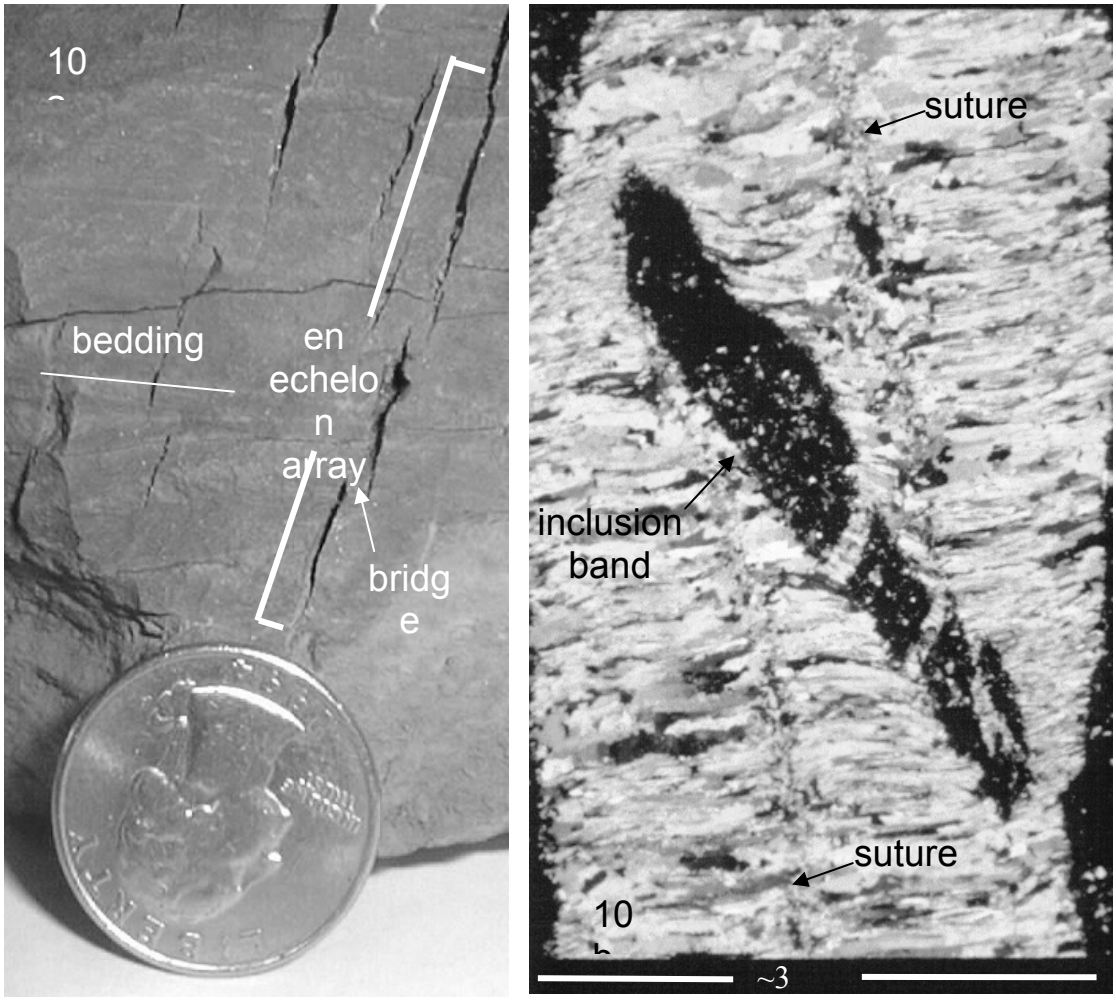

Figure 10. Tectonic veins in the Passaic Formation are commonly filled with fibrous calcite displaying medial sutures (10b) indicating synchronous filling or healing of the fracture during opening and growth. Fractures grow by linking smaller fractures; arranged in en echelon arrays (10a), into larger ones. Figure 10a is from a hand sample of red mudstone in the upper part of the Passaic Formation, Raritan Township, Hunterdon County. Photomicrograph (10b) shows details of the vein-fill morphology. The band of host rock in the central field of view shows that two fractures coalesced into one by growth and linkage; that is, bridges between separate and adjacent fractures (such as shown to the left) became engulfed and included into vein-fill complexes of larger fractures.

ATTITUDE, GEOMETRY AND DISTRIBUTION OF STEEPLY DIPPING JOINTS AND VEINS

Joints and veins mapped in a 750-sq. km. area in the central part of the basin display three strike maximums (Figure 1). The NE-SW maximum (**S1**) strikes about N36°E to N50° E, subparallel to the basin's northwestern, faulted margin. The NNE-SSW maximum (**S2**) strikes about N16° to N30 ° E subparallel to intrabasin faults and regional dikes in Pennsylvania (Figure 1). A third strike maximum (**S3**) varies from about N5 °W to N10 ° E and occurs more commonly in the eastern part of the basin in association with early Jurassic rocks (Monteverde and Volkert 2005). S1 through S3 fracture sets and their complimentary cross fractures locally occur together so that many different sets mark a single location. More commonly, only one or two steeply dipping sets fracture any single outcrop. Other gently- to moderately dipping fractures sets scattered throughout the basin include shear fractures in warped strata on faulted hanging walls; cooling and other fractures in igneous dikes, sills, and basalt flows, and opening-mode shear fractures in rocks subjected to sub-horizontal compressive stresses. Steeply dipping extension fractures and complimentary cross-joints are by far the most prevalent sets and the focus here.

S1 fractures are generally older than S2, which are older than S3. S1 veins, joints, and brittle deformation zones (Figure 11) occur in strata of Late Triassic through Early Jurassic age. S1 veins in Triassic sedimentary rocks are locally folded normal to bedding (Figures 7e and 7f) from sedimentary compaction during burial and lithification, predominantly dip about 60° to 80° southeast in strata dipping gently northwest. They also show the most complex vein-fill morphologies including crack-seal banding (Figure 7b), recrystallization of vein-fill with mosaic calcite (Figure 7b), and localized hydrothermal alteration (bleaching) of fracture walls from the reduction or removal of iron. Hydrothermal fluids convectively circulating in basin strata during the Late Triassic to Early Jurassic caused localized high-temperature (>100°C) alteration of earlier diagenetic minerals (Steckler and others, 1993; Van de Kamp and Leake, 1996).

S2 veins and cross joints are abundant in Triassic and Jurassic strata, strike NNE-SSW subparallel to the major segments of the intrabasinal fault systems and diabase dike swarms around the southwestern parts of the basin (Figure 1). They mostly dip steeply at about 70° to 80° east, and are most densely developed in the hanging walls of the Flemington and Hopewell faults (Herman, 1997). S2 veins commonly consist of fibrous calcite cements (Figures 7a, 7c, and 8b) and locally cut across (Figure 9b) and butt into S1 fractures (Herman 2001). S1 brittle deformation zones occur as strain-hardened columnar walls in early Jurassic diabase near Pennington, Mercer County (Figure 11). Later S2 fractures and shear planes cut these early structures. The structural link between S1 and S2 fractures is visible in outcrop where *en echelon* fractures with hackly surfaces and intermediate strikes bridge S1 and S2 surfaces (Figure 12). These transitional fractures propagate away from S1 crack tips and curve towards and into major S2 fracture surfaces, thereby preserving evidence of the geometric transition between the overlapping fracture sets and their relative ages. In places, S1 veins form en echelon arrays with crack tips that swing into alignment with array boundaries of later S2 fracture strikes (Figure 13).

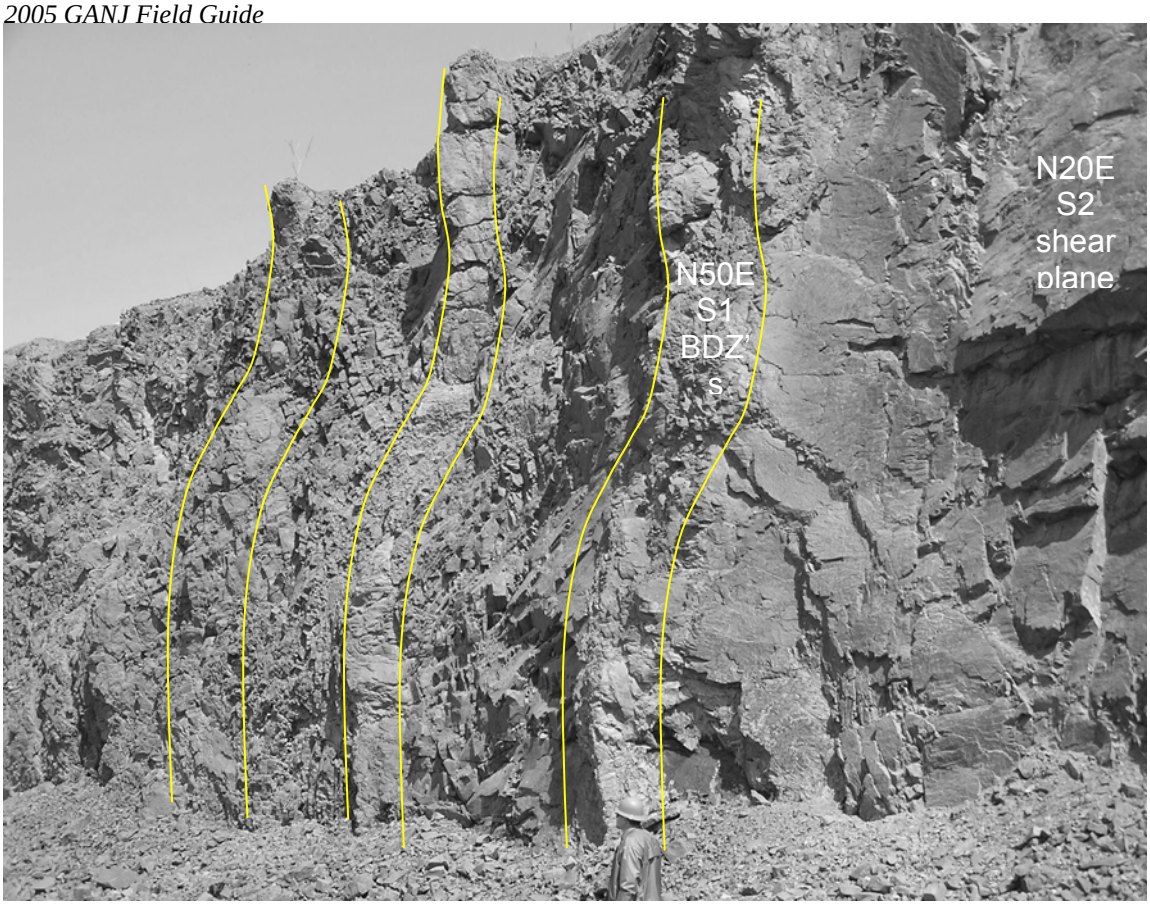

Figure 11. Brittle deformation zones (BDZs) form columnar structures striking parallel to S1 fractures (about N50E) in early Jurassic diabase, Pennington trap rock quarry, Hopewell Township, Mercer County. View facing northeast. The person standing at the bottom center provides a scale.

S3 fractures are interpreted as late-stage fractures that cut across and terminate against both earlier sets (S1 and S2), as best seen in borehole images obtained using a digital optical televiewer (Figures 14 and 15). An optical televiewer is a geophysical sonde that is deployed in bedrock wells to gain a three-dimensional (3D) record of subsurface geological features. 3D records include the depth and orientation of identified features (Figure 16) and the borehole orientation (Figure 17).

The NJGS has mapped sedimentary bedding in Triassic sedimentary bedrock and igneous layering in Jurassic diabase and basalt and associated fractures using OPTV and ATV records from more than 30 locations in the New Jersey part of the basin (Figure 18). All records were collected in 6- and 8-inch-diameter water wells ranging in depth from about 20 ft to 600 ft. These records provide information on the distribution and arrangement of fractures that becomes an integral part of hydrogeological frameworks developed for ground-water-resources projects. OPTV records (Figures 19, 20, and 21) are used to corroborate S1-through-S3 fracture geometry observed in outcrop and make it possible to inspect the configuration of fracture sets in three dimensions (Figure 17).

Figure 12a. S2 fracture set terminating against S1fractures in red mudstone cropping out along a railroad cut in Hopewell Township, Mercer County.

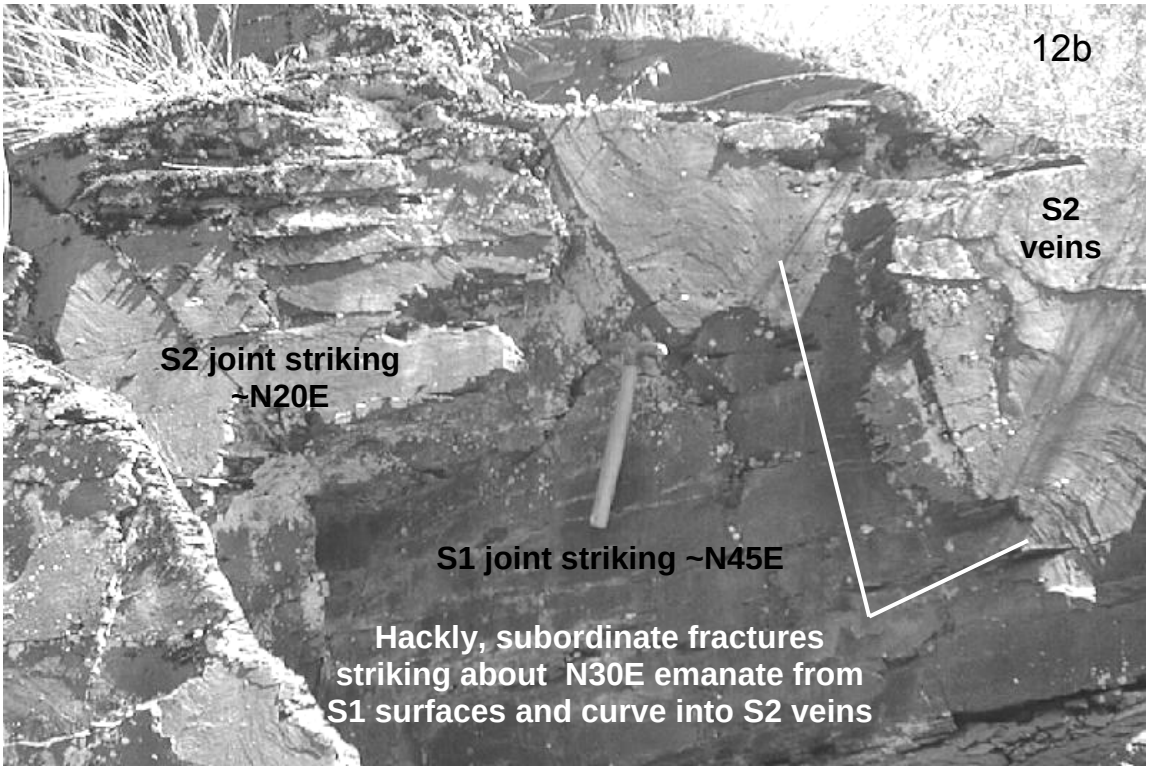

Figure 12b. A progressive strain history is recorded locally where two different fracture sets overlap. In this case, subordinate, hackley joints and veins striking midway between S1 and S2 strike maximums record incremental finite extension and help establish the relative timing of fracturing events.

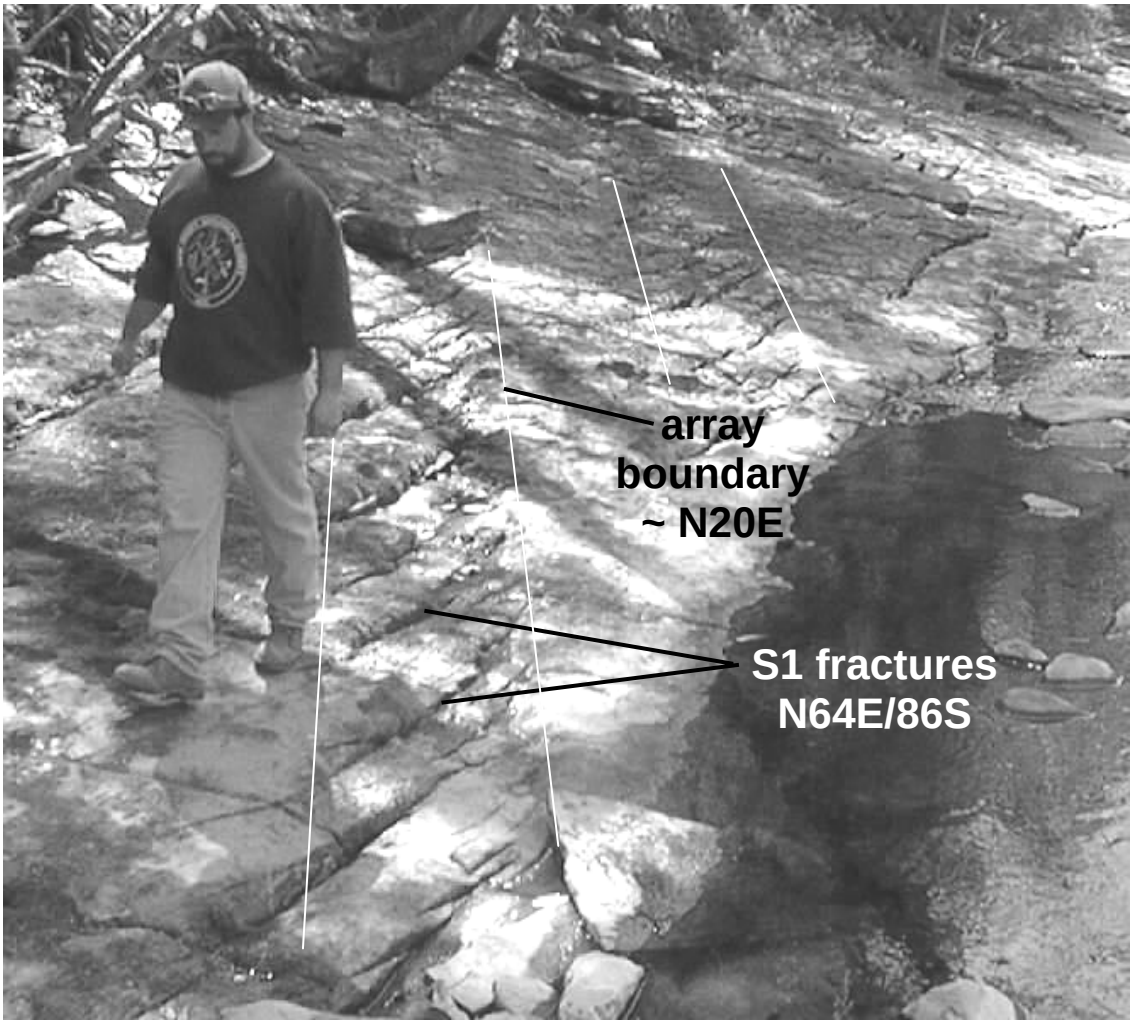

Figure 13. S1 extension fractures are early fractures arranged in en echelon, conjugate arrays with boundaries and crack tips that locally align along S2 fracture orientations. Outcrop of Lockatong Formation along Wickecheoke Creek, Delaware Township, Hunterdon County.

Moreover, OPTV provides detailed, visual records of small-scale structural relationships, including localized, normal dip-slip shear offset of Triassic sedimentary strata across individual fractures (Figures 19a and 20d).

S3 fractures are common in the northeast parts of the basin near N-S striking fault segments of the intrabasin fault systems (Figure 1) and in southeastern parts of the basin north of the Trenton Prong (Figure 18). The E-W striking, S3 extension fractures lie along the strike of S3 cross-fractures in structural domains exhibiting strain effects of late-phase compression and wrench faulting.

Extension fractures in Jurassic diabase and basalt were measured at five locations in New Jersey using an OPTV (Figure 22). Five wells at three locations were in Jurassic diabase and four wells at two locations were in the Orange Mt. Basalt. Fractures in igneous rocks commonly strike along both S2 and S3 trends (Figure 22; and Monteverde, 2000; Monteverde and Volkert, 2005). S1 fractures are localized and uncommon.

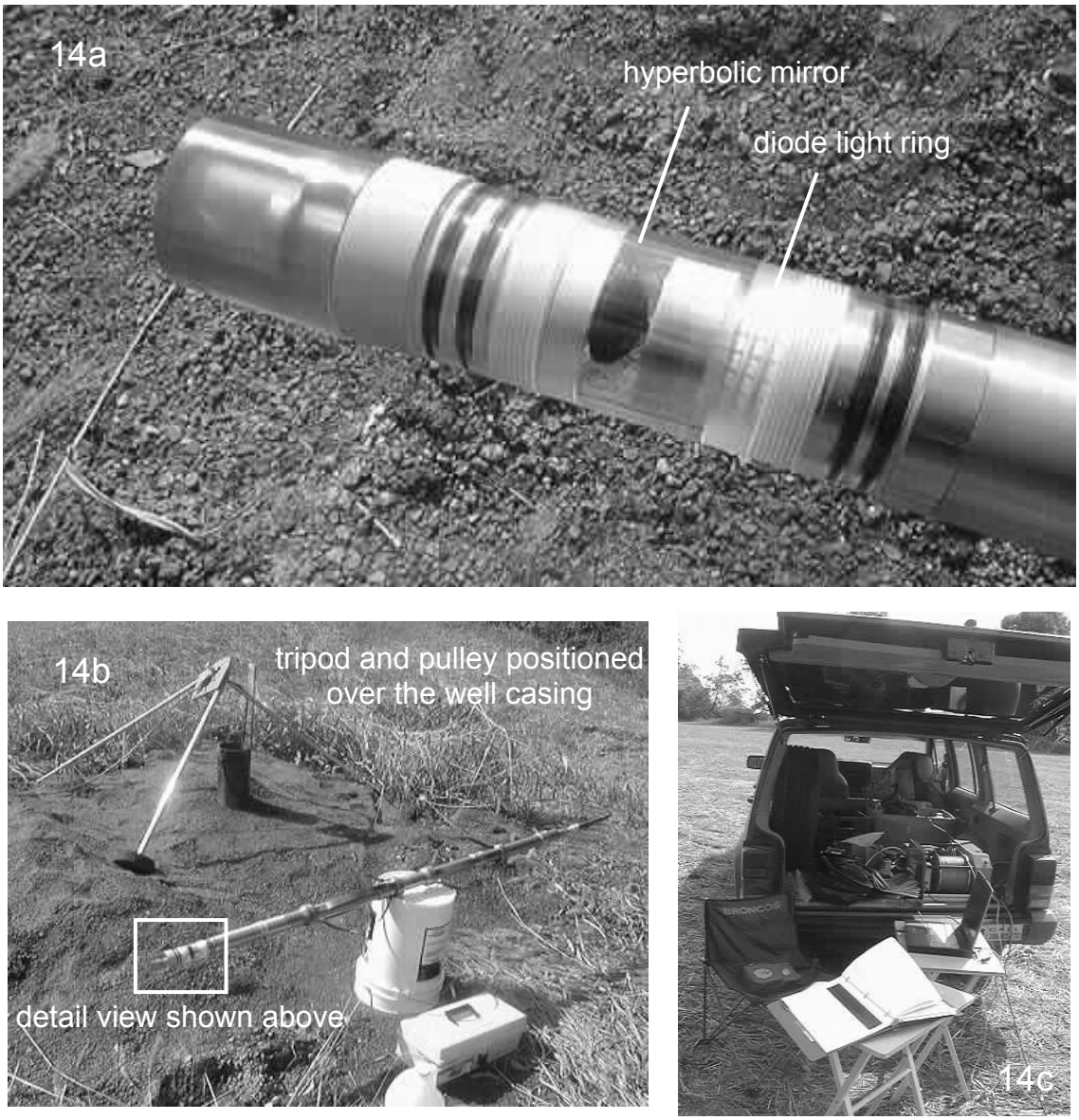

Figure 14. The New Jersey Geological Survey deploys a Robertson Geologging, Ltd[1]. digital optical televiewer for mapping subsurface geological features in 6- and 8-inch-diamater water wells. Top photo (14a) shows details of the bottom part of the sonde assembly, including the diode light ring and the hyperbolic mirror. The light emanating from the diodes is reflected off the borehole to the mirror and into the digital camera (see figure 15). Bottom left photo (14b) shows the sonde next to the tripod-and-pulley assembly used to lower the probe into position in the borehole with a coaxial cable spooled on a winch (14c). The cable transmits the digital signal to a surface acquisition system that includes a data logger and a laptop personal computer providing real-time display during data acquisition and storage of the digital data record.

[1]Use of trade, brand, or company names is for identification purposes only and does

Figure 15. Schematic diagrams showing details of the OPTV sonde assembly and borehole deployment (15a) and how a cylindrical borehole image is 'unrolled' for display during data processing (15b).

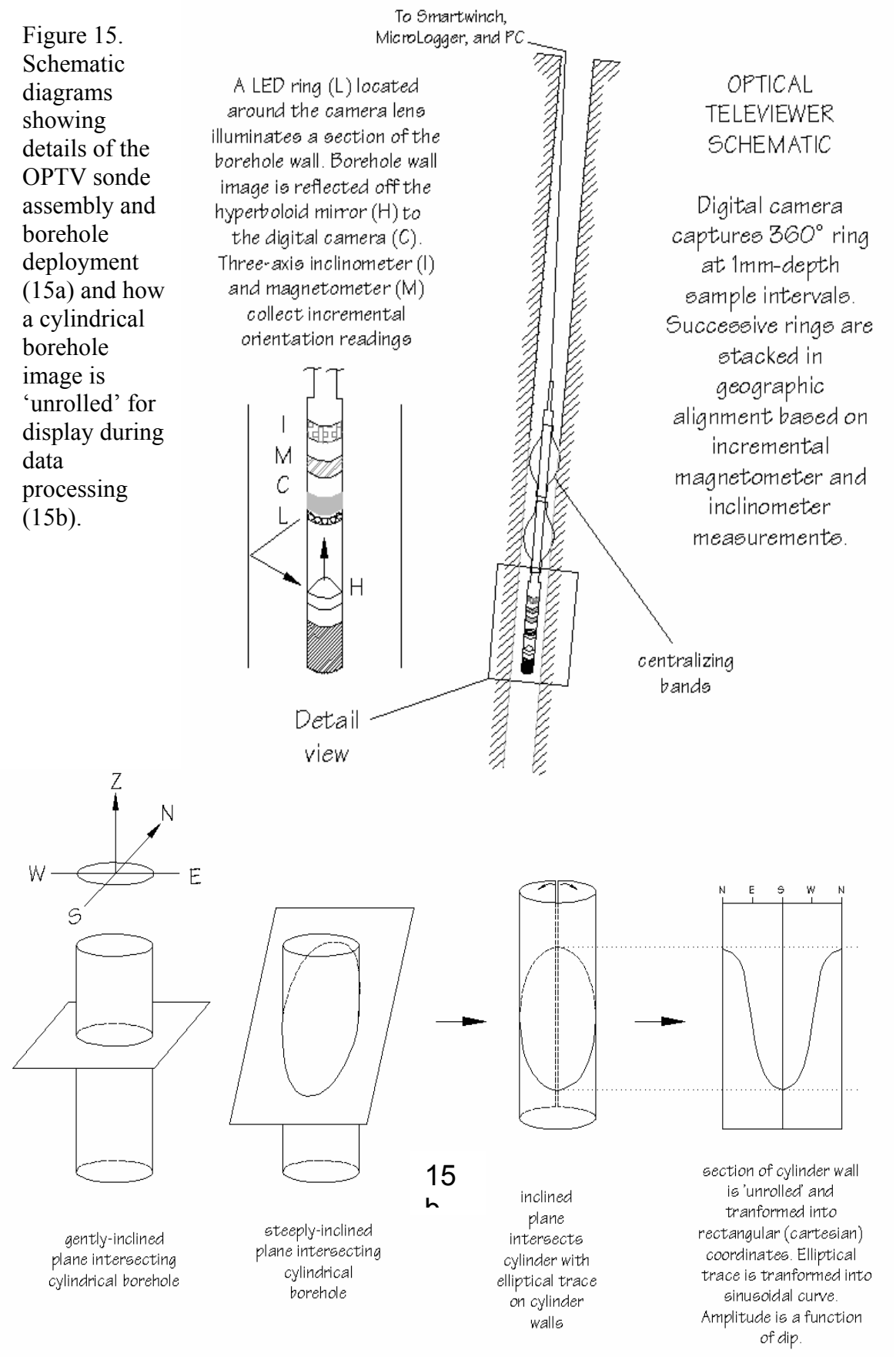

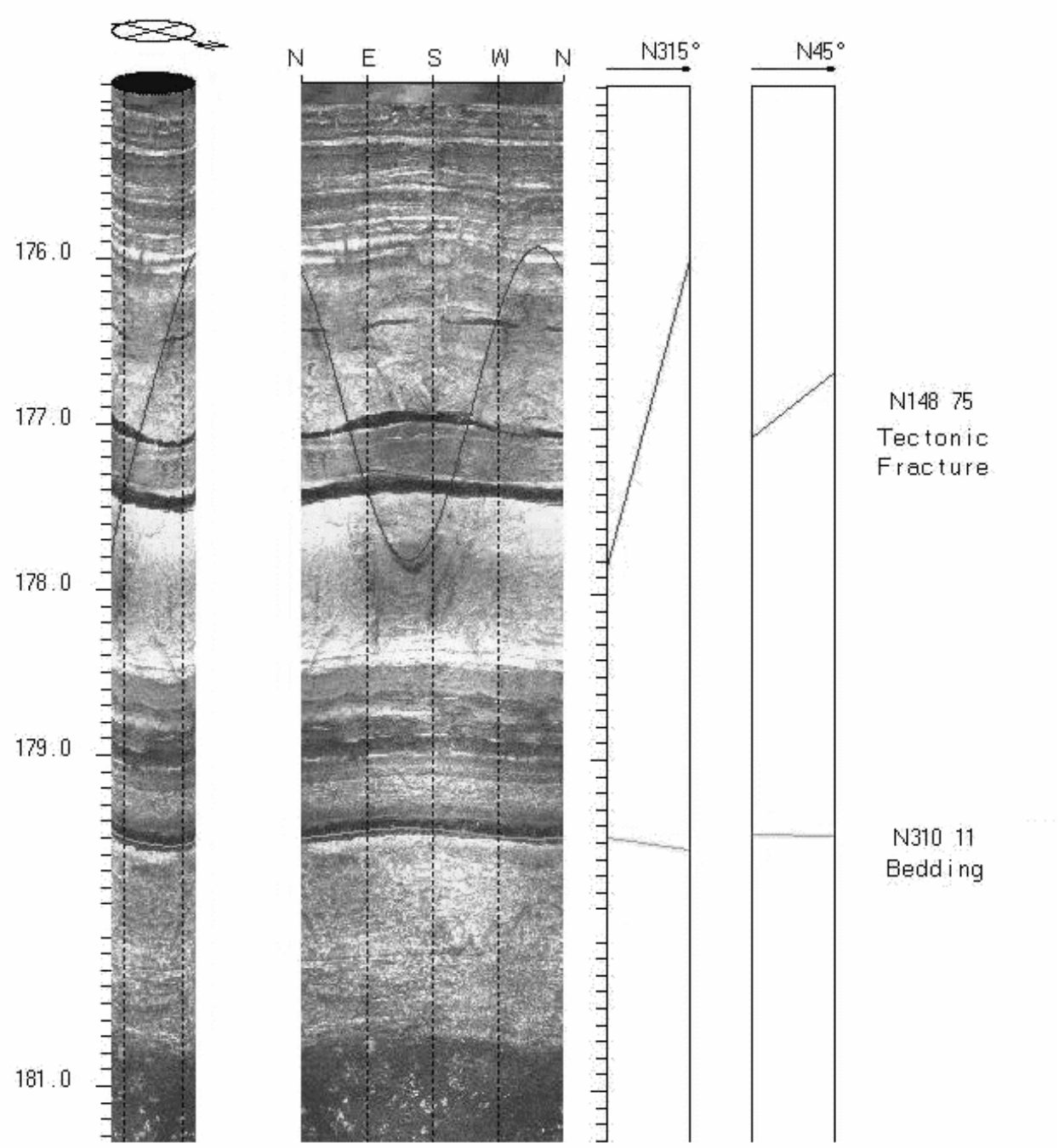

Figure 16. Interpreted OPTV records of borehole walls include a virtual, wrapped-core display (left) and the unrolled borehole image (center). The line diagrams to the right show apparent dips of interpreted structures from two orthogonal perspectives. Annotation on the far right denotes dip azimuths of interpreted features. The interpreted records are generated at 1/12 scale and stored as JPEG digital images for archiving and display.

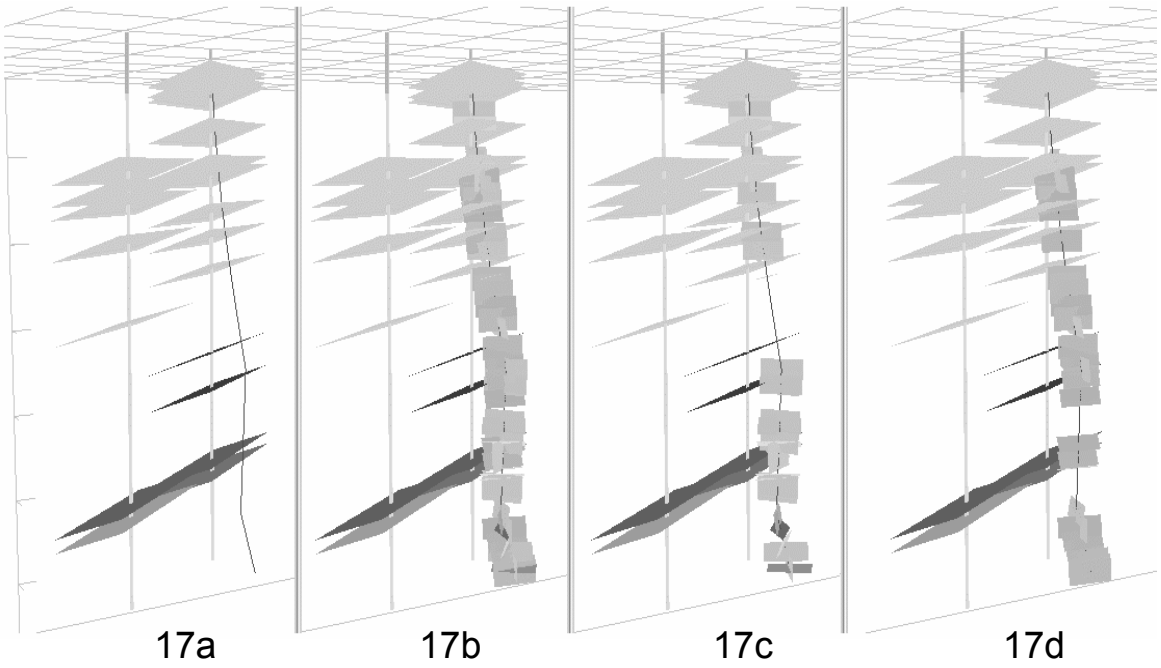

Figure 17. Paneled views from a computer-based geographic information system 3D model of a water-well field developed in the lower part of the Passaic Formation in East Amwell Township, Hunterdon County. Grid cells at the top of each panel and tick marks to the left mark 50-ft. intervals. Driller-reported water-bearing zones are assumed to parallel beds and are plotted along the vertical projection of two wells. Water-bearing zones dip at shallow angles from right to left. Darker planes represent higher-yielding zones. The borehole geometry for the well on the right was generated from OPTV data and shows that the borehole has an irregular shape that drifts in a direction opposite of bedding dip (17a). All measured fractures are plotted along the borehole in 17b. Only S1 fractures are plotted in 17c and only S2 fractures are shown in 17d. S1 and S2 fracture sets occur locally in isolation but also locally overlap. The borehole drift is affected by the 3D spatial arrangement of the different fracture sets, with dogleg angles in the borehole trace corresponding to the occurrence of different fracture sets. Also, higher-yielding water-bearing zones correspond to areas of overlapping S1 and S2 fracture sets.

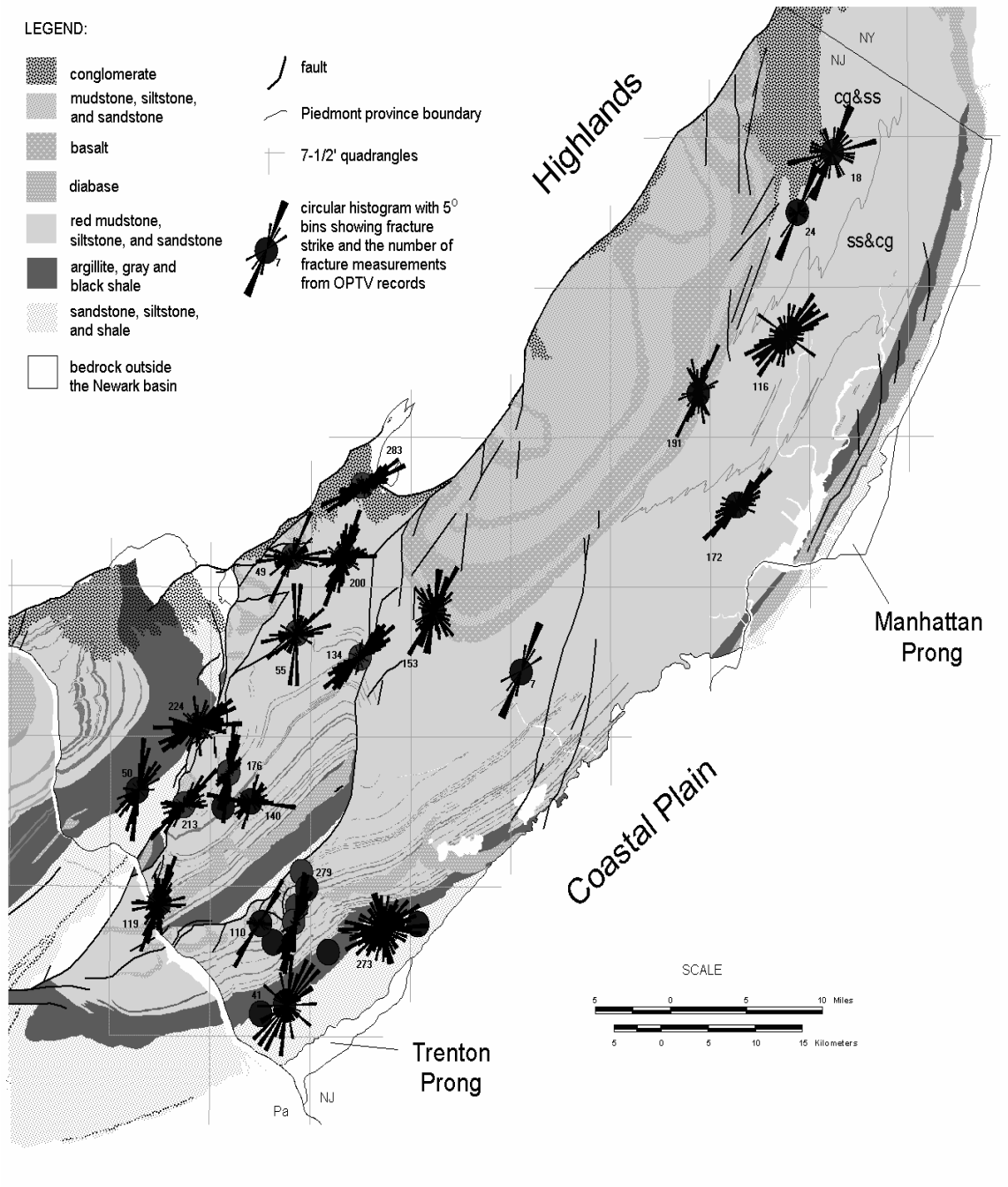

Figure 18. Generalized bedrock geology map of the eastern part of the Newark Basin showing fracture-strike histograms for some of the locations where OPTV data have been collected and analyzed by the NJGS.

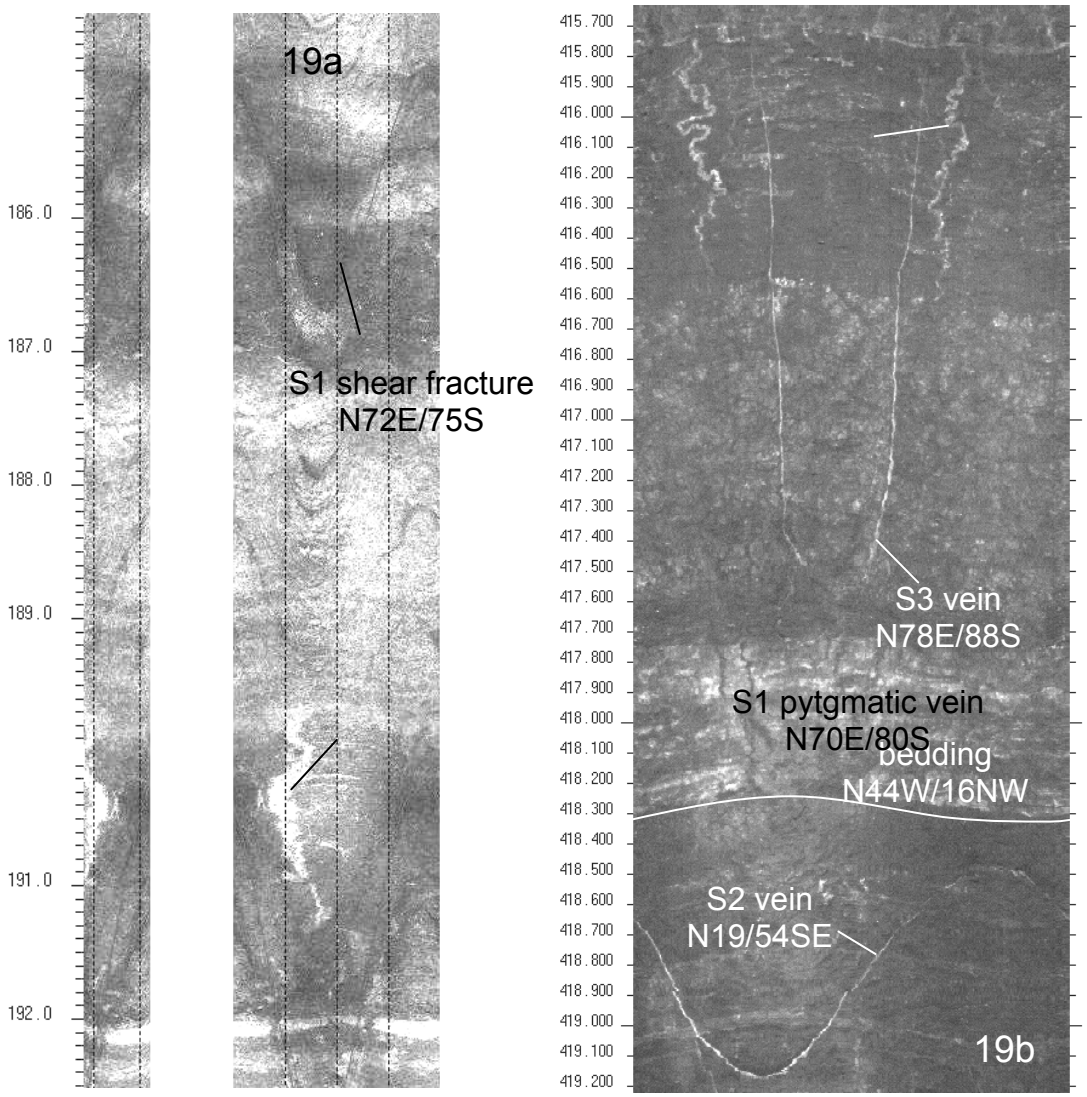

Figure 19. Processed OPTV borehole record (19a) and unprocessed OPTV borehole image (19b) showing examples of S1, S2, and S3 fracture geometry in the Lockatong Formation, Raritan Township, Hunterdon County. Figure 19a shows folded S1 veins and normal dip-slip offset of beds across a S1 shear fracture. Figure 19b also shows a pytgmatically-folded S1 vein and later S2 and S3 veins. Orientation of OPTV records the same as shown in figure 16.

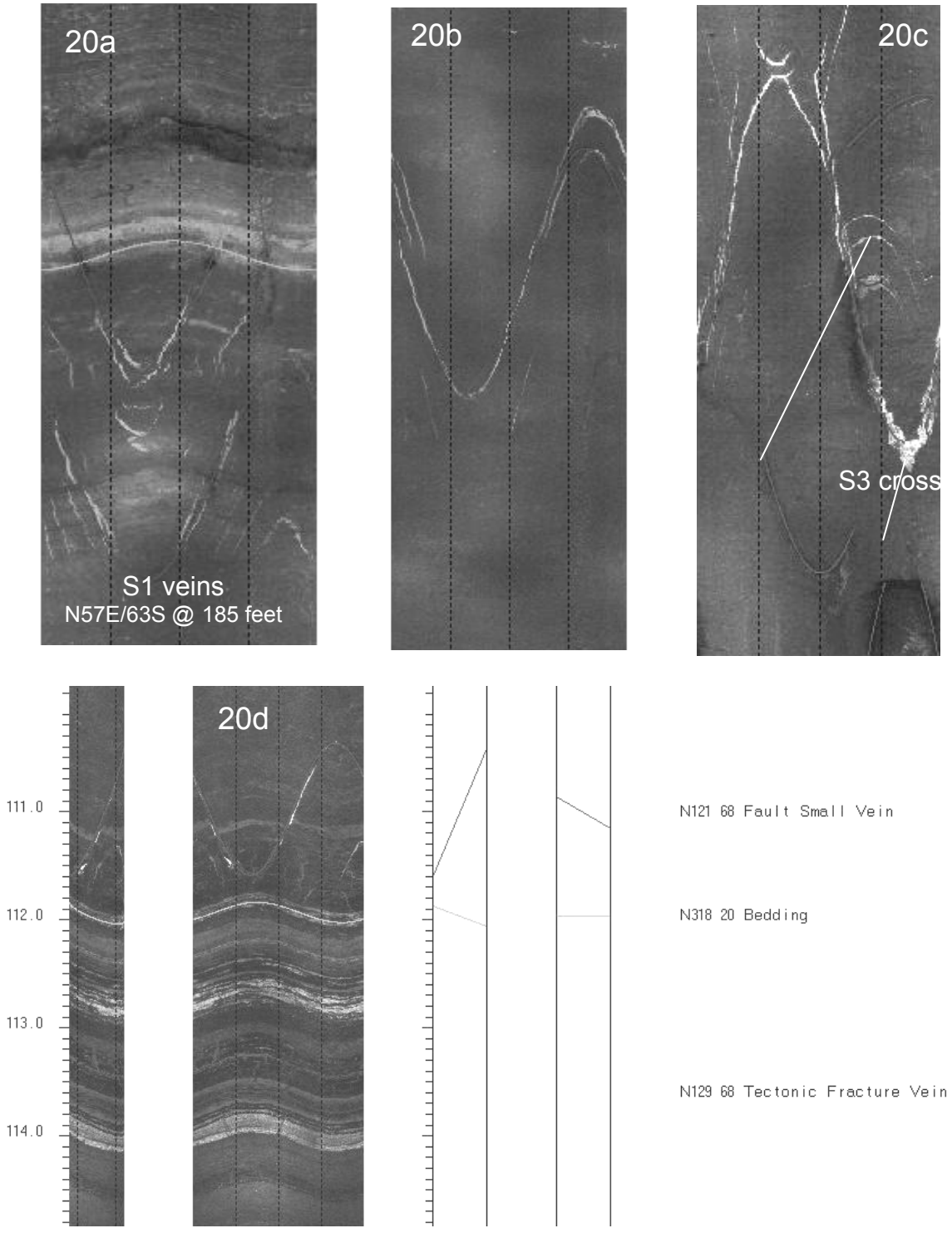

Figure 20. Processed OPTV images showing S1, S2, and S3 vein geometry in red mudstone and gray and black shale in the middle part of the Passaic Formation, East Amwell Township, Hunterdon County. Orientation of images the same as for figure 16. Orientations next to classified structures in the bottom diagram indicate feature dip azimuths. Depth in feet below land surface.

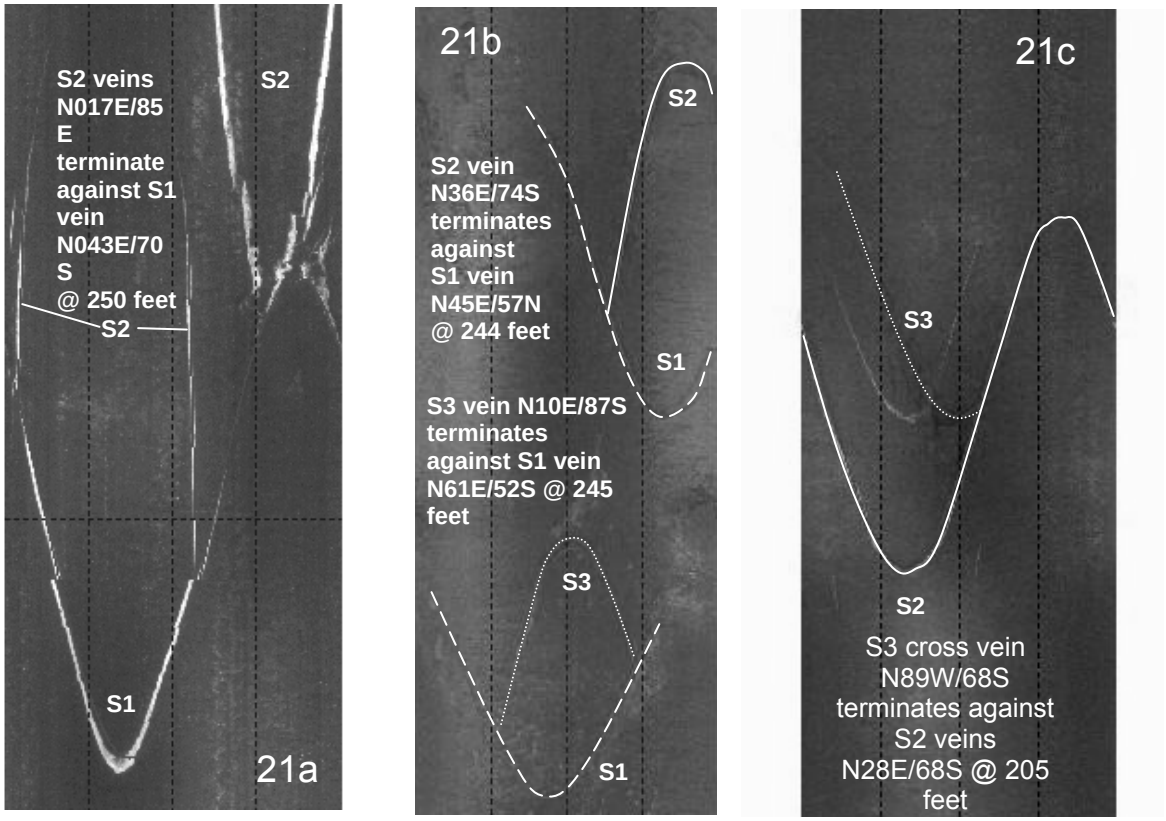

Figure 21. Fracture geometry in three OPTV borehole records. Left record (21a) shows S2 veins terminating against S1 veins in red mudstone from the lower part of the Passaic Formationm, Hopewell Township, Mercer County. Middle record (21b) shows both S2 and S3 veins terminating against S1 veins in red mudstone from the middle part of the Passaic Formation, Hopewell Township, Mercer County. Right image (21c) shows S3 vein terminating against a S2 vein in red mudstone of the middle Passaic Formation, East Amwell Township, Hunterdon County. Depths in feet below land surface.

The multiple sets of steeply dipping extension fractures show some similar geometric and spatial properties. For example, the surface area of extension-fracture walls, and the spacing between fractures measured normal to a fracture surface commonly decrease with the thickness of the fractured layer; a feature observed in sedimentary rocks elsewhere (Pollard and Aydin, 1988; Huang and Angelier, 1989; Narr and Suppe, 1991, Gross, 1993). Inter-fracture spacing, or fracture density, is measured normal to fracture walls and locally ranges from less than 1 fracture per meter to more than 50 fractures per meter near the trace of mapped faults (Herman, 1997). Fracture trace lengths of 1 to 5 meters are common in all bedrock units, and mechanical (fracture) layering in sedimentary strata commonly ranges from < 1 m to about 2 m thick (Figure 4b).

Most steeply dipping extension fractures are aligned *en echelon* with adjacent and overlapping, subparallel veins displaying systematic, stepped geometry (Figures 3a, 4a, 6a , 7g, and 10a). Curved country-rock bridges are commonly positioned between adjacent, isolated veins in outcrop (Figure 10a) or occur as remnant country-rock

inclusions (Figure 10b) encased by secondary mineral cements from linkage and growth of fractures. Sets of en echelon veins are commonly arranged in conjugate arrays (Figure 23) having the geometry of normal dip-slip shear zones (Type 2 arrays of Beach, 1975).

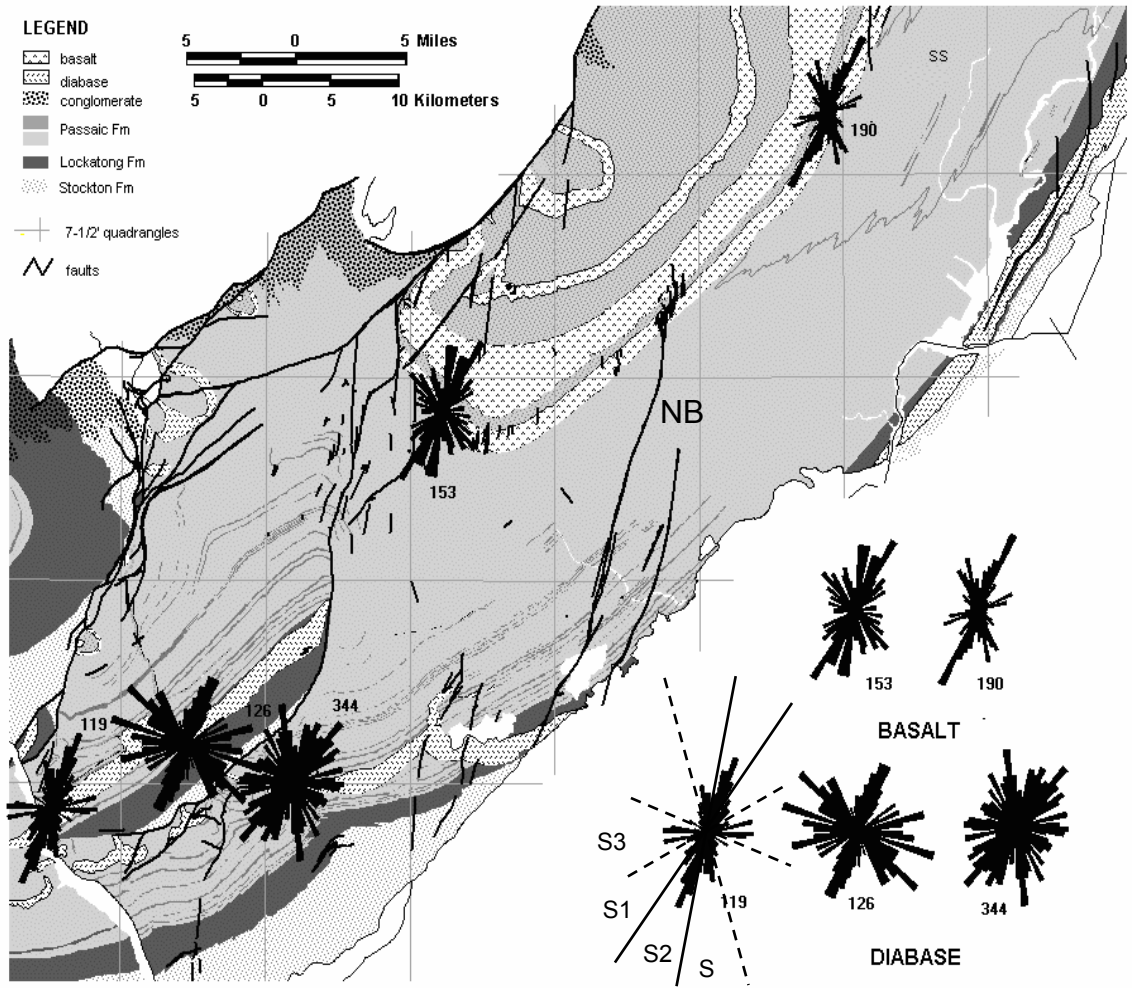

Figure 22. Generalized bedrock geology of the central part of the Newark Basin showing circular-histogram summaries of OPTV fracture data from 5 locations in Early Jurassic basalt and diabase in New Jersey. The numbers beside the histograms show the total number of fractures interpreted at each site. The fracture summary reflects stages identified from fractures mapped in outcrop (see Figure 1). SS – sandstone and siltstone facies of the Passaic Formation (Parker and others, 1988), NBF – New Brunswick fault.

Steeply-dipping, en echelon extension fractures arranged in conjugate arrays form in a tectonic environment having principal sub-horizontal tension and sub-vertical principal compressive stress (Figures 2 and 23). Their formation and growth stretches beds in both horizontal and vertical directions and are responsible for producing gentle stratigraphic dips by imparting apparent angular rotations of beds normal to fracture surfaces (Figures 24 and 25). Spaced sets of tectonic veins therefore developed in the basin as a pervasive strain mechanism allowing a thick pile of heterogeneous layered rocks to simultaneously stretch and sag (Figure 26). Tightly spaced swarms of veins probably served as loci for subsequent fault development in agreement with the reported dynamics of Type 2 en echelon cracks where crack arrays weakened a rock mass and later served to localize shear zones (Nicholson and Pollard, 1985).

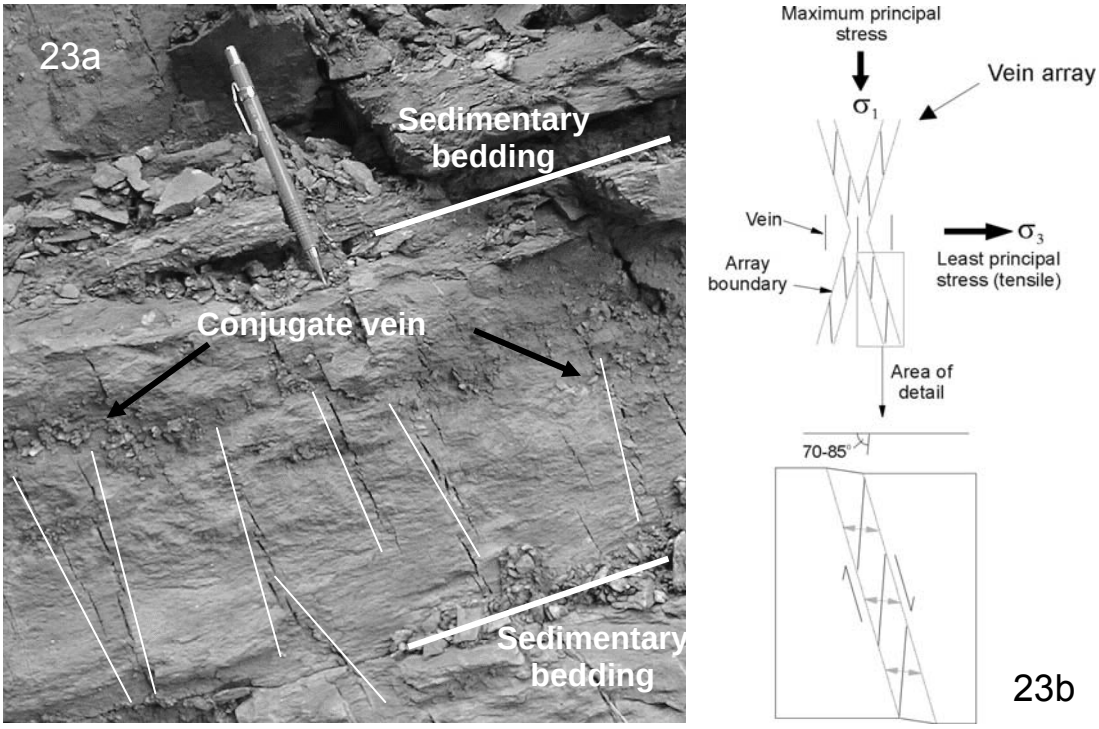

Figure 23. Steeply dipping extension fractures form in *en echelon* alignment within conjugate arrays having the geometry of normal dip-slip shear zones. Individual veins are arranged in conjugate veins arrays as seen above in profile (23a) from an excavation in red mudstone of the Passaic Fm., East Amwell Twp., Hunterdon County, NJ. S2 veins in the hanging wall of the Flemington fault have an average dip of about 70^o when bedding is restored to a pre-tilt (horizontal) alignment (Herman, 2001). The 70^o average dip directly agrees with the angle of inclined-shear failure reported for material moving in faulted, extended hanging walls (Xiao and Suppe, 1992; Dula, 1991, Withjack and others, 1995).

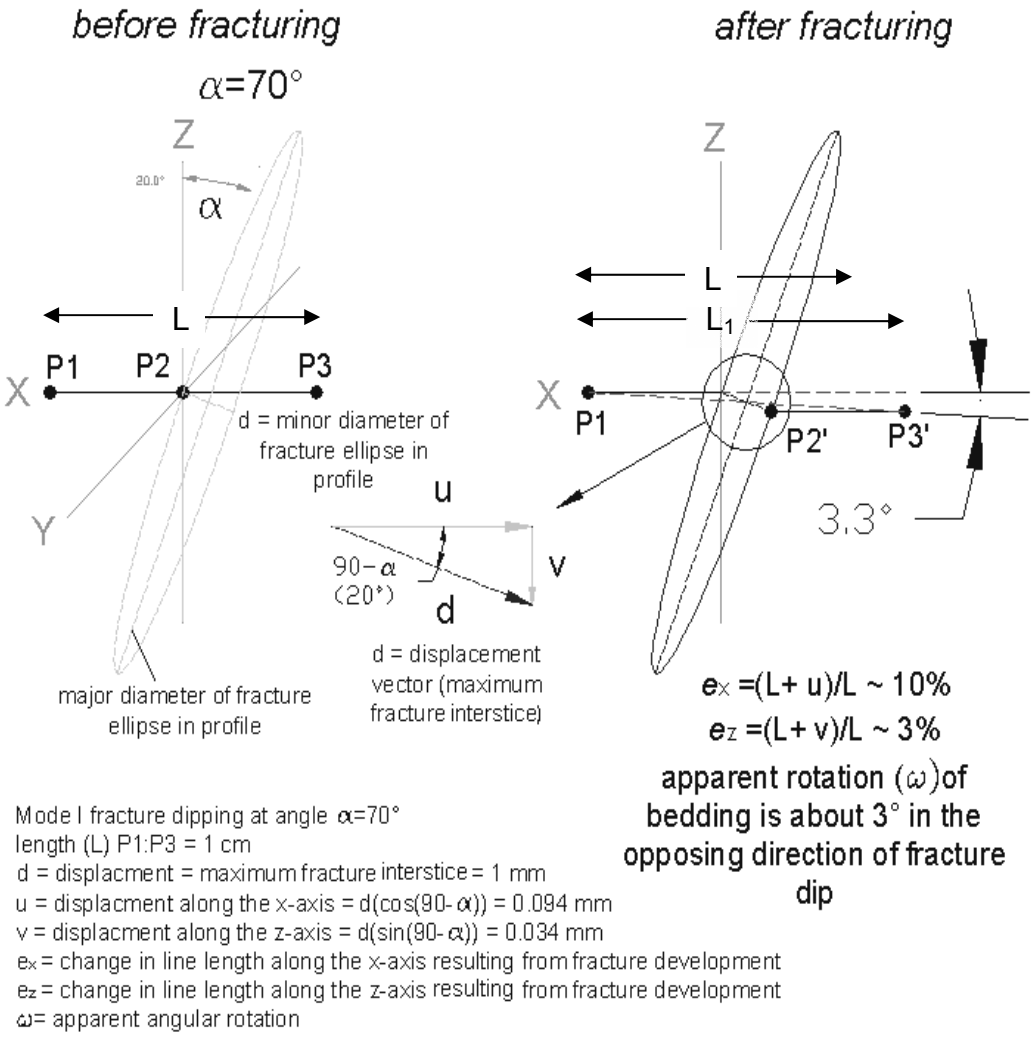

Figure 24. Finite strain analysis of an extension (Mode I) fracture in profile. Sub-horizontal bedding corresponds with the XY plane. Bedding is positively extended
both horizontally (**u**) and vertically (**v**) and apparently rotated in a direction opposite that of fracture dip as a result of extensional opening. Displacement of reference points P2 and P3 into their opened positions (P2' and P3') illustrates how steeply inclined fractures result in an apparent angular rotation of a bed across the opening. This exercise show and a fracture interstice of 1 cm imparts about 10% horizontal stretching ($\mathbf{e}_x$), 3% vertical stretching ($\mathbf{e}_z$), and about a 3° apparent rotation (**w**) tilt of beds. Sub-horizontal line L is stretched with an extended length of L_1.

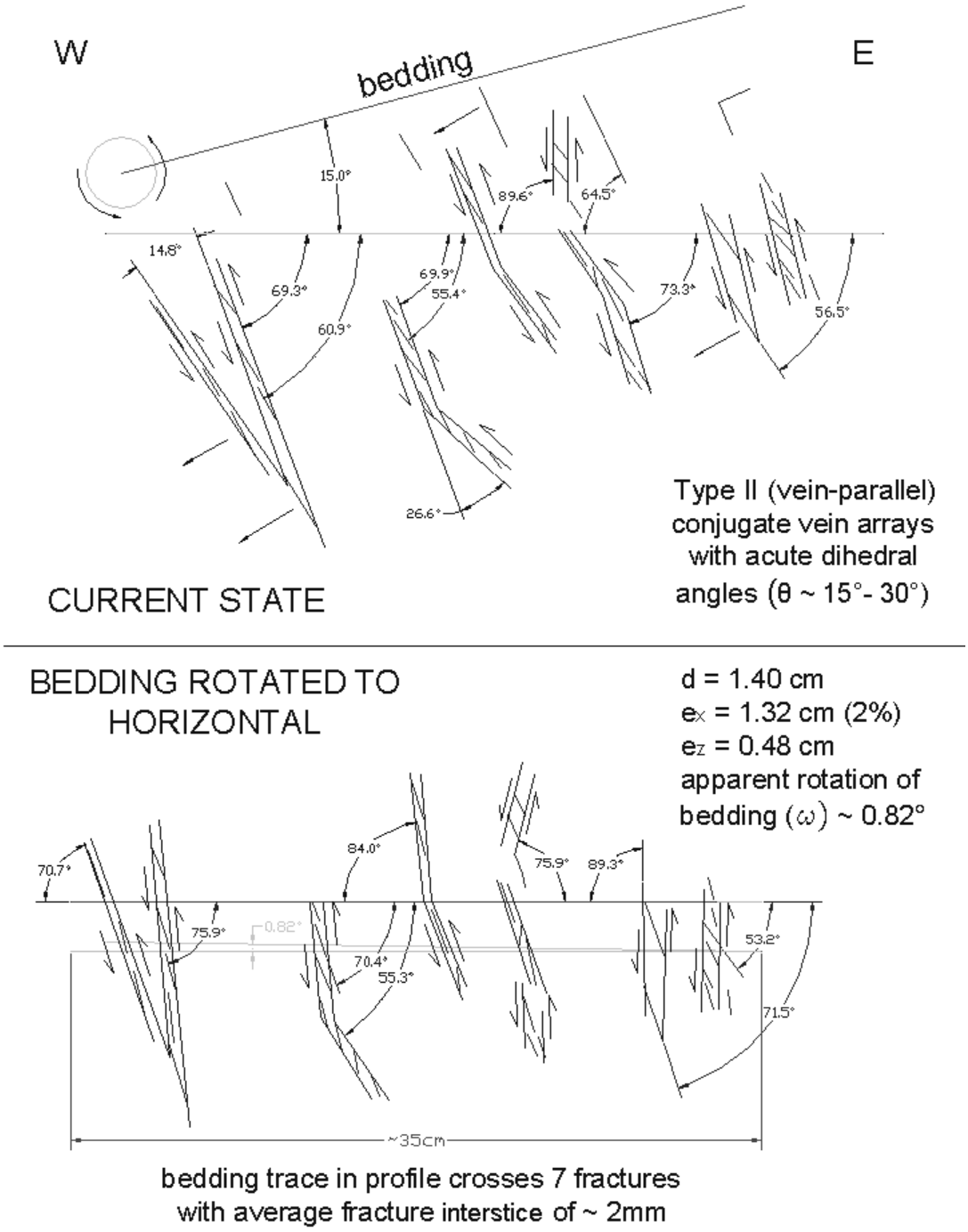

Figure 25. Profile view of vein-array geometry and finite-strain calculations for fractured red mudstone of the Passaic Formation in the hanging wall of the Flemington fault (see figure 23 for photo showing vein geometry). In the current state (top), bedding dips anout 14° West and fractures dip about 55 ° to 65° East within arrays having boundaries dipping 70° to 90° East. Angles between array boundaries range from about 15° to 30°. Fracture dips average about 70° following rotation of bedding back to horizontal (14 ° clockwise). For the strain analysis (bottom), a reference line 35 cm long was drawn parallel to bedding across seven steeply inclined fractures with an average fracture interstice of 2mm. In this case, based on the geometry and strain relations outlined in figure 24, bedding was stretched horizontally about 2% and rotated about 1°

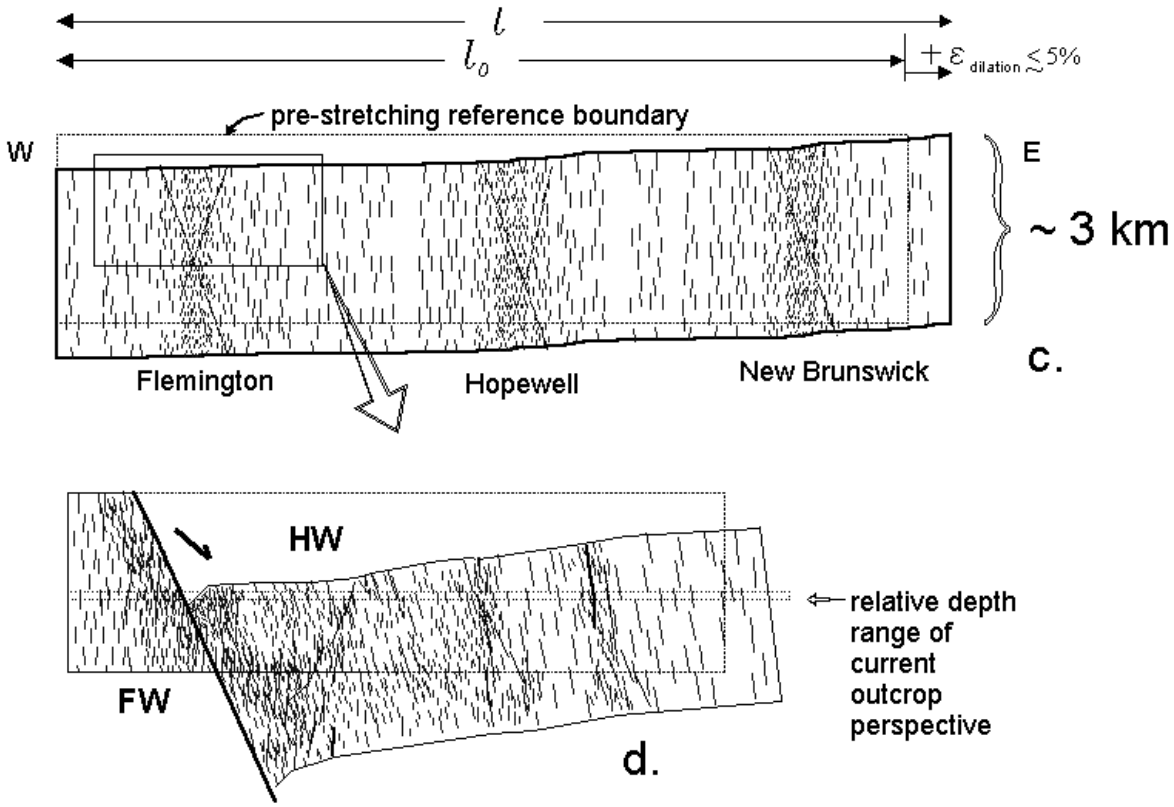

Figure 26. A schematic profile of basin strata showing progressive strain effects associated with the S2 fracture swarms extending from Flemington to New Brunswick, NJ. Location of profile shown in Figure 28.

JOINTING AND VEINING WITH RESPECT TO THE REGIONAL TECTONICS

Extension fractures are an integral part of the basin's structure. They reflect accumulated brittle strain as part of the regional tectonic history. Their orientation, distribution, morphology and vein-fill mineralogy record the incremental strain and pore-fluid chemistry developed during the various rifting, shifting, and drifting events that shaped the basin and surrounding bedrock following the Middle Triassic period. Absolute and relative ages of the multiple fracture sets are partly constrained by the rocks they affect and the ways they interact geometrically.

S1 fracture sets are more common in late Triassic rocks (Figure 1), S3 fractures are more common in early Jurassic rocks (Figures 1 and 22), and S2 fractures are common in all of these rocks. Folded S1 veins in strata within the hanging wall blocks of the border faults (7f), and subparallel segments of the Hopewell fault system (Figure 7e) reflect early dip-slip shear fracturing and synchronous lithologic compaction from sedimentary loading. Dip-slip extensional faulting on S1 faults followed preexisting crustal faults cutting basement and stemming from Paleozoic continental collision and suturing (Ratcliffe, 1971; Lindholm, 1978)). Early Mesozoic strata along the length of the border

fault system locally intersect normal faults marked by footwall blocks of Precambrian and early rocks (Drake and others, 1996). Late Triassic conglomerate beds elsewhere along the western border unconformably onramp older basement along cross-strike contacts between tip lines of overlapping fault segments. At these locations, referred to as relay ramps by Schlische (1992), beds are tilted and strike at high angles to the basin's axis. These structures bear a strong resemblance to, and have similar geometry to the inter-fracture bridges seen at the microscopic (Figure 10b) and outcrop scales (Figure 10a and 23a) denoting fracture coalescence. Late Triassic strata also thin locally over structural arches oriented along S1 cross trends as a result of differential fault slip (Schlische, 1992). These relationships together point to the likelihood of early S1 fracturing and concomitant dip-slip faulting of Late Triassic strata along S1-striking fault segments.

S1 fracture sets in Late Triassic sedimentary bedrock and Early Jurassic diabase indicate prolonged NW-SE tectonic extension normal to the structural axis of the basin (about N40^{o}E to of N70^{o}E) throughout the Late Triassic and into the Early Jurassic. The structural transition from S1- to S2-stage fracturing may have occurred during a relatively short time span as suggested by outcrops where fractures striking between S1 and S2 maximums are comparatively limited in physical size and distribution with respect to S1 and S2 maximum sets (Figure 12b). S2 maximums are aligned about 30^{o} counterclockwise with respect to S1 maximums (Figure 1). This agrees with the predicted angular arrangement of overlapping and stepped faults reported from analog clay model and sandbox studies of oblique-rift and strike-slip models (Schlische and others, 2002; McClay and Bonora, 2001) and reflects rotation of the developing North American plate preceding the onset of sea-floor spreading (Figure 27).

The S2 extension phase reflects a period of accelerated crustal stretching and basin subsidence that affected continental crust throughout the region (Figures 28 and 29) during the early Jurassic. Crustal-scale faults developed in the center of the basin during this period with S2 fracture sets having the highest densities and frequencies in fault blocks of the Flemington (Herman, 1997), Hopewell (Monteverde and others, 2003), and New Brunswick fault systems (Stanford and others, 1998). S2 fractures sets in the Passaic Formation are mostly calcite cemented, are not folded, and therefore formed after consolidation of most Late Triassic sediments. Late Triassic bedrock and older basement are intruded by Early Jurassic dikes swarms having S2 alignment in the southwest part of the basin (Figure 1). But Early Jurassic sills and basalt are commonly cut by S2 structures in New Jersey (Figures 12 and 24). Laney and others (1995) mapped late-stage leucocratic dikes, zoned veins, hydrothermal veins, and strike-slip faults cutting the Lambertville diabase sill along S2 strikes.

A single Jurassic dike extending from the top of the Sourland Mountain (Lambertville Sill of Husch, 1992) is interpreted here to be part of a locally discordant S2 fracture phase that locally overprints S1 faults of the Hopewell fault system. The dike formed along a major crustal fissure that cuts the entire 9,000 feet of Passaic Fm and aligns with a fault that cuts across and offsets the Hopewell fault just northwest of Princeton, NJ (Figure 28). The Lambertville sill is fractured and sheared downward at a location between the dike and the fault with apparent right-lateral-normal oblique slip (119 fracture rose shown in Figure 22). These discordant, cross-cutting S2 structures floor into an oblique-slip, extensional duplex fault system near Princeton that forms a

major transform boundary extending eastward into the N.J. Coastal Plain with apparent right-lateral, dip-slip movement offsetting both Late Triassic and gneissic bedrock of the Trenton Prong (Figure 28). The fault relationship and geometry may be duplicated on concealed faults extending directly westward from the Trenton Prong in New Jersey toward the Chalfont fault system in Pennsylvania (Figure 29). These structures accommodated ESE extension and slumping failure in the center of the basin along with other intrabasinal fault systems. S2 extension on S1 faults also resulted in predominant

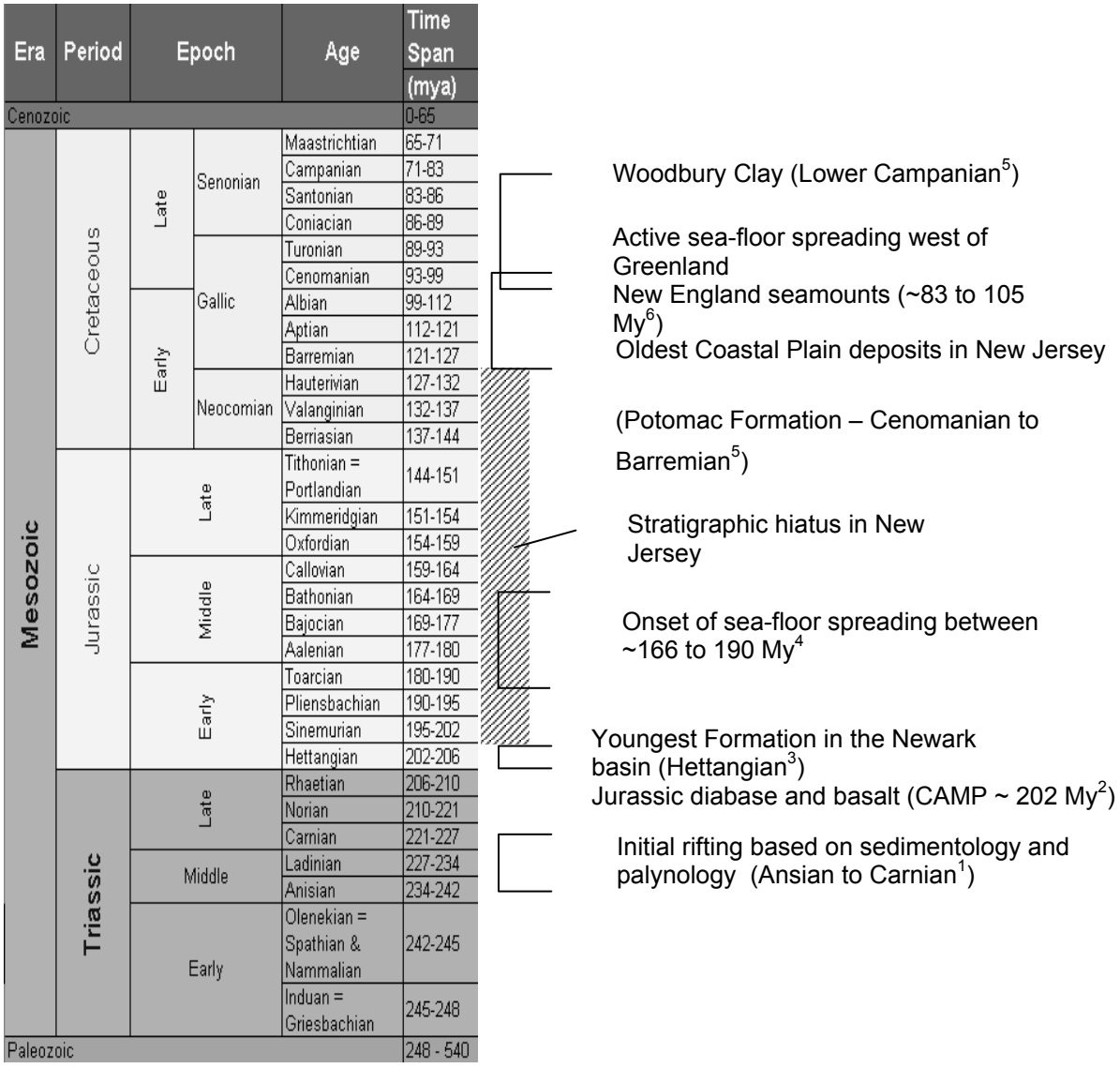

Era	Period	Epoch		Age	Time Span (mya)
Cenozoic					0-65
Mesozoic	Cretaceous	Late	Senonian	Maastrichtian	65-71
				Campanian	71-83
				Santonian	83-86
				Coniacian	86-89
			Gallic	Turonian	89-93
				Cenomanian	93-99
		Early		Albian	99-112
				Aptian	112-121
				Barremian	121-127
			Neocomian	Hauterivian	127-132
				Valanginian	132-137
				Berriasian	137-144
	Jurassic	Late		Tithonian = Portlandian	144-151
				Kimmeridgian	151-154
				Oxfordian	154-159
		Middle		Callovian	159-164
				Bathonian	164-169
				Bajocian	169-177
				Aalenian	177-180
		Early		Toarcian	180-190
				Pliensbachian	190-195
				Sinemurian	195-202
				Hettangian	202-206
	Triassic	Late		Rhaetian	206-210
				Norian	210-221
				Carnian	221-227
		Middle		Ladinian	227-234
				Anisian	234-242
		Early		Olenekian = Spathian & Nammalian	242-245
				Induan = Griesbachian	245-248
Paleozoic					248 - 540

Figure 27. Mesozoic time summary of regional geological and tectonic events in the Newark basin region. Time scale adapted from Gradstein and others (1995). [1]Manspeizer and Cousminer (1988), Olsen and others (1996); [2] Sutter (1988); Dunning and Hodych (1990); [3]Olsen and Kent (1996); [4]Benson (2002); [5]Owens and others (1998); [6]Duncan(1984)

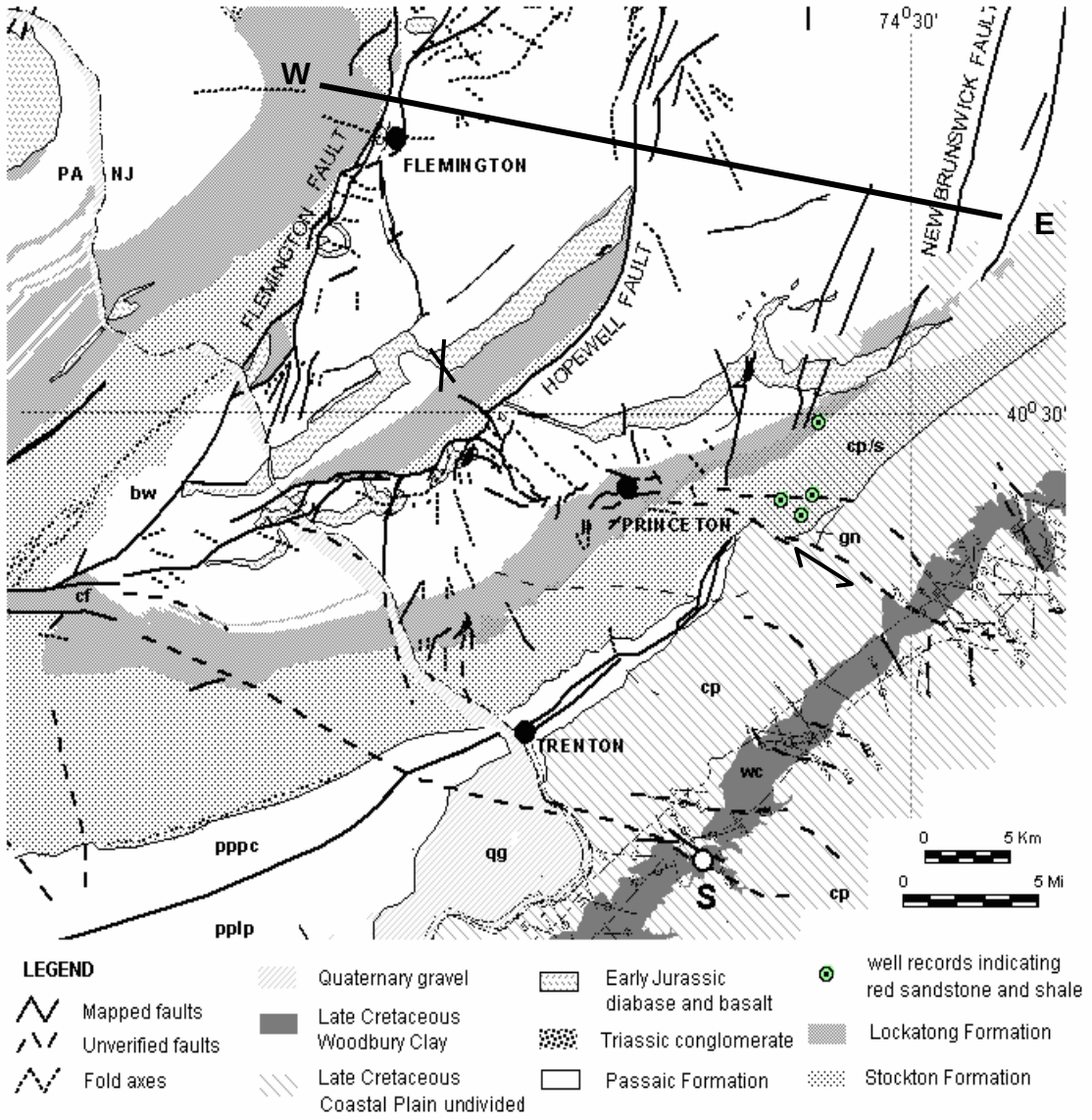

Figure 28. Generalized bedrock geology in the vicinity of the southeastern part of the Newark basin showing the location of inferred faults and/or fracture swarms that cut Late Cretaceous coastal plain deposits and older basement in the Trenton Prong and Pennsylvania Piedmont. These faults may have formed initially as oblique right-lateral-normal faults during late stages of rifting but were reactivated as oblique left-lateral-reverse faults from subsequent compression and basin inversion. The Late Cretaceous Woodbury Clay is fractured and apparently offset along the strike of lineaments shown above (lineament interpretation of synthetic aperture radar imagery, Aero Services Corp, 1980, 1:100,000 scale, on-file at the NJGS office). Permanent notes of the NJGS include records of steep dips and complex structures in the Woodbury Clay at location **S** that have been attributed to sedimentary slumping and/or freeze-thaw inversion. Apparent offset of the Woodbury Clay in New Jersey is consistent with oblique uplift (left-lateral reverse) on inerred faults that probably link with the Chalfont fault system (cf) in Pennsylvania. Abbreviations: gn – weathered gneiss, qg - Quaternary gravel, bw – Cambrian-Ordovician carbonates in the

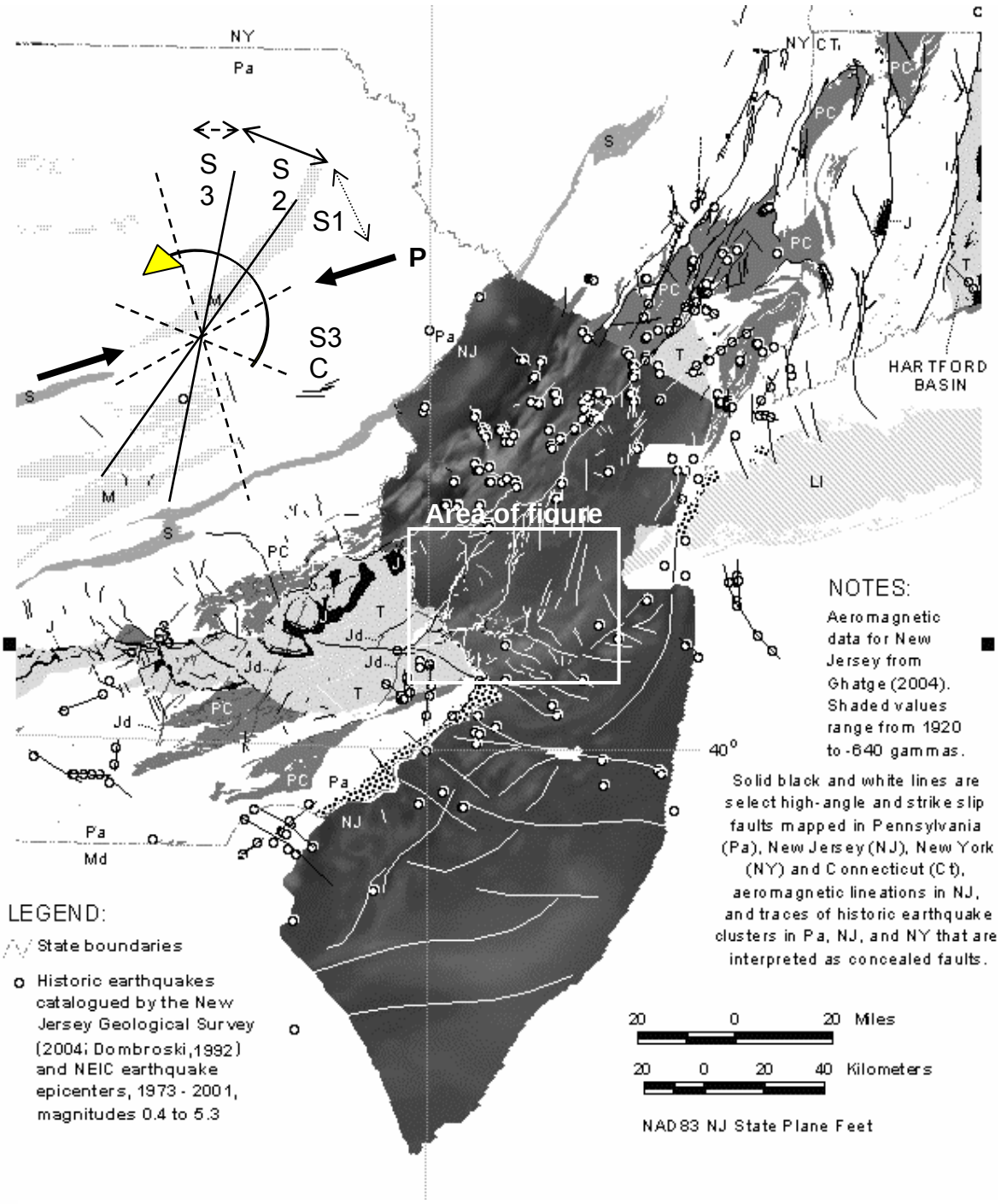

Figure 29. A regional wrench-fault system interpretation centered on New Jersey is shown in relation to a diagram illustrating the fracture geometry outlined for the Newark basin. Generalized bedrock geology from GIS coverage of Pennsylvania (Berg and others, 1980; http://www.dep.state.ct.us/gis/), New York (Fischer and others, 1980; http://www.dep.state.ct.us/gis/), and Connecticut (Rodgers, 1985; http://www.dep.state.ct.us/gis/). Solid lines represent mapped, concealed, and inferred faults that are interpreted to have been active during and since the Late Triassic. Historical earthquake epicenters show areas of currently tectonic activity in the region. Bedrock polygons include M – Mississipian, S – Silurian, T – Triassic, J – Jurassic bedrock. Jd – Jurassic dike. LI – Long Island. P – direction of current horizontal

right-lateral, normal slip along border faults (Ratcliffe and Burton, 1985). Merguerian and Sanders (1994) mapped chevron folds plunging N75^{o}W in the Lockatong Fm at the base of the Palisades sill and interpreted them as resulting from intrusive flow emplacement toward the NE, along the S2 stretching direction outlined here. Therefore, the combined body of evidence points to S2-stage extension fracturing lasting throughout the estimated ~ 580 Ky duration of magmatic activity in the basin (Olsen and others, 1996b) beginning near the onset of the early Jurassic at about 201 Mya (Sutter, 1988; Dunning and Hodych, 1990).

The structural transition between S2 and S3 extension fractures is apparently continuous, resulting in upward curving fractures and faults reflecting a ~30 ^{o} to 40^{o} counterclockwise reorientation of the principal stretching direction that postdates lithification of early Jurassic basalt. S2-striking faults of the New Brunswick fault system have fault tips of S3 orientation in basalt of the Watchung Mt. Region (Figure 23). Upward twisting, curvilinear jointing in these basalts (Faust, 1978) may also record this increment of rotation strain.

S3 fractures are more locally restricted in their occurrence and more problematic with respect to their tectonic history insofar as they appear to stem from both late phases of extension and subsequent compression. During S3 extension, the basin appears to have been strongly stretched E to ENE with concurrent development of N-S to WNW striking, high-angle, oblique-slip normal faults (Figure 28). S3 extension fractures striking about N-S are common near faults having these same strikes in the Watching Mt region as well as southward near Princeton and Trenton, NJ. Late-stage leucocratic, magmatic dikes as much as a couple of meters thick and smaller, zoned veins commonly cut diabase sheets at steep angles along S3 trends in the Early Jurassic Lambertville diabase sill near Hopewell, NJ (Laney and others, 1995). Dikes and veins striking along S3 directions have also been mapped in the Pennington and Rocky Hill diabase sheets (NJGS permanent notes). S3 extension fractures, dikes, and faults that cut across and offset S1 and S2 features exhibit a finite counterclockwise rotation of the principal extension direction of about 70^{o} that began during S1-stage rifting in the Late Triassic before the onset of regional tectonic compression and basin inversion. Continental rifting probably ended at the onset of sea-floor spreading and development of the drift-stage, 'passive' continental margin', estimated to have ranged from about 166 to 190 Mya in the Early- to Middle Jurassic (Figure 27). The combined S2 and S3 extension events may have lasted as long as the S1 event but were far more pronounced with respect to accumulated crustal strains.

S3 cross fractures strike about E-W, complimentary to S3 extension fractures. In areas where the two opposing directions of principal strain overlap, S3 cross fractures strike subparallel to later extension fractures (SC3 sector in Figure 1) formed during subsequent compression (Figure 2). In southeastern parts of the basin near Pennington and Princeton, NJ, dominant populations of SC3, E-W striking veins occur in systematic arrays striking subparallel with the regional, contemporary tectonic stress field (principal NE-SW horizontal compression shown in Figures 1 and 29). In areas of SC3 influence, S2 and S3 vein fibers in the Passaic Fm locally show complex, incremental stretching and shearing of basin strata that are cut by faults forming positive flower structures (Harding, 1985) with uplifted and folded Late Triassic and Early Jurassic bedrock involving high-angle block faults (Figure 28). In eastern Pennsylvania, small diabase dikes cut Late Triassic

strata along cross-strike fault segments that fold Early Jurassic diabase and align with NW striking lineaments, and gently-plunging open folds in the continental foreland of Pennsylvania (see STOP 3, Figure 1 of the field guide) where Late Paleozoic structures also have NE-plunging terminations in the Valley and Ridge province (Figure 29). These structures are rooted in adjacent bedrock of the oceanic margin where coastal plain strata are fractured (Owen and Sohl, 1969) and apparently offset together with gneissic bedrock of the Trenton Prong (Figure 29). Magnetic (Figure 29) and gravity anomalies in the region help identify concealed basement structures that are an integral part of this structural system. The overall data point to systems of large-scale block faults that continue to transform crustal strata throughout the region today. The age, map extent and geometry of this regional wrench fault system are elusive but have had major components defined from previous mapping during the past half century (Drake and Woodward, 1963; Woodward, 1964; Sheridan, 1976; Arthaud and Matte, 1977; Root and Hoskins, 1977; Sumner, 1978, Manspeizer and Cousminer, 1988).

Early Jurassic SE- and ESE-directed extension and rift faulting within the eastern continental margin of North America evolved into NE-SW-directed compressional wrench faulting, possibly beginning in the Early to Middle Jurassic (Figure 27) that continues today along a similar trend (Figure 29; and Goldberg and others, 2003). The wrench fault system proposed here accounts for late-stage fracture patterns in the basin that formed within the 'passive, drift stage' of tectonism. High-angle faults that locally uplifted and skewed crustal blocks in the southeastern, hinterland parts of the basin involve many concealed faults that link structures from the continental margin to transform faulting in the western Atlantic Ocean basin (Hutchinson and others, 1986; Hutchinson and Klitgord, 1988, Klitgord and others, 1998). This fault system also probably involves Cenozoic strata in areas of neotectonic activity associated with historical seismicity, as observed elsewhere in the eastern North American continental margin (York and Oliver, 1992). Many extensional fractures in the NB are favorably aligned for continued growth in the contemporary stress regime, probably resulting in crack-tip modifications to existing fractures.

The tectonic model proposed here has the initial SC3 compressive push oriented about E-W, almost directly opposed to the latest phase of S3 extension. Future mapping and research may resolve the apparent contradictions between this model and those portraying initial, post-rift oriented compression directed NW-SE, approximately normal to the current structural grain of the continental margin (Goldberg and others, 2003; Schlische, 2003).

REFERENCES

Arthaud, Franics, and Matte, Phillipe, 1977, Late Paleozoic strike-slip faulting in southern Europe and northern Africa: Result of a right lateral shear zone between the Appalachian and the Urals: Geological Society of America Bulletin, v. 88, p. 1305-1320

Beach, A. 1975, The geometry of en-echelon vein arrays: Tectonophysics, v. 28, p. 245-263.

Benson, R.N., 2002, Age estimates of the seaward dipping volcanic wedge, earliest oceanic crust, and earliest drift-stage sediments along the North American Atlantic

continental margin, *in* Hames, W.E., McHone, J.G., Renne, P.R., and Ruppel, C., eds., The Central Atlantic Magmatic Province: American Geophysical Union, Geophysical Monograph, v. 136, p. 61-76.

Berg, T. M., and 8 others, compilers, 1980, Geologic map of Pennsylvania: Commonwealth of Pennsylvania Topographic and Geological Survey Map 1, 2 pl., scale 1:250,000.

de Boer, J. Z., and Clifford, A. E., 1988, Mesozoic tectogenesis: Development and deformation of 'Newark' rift zones in the Appalachian (with special emphasis on the Hartford basin, Connecticut), *in* Manspeizer, Warren, ed., Triassic-Jurassic Rifting, Continental Breakup, and the Origin of the Atlantic Ocean and Passive Margin: Elsiever, New York, Chapter 11, p. 275-306.

Dombroski, D. R., 1992, Catalog of New Jersey earthquakes through 1990: N.J. Geological Survey Geological Survey Report 31, 16 p.

Drake, A. A., Jr., Volkert, R. A., Monteverde, D. H., Herman, G. C., Houghton, H. H., and Parker, R. A., 1996, Bedrock geologic map of northern New Jersey: U. S. Geological Survey Miscellaneous Investigation Series Map I-2540-A, scale 1:100,000, 2 sheets.

Drake, C. L., and Woodward, H. P., 1963, Appalachian curvature, wrench faulting, and offshore structures: New York Academy of Science Transactions, Series 2, V. 26., p. 48-63.

Dula, W. F., 1991, Geometric models of listric normal faults and rollover folds: American Association of Petroleum Geologists Bulletin, v. 75, no. 10, p. 1609-1625.

Duncan, R. A., 1984, Age progressive volcanism in the New England Seamounts and the opening of the central Atlantic Ocean, J. Geophysical Research, v. 89, p. 980-990.

Dunning, G. R., and Hodych, J. D., 1990, U-Pb zircon and baddeleyite age for the Palisade and Gettysburg sills of northeast United States: Implications for the age of the Triass-Jurassic boundary: Geology, v. 18, p. 795-798.

Durney, D. W., and Ramsay, J. G., 1973, Incremental strains measured by syntectonic crystal growths, *in* DeJong, K. A. and Scholten, R., eds., Gravity and Tectonics: New York, Wiley-Interscience, p. 67-96.

El Tabakh, M. E., Schreiber, B. C., and Warren, J.K., 1998, Origin of fibrous gypsum in the Newark rift basin, eastern North America: Journal of Sedimentary Research, v. 68, no. 1., p. 88-99.

El Tabakh, M. E., Riccioni, Rita, and Schreiber, B. C., 1997, Evolution of late Triassic rift basin evaporites (Passaic Formation): Newark basin, eastern North America: Sedimentology, v. 44, p. 767-790.

Faust, G. T., 1978, Joint systems in the Watchung basalt flows, New Jersey: U.S. Geological Survey Professional Paper 864-B. 46 p.

Fisher, D. W., Isachsen Y. W. and Rickard, L. V., 1970,Geologic Map of New York State, New York State Museum and Science Service, Geologic Survey Map and Chart Series, scale 1:250,000, 5 sheets.

Ghatge, S. L., 2004, Magnetic anomalies of New Jersey, N.J Geological Survey Digital Geodata Series DGS04-3, ArcView shapefile coverage, scale 1:500,000.

Goldberg, D., Lupo, T., Caputi, M., Barton, C., and Seeber L., 2003, Stress Regimes in the Newark Basin Rift: Evidence from Core and Downhole Data, i*n*: LeTourneau,

P. M. and Olsen, P. E., eds.,The Great Rift Valleys of Pangea in Eastern North America, v.1, Tectonics, Structure, and Volcanism, Columbia University Press, New York, Chapter 7, p.

Gradstein, F. M., F. P. Agterberg, J. G. Ogg, J. Hardenbol, P. van Veen, J. Thierry, and Z. Huang, 1995, A Mesozoic Time Scale. Journal of Geophysical Research 99 (B12): p. 24.051-24.074.

Groshong, R. H., 1988, Low-temperature deformation mechanisms and their interpretation: Geological Society of America Bulletin, V. 100, p. 1329-1360.

Gross, M. R., 1993, The origin and spacing of cross joints: examples from the Monterey Formation, Santa Barbara Coastline, California: Journal of Structural Geology, v. 15, p. 737-751.

Harding,T. P. , 1985, Seismic characteristics and identification of negative flower structures, positive flower structures, and positive structural inversion**:** American Association of Petroleum Geologists Bulletin, v. 69, p. 582-600.

Herman, G.C., 1997, Digital mapping of fractures in the Mesozoic Newark basin, New Jersey: Developing a geological framework for interpreting movement of groundwater contaminants: Environmental Geosciences, v. 4, no. 2, p. 68-84.

Herman, G. C., 2001, Hydrogeological framework of bedrock aquifers in the Newark Basin, New Jersey, in LaCombe, P.J. and Herman, G.C., eds., Geology in Service to Public Health, Eighteenth Annual Meeting of the Geological Association of New Jersey, p. 6-45.

Hodgson, R. A., 1961, Regional study of jointing in Comb ridge-Navajo Mountain Area, Arizona and Utah, American Association of Petroleum Geologists Bulletin, v. 45, p. 1-38.

Huang, Q., and Angelier, J., 1989, Fracture spacing and its relation to bed thickness: Geological Magazine, v. 126, p. 355-362.

Husch, J. H., 1988, Significance of major- and trace-element variation trends in Mesozoic diabase, west-central New Jersey and Eastern Pennsylvania, in Froelich, A. J., and Robinson, G. R., Jr., eds., Studies of the Early Mesozoic basins of the eastern United States: United States Geological Survey Bulletin 1776, p. 141-150.

Hutchinson, D. R. and Klitgord, K. D., 1988, Evolution of rift basins on the continental margin of southern New England, *in* Manspeizer, W., ed.., Triassic-Jurassic Rifting, Continental Breakup, and the Origin of the Atlantic Ocean and Passive Margin, Elsevier, New York, NY, Chapter 4, p. 82-97.

Hutchinson, D. R. Klitgord, K. D., and Detrick, R. S., 1986, Rift basins of the Long Island platform: Geological Society of America Bulletin, v. 97, p. 688-702.

Klitgord, K. D., Hutchinson, D. R., and Schouten, H., 1998, Tectonic features and geophysical Lineaments; *in* Sheridan, R. E., and Grow, J. A., eds., The Geology of North America, V. I-2, The Atlantic Continental Margin, U.S.: Geological Society of America, Plate 2C.

Laney, S. E., Husch, J. M., and Coffee, Cheryl, 1995, The petrology, geochemistry and structural analysis of late-stage dikes and veins in the Lambertville sill, Belle Mead, New Jersey: Northeastern Geology and Environmental Sciences, V. 17, no. 2., p. 130-145.

Lindholm, R. C., 1978, Triassic–Jurassic faulting in eastern North America—A model based on pre-Triassic structures: Geology, v. 6, p. 365–368.

Lucas, M., Hull, J., and Manspeizer, W., 1988, A foreland-type fold and related structures of the Newark rift basin, in Manspeizer, W., ed., Triassic-Jurassic Rifting, Continental Breakup, and the Origin of the Atlantic Ocean and Passive Margin, Elsevier, New York, NY, Chapter 12, p. 307-332.

Manspeizer, W., and Cousiminer, H.L., 1988, Late Triassic-Early Jurassic synrift basins of the U.S. Atlantic margin; *in* Sheridan, R. E., and Grow, J. A., eds., The Geology of North America, V. I-2, The Atlantic Continental Margin, U.S.: Geological Society of America, Chapter 10, p. 197-216.

McClay, Ken, and Bonora, Massimo, 2001, Analog models of retraining stepovers in strike-slip fault systems: American Association of Petroleum Geologists Bulletin, v. 85, no. 2, p. 233-260

Merguerian, Charles, and Sanders, J. E., 1994, Implications of the Graniteville xenolith for flow directions of the Palisades magma, *in* Benimoff, A. I., ed., The Geology of Staten Island, New York,: Eleventh Annual Meeting of the Geological Association of New Jersey, p. 59.

Monteverde, D. H. 2000, Bedrock Geology of the Roselle Quadrangle, Union and Essex Counties, New Jersey: : N.J. Geological Survey Open-File Map OFM 34, scale 1:24000.

Monteverde, D. H., Stanford, S. D., and Volkert, R. A., 2003, Geologic Map of the Raritan Quadrangle, Hunterdon and Somerset Counties, New Jersey: N.J. Geological Survey Geologic Map Series GMS 03-2, scale 1:24000.

Monteverde, D. H. and Volkert, R. A., 2005, Bedrock Geologic Map of the Chatham Quadrangle, Morris, Somerset and Union Counties, New Jersey: N.J. Geological Survey Geologic Map Series GMS 04-2, scale 1:24000.

Narr, W., and Suppe, J., 1991, Joint spacing in sedimentary rocks: Journal of Structural Geology, v.13, p.1037-1048.

New Jersey Geological Survey, 2000, Bedrock Geology and Topographic Base Maps of New Jersey, 1:100,000 scale, New Jersey Geological Survey Compact Disc Series CD-01.

New Jersey Geological Survey, 2004, Earthquakes Epicentered In New Jersey: N.J. Geological Survey Digital Geoedata Series DGS04-1, ArcView GIS point shapefile of 145 earthquake epicenters.

Nicholson, R., and Pollard, D. D., 1985, Dilation and linkage of echelon cracks. Journal of Structural Geology, v. 7, p. 583–590.

Olsen, P. E. and Kent, D. V., 1996, Milankovitch climate forcing in the tropics of Pangea during the Late Triassic. Palaeogeo. Palaeoclim. Palaeoecol. 122, p. 1-26.

Olsen, P. E., Kent, D., Cornet, Bruce, Witte, W. K., and Schlische, R. W., 1996a, High-resolution stratigraphy of the Newark rift basin (early Mesozoic, eastern North America), Geological Society of America Bulletin, v. 108, p. 40-77.

Olsen, P. E., Schlische, R. W., and Fedosh, M. S., 1996b, 580 Ky Duration of the Early Jurassic flood basalt event in eastern North America estimated using Milankovitch Cyclostratigraphy, in The Continental Jurassic, Morales, Michael, ed.: Museum of Northern Arizona Bulletin 60, p. 11-22.

Olsen, P. E., Withjack, M. O., and Schlische, R. W., 1992, Inversion as an integral part of rifting: An outcrop perspective from the Fundy basin, eastern North America: Eos--American Geophysical Union Transactions, v. 73, no. 43, p. 562.

Owens, J. P., Sugarman, P. J., Sohl, N. F., Parker, R. A., Houghton, H. F., Volkert, R. A., Drake, A. A., Jr., and Orndorff, R.C., 1998, Bedrock Geologic Map of Central and Southern New Jersey, U. S. Geological Survey Miscellaneous Investigation Series Map I-2540-B, scale 1:100,000, 4 sheets.

Owens and Sohl, 1969, Shelf and Deltaic Paleoenvironments in the Cretaceous-Tertiary Formations of the New Jersey Coastal Plain, in Subitzky, Seymour, ed., Geology of selected areas in New Jersey and Pennsylvania, Rutgers University Press, New Brunswick, New Jersey, p. 235-278.

Parker, R. A., Houghton, H. F., and McDowell, R. C., 1988, Stratigraphic framework and distribution of early Mesozoic rocks of the northern Newark basin, New Jersey and New York, *in* Froelich, A. J., and Robinson, G. R., Jr., eds., Studies of the Early Mesozoic basins of the eastern United States: United States Geological Survey Bulletin 1776, p. 31-39.

Parnell, J. and Monson, B., 1995, Paragenesis of hydrocarbon, metalliferous and other fluids in Newark Group basins, Eastern U.S.A., Institute of Mining and Metallurgy, Transactions, Section B: Applied Earth Science; v. 104, p. 136-144.

Pollard, D.P., and Aydin, A., 1988, Progress in understanding jointing over the past century: Geological Society of America Bulletin, vV. 100, p. 1181-1024.

Pratt, L.M., Shaw., C.A., and Burruss, R.C., 1988, Thermal histories of the Hartford and Newark rift basins inferred from maturation indices of organic matter, in Studies of the Early Mesozoic basins of the Eastern United States, Froelich, A.J. and Robinson, G.R., Jr., eds., U.S. Geological Survey Bulletin 1776., p. 58-62.

Ramsay, J. G., 1980, The crack-seal mechanism of rock deformation: Nature, 284, p. 135-139.

Ramsay, J. G., and Huber, M. I., 1983, The techniques of modern structural geology, v. 1: Strain analysis: London, England, Academic Press, 307 p.

Ramsay, J. G., and Huber, M. I., 1987, The techniques of modern structural geology, v. 2: Folds and fractures: London, England, Academic Press, 700 p.

Ratcliffe, N. M., 1971, The Ramapo fault system in New York and adjacent northern New Jersey: A case of tectonic heredity: Geological Society of America Bulletin, v. 82, p. 125-142.

Ratcliffe, N.M., and Burton, W.C., 1985, Fault reactivation models for the origin of the Newark basin and studies related to U.S. eastern seismicity: U.S. Geological Survey Circular 946, p. 36-45.

Reed, J. C. Jr. and Bush, C. A., 2004, Generalized Geologic Map of the Conterminous United States, National Atlas of the United States, Version 1.1, scale 1:7,500,000, http://pubs.usgs.gov/atlas/geologic/.

Rodgers, John , 1985, Bedrock geologic map of Connecticut: Connecticut Geological and Natural History Survey, 2 sheets, scale 1:125,000.

Root, S. I., and Hoskins, D. M., 1977, Lat 40^{o}N fault zone, Pennsylvania: A new interpretation: Geology v. 5, p. 719-723.

Sanders, J., E., 1963, Late Triassic tectonic history of Northeastern United States, American Journal of Science, v. 261, p. 501-524.

Schlische, R. W., 1992, Structural and stratigraphic development of the Newark extensional basin, eastern North America: Evidence for the growth of the basin and

its bounding structures: Geological Society of America Bulletin, v. 104, p. 1246-1263.

Schlische, R. W., 1993, Anatomy and evolution of the Triassic-Jurassic continental rift system, eastern North America: Tectonics, v. 12, p. 1026-1042.

Schlische, R.W., 2003, Progress in understanding the structural geology, basin evolution, and tectonic history of the eastern North American rift system, in LeTourneau, P.M., and Olsen, P.E., eds., The Great Rift Valleys of Pangea in Eastern North America , v. 1, Tectonics, Structure, and Volcanism: New York, Columbia University Press,
p. 21-64.

Schlische, R. W., and Olsen, P. E., 1988, Structural evolution of the Newark Basin, in Husch, J. M., and Hozik, M. J., eds., Geology of the central Newark Basin, field guide and proceedings: 5th Annual Meeting of the Geological Association of New Jersey, Rider College, Lawrenceville, N.J., p. 43-65.

Schlische, R. W., Withjack, M. O., and Eisenstadt, Gloria, 2002, An experimental study of secondary deformation produced by oblique-slip normal faulting: American Association of Petroleum Geologists Bulletin, v. 86, no. 5., p. 885-906.

Sheridan, R. E., 1976, Conceptual model for the block-fault origin of the North American Atlantic continental margin geosyncline: Geology, v. 2., p. 465-468.

Simonson, B. M. and Smoot., J. P., 1994, Distribution and origin of macropore-filling cements in nonmarine mudstones, early Mesozoic Newark Basin, New Jersey and Pennsylvania: Geological Society of America, Abstracts with Programs. v. 26, no. 7, p. 337

Smoot, J. P., and Olsen, P. E., 1994, Climatic cycles as sedimentary controls of rift-basin lacustrine deposits in the early Mesozoic Newark Basin based on continuous core, *in* Lomando, T., and Harris, M., eds., Lacustrine depositional systems: Society of Sedimentary Geology (SEPM) Core Workshop Notes, v. 19, p. 201-237.

Smoot, J. P. and Simonson, B. M., 1994, Alkaline authigenic minerals in the early Mesozoic, Newark Basin, NY, NJ, PA; evidence for late fluid movement through mudstones: American Association of Petroleum Geologists and Society of Economic Paleontologists and Mineralogists Abstracts with Programs, 1994 AAPG annual convention, p. 261-262.

Stanford, S. D., 1993, Surficial Geologic Map of the Princeton Quadrangle, Mercer, Middlesex, and Somerset Counties, New Jersey, NJGS Open-file Map OFM 11, Scale 1:24,000.

Stanford, S. D., Monteverde, D. H., and Volkert, R. A., 1998, Geology of the New Brunswick Quadrangle, Middlesex and Somerset Counties, New Jersey, N.J. Geological Survey Open-file Map OFM 23, scale 1:24,000.

Steckler, M.S., Omar, G.I., Karmer, G.D., and Kohn, B.P., 1993, Pattern of hydrothermal circulation within the Newark basin from fission-track analysis: Geology, v., 21, p. 735-738.

Sumner, J. R., 1978, Geophysical investigation of the structural framework of the Newark-Gettysburg Triassic basin, Pennsylvania: Geological Society of America Bulletin, v. 88, p. 935-942.

Sutter, J.F., 1988, Innovative approaches to the dating of igneous events in the early Mesozoic basins of the eastern United States, *in* Froelich, A.J., and Robinson, G.R.,

Jr., eds., Studies of the early Mesozoic basins of the eastern United States: U.S. Geological Survey Bulletin 1776, p. 194-200.

Swanson, M. T., 1986, Preexisting fault control for Mesozoic basin formation in eastern North America: Geology, v. 14, p. 419–422.

Van de Kamp, P. C. and Leake, B. E., 1996, Petrology, geochemistry, and Na metasomatism of Triassic – Jurassic non-marine clastic sediments in the Newark, Hartford, and Deerfield rift basins, northeastern USA.:Chemical Geology v. 133, p. 89-124.

Van Houten, F. B., 1964, Crystal casts in upper Triassic Lockatong and Brunswick Formations: Sedimentology, v. 4., p. 301-313.

Van Houten, F. B., 1965, Composition of Triassic Lockatong and associated formations of Newark Group, central New Jersey and adjacent Pennsylvania: American Journal of Science, v. 263, p. 825-863.

Wiltschko, D. V. and Morse, J. W., 2001, Crystallization pressure versus "crack seal" as the mechanism for banded veins, Geology, v. 29; no. 1; p. 79-82.

Withjack, M. O., Islam, Q. T., and La Pointe, P. R., 1995, Normal faults and their hanging-wall deformation: An experimental study: American Association of Petroleum Geologists Bulletin, v. 79, No. 1, p. 1-18.

Withjack, M. O., Schlische, R. W. and Olsen, P. E., 1998: Diachronous rifting, drifting, and inversion on the passive margin of eastern North America: An analogue for other passive margins: American Association of Petroleum Geologists Bulletin, v. 82,
p. 817-835.

Woodward, H. P., 1964, Central Appalachian tectonics and the deep basin: American Association of Petroleum Geologists Bulletin, v. 48, no. 3, p. 338-356.

York, J. E., and Oliver, J. E., 1992, Cretaceous and Cenozoic faulting in eastern North America: Geological Society of America Bulletin: v. 87, No. 8, p. 1105–1114.

Xiao, H., and Suppe, J., 1992, Origin of rollover: American Association of Petroleum Geologists Bulletin, v. 76, no. 4, p. 509-529.

FIELD GUIDE

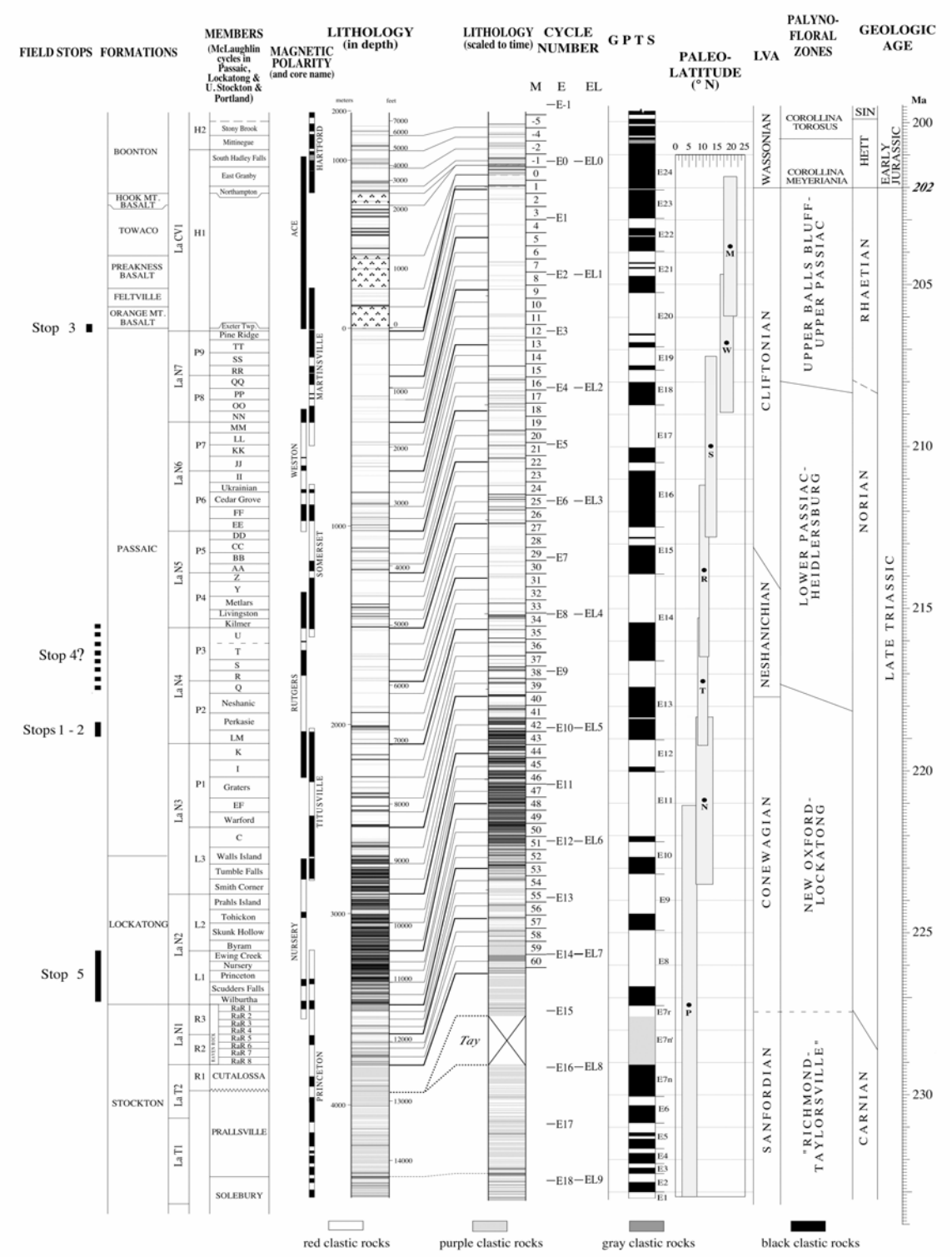

Newark basin astronomically calibrated geomagnetic polarity time scale derived from the Newark basin coring project (1990-1993) showing the relative stratigraphic position and age of the field stops.

ROAD LOG

Newark Basin - View from the 21st Century Field Trip Road Log

Segment Start / Stop (mi)		Segment Directions
0.0	0.3	From TCNJ Pkg Lot 4 entrance, proceed N/E on service road to Rt 31 (Pennington Rd).
0.3	1.8	Turn R (N) onto Rt 31 and proceed to entrance to I-95 (South to PA)
1.8	6.0	Proceed S on I-95 to Exit 1 (Rt 29)
6.0	15.5	Proceed N on Rt 29 to jct with Rts 179 & 518
15.5	16.7	Continue N on Rt 29 to exit ramp for Rt 202S
16.7	24.3	Proceed S on Rt 202 to jct with PA 413
24.3	32.9	Turn R (N) on PA 413 and proceed to jct with PA 611
32.9	38.2	Bear R (N) onto PA 611 and proceed to jct with PA 412
38.2	42.0	Continue N on 611 to jct with Trauger's Crossing Rd *Travel time: Approx 70 minutes from TCNJ to Stop 1.*

Stop 1 - Haycock Mt.; Stop Leader: Dr. Roy Schlische, Rutgers University

42.0	43.1	From PA 611/Trauger's Crossing Rd, jct, proceed N on PA 611 to jct with Rt 32
43.1	47.4	Turn R (E) onto Rt 32 and proceed to bridge over Delaware R. (Bridge St)
47.4	47.6	Turn L (E) onto Bridge St and follow over Delaware R. to jct with Church St. in Milford, NJ.
47.6	49.0	Turn L (N) onto Church St., then R (N) onto Spring Garden St (Hunterdon Co 627), proceed to jct with Spring Garden Rd (suitable for bus turnaround) *Travel time: Approx 25 minutes from Stop 1 to Stop 2.*

Stop 2 - Pebble Bluff; Stop Leader: Dr. Paul Olsen, LDGO, Columbia University

49.0	50.4	From jct of Co Rd 627 & Spring Garden Rd., proceed S on Hunterdon Co 627, then E & S on Church St to jct with Bridge St.
50.4	50.6	Turn L (E) on Bridge St and proceed to "T" junction with Rt 619
50.6	54.1	Bear R (S) onto Rt 619 and proceed south to Bridge St. in Frenchtown, NJ
54.1	54.3	Turn L (E) onto Bridge St. and proceed to jct with Rt 12 (sign on right)
54.3	64.7	Turn R (E) onto Rt 12 and proceed to jct with Old Croton Rd.

64.7	64.9	Turn L (N) onto Old Croton Rd and proceed to Mine Brook Park pkg lot on right *Travel time: Approx 40 minutes from Stop 2 to Stop 3.*

Stop 3 - Mine Brook Park; Stop Leader: Dr. Greg Herman, NJ Geological Survey

LUNCH

64.9	65.1	From Mine Brook Park, proceed S on Old Croton Rd. to jct with Rt 12
65.1	66.2	Turn L (E) onto Rt 12, proceed to 12 / 31 / 202 traffic circle
66.2	71.7	Bear R (S) onto Rt 31 / 202, proceed to exit for Rt 31 South
71.7	75.8	Proceed south on Rt 31 to jct with Rt 518
75.8	82.2	Turn L (E) onto Rt 518 and proceed to jct with Rt 601
82.2	85.3	Turn L (N) onto Rt 601 and proceed to 3M plant entrance. *Travel time: Approx 35 minutes from Stop 3 to Stop 4*

Stop 4 - Hopewell Fault; Stop Leader: Mr. Steve Laney

85.3	88.4	From 3M plant entrance, proceed S on Rt 601 to jct with Rt 518
88.4	94.8	Turn R (W) onto Rt 518 and proceed to jct with Rt 31
94.8	102.0	Turn L (S) onto Rt 31 and proceed to jct with I-95 (South to PA)
102.0	104.7	Enter I-95 (South to PA) and proceed West to Exit 2 (Rt 579)
104.7	105.7	Proceed South on Rt 579 to jct with Rt 634
105.7	106.0	Turn L (E) onto Rt 634 (Upper Ferry Rd) and proceed to Naval Air Warfare Center pkg lot *Travel time: Approx 35 minutes from Stop 4 to Stop 5*

Stop 5 - Naval Air Warfare Center; Stop Leader: Mr. Pierre Lacombe, US Geological Survey

106.0	106.7	From N.A.W.C. pkg lot, proceed East on Rt 634 to jct with Scotch Rd (Rt 611)
106.7	107.1	Turn L (N) onto Scotch Rd and proceed to jct with Carlton Ave.
107.1	107.9	Turn R (E) onto Carlton Ave, proceed to jct with Rt 31 (Pennington Rd)
107.9	108.2	Proceed straight into entrance to TCNJ, bear R (E / S) onto service road, proceed to pkg lot 4. End Field Trip. *Travel time from Stop 5 to TCNJ: Approx 10 minutes.*

Stop 1. Normal Faults in the Passaic Formation at Haycock Mountain, PA

Roy W. Schlische & Martha Oliver Withjack
Department of Geological Sciences
Rutgers University
Piscataway, NJ 08854

A set of meter-scale normal faults cuts red mudstone of the middle Passaic Formation (Figure 1). The normal faults strike ~030° and generally dip 40°-50° to the SE. Slickenlines are steeply raking, indicating predominantly dip-slip movement. Like most larger intrabasinal faults in the Newark basin, these faults are oblique to the strike of fault segments of the border-fault system (the strike of the nearest segment of the border-fault system is ~060°). Experimental clay modeling of oblique deformation (Schlische et al., 2002) indicates that secondary faults (equivalent to the intrabasinal faults) form subperpendicular to the extension direction and undergo dip-slip displacement, whereas the reactivated master fault (equivalent to the border fault) undergoes oblique-slip displacement.

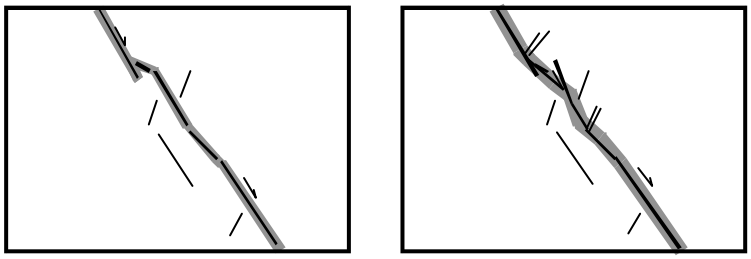

Figure 1. Sketch of normal-faulted Passaic Formation at Haycock Mountain (left) and inferred evolution of normal faults (right) based on geometries at Haycock Mountain. From Withjack and Olsen (1999).

Fault 2 (Figure 1) has the smallest displacement and narrowest zone of breccia and gouge; fault 4 has the highest displacement and widest zone of breccia and gouge. These faults obey an approximately linear scaling relationship between fault width and fault displacement (e.g., Hull, 1988; Knott, 1994; Figure 2). The sequence going from fault 2 to 3 to 1 to 4 likely reflects stages in the evolution of normal faults with increasing displacement (Figure 1).

The Haycock Mountain outcrop is ~5 km NE of the location of the NB1 seismic-reflection profile and about 6 km NW of the Cabot well, both of which provide important

information about the subsurface geometry of the Newark basin (Schlische and Withjack,

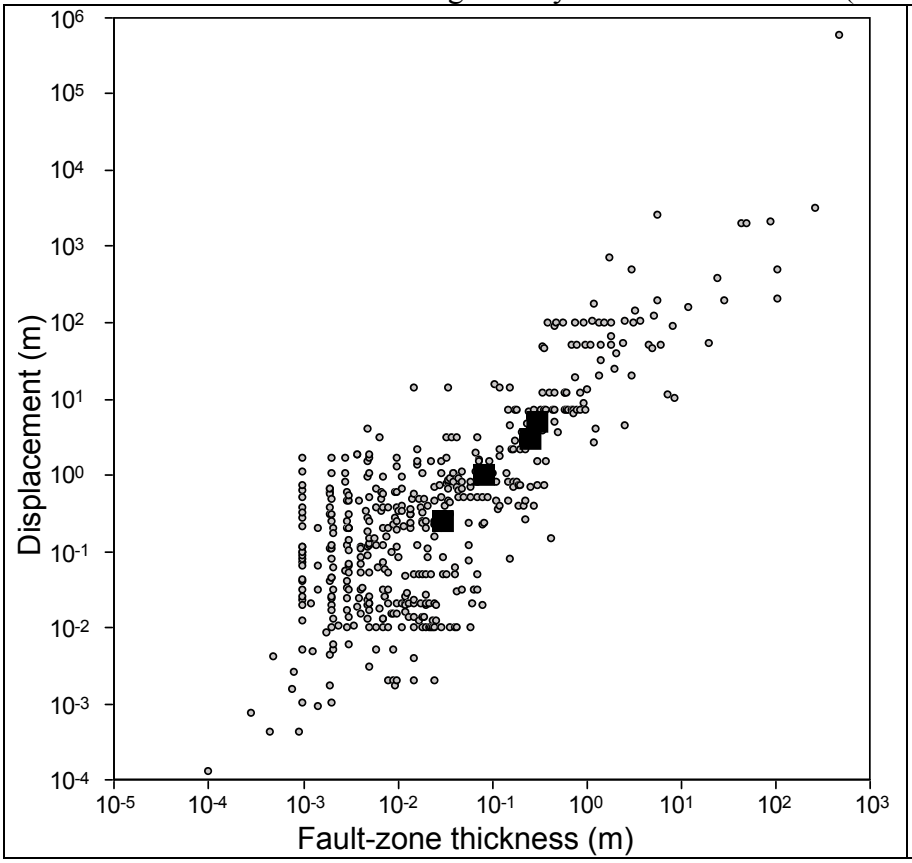

Figure 2. Log-log plot of fault displacement vs. fault-zone thickness. Small circles show data from Hull (1988), Knott (1994), and Knott et al. (1996). Large black squares are data from the four largest faults at Haycock Mountain.

2005). The seismic profile (Figure 3) shows a shallow-dipping border-fault system, which is consistent with the interpretation that it is a reactivated Paleozoic contractional structure (e.g., Ratcliffe et al., 1986). The footwall block contains a number of reflections that are subparallel to the border fault and are also likely Paleozoic contractional faults.

According to Withjack and Olsen (1999), the exposure belongs to the upper part of Member K of the Passaic Formation (nomenclature of Olsen et al., 1996). Deposition occurred mostly in playas. A prominent bed contains vugs that were once filled with evaporite minerals. Silt bands likely represent slightly deeper or more permanent shallow lakes. Red beds similar to those outcropping here account for more than 80% of the Passaic Formation.

Although this outcrop is less than 4 km from the border fault, the sedimentary rocks are fine grained. Two possibilities account for this observation: (1) The hanging-wall block and axial sources contributed more sediment than the footwall block, as in many modern rift basins (e.g., Gawthorpe and Leeder, 2000). (2) The present-day boundary fault of the basin was not the outermost border fault during deposition (Figure 4). In Late Triassic time, coarser sediments accumulated in the hanging walls of border faults located to the NW of the present-day border fault. Subsequent erosion (up to 5 km in places; Steckler et al., 1993; Malinconico, 1999) removed these coarse-grained strata and exposed the Paleozoic and Precambrian rocks.

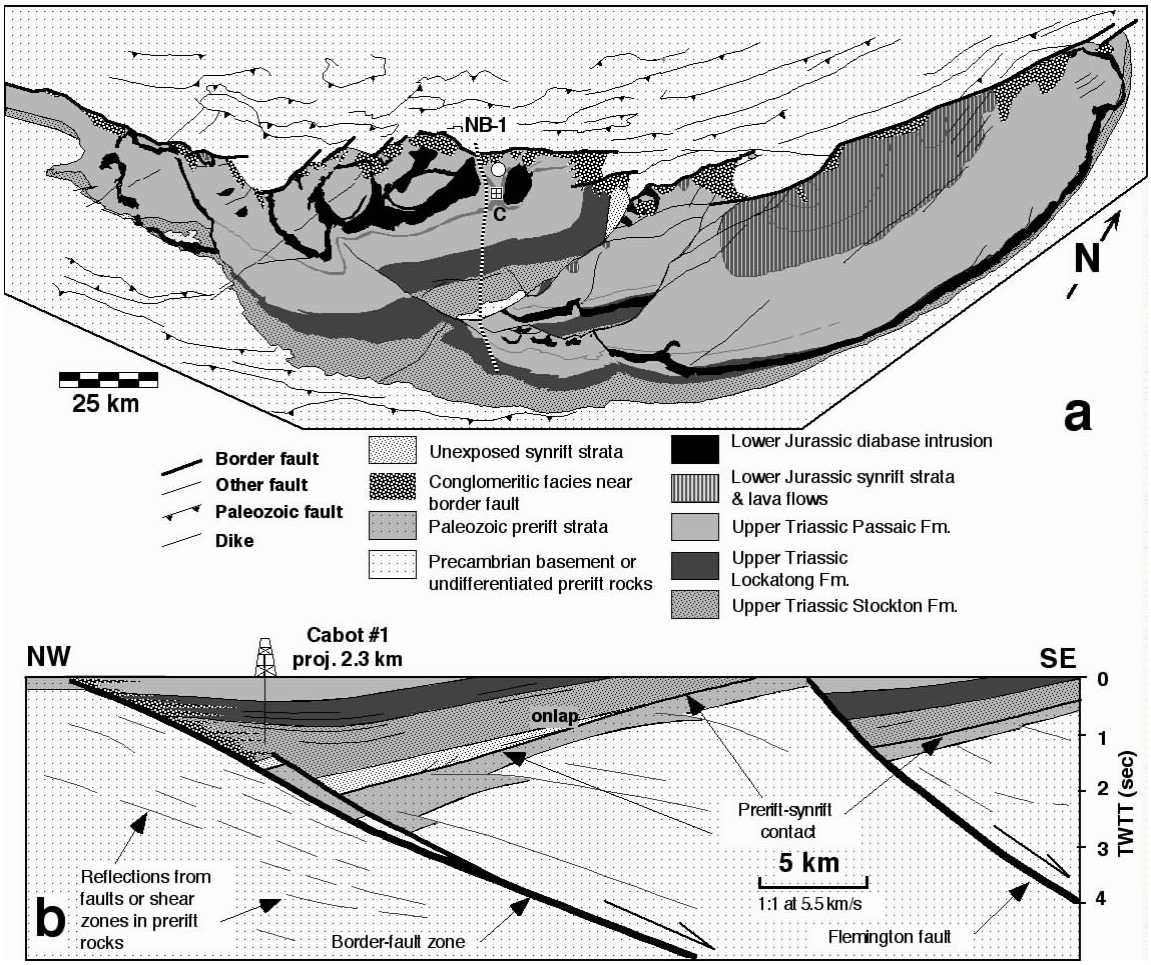

Figure 3. (a) Geologic map of the Newark basin showing location of the NB-1 seismic-reflection profile, the Cabot #1 well (C), and the Haycock Mountain outcrop (circle). (b) Interpretation of line NB-1 constrained by surface geology and the nearby Cabot #1 well. Modified from Schlische and Withjack (2005).

REFERENCES

Gawthorpe, R.L., and Leeder, M.R., 2000, Tectono-sedimentary evolution of active extensional basins: Basin Research, v. 12, p. 195-218.

Hull, J., 1988, Thickness-displacement relationships for deformation zones: Journal of Structural Geology, v. 10, p. 431-435.

Knott, S.D., 1994, Fault zone thickness versus displacement in the Permo-Triassic sandstones of NW England: Journal of the Geological Society, London, v. 151, p. 17-25.

Knott, S.D., Beach, A., Brockbank, P.J., Brown, J.L., McCallum, J.E., and Welbon, A.I., 1996, Spatial and mechanical controls on normal fault populations: Journal of Structural Geology, v. 18, p. 359-372.

Malinconico, M.L., 1999, Thermal history of the Early Mesozoic Newark (NJ/PA) and Taylorsville (VA) basins using borehole vitrinite reflectance: conductive and advective effects: Geological Society of America Abstracts with Programs, v. 31, n. 2, p. A-31.

Olsen, P.E., Kent, D.V., Cornet, B., Witte, W.K., and Schlische, R.W., 1996, High-resolution stratigraphy of the Newark rift basin (early Mesozoic, eastern North America): Geological Society of America Bulletin, v. 108, p. 40-77.

Ratcliffe, N.M., Burton, W.C., D'Angelo, R.M., and Costain, J.K., 1986, Low-angle extensional faulting, reactivated mylonites, and seismic reflection geometry of the Newark basin margin in eastern Pennsylvania: Geology, v. 14, p. 766-770.

Schlische, R.W., Withjack, M.O., and Eisenstadt, G., 2002, An experimental study of the secondary deformation produced by oblique-slip normal faulting: AAPG Bulletin, v. 86, p. 885-906.

Schlische, R.W., and Withjack, M.O., 2005, The early Mesozoic Birdsboro central Atlantic margin basin in the Mid-Atlantic region, eastern United States: Discussion: Geological Society of America Bulletin, v. 117, p. 823-828.

Steckler, M.S., Omar, G.I., Karner, G.D., and Kohn, B.P., 1993, Pattern of hydrothermal circulation with the Newark basin from fission-track analysis: Geology, v. 21, p. 735-738.

Withjack, M.O., and Olsen, P.E., 1999, Rift Basins and Passive Margins Tectonics Seminar, Mobil Technology Company, July 14-24, 1999.

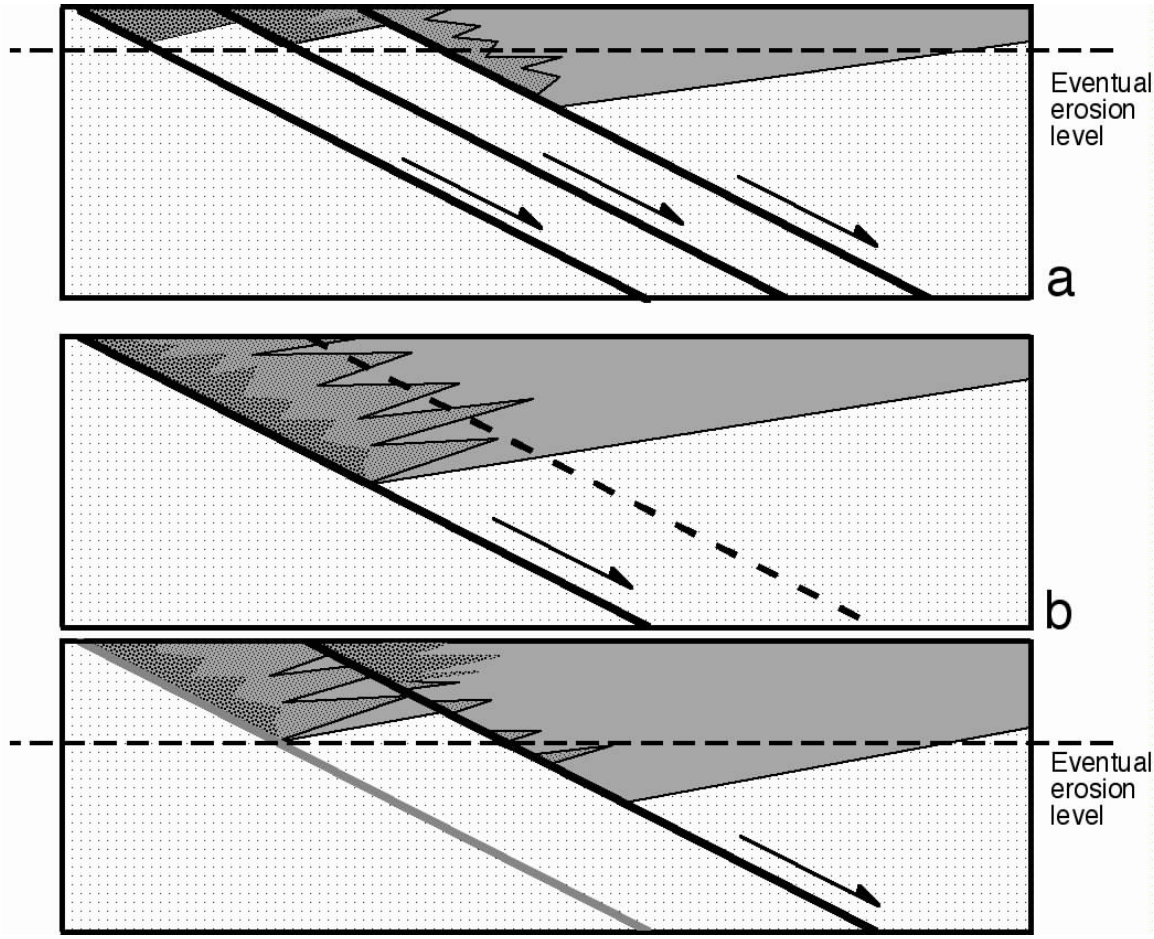

Figure 4. Schematic cross sections showing border-fault development during deposition. (a) Model with multiple active faults. Coarse-grained sediments preferentially accumulate in hanging walls of outer border fault. Later erosion removed these sedimentary rocks. (b) Model with basinward migration of border faults. During

the early stages of rifting, the outer border fault was active, and coarse-grained sediments accumulated in its hanging wall. During the later stages of rifting, the inner border fault became active, and coarse-grained sediments accumulated in its hanging wall. Later erosion removed the coarse-grained sedimentary rocks. From Withjack and Olsen (1999).

Stop 2. Upper Member L-M and Perkasie Member of the Passaic Fm. Pebble Bluff, Milford, NJ.

P. E. Olsen, J. P. Smoot, and J. H. Whiteside

Latitude and Longitude: (aprox.) 40°34.60'N, 75°08.27'W
Stratigraphic Unit: Passaic Formation
Age: Norian; ~215 Ma
Main Points:

1. Passaic Formation near border fault and coarse facies of interval at Stop 1.
2. Milankovitch cyclicity, and deeper water units extending into conglomeratic facies
3. Comparision to central basin facies
4. Fossiliferous outcrops
5. Reptile footprint faunules

These outcrops (Fig. 1), also described by Van Houten (1969, 1980), Arguden and Rodolpho (1986), Olsen and Flynn (1989), and Olsen et al., 1989) are less than 2.4 km to the southeast from the border fault and consist of thick sequences (>20 m) of red conglomerate and sandstones alternating with cyclical black, gray, and red mudstone and sandstone. Dips average 10-15° NW, and there several faults, downthrowing to the east, between the largest outcrops. These outcrops are part of the cyclical and quasiperiodic lacustrine to fluvial succession of the central Newark basin in which lake depth responded profoundly to Milankovitch climate forcing (Olsen, 1996; Olsen and Kent, 1996; Olsen and Kent, 1999). The thickest gray beds at this stop (see Figures 1 and 2) are the Perkasie Member, marking a 405 ky McLaughlin cycle within the wetter part of a 1.75 m.y. modulating cycle (P2) and a wetter part of a 3.5 m.y. Laskar cycle (La4). The red conglomerates in the lower parts of the section are the coarse lateral equivalents of the red mudstones seen at Stop 1.

The Perkasie Member consists of Van Houten cycles and compound cycles showing the same pattern as the Lockatong (Olsen, 1986; Olsen and Baird, 1986). It consists of two sequential 100 ky) year cycles, each containing two well developed ~20 ky Van Houten cycles and weakly developed red and purple Van Houten cycle, succeeded upwards by red clastics (Figure 2). McLaughlin named the lower set of gray beds member N and the upper member O, which I have renamed short modulating cycle N and O, respectively. Underlying strata at these outcrops comprise the drier parts of member L-M, and these are largely conglomeritic at this site.

Conglomerates at Pebble Bluffs occur in three basic styles. 1) Poorly-bedded boulder-cobble conglomerate with pebbly sandstone interbeds. Matrix rich conglomerates are in places matrix-supported. These appear to define lenses that are convex-upward and bounded by the largest clasts at their edges and tops. These lenses appear to be debris flow lobes, in which some of the matrix may have been partially washed out by rain during periods of non-deposition. If correctly identified, the flow lenses are typically less than 30 cm thick and less than 5 m wide, similar to debris flows formed on mid to lower portions of steep fans. Pebbly sandstone and muddy sandstone include "trains" of isolated

cobbles often oriented vertically. These cobble trains represent thin, low viscosity debris flows that are stripped of their matrix by shallow flash-flood streams. The sandstones appear to be broad, shallow stream deposits that may include hyperconcentrated flow as indicated by flat layering defined by the orientation of granules. At this locality, this style of conlomerte occurs in the upper part of member M-L.

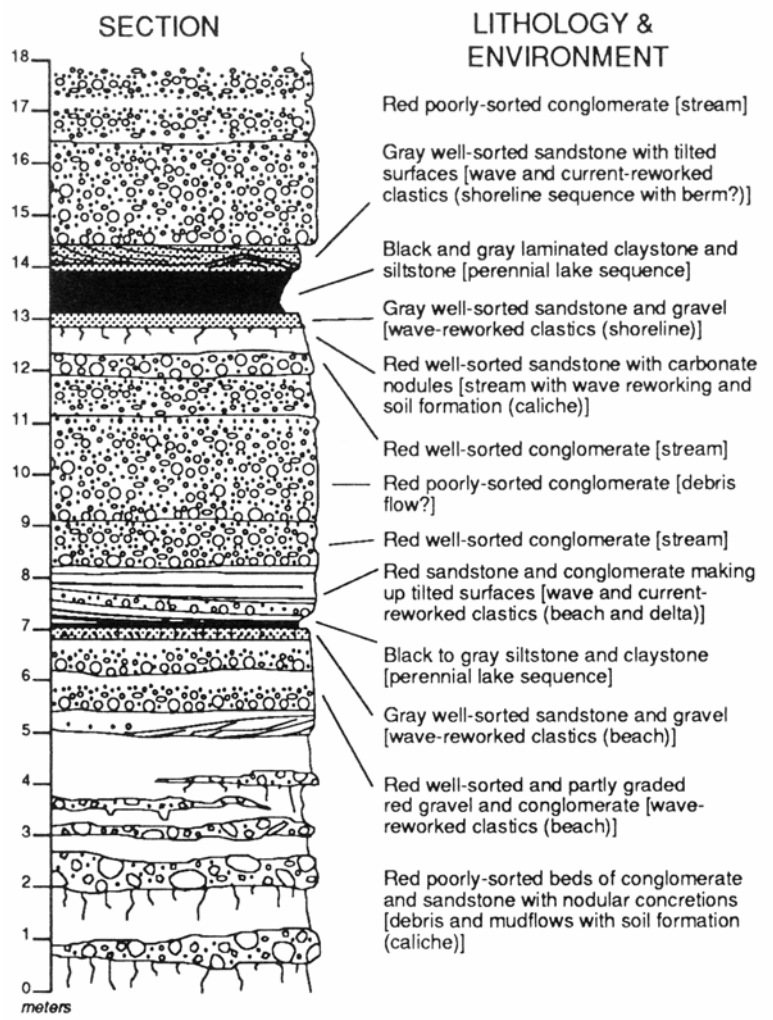

Figure 1 Measured section of the Passaic Formation at Pebble Bluff, Stop 2, showing the interfingering of debris flow, shoreline, and perennial lake deposits. (Olsen et al., 1989).

2) Well-defined lenticular beds of pebble-cobble conglomerate separated by pebbly muddy sandstones with abundant root structures. The conglomerate beds are channel-form with abundant imbrication. Some internal coarsening and fining sequences are consistent with longitudinal bars (Bluck, 1982). Finer grained deposits resemble less-incised channels and overbank deposits. There are some hints of thin debris flow sheets. Abundant root structures filled with nodular carbonate suggest soil caliche. Again these types of conglomerates are here almost entirely within member L-M although some occur in the gay parts of the Perkasie Member.

3) Grain-supported cobble-pebble conglomerate with sandy matrix. Granules and coarse sand show high degree of sorting suggesting wave reworking of finer fractions

(LeTourneau and Smoot, 1985; Smoot and LeTourneau, 1989). These are associated with gray and black shales and oscillatory-rippled sandstones in Van Houten cycles. No unequivocal bar-form structures or imbricate ridges have been observed. These types are here restricted to the gray parts the Perkasie Member.

Laterally-continuous black and gray siltstones and claystones within division 2 of Van Houten cycles contain pinch-and-swell laminae, abundant burrows, and rare conchostracans. These are definitely lacustrine deposits, almost certainly marginal to the finer-grained facies more centrally located in the basin. These lacustrine sequences mark transgressions of perennial lakes over the toes of alluvial fans, much as LeTourneau and Smoot (1985) and LeTourneau (1985) described in marginal facies of the Portland Formation in the Hartford basin of Connecticut. Division 2 of cycles comprising the Perkasie Member were produced by lakes which were almost certainly shallower than those which produced the microlaminated, whole fish- and reptile-bearing units in other parts of the Newark basin section. They evidently were deep enough, however, to transgress over at least the relief caused by the toes of alluvial fans. To what degree have more subtle transgressions of shallower lakes modified clastic fabrics elsewhere in this section?

The restriction of the conglomerate facies to the vicinity of the border fault and the association of debris flow and shallow stream deposits is consistent with an alluvial fan model (i.e., Nilson, 1982). Channel-form conglomerates suggest flash-flooding streams that are still consistent alluvial fans; but the abundance of interbedded fine sandstone suggest lower slopes than for the debris flow deposits. All of the deposits resemble distal low-slope fans or in the case of the coarse debris flow conglomerates, more distal parts of steep fans. Intercalation of lacustrine shales would appear to demand low slops. Coarsening up sequences of wave-formed deposits suggest intermittent introduction of material in receding lakes. This is probably a climatic as opposed to tectonic response because the shallowing is recognized basin-wide. Therefore, even the coarsest deposits accumulated on relatively low slopes. The requirement of low slopes means the present basin fault does not necessarily mark the apex and more likely the fans extended several miles beyond the present basin boundary (Smoot. 1991). The fans could have extended away from the present basin as thin veneers on pediment surfaces on basement, with fan material being continuously recycled basinward. This is consistent with the observations of a number of workers (Van Houten, pers. comm.; Manspeizer, pers. comm.) who noted that many of the clasts in the debris flow and poorly-sorted stream deposits are relatively well- rounded and mixed with highly-angular clasts.

Individual Van Houten cycles of the Perkasie Member in this area average 7 m thick, as compared with a mean of 6.5 m for the same cycles at the Bucks County Crushed Stone Quarry. The thickness of the ~100 ky cycles increase as well from 20.3 m at Ottsville to 28.1 m in this area (Figure 3). At New Brunswick, New Jersey, closer to the east side of the basin, the cycles are a mean of 4.4 m. This thickening towards the border fault is typical of most of the Newark Supergroup and dramatically illustrates the asymmetrical character of the half-graben. The trend to greater fossil richness is evident at this outcrop as is typical for more marginal facies of the Passaic Formation. The conchostracans present in the upper parts of division 2 in the upper black shale cycle in the second short modulating cycle of the Perkasie are absent in the more basinward exposures.

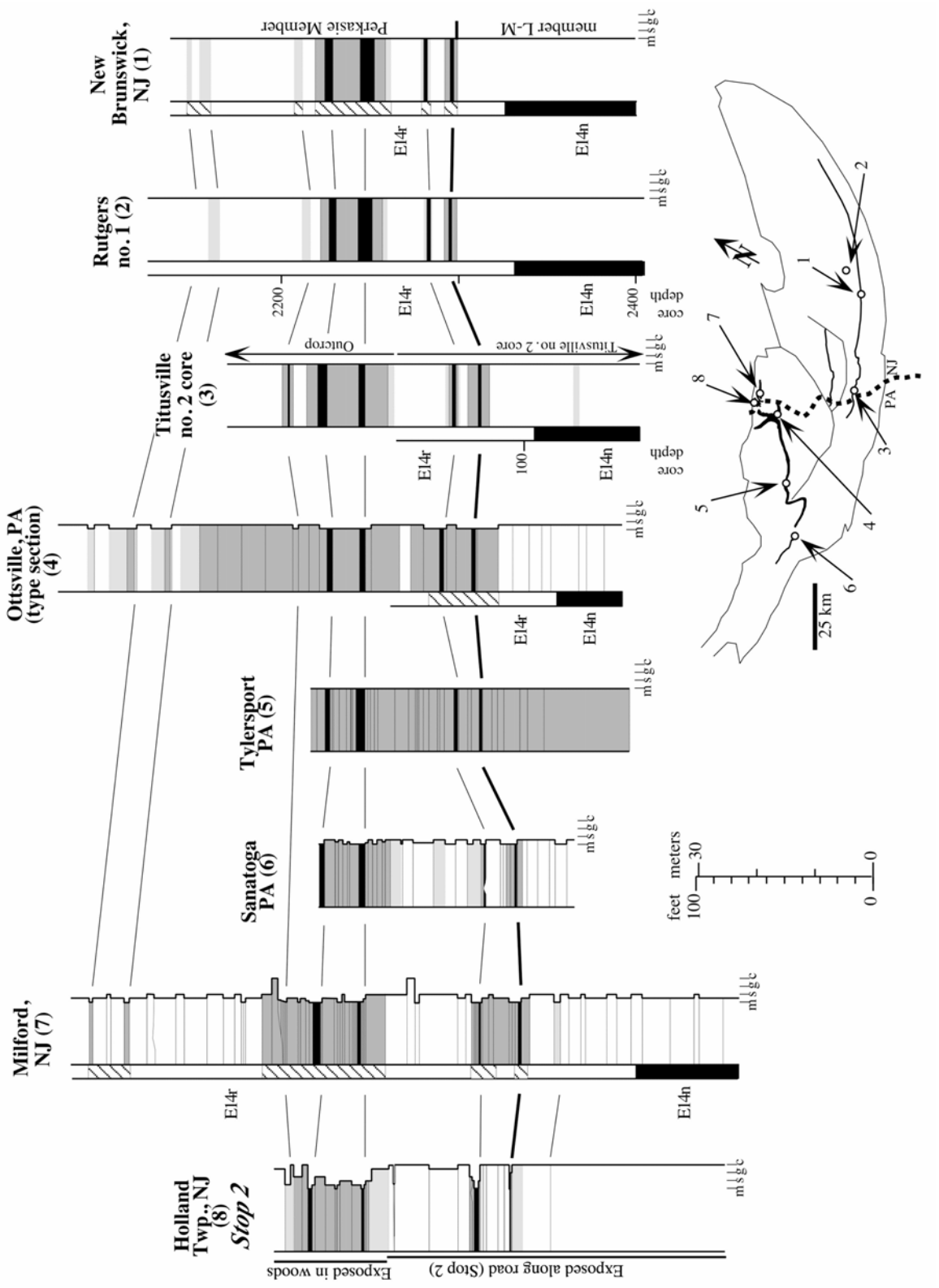
New Brunswick, NJ (1)
Perkasie Member
member L.-M
Rutgers no. 1 (2)
Titusville no. 2 core (3)
Outcrop
Titusville no. 2 core
core depth
2200
2400
100
Ottsville, PA (type section) (4)
Tylersport PA (5)
Sanatoga PA (6)
Millford, NJ (7)
Holland Twp., NJ (8)
Stop 2
E14r
E14n
Exposed along road (Stop 2)
Exposed in woods
feet
meters
100
30
0
0
25 km
PA
NJ
1
2
3
4
5
6
7
8

Figure 2. Lateral correlation of the lower part of the Perkasie Member in outcrops and cores. Locations of sites are: 1, Rt. 18, New Brunswick, NJ ; 5, NE extension, PA Turnpike, Tylersport, PA; 6, quarry, Sanatoga, PA; 7, road outcrops in and near Milford, NJ; 8, Pebble Bluff, Holland Township, NJ (Stop 2) (from Olsen et al., 1996). For lithologies: white represents red; light gray, represents purple; gray, represents gray; and black, represents black. For magnetic polarity: black is normal and white is reverse.

The central basin facies of the Perkasie Member, consisting largely of fine-grained playa deposits is remarkably devoid of fossils. However, at localities such as these, closer to the border fault, fossils of many kinds are actually quite common. This I believe to be due to two factors: 1) desiccation patterns; and 2) variability of accumulation rate. In the central facies of the Newark basin the Passaic (and Lockatong) are profoundly mud dominated. On the flat playas during dry phases of Van Houten cycles, the high frequency of wetting and drying events produce a desiccation breccia fabric that destroys most trace and aquatic fossils. Second, and probably more importantly, the accumulation rate in the center of the Newark basin was probably extremely even with a precompaction rate of only 1 mm or so a year. Such evenness of accumulation means that remains of plants or animals are not buried quickly enough to remove them from the high recycling rate part of the terrestrial ecosystem. In contrast, closer to the border fault, accumulation rates were much more erratic both vertically and horizontally. This is evident from the scale of individual deposition events, which is both on average larger and more erratic near the border fault than at the center of the basin. Hence, there is a much higher potential for swift burial and escape from ecosystem recycling

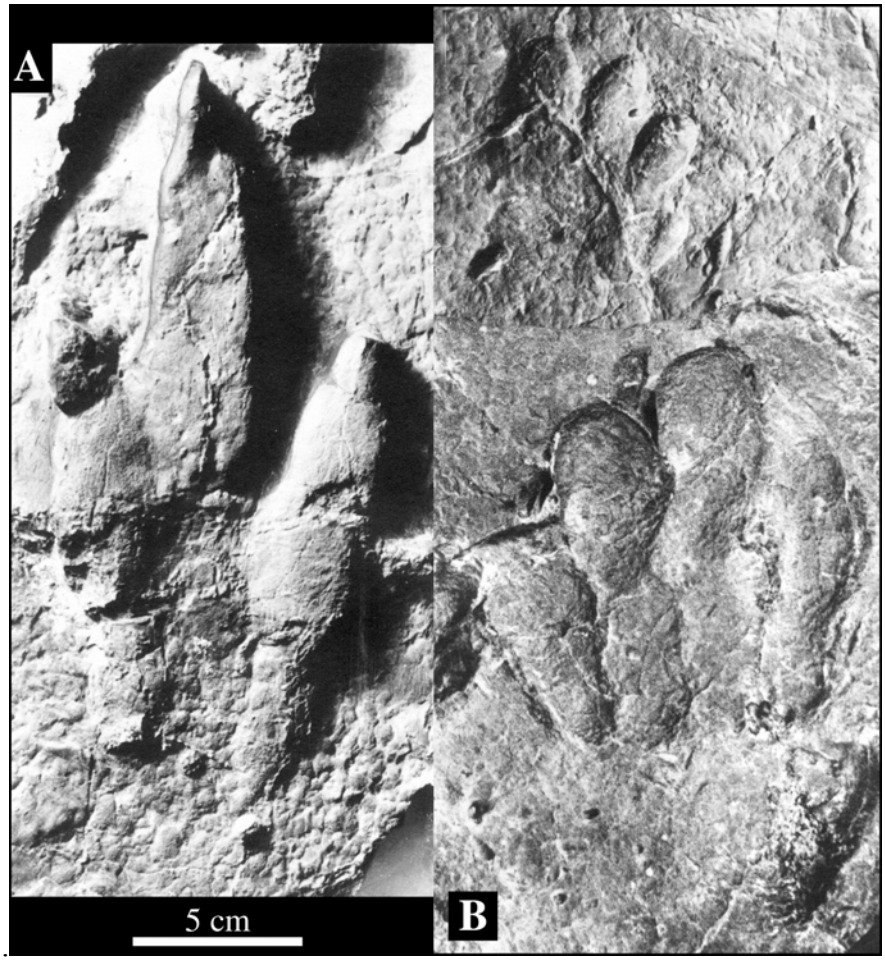

Figure 3. Examples of tracks from the Smith Clark Quarry, Perkasie Member, Milford, NJ: A, *Atreipus sulcatus*; B, *Brachychirotherium parvum*. From Baird (1957).

At this particular outcrop, complete fossil specimens are rare but nearby outcrops have produced a wealth of material. The nearby abandoned Smith Clark quarry is such an example. The Smith Clark Quarry was in operation in the late l9th to 20th century and was developed to quarry flagstones from exposures of the short modulating cycle O of the Perkasie Member (Drake et al., 1961) of the Passaic Formation at Milford, NJ (Figure 2). The gray footprint-producing horizons in the Smith Clark Quarry have produced the types and much associated material of *Atreipus milfordensis*, *A. sulcatus* (Baird, 1957; Olsen and Baird, 1986), *Brachychirotherium parvum* (Hitchcock, 1889), *B. eyermani* (Baird, 1957), *Apatopus lineatus* (Bock, 1952a), and *Rhynchosauroides hyperbates* (Baird, 1957), as well as examples of *Grallator parallelus* (Baird, 1957), *Rhynchosauroides brunswickii* (Baird, 1957), "*Coelurosaurichnus* sp." (Olsen and Baird, 1986), and an uncertain tridactyl form (Baird, 1957) (Figure [i]). Associated gray sandstones have produced an important megafossil plant assemblage and a probable phytosaur tooth (Newberry, 1888; Bock, 1969; Axsmith et al., 2004; Gallagher, pers.

comm.) including *Glyptolepis playsperma* and *G. keuperiana* (Cornet, 1977), *G. delawarensis* (Bock, 1969), *Pagiophyllum* spp., (?) *Cheirolepis munsteri*, *Clathropteris* sp., and *Equisetites* spp. The interesting, unique specimen of the plant fossil *Ginkgoites miliordensis* Bock, 1952b (ANSP uncatalogued), from the Smith Clark quarry, was destroyed on loan in 1974 (Spamer, 1988), so comparisons cannot now be satisfactorily made regarding its relationship to other fossil plants. Axsmith et al. (2004) have recently reviewed this floral assemblage. An isolated serrated tooth has also been found (by Andrew Ballet) in exposed gray sandstone relatively high in the section at the quarry (W. Gallagher, pers. comm.). The serrated tooth is comparable to the rear teeth of heterodont phytosaurs, but is not diagnostic at a lower taxonomic level than Phytosauria. Other teeth and bones could certainly be found.

At a nearby outcrop along Mill Road on the north side of Hackihokake Creek to the northeast, purplish and red footprint bearing beds of the Van Houten cycle overlying the gray beds of short modulating cycle O have produced *A. millordensis*, the type of *Chirotherium lulli* (Bock, 1952a; Baird, 1954), cf. "*Coelurosaurichnus* sp." (a different form than previously mentioned), and numerous small *Grallator* (PU 19910). Nearby exposures have also yielded clam shrimp in short modulating cycle O.

What is important about these particular footprint assemblages, is that on the whole, it is very similar to the assemblages from Lyndhurst, NJ (?Kilmer Member) which is about 3 m.y. younger and an assemblage from the lower Lockatong that is about 7 m.y. older (Olsen and Flynn, 1989), demonstrating very slow rates of faunal change through the Late Triassic.

As mapped by Ratcliffe et al. (1986) on the basis of surface geology, drill cores, and a Vibroseis profile, the border fault in this area is a reactivated imbricate thrust fault zone dipping 32°SE. Core and field data reveal Paleozoic mylonitic fabrics of ductile thrust faults in Precambrian gneiss and early Paleozoic dolostone overprinted by brittle cataclastic zones of Mesozoic normal faults which form the border fault system of this part of the Newark basin (see Stop 1).

REFERENCES

Arguden, A.T., and Rodolfo, K.S., 1986, Sedimentary facies and tectonic implications of lower Mesozoic alluvial-fan conglomerates of the Newark basin, northeastern United States. Sedimentary Geology, v. 51, p. 97–118.

Axsmith, B.J., Andrews, F.M., Fraser, N.C., 2004, The structure and phylogenetic significance of the conifer *Pseudohirmerella delawarensis* nov. comb. from the Upper Triassic of North America. Review of Palaeobotany and Palynology, v. 129, p. 251-263

Baird, D., 1954, *Chirotherium lulli*, a pseudosuchian reptile from New Jersey. Bulletin of the Museum of Comparative Zoology (Harvard University), v. 111. p. 166-192.

Baird, D., 1957, Triassic reptile footprint faunules from Milford, New Jersey: Bulletin of the Museum of Comparative Zoology (Harvard University), v. 117, p. 449-520.Bluck, 1982

Bock, W., 1952a, Triassic reptilian tracks and trends of locomotive evolution: Journal of Paleontology, v. 26, p. 395-433.

Bock, W., 1952b, New eastern Triassic ginkgos. Bulletin of the Wagner Free Institute of Sciences of Philadelphia v. 27, p. 9-14.

Bock, W., 1969. The American Triassic Flora and Global Distribution, vols. 3 and 4. Geological Center, North Wales, PA, USA, 406 p.

Cornet, B., 1977, The palynostratigraphy and age of the Newark Supergroup. Ph.D. thesis, University of Pennsylvania, 505 p.

Drake, A.A., Jr., McLaughlin, D.B., Davis, R.E., 1961, Geology of the Frenchtown Quadrangle, New Jersey-Pennsylvania. U.S. Geological Survey, Geologic Quadrangle Map GQ-133.

Hitchcock, C.H., 1889, Recent progress in ichnology. Proc. Boston Soc. Nat. Hist., XXIV, pp. 117-127.

Kent, D.V. and Tauxe, L., 2005, Corrected Late Triassic latitudes for continents adjacent to the North Atlantic: Science, v. 307, p. 240-244.

LeTourneau, P.M., 1985, The sedimentology and stratigraphy of the Lower Jurassic Portland Formation, central Connecticut [M.Sc. thesis], Wesleyan University, Middletown, 247 p

LeTourneau, P.M. and Smoot, J.P., 1985. Comparison of ancient and modern lake margin deposits from the Lower Jurassic Portland Formation, Connecticut, and Walker Lake, Nevada. Geol. Soc. Am. Abstr. Programs, v. 17, p. 31

Newberry, J. S., 1888, Fossil fishes and fossil plants of the Triassic rocks of New Jersey and the Connecticut valley. U.S. Geological Survey Monographs 14, p. 1-152.

Nilsen, T.H., 1982, Alluvial fan deposits, *in* Scholle, P.A. and Spearing, D. (eds.), Sandstone depositional environments: American Association of Petroleum Geologists Memoir 31, p. 49-86.

Olsen, P.E., 1986, A 40-million-year lake record of early Mesozoic climatic forcing. Science 234, p. 842-848.

Olsen, P.E. and Baird, D., 1986, The ichnogenus *Atreipus* and its significance for Triassic biostratigraphy, in Padian, K. (ed.), The Beginning of the Age of Dinosaurs: Faunal Change Across the Triassic-Jurassic Boundary. Cambridge University Press, p. 61-87.

Olsen, P.E. and Flynn, J., 1989, Field guide to the vertebrate paleontology of Late Triassic rocks in the southwestern Newark Basin (Newark Supergroup, New Jersey and Pennsylvania). The Mosasaur v. 4, p. 1-35.Olsen and Kent, 1996

Olsen, P.E. and Kent, D.V., 1996, Milankovitch climate forcing in the tropics of Pangea during the Late Triassic. Palaeogeography, Palaeoclimatology, Palaeoecology v. 122, p. 1-26.

Olsen, P.E. and Kent, D.V., 1999, Long-period Milankovitch cycles from the Late Triassic and Early Jurassic of eastern North America and their implications for the calibration of the early Mesozoic time scale and the long-term behavior of the planets. Philosophical Transactions of the Royal Society of London (series A) v. 357, p. 1761-1787.

Ratcliffe, N.M., Burton, W.C., D'Angelo, R.M. and Costain, J.K., 1986, Low-angle extensional faulting, reactivated mylonites, and seismic reflection geometry of the Newark Basin margin in eastern Pennsylvania. Geology v. 14, p. 766-770.

Smoot, J.P. and LeTourneau, P.M., 1989. Wave-formed shore line deposits on aI1uvial fans: Examples from modern pyramid and Walker Lake, Nevada, and early

Mesozoic Newark Supergroup. In: 28th Int. Geol. Congr., Washington, D.C., Abstr., v. 3, v. 141-142.

Spamer, E.E., 1988, Catalogue of type specimens of fossil plants in the Academy of Natural Sciences. Academy of Natural Sciences of Philadelphia, Proceedings, v. 140, p. 1-17.

Van Houten, F.B., 1969, Late Triassic Newark Group, north central New Jersey, and adjacent Pennsylvania and New York, in Subitzky, S.S. (ed.), Geology of Selected Areas in New Jersey and Eastern Pennsylvania. Rutgers University Press, p. 314-347.

Van Houten, F.B., 1980, Late Triassic part of the Newark Supergroup, Delaware River section, west-central New Jersey, in Manspeizer, W. (ed.), Field Studies of New Jersey Geology and Guide to Field Trips, 52nd Annual Meeting, New York State Geological Association, Rutgers University, p. 264-276.

STOP 3: STRATIGRAPHY AND STRUCTURE OF THE PASSAIC FORMATION AND ORANGE MOUNTAIN BASALT AT MINE BROOK PARK, FLEMINGTON, NEW JERSEY

By Greg Herman

INTRODUCTION

Splay faults in the Flemington fault zone are exposed in Walnut Brook at Mine Brook Park, Flemington, NJ. Faults cut the uppermost part of the Passaic Formation and overlaying Orange Mt. Basalt. Stratigraphic contacts between the units and fault-related structures are exposed in the beds and banks of Walnut Brook for about 400 ft beginning at the bridge crossing Walnut Brook on Capner Street and proceeding north. The exposures are most accessible by the footpath located across Capner Street from the paved parking lot on the North side of the Park. The entrance to the footpath is just to the south (before) the electrical transfer station adjacent to the Morales nature preserve. Once entering the footpath, proceed north about 50 yards until you see a path to the right angling down toward the brook. The traverse begins at the Passaic Fm and Orange Mt contact exposed in the east bank of the brook and proceeds south towards the bridge. Walnut Brook is subject to flash flooding, as it drains the relatively impermeable uplands of the Hunterdon Plateau underlain by the Lockatong Formation Flood events often create new outcroppings but also cover old ones with thick sedimentary bar deposits.

Geological Setting

Mine Brook Park in Flemington, New Jersey is located in the eastern part of the Flemington fault zone (Figure 1, and Houghton and others, 1992). The Flemington fault (FF) is the main fault in this major intrabasinal fault system that strikes about N20^{o}E in the central part of the Newark basin (see Herman, Figure 1 this volume). The FF links border faults on the NW margin of the basin with the Chalfont fault in eastern Pennsylvania (Figure 1). The fault zone is composed of many branching, splaying, and interconnected fault segments (Figures 1, 2, and 3) in the eastern part of the fault zone. The Flemington fault trace is mapped about 1000 ft to the west of this stop where it is concealed by alluvium. Most faults in the fault zone area show apparent normal dip-slip offset, with major faults dipping south and east (Herman and others, 1992; and unpublished quadrangle maps by Monteverde and others, NJ Geological Survey, in preparation). However, smaller-scale structures mapped in the brook dip more commonly North and West.

Maximum, apparent, normal dip slip on the FF occurs in the area of the Sand Brook syncline where Preakness Basalt is in fault contact with the upper part of the Stockton Formation (Figure 2). Here, there is about 13,000 feet of stratigraphic separation but about 22,000 feet interpreted displacement on the fault system based on stratigraphic thickness of Late Triassic and Early Jurassic strata (Houghton and others (1992; Olsen and others, 1996) and cross-section interpretations by Drake and others (1996). Near Mine Brook Park, there is about 11,000 feet of apparent stratigraphic offset across the entire fault zone.

Small faults in the FF zone at Mine Brook Park cut and deform the uppermost Passaic Fm and suprajacent base of the Orange Mt. Basalt. The amount of offset along the fault segment at this local has not been determined although the sense of displacement can be seen in outcrop-scale structures. Mine Brook Park is named from it's association with the Flemington copper mine, located about 2000 ft south of the park along the course of Walnut Brook (Figure 2).

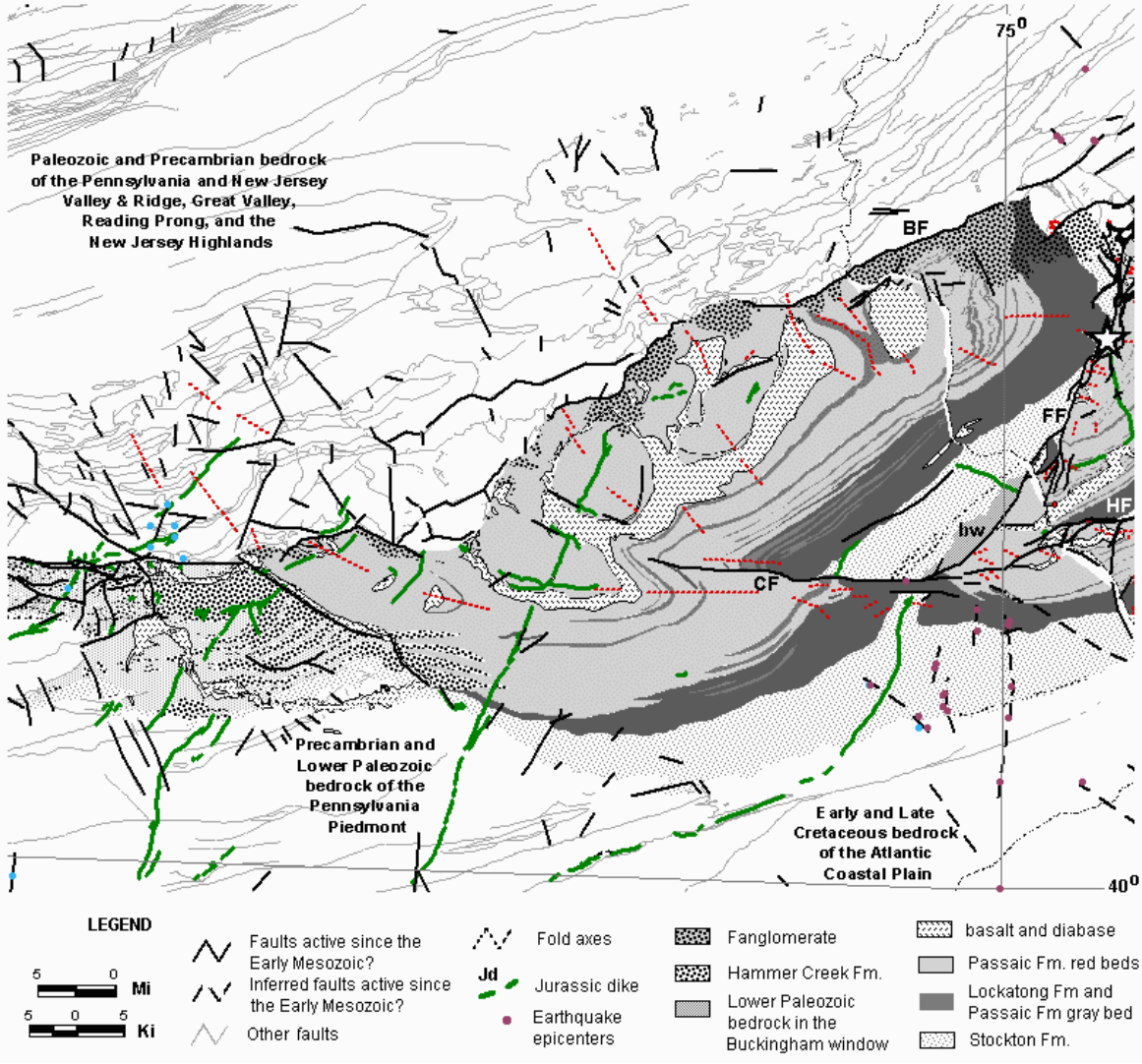

Figure 1. Bedrock geology map of the western part of the Newark basin showing faults interpreted to have been active since the Early Mesozoic and historical earthquake epicenters (see Herman, figure 29 of this volume). BF – border fault(s), CF – Chalfont fault, FF – Flemington fault, HF – Hopewell fault, bw - Buckingham window. Bedrock geology adapted from GIS coverage by the N.J. Geological Survey (2000), and Berg and others (1980); http://www.dcnr.state.pa.us/topogeo/map1/bedma.htm. The star highlights the location of Mine Brook Park, Flemington, NJ.

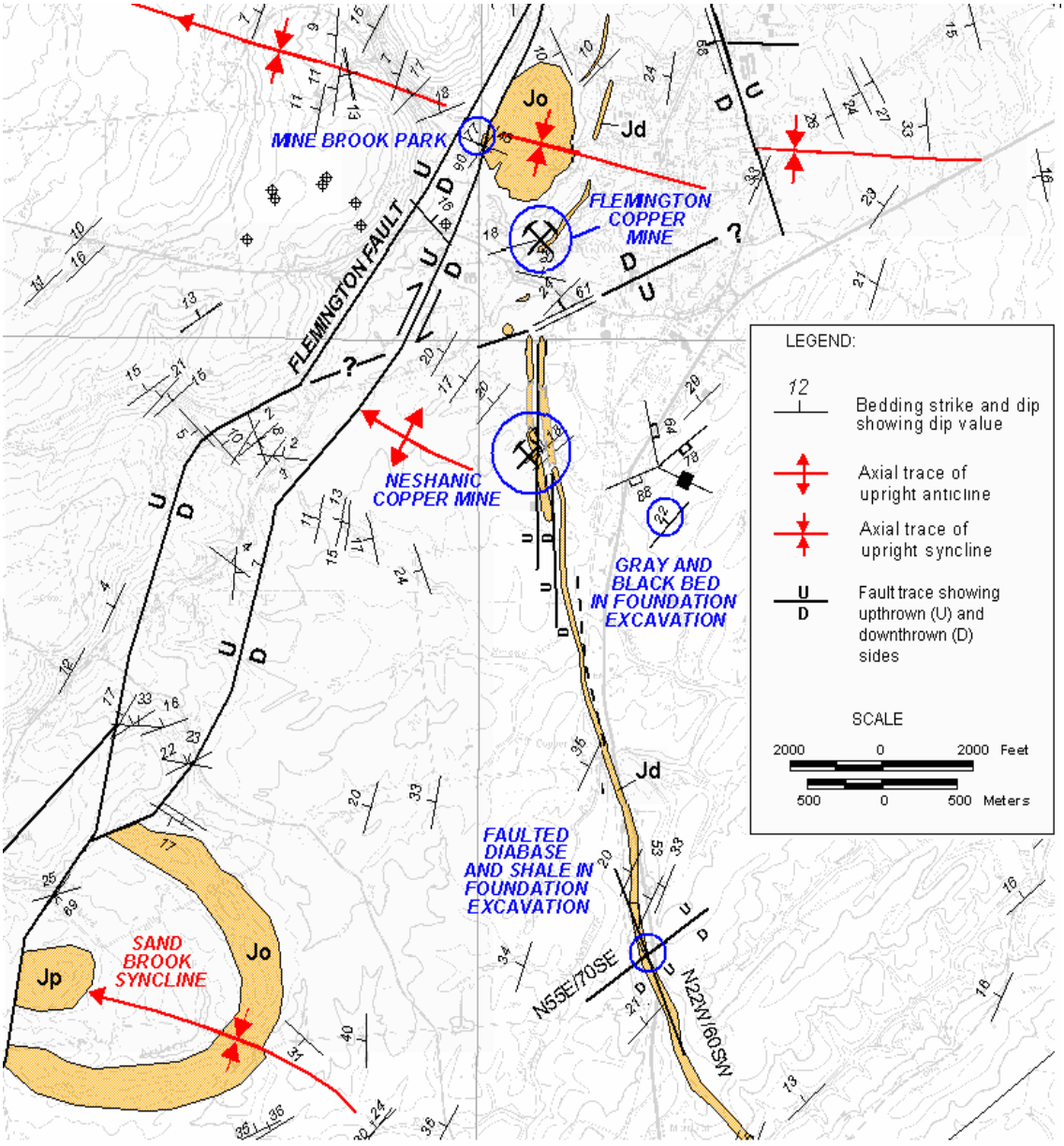

Figure 2. Generalized bedrock geology map of the Flemington fault zone in the vicinity of the Flemington and Neshanic copper mines, Raritan Twp., Hunterdon County, N.J. JO – Orange Mt. Basalt, JP – Preakness Basalt, Jd – Jurassic diabase. Circled stations with annotation are notable outcrops recently obtained from basement excavations, old mine workings, and natural outcrops where the NJGS has filed permanent notes of geological details. Of particular note is the Neshanic Copper Mine, recently exposed during subsoil excavation for a housing development in the fall of 2002. The permanent note includes a photographic record , video clips and other details of the mine excavation

Stop 3. Stratigraphy and structure of the Flemington fault zone in Walnut Brook at Mine Brook Park, Flemington, NJ

The fault at Mine Brook park is exposed in the bed and banks of Walnut Brook beginning beneath the bridge on Capner Street and continuing north about 400' where the brook takes an abrupt, westerly bend and continues northward (Figure 3). As one approaches the bend from the south, the contact between the Exeter Twp (VV) Member of the Passaic Fm. and the overlying Orange Mt. Basalt is seen in the eastern bank

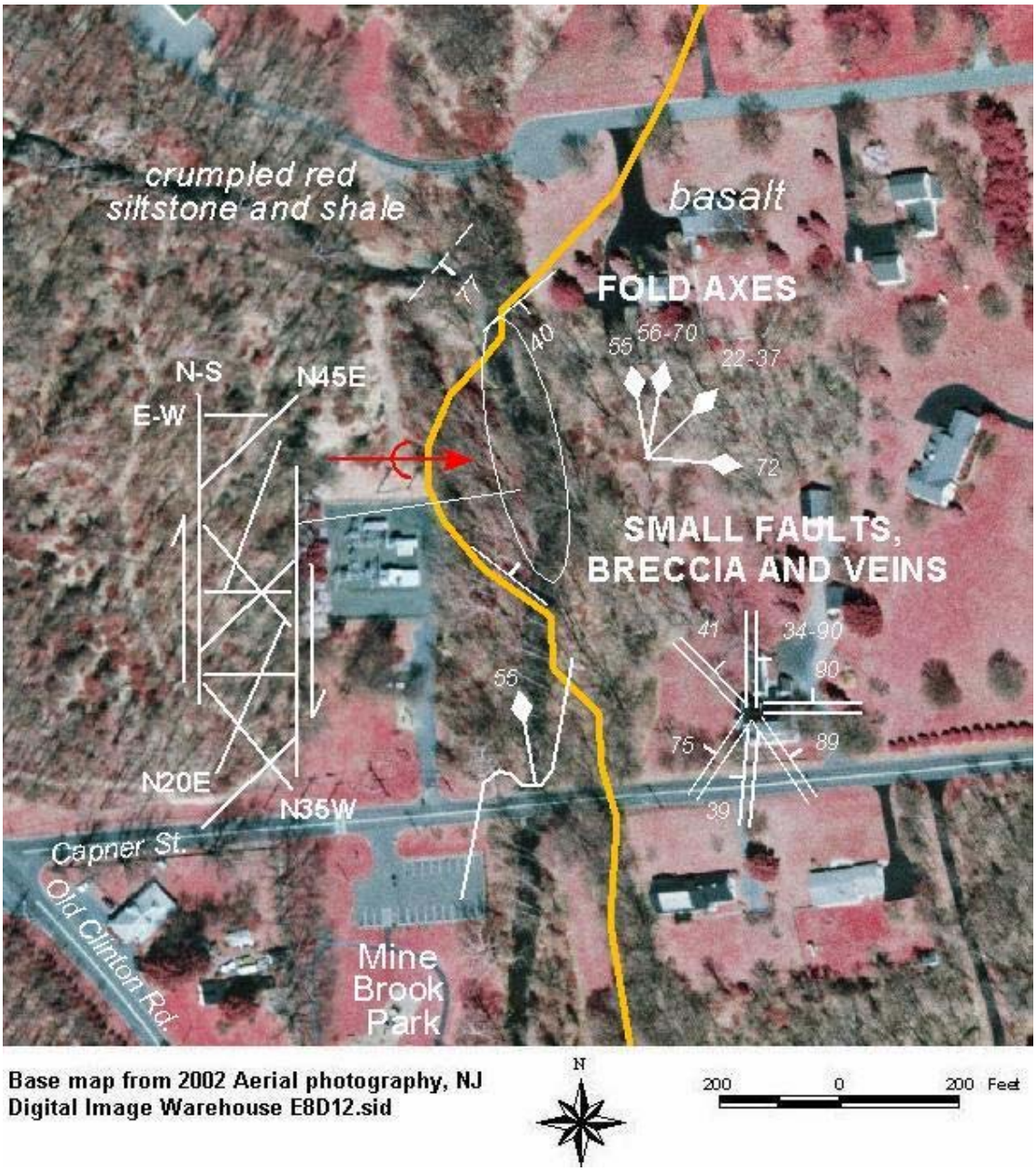

Figure 3. Aerial photograph showing the location and summary of structural fabric exposed in the streambed and banks of Walnut Brook.

(Figure 4). The contact is a parallel unconformity that strikes and dips about N50E/40SE. Immediately to the north of the contact, the Passaic Fm is tectonized with slickensided shear planes and multiple fracture surfaces. Anastomosing shear zones in the Passaic Formation strike about N-S to N20E and dip moderately to steeply southeastward, impart a heterogeneous texture to the faulted sequence with sheared red siltstone and mudstone bounding less deformed blocks of the same material. Slickensided shear planes that strike and dip about N-S and dip gently westward show reverse dip-slip indicators. The sheared Passaic Fm. dips east beneath relatively undeformed red shale seen in the upper banks of the stream cut. More tectonized red siltstone and shale is exposed in the bed and the banks of the stream continuing west around the bend and upstream to the north before encountering highly-fractured Lockatong Formation across the concealed trace of the main fault. It is common to encounter red Passaic Formation that is densely fractured and highly weathered into elongate, crumbly 'pencils' of siltstone.

The contact between the Passaic Fm and the Orange Mt. Basalt is intermittently exposed at a few other locations in the stream because of temporal changes in streambed geometry and migration of thick alluvial bars composed of shale and argillite boulders, cobbles, and gravel deposited during floods. Recent scouring of the banks of the east bank immediately south and west of the aforementioned contact exposed the most complete stratigraphic record of the siltstone and basalt contact to date. Weathered basalt overlies about 5 to 6 ft of dark gray hornfels striking and dipping N48E/35S. Toward the

Figure 4. The stratigraphic contact between the Passaic Formation and the overlying Orange Mt. Basalt is exposed at many places along the banks of Walnut Brook. The contact pictured above is found on the east bank about 400 ft north of the Capner Street Bridge. The contact strikes and dips about N18E/25SE. The Passaic Fm siltstone beds are thermally altered for about 6 ft below the contact and highly weathered.

bottom of the hornfels there is a thin, 4 to 5" thick, copper-mineralized gray about 4 feet below the contact. The gray bed is altered to light grayish brown and has green malachite ($CuCO_3 \cdot Cu(OH)_2$) coating fracture surfaces. A second gray unit occurs in red siltstone and shale about 13 to 15' below the contact. This gray bed is about a foot thick and is mottled light to dark gray shale. Another contact is frequently exposed in the western stream bank downstream about 250 ft where bedding strikes and dips N52W/49NE, thereby defining the southern limb of a syncline plunging moderately eastward with Orange Mt basalt lying in the trough axis (Figure 3).

The fault zone at Mine Brook Park contains many brittle features including basalt breccia, mineralized veins, slickensided shear planes and drag folds. Limestone-cemented breccia planes are primary structures that strike about N-S to N10^{o}E (Figure 3) and N35^{o}W. These breccia interconnect with networks of fractures including carbonate-filled veins and slickensided shear planes. Together they form rhomb-shaped fault slices (Figures 3 and 5) that are bounded by conjugate planes dipping moderately to steeply east and west. The rhomb-shaped fault slices observed in the brook have the same geometry of interconnecting fault segments seen at smaller scales in map patterns of the area (Figure 2) and elsewhere in the basin (see Herman, this Volume, Figure 19).

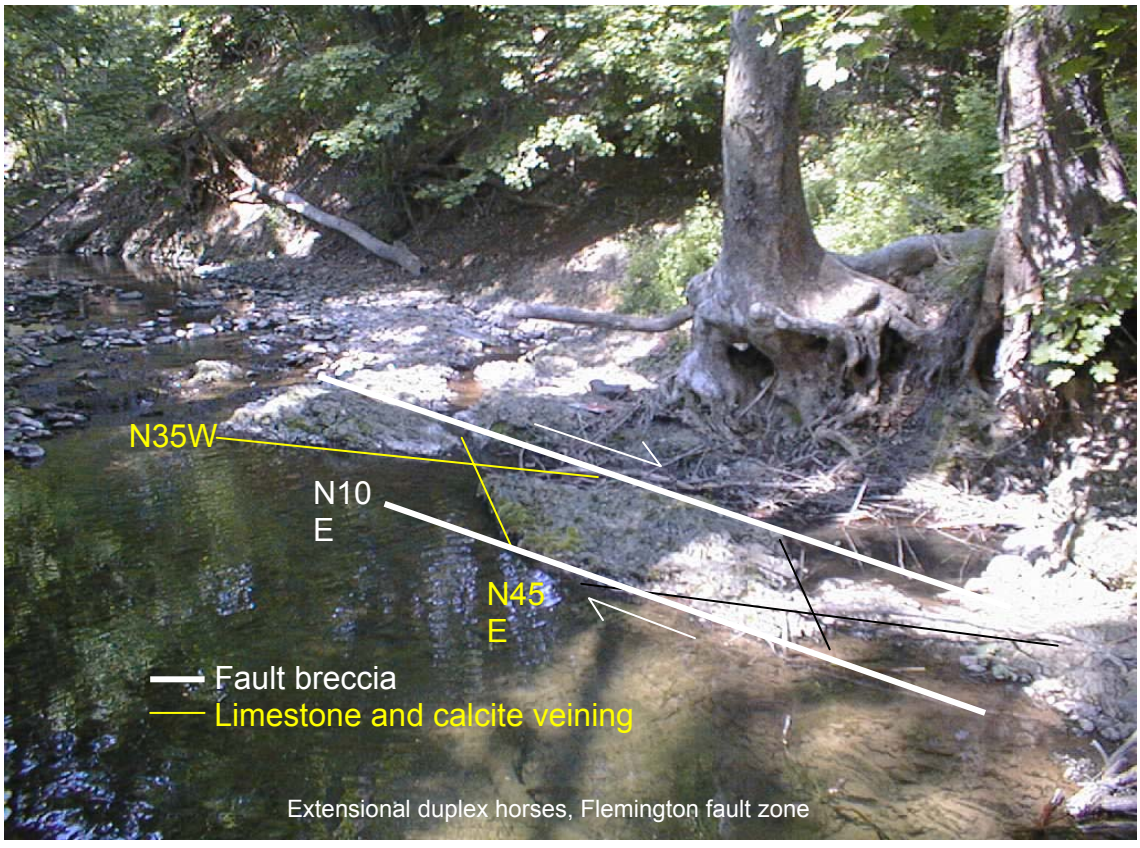

Figure 5. Systems of small faults composed of carbonate-cemented basalt breccia, slickensided shear planes, and carbonate veins link together to form a series of rhomb-shaped fault slices arranged as an extensional duplex fault system having oblique right-lateral strike slip and normal dip-slip strain.

The basalt breccia is composed of gravel- to cobble basalt aggregates floating in microcrystalline calcium-carbonate cement (Figure 6). The cement is light-bluish gray limestone rather than the fibrous or mosaic, white sparry calcite cements that commonly fills extension veins mapped elsewhere in the basin (see Herman, this volume). The limestone cement probably results from the precipitation of calcium carbonate from hydrothermal fluids circulating in the fault zone and perhaps driven by emplacement of the nearby Jurassic diabase dikes mapped to the east and south of Mine Brook Park (Figure 2). Carbonate sheet veins are commonly found in young orogenic belts and intercontinental rift zones with strike-slip faulting, with or without associated volcanic activity. They require carbonate-rich sediments in the subsurface and deep-water circulation. Circulating ground waters are channeled by faults and fractured rocks and mineralized by dissolution of subsurface carbonate rocks. These deposits commonly include calcium-carbonate scinter and travertine that form at temperatures in the 100^{o} to 200^{o} C range. The basalt breccia probably stem from explosive disruption of the country rock by hydrothermal fluid and steam injected along fractures. Explosive brecciation of country rock occurs when steam vents linked to hot springs become sealed, resulting in overpressured conduits that eventual explode. Each hydrothermal explosion fragments the surrounding rock producing new pathways for water to ascend to the surface.

Networks of systematic extension fractures occurring in the streambed and banks of Walnut Brook are also locally filled with the microcrystalline limestone that forms the breccia matrix (Figure 6). These veins locally show composite, banded morphologies and strike at a number of systematic directions (Figure 7). The carbonate veins are locally folded with an asymmetric geometry indicating oblique, right-lateral normal dip slip (Figure 8). This same type of folding also occurs in Passaic Fm red beds in the eastern bank of the brook immediately beneath the bridge (Figure 8), although recent dumping of large rock boulders by the base of the bridge has locally covered outcrops showing the drag folds in the Passaic.

Exposures of the fault splay at Mine Brook Park provide an excellent opportunity to examine the stratigraphic contact between the uppermost Passaic Formation and the overlying Orange Mt. Basalt. It also provides opportunities to examine detailed structures associated with a major intrabasinal fault developed during intermediate and late stages of basin extension (see Herman this volume). Moreover, this sequence of outcrops includes the only location in the basin where hot-spring types of deposits are reported.

Figure 6. Primary fault fabrics include basalt breccia floating in a matrix of light bluish gray, microcrystalline limestone originating from hydrothermal fluid movement in the fault zone and in close proximity to diabase dikes extending from the top of the Sourland Mountain diabase (Lambertville sill of Husch (1988).

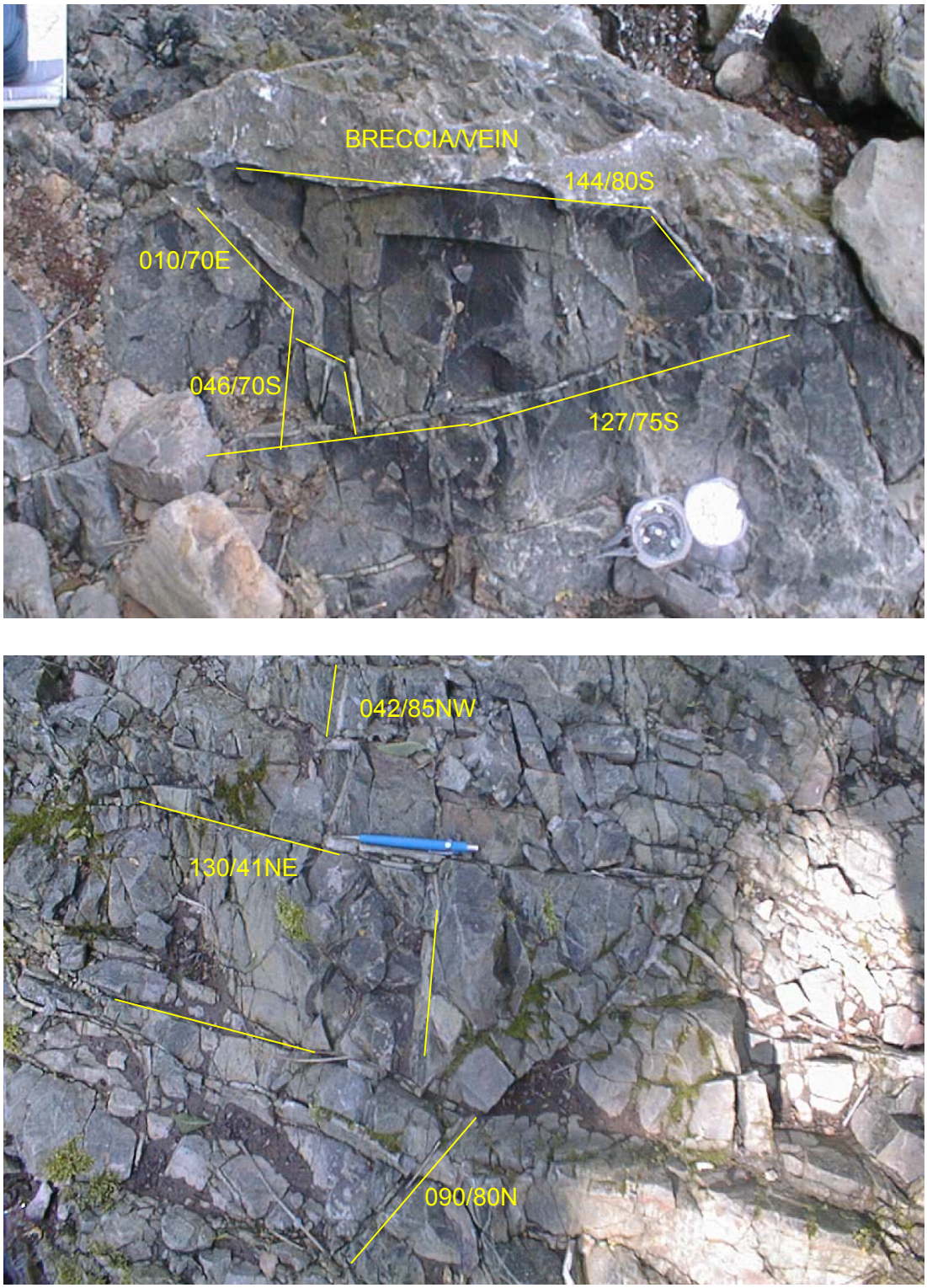

Figure 7. Microcrystalline limestone veins cut the fractured and brecciated basalt at various orientations. Both views are of subhorizontal surfaces in the streambed that stand above water level during periods of relatively low stream flow.

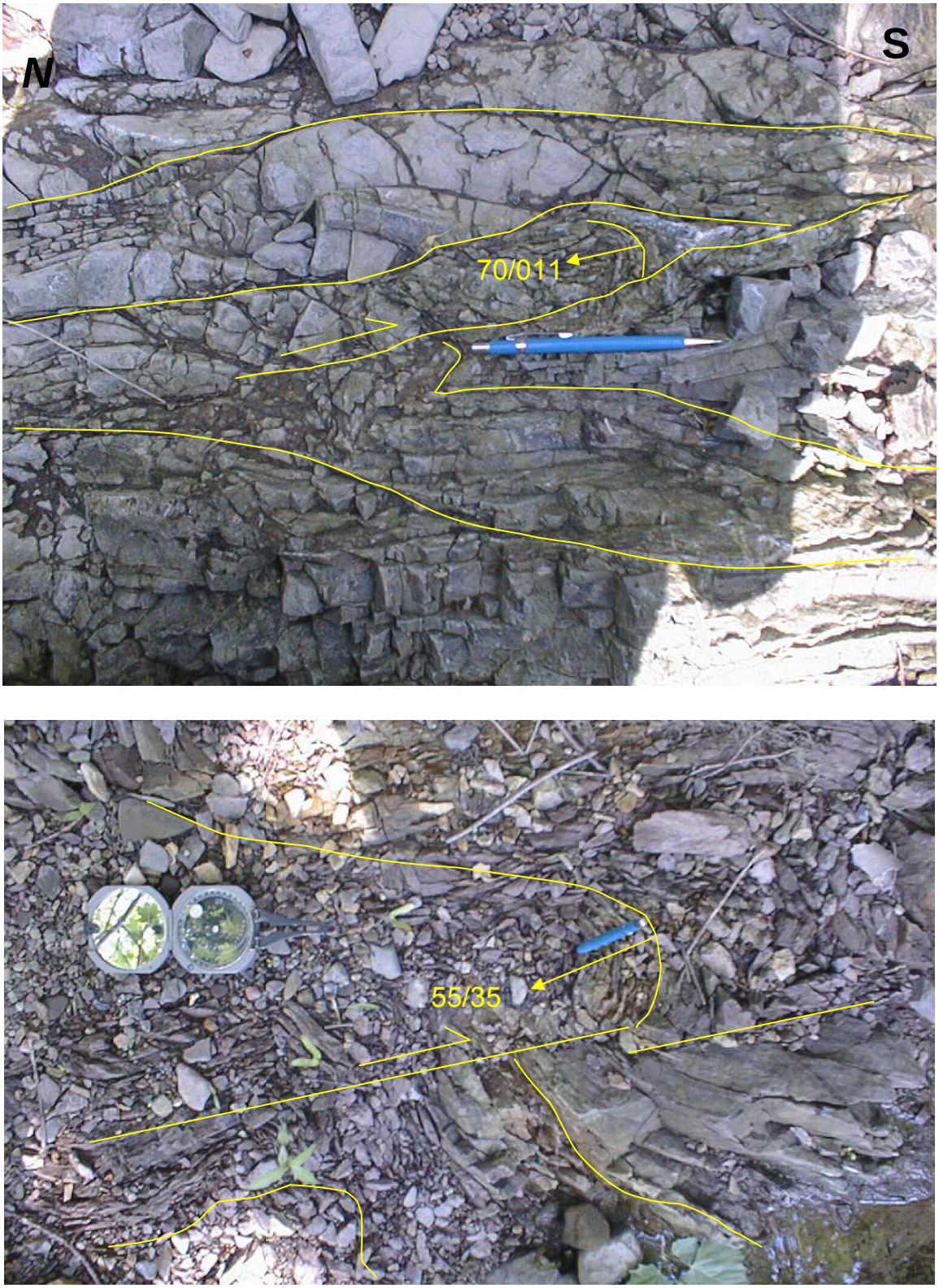

Figure 8. Asymmetric drag folds in fractured basalt (top) and red siltstone (bottom) in the fault zone in Walnut Brook at Mine Brook park. Both views are looking down at sub-horizontal surfaces in the streambed. Folding indicates a right-lateral strike slip strain component for the fault zone.

References

Drake, A. A., Jr., Volkert, R. A., Monteverde, D. H., Herman, G. C., Houghton, H. H., and Parker, R. A., 1996, Bedrock geologic map of northern New Jersey: U. S. Geological Survey Miscellaneous Investigation Series Map I-2540-A, scale 1:100,000, 2 sheets.

Houghton, H. F., Herman, G. C., and Volkert, R. A., 1992, Igneous rocks of the Flemington Fault zone: Geochemistry, structure, and stratigraphy, *in* Puffer J. H. and Ragland, P. C., eds, Eastern North American Mesozoic Magmatism, Geological Society of America Special Paper 268, p. 219-232.

Herman, G. C., Houghton, H. F., Monteverde, D. H., and Volkert, R. A., 1992, Bedrock geologic map of the Flemington and Pittstown 7-1/2' quadrangles, Hunterdon County, New Jersey: N.J. Geological Survey Open-file Map OFM-10, 1:24,000 scale

Husch, J. H., 1988, Significance of major- and trace-element variation trends in Mesozoic diabase, west-central New Jersey and Eastern Pennsylvania: *in* Froelich, A. J., and Robinson, G. R., Jr., eds., Studies of the Early Mesozoic basins of the eastern United States: United States Geological Survey Bulletin 1776, p. 141-150.

New Jersey Geological Survey, 2000, Bedrock Geology and Topographic Base Maps of New Jersey, 1:100,000 scale, New Jersey Geological Survey Compact Disc Series CD-01.

Olsen, P. E., Kent, D., Cornet, Bruce,Witte, W. K., and Schlische, R. W., 1996, High-resolution stratigraphy of the Newark rift basin (early Mesozoic, eastern North America), Geological Society of America Bulletin, v. 108, p. 40-77.

STOP 4. STRUCTURE OF THE HOPEWELL FAULT, NORTH SEGMENT, BELLE MEAD, NJ

Stephen E. Laney, CPG 7519

ABSTRACT

The central part of the Hopewell fault in New Jersey forms an arcuate scarp extending from near Hillsborough on the north end to near Harbourton at the southwest end. The Hopewell Fault has been typically characterized as being a normal fault structure, juxtaposing the Passaic formation hanging wall against the older Lockatong and Stockton formations footwall. Mapping conducted near Belle Mead, NJ indicates that the fault zone is a shear zone at least 500 feet wide. Four areas within the fault zone were studied. The innermost part of the exposed deformation in the footwall consists of large-scale drag folding and reverse faulting, the middle part by a dextral strike-slip zone and the outer part by a heavily brecciated zone. The hanging wall consists of relatively undeformed mudstone. Brittle deformation dominates the shear zone, but brittle-ductile features are common. This is the first field evidence of right-lateral movement on the fault.

INTRODUCTION

The Hopewell Fault is located in the central part of the Newark basin in central New Jersey. The Newark basin is part of the larger Birdsboro basin in the Central Atlantic Region of Eastern North America (Faill, 2005). The Birdsboro basin is part of a chain of rift basins that extends along the east cost of North America. These basins were formed as a result of the breakup of Pangea and the opening of the Atlantic Ocean between 230 and 175 Ma (Sanders, 1963; Cornet and Olsen, 1985; Klitgord and Schouten, 1986). The Newark basin is a half-graben hinged on the east side and bordered on the west by a system of dip-slip and strike-slip faults.

The Hopewell fault is one of the major intrabasinal Mesozoic faults in New Jersey that offsets the Mesozoic section from the Stockton Formation to the Passaic Formation. In New Jersey, the Hopewell fault is approximately 35 miles in length. The central part of the fault forms an arcuate fault scarp approximately 15 miles in length extending from near Hillsborough, NJ on the north end, south-southwest through Hopewell, NJ then to near Harbourton at the southwest end (USGS, 1998). At the northeast end, the fault scarp disappears near Belle Mead/Hillsborough, NJ. At this point, the fault splays into 3-5 segments extending to the north to merge with the Ramapo Fault near Pluckemin, NJ (U.S.G.S., 1996). Figure 1 is a site location map. The study area for this paper is located approximately 7.5 miles south of the north end of the fault escarpment, on Roaring Brook.

Near Hopewell, NJ, the scarp strikes northeast, dips southeast and has a topographic relief of at least 260 feet. The highlands formed north of the fault in this area are referred to as the Sourland Mountains, due to their poor drainage. From this point towards the west many splinter faults striking south-southwest splay off of the main fault.

At the west end of the Hopewell fault in New Jersey south of Lambertville, the fault strikes east-west and continues across the Delaware River into Pennsylvania as the Pidcock Creek Fault, then intersecting with the larger Chalfont Fault (Ratcliffe and Burton, 1988).

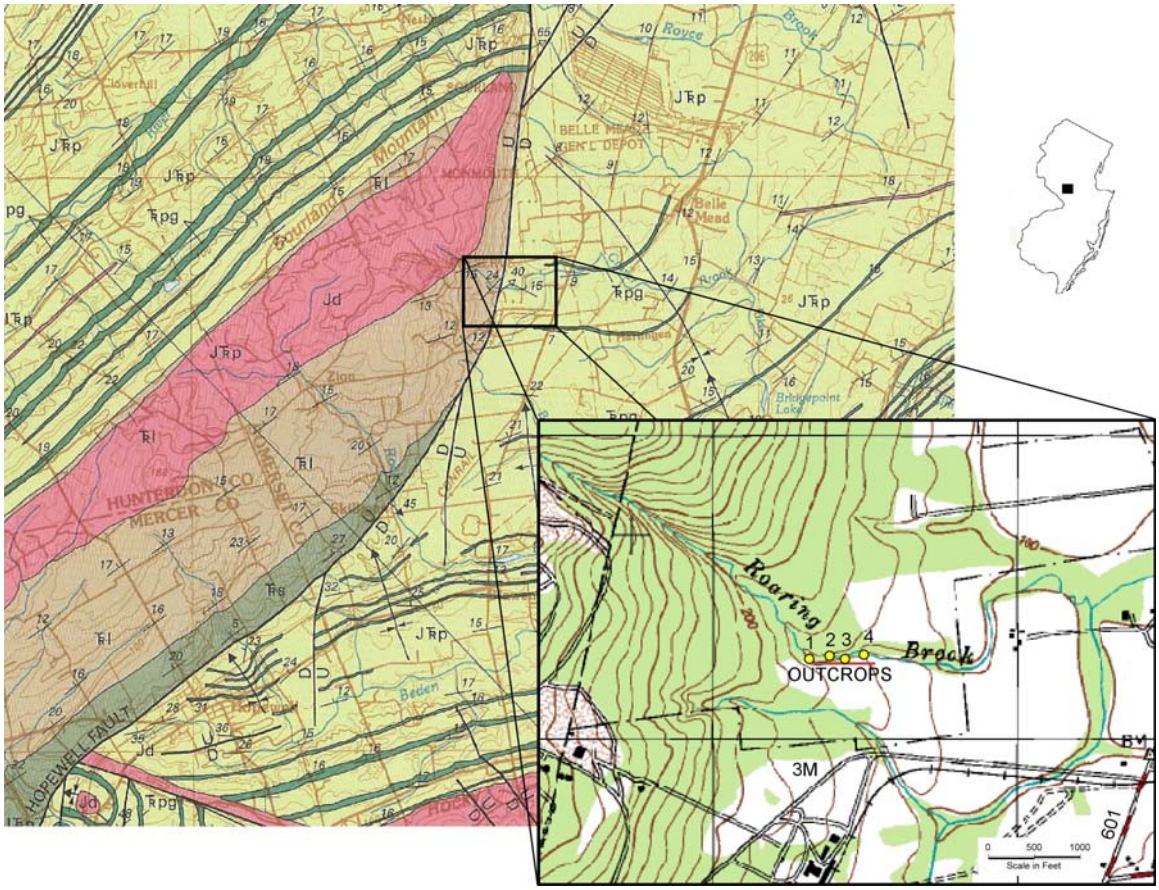

Figure 1. Site Location Map, Somerset County, Belle Mead, NJ (U.S.G.S. 1954, 1998)

Previous Investigations

The Hopewell fault was originally mapped for the first Geologic Map of New Jersey (Lewis and Kummel, 1910-1912) with roughly the same geomorphology as during more recent years. The fault is shown as a normal fault, downthrown to the south-southeast and dipping approximately 80 degrees south. More recent mapping shows the fault dipping 45-50 degrees south (Parker and Houghton, 1990; U.S.G.S., 1998).

Newark basin-fill strata have been offset by two major intrabasinal faults, the Flemington and the Hopewell faults. Sanders (1962, 1963) described 2 miles of dip-slip displacement and up to 12 miles of right-lateral displacement on the Hopewell fault. Schlische and Olsen (1988) described the Flemington and Hopewell faults as having developed late in the history of the basin to accommodate regional extension. They estimated the regional extension direction to be east-southeast.

Jones (1994) described the Hopewell fault as a predominantly normal-displacement fault that has 1-2 miles of dip separation and suggests that faulting may have been coeval with sedimentation. He also documents the presence of transverse folds in the hanging wall adjacent to the fault. Laney and Gates (1995) described a splay off of the north segment of the Hopewell fault near the study area as having a right-lateral movement sense.

Ratcliffe and Burton (1985) interpreted the strike-slip movements of intrabasinal faults as the result of their orientation relative to the early Mesozoic southeast extension direction. Fault segments oriented north-south in this stress field would have right-lateral slip, whereas those oriented east-west would have left-lateral slip components. Northeast- and NW-trending segments would show oblique movement. In this stress field, the Hopewell fault would have right-lateral displacement along its N-S section (study area) and left-lateral displacement along its E-W section to the southwest (Ratcliffe and Burton, 1988; Schlische and Olsen, 1988).

Schlische (1992) described a regional orthogonal fracture system composed of nearly vertical NE-striking faults related to the regional NW-SE extension direction and NW-striking fractures related to local extension in a NE-SW direction as a result of the downwarping of the inner basin. He described the Hopewell fault as having a throw of 1-2 miles based upon the separation of stratigraphic units.

Stratigraphy

The Hopewell fault offsets late Triassic to Early Jurassic age sedimentary rocks of the Newark basin. Rocks within the Newark basin are composed predominantly of "red bed" sequences of fluvial and shallow-to-deep-water lacustrine sediments (Olsen et al, 1996). Sedimentation is considered to have been contemporaneous with basin subsidence (Schlische, 1992). Tholeiitic magma was intruded as diabase sills and extruded as flood basalts at 201 Ma (Husch et al, 1988: Sutter, 1988; Dunning and Hodych, 1990; Husch, 1992).

The stratigraphy in the study area from youngest to oldest consists of the Passaic, Lockatong, and Stockton formations. Rocks of the Passaic formation occur in sequences of red-brown silty, shaley mudstones and sandy siltstones. The rheology of these two rocks types is such as to form massive, homogenous and hard siltstones and crumbly, easy eroded mudstones. Rocks of the Passaic formation form the hanging wall of the Hopewell fault in the study area.

The Lockatong formation generally consists of dark red-brown and grey argillite having massive bedding with shale partings. These rocks are sodium-rich and were deposited in shallow to deep lacustrine (lake) environments. Rocks of the Lockatong formation occur in the footwall of the fault in the study area.

Also in the footwall and below the Lockatong is the Stockton formation. The Stockton is a fluvial arkosic sandstone consisting of thick beds of conglomerate and sandstone with interbedded red-brown mudstone and siltstone (Olsen, 1980; Olsen et al, 1996).

In addition to these sedimentary rocks, a diabase sill was intruded into the Lockatong formation and forms the backbone of the Sourland Mountains in the study area. The sill is referred to as the Lambertville sill. The argillite has been contact

metamorphosed into hornfels adjacent to the sill. The diabase sill has also been truncated by the Hopewell fault. The fault developed after intrusion of the sill thus constraining the time of intrabasinal faulting to post-201 Ma.

DESCRIPTION

The study area is located along Roaring Brook in a forested area approximately 0.8 miles west of County Route 601 in Somerset County, Belle Mead, New Jersey (see Figure 1). The area is located approximately 0.2 miles north of the main entrance road to the 3M quarry. It is located approximately 5 miles northeast of Hopewell, NJ. The fault scarp has a relief of approximately 400 feet in the study area.

Roaring Brook flows southeast along the northeast border of the 3M property. Where the Brook intersects the Hopewell fault zone, it bends sharply to the east for approximately 700' before bending back toward the southeast. It is along the east segment of the Brook where the outcrops studied in this paper are located (see Figure 1).

A local area of interest is Roaring Rocks, located in the source area for the Roaring Brook, which is spring fed. The Roaring Rocks form a rock glacier. With sufficient rainfall, the loose rock beneath the larger diabase rock boulders (up to 20' long) will roll and bang together resulting in a roaring sound from beneath the boulders, thus the name.

There are four outcrops within the fault zone which were studied and mapped (see Figure 1). These outcrops are numbered 1-4. Outcrops 1-3 are located in the footwall of the Hopewell fault. Outcrop 4 is located in the hanging wall. The Hopewell fault in the study area strikes north-northeast. The section of outcrops is aligned east-west. The estimated width of the fault zone is at least 500' in the study area.

Kinematic Indicators

Kinematic indicators on fault surfaces and internal to the rock and their interrelations were used to determine slip directions and relative timing of fractures. The kinematic indicators observed include grooved and stepped slickensides, slickenlines on slickensides, imbricate slickenfibers, sigmoidal lenses, bookshelf faulting and drag folding. These indicators are abundant in Outcrops 1 and 2.

Slickensides with tool markings are evident as polished surfaces bounding argillite slabs and as pull-apart structures. Slickenlines on slickensides (Fleuty, 1975) composed of primarily chlorite and possibly actinolite are abundant. They appear mainly as aligned slickenfibers ranging from 2 mm to 1 cm in length on fracture surfaces. These growth fibers form imbricate accretion steps. The long axis of each fiber is parallel to the direction of fault extension during slip. The sense of imbrication of the fibrous steps gives the sense of movement on the fault. An example would be that the missing block moved in the direction that the rough slickenlines point. Stepped slickensides are interpreted in the same manner (Durney and Ramsay, 1973; Hancock, 1985; Tanner, 1989).

The tapered ends or tails of sigmoidal lenses are bent to point in the direction of movement of the opposing block. These tails are interpreted to have rotated. A sigmoidal lens created by dextral (right lateral) faulting would have a flattened "S" shape. A lens created by sinistral (left lateral) faulting would have a flattened "Z" shape.

The presence of chlorite slickenlines in the faulted rocks indicate that zeolite-lower greenschist metamorphic grade was attained during deformation (Laney & Gates, 1996). Based upon the brittle kinematic indicators and associated metamorphic minerals, faulting is interpreted to have occurred at depths of 2-10 miles and temperatures of 200-300ºC (Sibson, 1986). The bent or rotated tails of sigmoidal blocks are not due to high-temperature/pressure ductile deformation. Instead, they are formed by reaction-enhanced ductility during displacement (White and Knipe, 1978) whereby a combination of metamorphic reactions and cataclastic flow accommodate the strain and cause the rocks to appear ductile at low temperatures. The rock is broken into grains by microfracturing and, if homogeneously distributed, are able to form the rotated tails (Rutter, 1986).

Outcrops

Rocks in the fault zone are exposed in four outcrops (see Figure 1). These outcrops line up to form a transect near perpendicular to the fault zone. The areas between outcrops are covered by alluvium and regolith. The outcrops will be discussed in order from deep within the footwall to the hanging wall.

Outcrop #1

Rocks in this outcrop are deformed by large-scale drag folding. It is considered to be a zone located the deepest into the footwall. Deformed rock occurring in this zone are exposed in the streambed for approximately 150 feet upstream of Outcrop #1. These outcrops expose only a two-dimensional view of the zone. Outcrop #1 provides a three-dimensional view of the folded rock.

Outcrop #1 consists of flinty grey-black to dark reddish brown hornfelsic argillite forming an outcrop approximately 25 feet long, four feet in height and striking approximately N50E (see Figure 2). Beds of argillite 6-8" thick dip NW40 degrees at the top of the exposure then dip steeply to vertical at the base of the outcrop. The outcrop has a hackly fracture appearance. Rock dipping vertically in the streambed are broken into blocks 2-12" in size. Recumbent folding occurs in several areas at the base of the outcrop. The apparent bedding surfaces are actually fracture surfaces along which thicker argillite beds were broken to accommodate stress. This results in fracture surfaces bounding slabs of argillite instead of beds. Many of these fracture surfaces have polished slickensides with chloritic slickenlines. Reverse faulting dominates the outcrop. .

Figure 2. Outcrop #1 looking north; showing sigmoidal lensing and slab structure.

The cross-sectional view of these slabs (see Figure 2) show internal fracturing oriented near perpendicular to the slab surface. The internal fractures form rectangular blocks resembling books. Each book is approximately 1-2 inches thick and 8-10 inches long, depending upon the slab thickness. The ends of each book are deformed into tails, each pointing in opposite directions, forming a sigmoidal lens. The orientation of the tails to each lens results in an overall "S" shape. This configuration indicates that reverse faults bound each slab. The movement sense derived from imbricate slickenlines and stepped slickensides confirms the reverse faulting.

Minor bookshelf faulting also occurs internal to slabs. The previously described books are tilted in the direction that the overlying slab moved. This internal faulting also indicates that reverse faulting occurred along the top of each slab. Minor oblique and lateral faulting is also evident.

Outcrop #1 shows an overall clockwise rotation of rocks resulting in large cylindrical folds forming rock lozenges striking north-northeast and paralleling the Hopewell fault zone. These cylindrical folds are the result of large scale drag folding whereby rocks in the footwall are squeezed then rolled parallel to strike. This folding mechanism dominated by simple shear forces is similar to rolling clay between your hands to form a pencil-shaped roll of clay.

Outcrop #2

Located downstream and east of Outcrop #1 approximately 160 feet, Outcrop #2 is dominated by indicators of dextral strike-slip movements. The outcrop is approximately 25 feet in length and three feet tall. Rock at Outcrop #2 also consists of flinty, grey black hornfelsic argillite. The rock is broken into slabs, but the slabs are not

as continuous as those described at Outcrop #1. There are no primary bedding features evident. The rock breaks along remnants of slab surfaces striking northeast that parallel the direction of lateral slip.

The primary kinematic indicators are bookshelf faulting, sigmoidal lensing and slickensides with slickenlines. The lensing and bookshelf faulting are not confined to the interior of slabs as at Outcrop #1. Instead, lensing permeates the rock vertically and horizontally welding the rock together. This results in a secondary foliation or weak planar cleavage structure. Faults bound individual bodies of rock showing cleavage, which may have been original slab structures. Rigid body rotation and resulting internal fracturing most likely formed the cleavage structure. The cleavage is made up of sigmoidal lenses ranging 2-4 inches in thickness and 12-24 inches in length (see Figure 3). Each lens is welded to its neighboring lenses. Tails are rotated toward the southwest at the top of each lens and toward the northeast at the base. Each lens appears to be slightly overturned toward the south.

Figure 3. Outcrop #2 looking east, showing sigmoidal lensing and cleavage structures. The rock is exposed showing structure in three dimensions. The right (west) end of the outcrop provides the most information. Here the outcrop forms a bench with a near vertical face and a horizontal shelf. Sigmoidal lenses are exposed on both surfaces. Lenses can be traced from the vertical face to the horizontal bench. The three-dimensional geometry of each lens would resemble a plate with edges curved in an "S" shape. The surfaces of each plate are cleavage planes welded onto the adjoining plate. A cleavage fold also occurs on this outcrop.

Field evidence for this part of the Hopewell fault zone indicates dextral (right-lateral) strike-slip faulting has occurred. The shear couple would strike NNE paralleling

the fault zone. There has been a longitudinal wrenching of the rock at Outcrop #2 as compared to a cylindrical rotation of rock at Outcrop #1.

Outcrop #3

Outcrop #3 is located approximately 250 feet downstream and east of Outcrop #2. This outcrop is located in the streambed so offers only a two-dimensional view (see Figure 4). The entire outcrop is exposed for approximately 100 feet, but the best exposure is near the middle of the outcrop.

Figure 4. Outcrop #3, looking northwest; breccia zone.

This part of the footwall is interpreted to be the closest to the hanging wall. The rock is a fault breccia having clasts from 0.25-12 inches in size. The breccia clasts consist of both sandstone and argillite. The outcrop studied consists of 95% quartzitic sandstone. Minor angular argillite clasts are present. The sandstone belongs to the Stockton formation, which is stratigraphically below and older than the Lockatong formation. The sandstone is red brown, medium grained, and non-calcareous. The fault breccia is cohesive and cemented by limonite, hematite and fault gouge. The fault gouge consists of a granular matrix of clay, sand and argillite that binds the clasts together by compaction. The gouge matrix is most likely a cataclasite, but petrographic analysis was not performed as part of this investigation. The iron oxides commonly display an iridescent play of colors. Black, chloritic slickensides commonly coat breccia clasts. This rock type would have a very low porosity/permeability.

On outcrop in the stream, the rock is crumbly, very weathered and grey in color. Adjacent to the stream, the rock is hard but has a crumbly fracture. This characteristic is strikingly different than the previous outcrops studied, which were composed of hard, flinty argillite. Breccia composed of mainly argillite most likely subcrops between Outcrops #2 and #3. Cobbles and small boulders of this rock type are found around and downstream of Outcrop #3.

Outcrop #4

Outcrop #4 is located in the streambed approximately 200 feet downstream of Outcrop #3. The exposure is small as compared to the others, only being approximately 20' in length. The west end of the outcrop provides the best exposure. Rock at this outcrop consists of silty mudstone. The mudstone is red-brown, crumbly, well-bedded, strikes N15E and dips SE40 degrees. A major joint strikes N30E and dips NW60 degrees. At the east end of the outcrop, the mudstone strikes roughly E-W and dips toward the north.

The rock exposed at Outcrop #4 is interpreted as belonging to the Passaic formation. It is located in the hanging wall of the fault zone. The mudstone is relatively undeformed as compared to the other rock studied.

The regional structure of the Passaic mudstone (see Figure 1) adjacent to the Hopewell fault zone in the study area has the rock forming a broad syncline plunging toward the northwest with the west limb terminating against the fault (Parker and Houghton, 1990). The east end of Outcrop #4 is consistent with the synclinal structure. The west end of the outcrop is dipping away from the footwall and has joints dipping toward the fault. These structures are most likely due to local drag folding in the hanging wall.

Fracture Analysis

Figures 5a-f show rose diagrams and polar plots for fracture data collected at each outcrop. The petals on the rose diagrams represent strike directions and dips are represented using the right-hand rule, i.e. dip is to the right of the strike direction when viewed from the center of the diagram to the azimuth. The polar plots are equal area, lower hemisphere projections. Because of the lack of sufficient structural data, diagrams and plots are not provided for Outcrop #4.

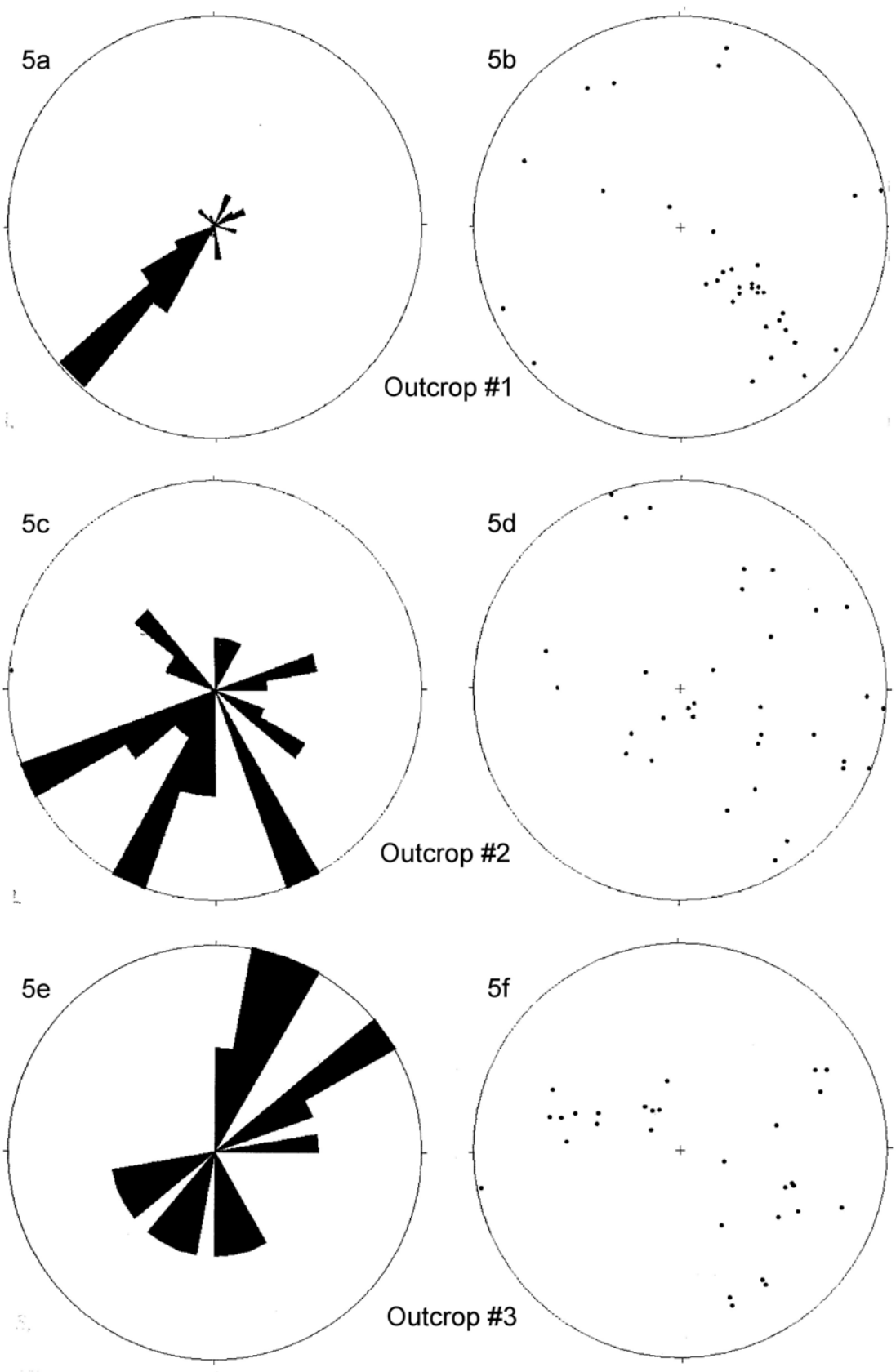

Figure 5. Rose Diagrams and polar plots; equal area, lower hemisphere projections.

Figure 5a is a rose diagram for fractures mapped at Outcrop #1.The diagram shows the majority of fractures striking northeast-southwest and dipping toward the northwest. Figure 5b is a polar plot for Outcrop #1. The half girdle in the southeast quadrant shows the progressive dip of fracture/slab surfaces toward near vertical along the perimeter of the plot.

Figure 5c is a rose diagram for Outcrop #2 and Figure 5d is the corresponding polar plot. The rose diagram shows the majority of fractures still striking toward the south-southwest and dipping toward the northwest. However, the polar plot shows poles scattered randomly without the uniform clustering shown for Outcrop #1. There is a weak conjugate set of fractures formed in the northeast and southwest quadrants. This fracturing is most likely due to compression of the rock from forces paralleling the strike of the fault zone.

Figure 5e is a rose diagram for Outcrop #3 and Figure 5f is the corresponding polar plot. A well-formed conjugate set of fractures is shown on the rose diagram striking toward the northeast and dipping toward the southeast. The poles to these fractures form a cluster in the northwest quadrant. The remaining poles are scattered in the southeast quadrant. The conjugate set also indicates that the rock was subjected to compressional forces paralleling the strike of the fault zone. The southerly dip to these fractures may indicate that, due to the close proximity of the hanging wall, normal stresses from the drag of the hanging wall have influenced these fracture formations. The dip of the entire fault zone may parallel these fractures, giving the fault a dip of 45-55 degrees toward the east-southeast.

The single strike direction mapped at Outcrop #1 is consistent with a single-axis rotation of rocks. The fracture patterns mapped at Outcrops #2 and #3 suggest that the rocks were subjected to compressional forces due to lateral movement paralleling the Hopewell fault zone. If the rock in the footwall was subjected to compressional forces arising from more normal faulting, the acute angle of the conjugate set would be in the southeast quadrant.

CONCLUSIONS

The Hopewell fault zone as exposed in the study area is at least 500 feet thick and strikes north-northeast. The fault zone is actually a brittle shear zone having subparallel boundaries in which shear strain has been localized. The wall rock on opposite sides of the shear zone has been displaced relative to one another in a direction parallel to the plane of the shear zone. The shear directions are both lateral and vertical, resulting in an oblique fault movement.

Based upon the available exposures, three discrete deformed zones were mapped in the footwall. The hanging wall is relatively undeformed. Rocks in the footwall are strongly deformed and make up 95% of the exposed fault zone. The deformation in the footwall most likely gradually decreases in intensity with depth, whereas, deformation in the hanging wall is abrupt.

Rocks in the footwall have been subjected to at least three modes of deformation. Rock adjacent to the hanging wall has been heavily brecciated. This breccia zone is estimated to comprise at least 40% of the shear zone. Going deeper into the footwall, the

next zone consists of rock deformed by lateral and compressional forces resulting in dextral strike-slip faulting. This zone is estimated to comprise approximately 20% of the fault zone. The rock deepest into the footwall (approximately 500 feet from the hanging wall) has been deformed by compressional and rotational forces that resulted in reverse faulting and cylindrical drag folding.

The model that best describes the structural evolution of the north segment of the Hopewell fault is that proposed by Ratcliffe and Burton (1985; Schlische and Olsen, 1988). This model describes how a southeast regional extension direction would cause right-lateral movement on a fault segment oriented north-south within the extensional stress field. The kinematics identified in this study include (see Figure 6) rotation of rock in a normal sense deep in the footwall and right later movements at shallower depth. The north-northeast segment of the Hopewell fault studied in this paper is a right-lateral oblique fault as described by the model and the movement sense of the structures identified. The fault zone dips 35-55 degrees toward the east-northeast.

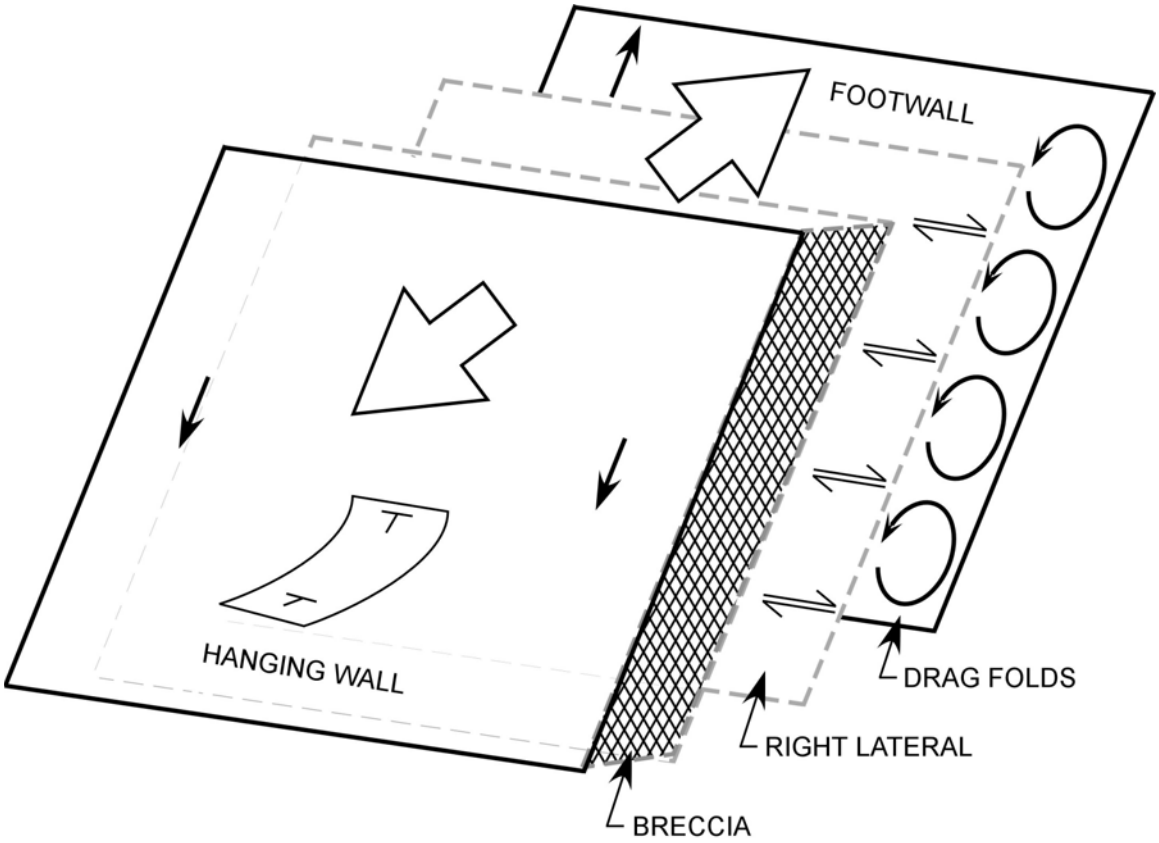

Figure 6. Schematic showing distribution of kinematic structures in the Hopewell shear zone.

Groundwater production from the Hopewell fault zone is one to two orders of magnitude higher than in adjacent rock (Houghton, 1988). Based upon the authors experience from studying the region around the 3M property adjacent to the fault study area, wells installed in the fault zone may produce 50-100+ gallons per minute (gpm) of

groundwater and exist under artesian conditions. Wells installed in the footwall outside of the fault zone produced < 10 gpm. Wells in the hanging wall produced on average 10-50+ gpm.

The Hopewell fault zone contains significant water resource potential. The increased production is likely due to the high storage potential and hydraulic conductivity found in the deformed rock located in the footwall, especially in the deeper drag-folded zone. The brecciated zone, because of the fault gouge, would act hydraulically as a confining layer.

ACKNOWLEGMENTS

The author thanks Doug Westover for his assistance in the preparation of figures for this paper. He also thanks 3M for entry to their property in order to access the study area.

REFERENCES

Burton, W.C. and Ratcliffe, N.M., 1985a. Compressional structures associated with right-oblique normal faulting of Triassic strata of the Newark basin near Flemington, New Jersey, Geological Society of America, Abstr. Program, 17 (1): 9.

Burton, W.C. and Ratcliffe, N.M., 1985b. Attitude, movement history and structure of cataclastic rocks of the Flemington fault -- Results of core drilling near Oldwick, New Jersey. U.S. Geological Survey, Miscellaneous Field Studies Map MF-1781.

Cornet, B. and Olsen, P.E., 1985. A summary of the biostratigraphy of the Newark Supergroup of eastern North America, with comments on early Mesozoic provinciality. In: R. Weber (editor), Congr. Latinoamerican de Paleontologia Mexico, III Simposium, Sobre Floras del Triasico Tardio, Fitogr. Paleoecol. Memo. Pp.67-81.

Dunning, G.R. and Hodych, J.P., 1990. U/Pb zircon and baddeleyite ages for the Palisades and Gettysburg sills of the northeastern United States: Implications for the age of the Triassic/Jurassic boundary: Geology, v. 18, p. 795-798.

Durney, D.W. and Ramsay, J.G., 1973. Incremental strain measured by syntectonic crystal growths. In: K.A. DeJong and R. Scholten (editors), Gravity and Tectonics. Wiley, New York, NY, pp. 67-96.

Faill, R.T., 2005. The Birdsboro Basin. Pennsylvania Geology, vol. 34, no. 4, pg. 2-11.

Fleuty, M.J., 1975. Slickensides and slickenlines. Geology Magazine, 112: 319-322.

Hancock, P.L., 1985. Brittle microtectonics: principles and practice. Journal of Structural Geology, 7: 437-457.

Houghton, H.F., 1988. Hydrogeologic study of water-well failures in argillite bedrock of Sourland Mountain, Somerset County, New Jersey, in 1982; New Jersey Geological Survey, Technical Memorandum 88-2, pp. 28.

Husch, J.M., Bambrick, T.C., Eliason, W.M., Roth, E.A., Schwimmer, R.A., Sturgis, D.S., and Trione, C.W., 1988. A review of the petrology and geochemistry of Mesozoic diabase from the central Newark basin: new petrogenetic insights: in Geology of the

Central Newark Basin, 5th Annual Meeting of GANJ, Field Guide and Proceedings, Oct. 7-9, 1988. p. 149-194.

Husch, J.M., 1992. Geochemistry and petrogenesis of the Early Jurassic diabase from the central Newark basin of New Jersey and Pennsylvania. Geological Society of America, Special Paper 268, p. 169-192.

Jones, B.D., 1994. Structure and stratigraphy of the Hopewell fault block, New Jersey and Pennsylvania. MS Thesis, New Brunswick, NJ. Rutgers University.

Klitgord, K.D. and Schouten, H., 1986. Plate kinematics of the central Atlantic. In: P.R. Vogt and B.E. Tucholke (Editors), The Western North Atlantic Region. (The Geology of North America, M.) Geophysical Society of America, Boulder, CO, p. 351-378.

Laney, S.E. and Gates, A.E., 1996; Three-dimensional shuffling of horses in a strike-slip duplex: an example from the Lambertville sill, New Jersey, Tectonophysics 258, p. 53-70.

Lewis, J.V.and Kummel, H.B., 1910-1912; Geologic Map of New Jersey, Revised 1931 and 1950, Department of Conservation and Economic Development, State of New Jersey.

Olsen, P.E., 1980. The Latest Triassic and Early Jurassic formations of the Newark basin (Eastern North America, Newark Supergroup). In: W. Manspeizer (Editor), Stratigraphy, Structure and Correlation: Field Studies of New Jersey Geology and Guide to Field Trips. 52nd Annual Meeting N.Y. Geological Association, Rutgers Univ., Newark, NJ. p. 2-41.

Olsen, P.E., Kent, D.V., Cornet, B., Witte, W.K. and Schlische, R.W., 1996. High-resolution stratigraphy of the Newark-rift basin (early Mesozoic, eastern North America); Geological Society of America Bulletin, V. 108, p. 40-77.

Parker, R.A. and Houghton, H.F., 1990. Bedrock geologic map of the Rocky Hill Quadrangle, New Jersey. U.S. Geological Survey Open-File Report 90-218.

Ratcliffe, N.M. and Burton, W.C., 1985. Fault reactivation models for the origin of the Newark basin and studies related to U.S. Eastern seismicity. U.S.Geological Survey Circ. 946: p. 36-45.

Ratcliffe, N.M. and Burton, W.C., 1988; Structural Analysis of the Furlong Fault and the Relation of Mineralization to Faulting and Diabase Intrusion, Newark Basin, Pennsylvania, In Froelich, A.J. and Robinson, G.R., Jr., eds. Studies of the Early Mesozoic Basins of the Eastern United States: U.S.Geological Survey Bulletin 1776, p. 176-193.

Rutter, E.H., 1986. On the nomenclature of mode of failure transitions in rocks. Tectonophysics, 122: 281-387.

Sanders, J.E., 1962. Strike-slip displacement on faults in Triassic rocks in New Jersey. Science, 136: p. 40-42.

Sanders, J.E., 1963. Late Triassic tectonic history of northeastern United States. American Journal of Science, 261: 501-524.

Schlische, R.W., 1992. Structural and stratigraphic development of the Newark extensional basin, eastern North America: Evidence for the growth of the basin and its bounding structures. Geological Society of America Bulletin 104: 1246-1263.

Schlische, R.W. and Olsen, P.E., 1988. Structural evolution of the Newark Basin. In: J.M. Husch and M.J. Hozik (Editors), Geology of the Central Newark basin. Field Guide Proc. 5th Annual Meet. Geological Association of New Jersey, p. 43-65.

Sibson, R.H., 1986. Brecciation processes in fault zones: Inference from earthquake rupturing. Pure Applied Geophysics, 124: 159-177.

Sutter, J.F., 1988. Innovative approaches to the dating of igneous events in the early Mesozoic basins: in Froelich, A.J. and Robinson, G.R., Jr. (Editors) Studies of the Early Mesozoic Basins in the eastern United States: U.S.G.S. Bulletin 1776. p. 194-200.

Tanner, P.W.G., 1989. Flexural-slip mechanism. Journal of Structural Geology, 11: 635-655.

United States Geological Survey, 1954; Rocky Hill, NJ Quadrangle, 7.5' Topographic Map.

United States Geological Survey, 1996; Bedrock Geologic Map of Northern New Jersey, A.A. Drake, Jr., R.A. Volkert, D.H. Monteverde, G.C. Herman, H.F. Houghton, R.A. Parker, and R.F. Dalton, Miscellaneous Investigations Series Map I - 2540-A.

United States Geological Survey, 1998; Bedrock Geologic Map of Central and Southern New Jersey, J.P. Owens, P.J. Sugarman, N.F. Sohl, R.A. Parker, H.F. Houghton, R.A. Volkert, A.A. Drake and R.C. Orndorff, Miscellaneous Investigations Series Map I -2540-B.

White, S.H. and Knipe, R.J., 1978. Transformation and reaction-enhanced ductility in rocks. Journal of the Geologic Society of London, 135: 513-516.

Stop 5. CORRELATION OF ROCKS UNITS AT THE NAVAL AIR WARFARE CENTER AND NEARBY CONTAMINATION SITE WITH THE NEWARK BASIN CORING PROJECT WELLS

Pierre Lacombe
U.S. Geologic Survey
810 Bear Tavern Road West Trenton, N.J.
placombe@usgs.gov

INTRODUCTION

The abundance of ground water contamination sites in fractured bedrock in the industrial parts of the United States is a major concern to the citizens and government. During 1980-1995, the U.S. Geological Survey Toxics Substances Hydrology Program began to investigate how to assess the flow of ground water through fractured bedrock at Mirror Lake, New Hampshire. In 2000, the USGS Toxics Program began a long term research project to investigate the flow and fate of contamination in fracture rock at the Naval Air Warfare Center (NAWC), West Trenton, N.J. (fig 1).

This investigation is coordinated with the U.S. Navy, its environmental contractors, and the NJDEP. The Navy's goal is to remediate contamination of trichloroethylene (TCE), its biodegradation products of dichloroethylene (DCE) and vinyl chloride (VC) as well as jet fuel that leaked during operation of the facility from about 1955 to 1998. South of NAWC is a former Auto Parts Manufacturer (APM) and a Bearings Parts Manufacturer (BPM) that also contaminated the fracture bedrock aquifer with TCE and other chemicals. The NAWC site overlies the Lockatong and Stockton Formations and the two industrial sites overlie the Stockton Formation. The two formations were previously mapped with a monolithic shallow northwest dip and a conformable contact (Owens and others, 1995).

The purpose of this paper is to show the local geologic framework using available natural gamma-ray and rock core logs from the three contamination sites and a local irrigation well. These logs are first correlated with one another then correlated with corehole data from the Newark Basin Coring Project (NBCP).

LOCAL GEOLOGY

Geologic mapping by Owens and others (1995), Lyttel and Epstein, (1984) and Hugh Houghton (1995, NJ Geological Survey, written commun.) show the strike and dip of the Lockatong and Stockton Formations about N40^{o}W and 15^{o}NW (fig. 1). They also show that the contact between the two formations is conformable at NAWC. However, they show numerous reverse faults at the contact on the west side of NAWC.

Geologic investigations by NBCP (Olsen and others, 1996) at the Nursery Road site collected rock core and geophysical logs for the complete thickness of the Lockatong Formation (fig. 2). Analysis of the rock core and logs allowed NBCP to divide the Lockatong Formation into 12 members. Each member represents a Milankovitch cycle and each member can be divided into five or six Van Houten cycles. A complete Van

Houten cycle consists of 4 major types of mudstone in a full cycle: red massive mudstone, light gray massive mudstone, dark gray laminated mudstone, and black carbon rich mudstone. The mudstone cycles are typical of a lacustrine environment of deposition. The members of the Stockton Formation are composed of conglomerate, sandstone, and shale typical of the fan type environment of deposition.

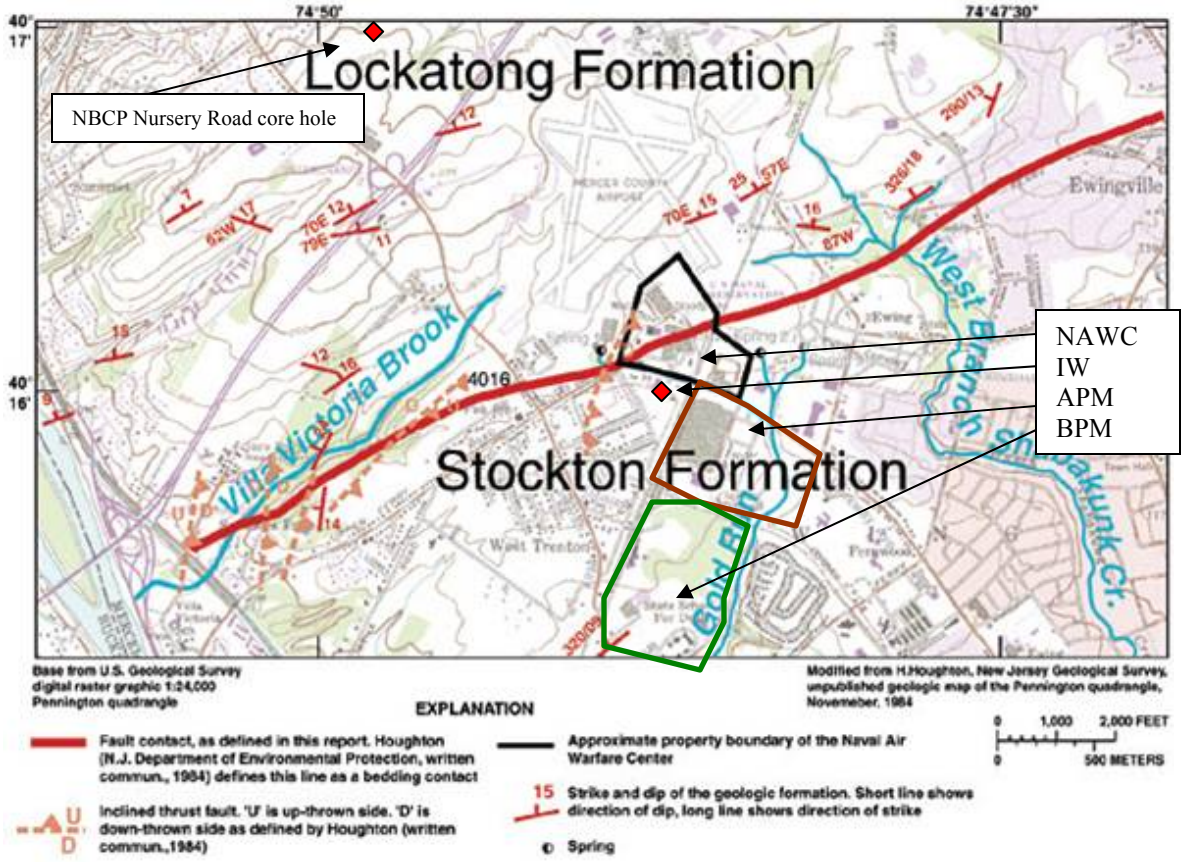

Figure 1. Geologic map showing the Stockton and Lockatong Formation and the location of the Naval Air Warfare Center (NAWC), local irrigation well (IW), former auto parts manufacture (APM), and bearings parts manufacture (BPM), and Newark Basin Coring Project (NBCP) Nursery Road core hole.

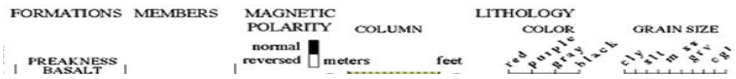

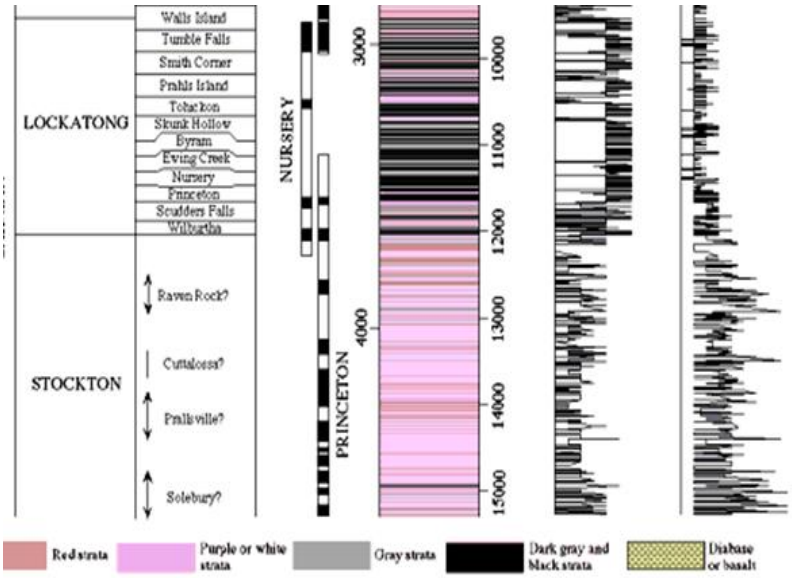

Figure 2. Members of the Lockatong and Stockton Formations and column showing rock color and grain size. (from Olsen and others, 1996)

Additional coring by NBCP on the Princeton University Campus eight miles northeast of NAWC collected rock core and geophysical logs for nearly the full thickness of the Stockton Formation. Analysis of the rock core and logs allowed the NBCP to divide the Stockton Formation into 4 members with tentative boundaries as to the top and bottom of each member.

GEOLOGY OF LOCKATONG FORMATION AT NAWC

Mapping of the geology of the Lockatong Formation at NAWC began with correlating about natural gamma-ray logs using signature anomalies within each log (fig 3). Lacombe, (2000) divided the Lockatong formation strata that underlies NAWC into 11 units (L-13 to L-23). Each gamma-ray based strata was defined as having a gamma high or a gamma low signature. The gamma ray stratigraphy was augmented by adding the rock description from core of borehole 43BR at NAWC (fig. 3). Rock descriptions were limited to four types of mudstone: red massive mudstone, light gray massive mudstone, dark gray laminated mudstone, and black carbon rich mudstone. The sections that Lacombe (2000 and 2002) published are enhanced here by including the four types of mudstone (fig.4). Section through NAWC shows the mudstone has a dip of 70o to 25^{o}NW. The strike of the bedrock is about N70^{o}E.

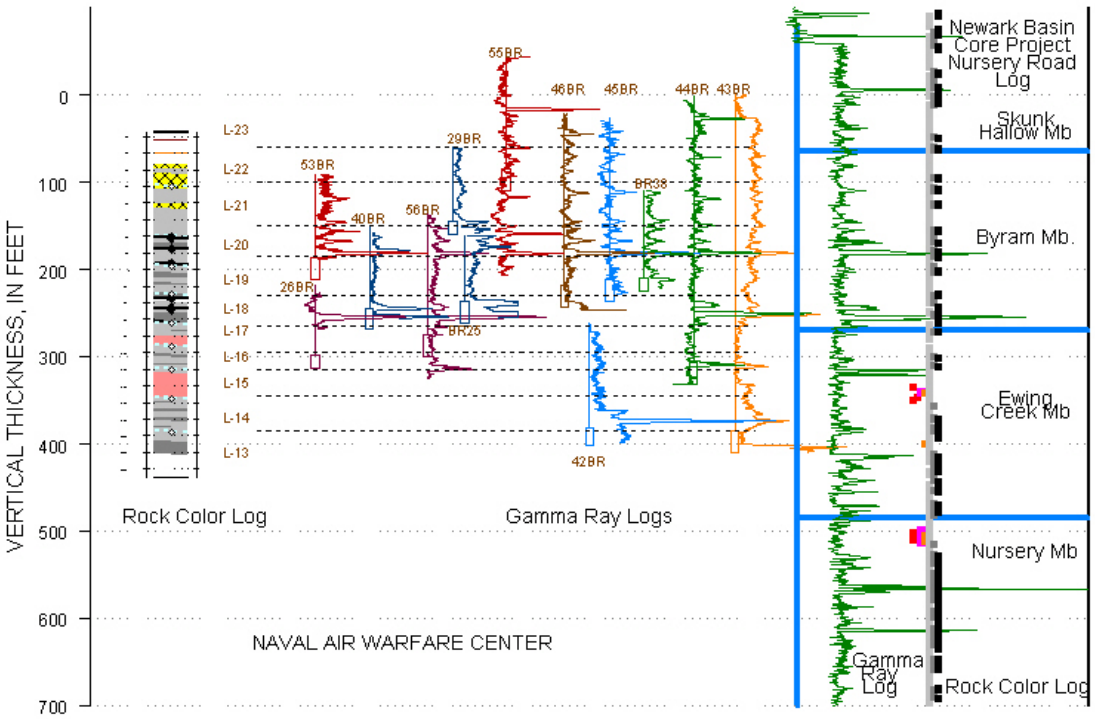

Figure 3. Thirteen natural gamma-ray logs from the Naval Air Warfare Center correlated with one another and divided into strata L-13 to L-23 and also divided into the four mudstones (red massive, light gray massive, dark gray laminated and black carbon rich). NAWC logs are correlated with Newark Basin Coring Project Nursery Road gamma-ray log and identified with the Ewing creek to Skunk Hallow member of the Lockatong formation. Rock color logs shown for the mudstone at NAWC and Nursery Road well.

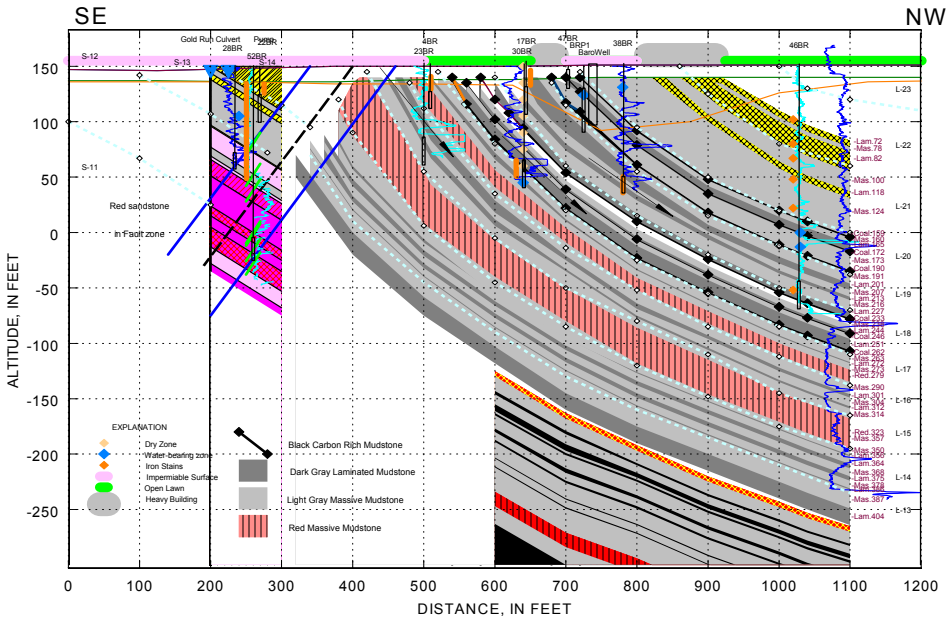

Figure 4. Section through NAWC showing gamma ray stratigraphy and the 42 rock color and nature of the mudstone strata in the Lockatong Formation (modified from Lacombe 2002). Location of the section through NAWC is shown in figure 9.

GEOLOGY OF STOCKTON FORMATION AT NAWC AND AT SITES SOUTH OF NAWC

Geologic mapping of the Stockton formation at NAWC is limited because there are only three widely spaced bedrock observation wells that have been drilled into the formation at the base. However, south of NAWC is a small private park with a 135 ft deep abandoned irrigation supply well (IW), a former automobile parts manufacturing facility (APM) with 15 bedrock observation wells that range in depth from 40 to 115 ft deep, and an active machine bearings parts manufacturer (BPM) with about 30 bedrock observations that range in depth from 40 to 250 ft deep. The USGS collected natural gamma-ray logs from all wells deeper than 40 ft and correlated gamma-ray logs for the BPM and APM sites (fig. 5). At this time, the drillers and the geologists' logs for the two sites have not been studied or correlated. However, rock cores for the APM site have been reviewed and the high gamma strata are red shale the low gamma strata are white sandstone and the intermediate gamma strata is red sandstone. With additional review of the BPM and APM drillers and geologists' logs, the interpretation of the gamma logs can be enhanced. The section through the BPM (fig. 6) shows northwest dipping strata of intercalated sandstone and shale. The strike and dip of the Stockton formation at two facilities is N45^{o}E and 27^{o}NW.

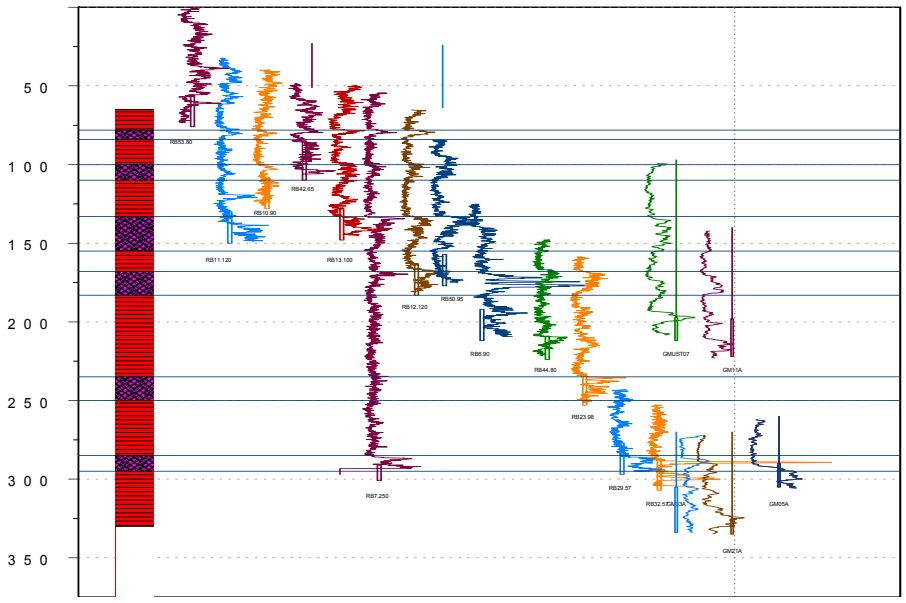

Figure 5. Thirteen natural gamma-ray logs from the bearing plant manufacture site (BPM) and 4 logs from the auto parts manufacturing site (APM) correlated with one another and divided into strata showing gamma high (red shale) and gamma low (red or white sandstone) zones.

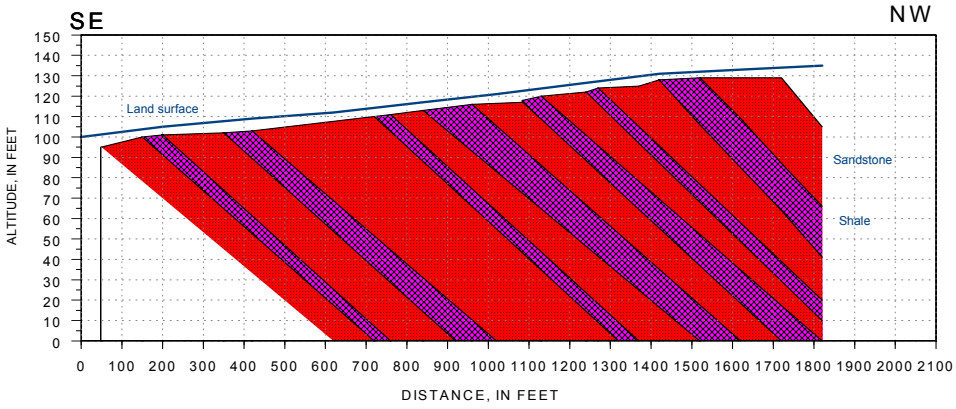

Figure 6. Section through the auto part manufacture and bearings parts manufacture site showing intercalated sandstone (dotted) and shale beds (crosshatch) of the Stockton Formation of the bedrock underling the two manufacturing sites. Location of the section through BPM and APM is shown in figure 9.

CORRELATION OF NAWC LOCKATONG STRATA WITH NURSERY ROAD CORE HOLE STRATA

The 450 foot long composite natural gamma-ray log of NAWC correlates remarkably wells with the gamma ray log for the Nursery Road core hole at the depth from about 1,750 to 2,220 ft below land surface (BLS) (fig. 3). The Nursery Road gamma high anomalies in the middle and at the bottom of the Byram Member are identical to the

anomalies in many of the wells at NAWC. Anomalies in the Skunk Hallow and Ewing Creek Members also match remarkably well. In addition, the rock color log for the NAWC well 43BR shows a 30 ft thick red mudstone at about 320 ft BLS. The Nursery Core log also shows a similar red stratum in the upper part of the Ewing Creek Member. The 10 ft thick red massive mudstone at NAWC at about 280 ft BLS does not correlate with a similar red mudstone in the upper Ewing Creek Member but there are no black or gray mudstone at this interval in the Nursery Core log. Two sets of three black carbon rich mudstone strata at 160 to 190 ft and 230 to 260 ft BLS at NAWC correlate well with the black mudstone in the middle and lower part of the Byram Member. Based on the gamma ray and rock color logs, the strata at NAWC correlates with the strata of the lower Skunk Hallow, Byram, and upper Ewing Creek Member of the Lockatong formation as defined in the Nursery core.

CORRELATION OF THE STOCKTON FORMATION STRATA FROM THE NAWC AND INDUSTRIAL SITES WITH STRATA FROM THE NURSERY ROAD AND PRINCETON CORE HOLE SITES

The correlation of the gamma ray logs from the IW, BPM, and APM wells with the NBCP wells is less well defined than the correlation of gamma ray logs for the Lockatong Formation. The Nursery Road and Princeton corehole gamma ray logs show that the Scudder's Falls and Wilburtha Member have many anomalously high gamma ray spikes (fig. 7) and that the Raven Rock member has only one anomalously high gamma ray spike that is located in its upper part. Further analysis of the gamma ray signature of the Raven Rock member shows that the member can be divided into a lower and upper Raven Rock member. The gamma ray signature of the upper member is shows a rather monotonous shale with a single gamma spike while the gamma ray signature for the lower member shows many interbedded sandstone and shale. Based on this simple interpretation it is possible that the IW well with its single high gamma ray anomaly is part of the Scudder’s Falls or Wilburtha Member but more likely it is part of the upper Raven Rock Member. Analysis of the gamma ray logs for the BPM and APM wells show many interbedded sandstone and shale beds typical of the lower half of the Raven Rock Member. With this correlation of gamma ray logs it is interpreted that the strata south of NAWC is the Raven Rock Member and is tentatively mapped as such.

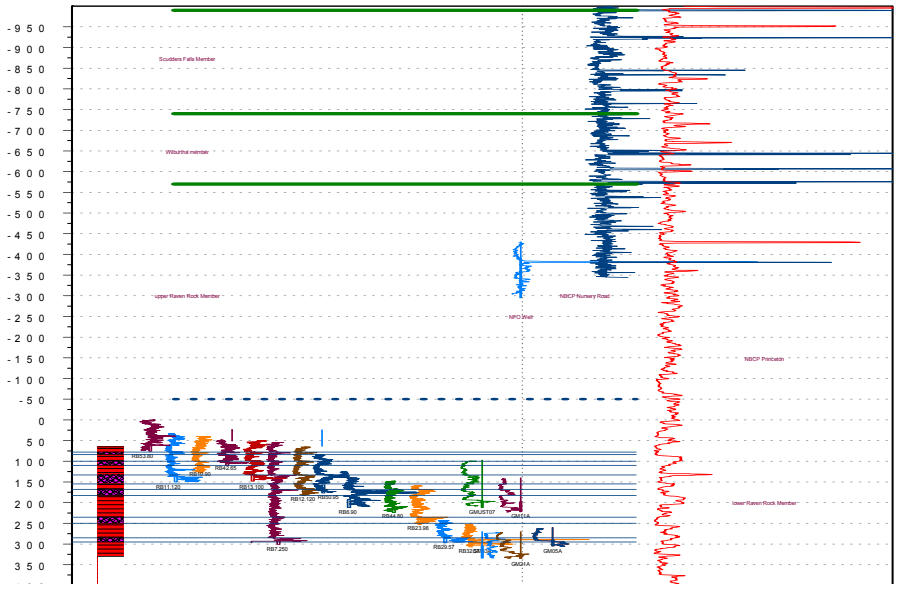

Figure 7. Correlation of the gamma ray logs from the two manufacturing sites and the irrigation well with the Newark Basin Coring Project wells at Nursery Road and Princeton. Raven Rock member is divided into an upper and lower strata based on gamma ray signature.

REVERSE FAULT

Rock core from four bedrock wells at NAWC show massive gouge zones, fault breccia, calcite infilling, slickenside, overturned bedding, abrupt bedrock changes, and many other characteristics of faulting. Excavations for local retail store on the south side of NAWC and for a veterinary hospital about 2000 ft west of NAWC show multiple fault features. Normal faulting is typical of the Newark Basin but reverse faulting also occurred in the Newark Basin during parts of the Jurassic. The rock core at NAWC and outcrops about 1 mile west of NAWC show overturned beds indicative of reverse faulting. The trend of the fault is north 45^{o}NE with a dip of 45^{o}SE. The few rock cores available from the APM show no fault features.

GEOLOGIC MAP AND SECTION OF THE STOCKTON AND LOCKATONG FORMATION

Correlations of the gamma ray logs from the NBCP, NAWC, IW, AMP, and BMP and the geomorphology of the land between the Nursery Road core site and the NAWC were used to create a geologic section and map of the area (fig. 9). The few natural outcrops and road cuts in the area are red and light gray, massive, and well indurated mudstone typical of parts of the Thumble Falls and Prahls Island members. Generally the natural outcrops occur along the crest of low linear ridges. The small valleys are likely underlain by the dark-gray and black laminated and highly fissile mudstone strata typical of the Smith Corner, lower Tohekon, Byram and the older members. Streams that flow

along the strike of these members are fed by ground water discharging from the rheologically weak fissile dark gray and black mudstone. The West Branch and East Branch of Shabakunk Creek cut across the members of both formations. The head water of both branches form multiple contributories in the Lockatong Formation but form a confluence immediately north of the Lockatong-Stockton contact. South of the contact the stream form a single channel with very few tributaries.

The strata that underlie NAWC are composed of more than 40 bedding units of three members of the Lockatong Formation. The strata that underlie APM and BPM are composed of more than 12 bedding units composed of sandstone and shale.

SUMMARY

The geologic framework of the Naval Air Warfare Center in West Trenton NJ is composed of northwest dipping red massive mudstone, light gray massive mudstone, dark gray laminated mudstone, and black carbon rich mudstone. Using these rock types and this structure the USGS in cooperation with the Navy and its environmental contractors has been able to better define the ground-water and contaminate flow at NAWC.

The Toxics Substances Hydrology Program of the USGS is investigating many facts of contamination in fractured bedrock. The facet of the extent of hydrogeology that is controlled by the local geology is of primary importance. The USGS will further convert this geologic framework into a hydrogeologic framework by incorporating the effects of offloading which open sealed fracture networks and preferential weathering that creates more primary and secondary porosity in the geologic unit.

ACKNOWLEDGEMENTS

The USGS would like to thank Jeff Dale, Edward Boyle and Debra Felton of the US Navy, Greg Herman and Bill Hanrahan and of the NJDEP and the many environmental scientists from ECOR Inc, EA Inc, and IT Inc, who have over the years collected and compiled data.

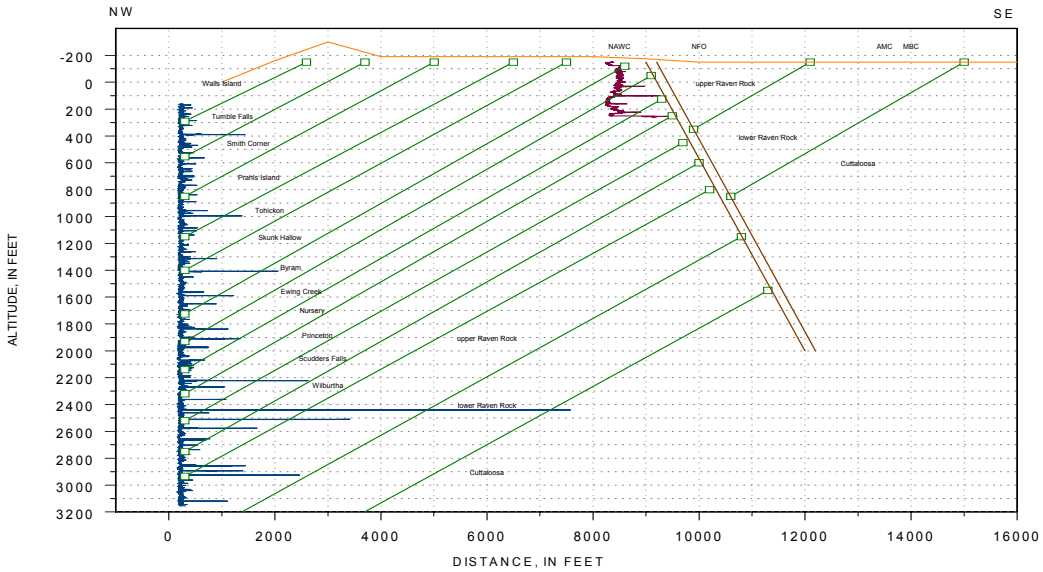

Figure 8 Section A-A' showing the members of the Lockatong and Stockton Formations at the NBCP Nursery Road Core site, NAWC, APM, and BPM sites.

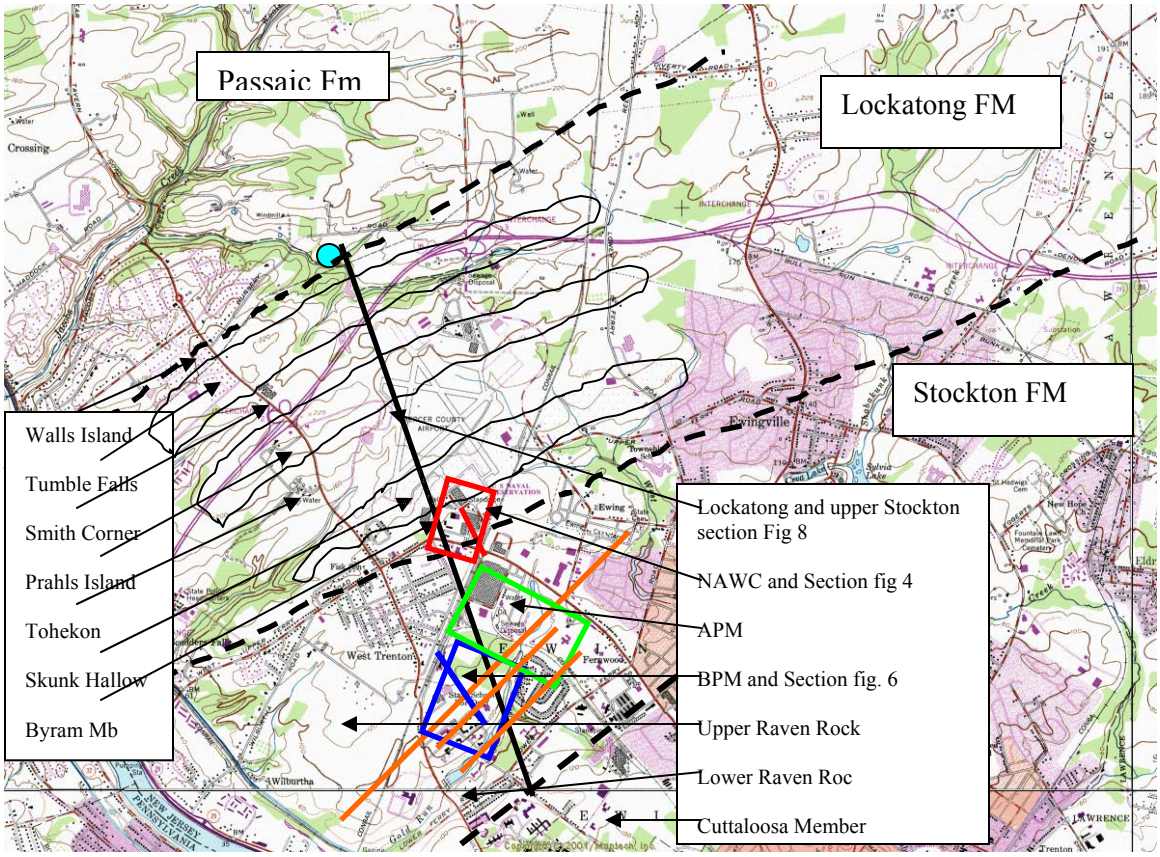

Figure 9 Topographic map show the outcrop areas of the members of the Lockatong and Stockton formations and near the Naval Air Warfare Center and the sections A, B and C

REFERENCES

Goldberg, D., Reynolds, D., Williams, C., Witte, W. K., Olsen, P. E., and Kent, D. V., 1994, well logging results from the Newark Rift Basin Coring Project. Scientific Drilling, 4 (4-6), pp. 267-279

International Technology Corporation, 1994, Remedial investigation report, Naval Air Warfare Center, Aircraft Division Trenton, N.J. Volume 1 of 3, IT Corporation, 165 Fieldcrest Avenue, Edison, NJ, Project Number 526538/529658, ~200 p.

Lacombe, P.J., 2000, Hydrogeologic framework, water levels, and trichloroethylene contamination, Naval Air Warfare Center, West Trenton, New Jersey, 1993-97: U.S. Geological Survey Water-Resources Investigations Report 98-4167, 139 p,

Lacombe, P.J., 2002, Ground-water levels and potentiometric surfaces, Naval Air Warfare Center, West Trenton, New Jersey, 2000: U.S. Geological Survey Water-Resources Investigations Report 01-4197, 48 p.

Owens, J. P., Sugarman, P., Sohl, Volkert, 1995. Geologic map of New Jersey, central sheet: Scale 1:100,000, U.S. Geological Survey Open-File Report; 95-253. 3 plates

Olsen, P. E., Kent, D. V., Cornet, Bruce, Witte, W. K. and Schlische, R.W., 1996, High resolution stratigraphy of the Newark Rift basin (early Mesozoic, eastern North America), GSA Bulletin: January 1996; v. 108; no. 1; p. 40- 77.

Olsen, P. E. and Kent, D. V., 1996, Milankovitch climate forcing in the tropics of Pangea during the Late Triassic. Palaeogeography, Palaeoclimatology, and Palaeoecology, v. 122, p. 1-26.

Smoot, J. P. and Olsen, P. E., 1994, Climatic cycles as sedimentary controls of rift basin lacustrine deposits in the early Mesozoic Newark basin based on continuous core. In Lomando, A. J. and Harris, M., Lacustrine Depositional Systems, SEPM Core Workshop Notes, v. 19, p. 201-237.

Compton, Robert R., 1962, Manual of Field Geology, John Wiley and Sons Inc. NYC, NY, 378 p.

Olson, P.E. 1996, Natural Gamma ray log data and rock core color log data. http://www.ldeo.columbia.edu/~polsen/nbcp/data.html

Van Houten F.B., 1962, Cyclic sedimentation and the origin of analcime rich Upper Triassic Lockatong Formation, West central New Jersey and adjacent Pennsylvania, American Journal of Science, v. 260, p. 561-576.

Van Houten F.B., 1964, Cyclic Lacustrine Sedimentation, Upper Triassic Lockatong Formation, Central New Jersey And Adjacent Pennsylvania, In Mermaid O.F., Ed., Symposium On Cyclic Sedimentation, Kansas Geological Survey Bulletin 169, P. 497- 531.

GANJ XXII
2005 Annual Meeting

Teachers Workshop

The Story of the

Wolf – to – Wale
&
Dino – to – Bird

AS TOLD IN THE FOSSIL RECORD

Presenter

Dr. George A. Randall
Rowan University Department
of Physics and Astronomy